

ADO 729869

Lyons

01

AFFDL-TR-71-6

**ANALYSIS OF LIMITED AUTHORITY
MANUAL CONTROL SYSTEMS**

LEE GREGOR HOFMANN

KISHOR V. SHAH

DUNSTAN GRAHAM

SYSTEMS TECHNOLOGY, INC.

3709

TECHNICAL REPORT AFFDL-TR-71-6

JULY 1971

Approved for public release; distribution unlimited.

20061017039

AIR FORCE FLIGHT DYNAMICS LABORATORY
AIR FORCE SYSTEMS COMMAND
WRIGHT-PATTERSON AIR FORCE BASE, OHIO

Best Available Copy

NOTICE

When Government drawings, specifications, or other data are used for any purpose other than in connection with a definitely related Government procurement operation, the United States Government thereby incurs no responsibility nor any obligation whatsoever; and the fact that the government may have formulated, furnished, or in any way supplied the said drawings, specifications, or other data, is not to be regarded by implication or otherwise as in any manner licensing the holder or any other person or corporation, or conveying any rights or permission to manufacture, use, or sell any patented invention that may in any way be related thereto.

Copies of this report should not be returned unless return is required by security considerations, contractual obligations, or notice on a specific document.

**ANALYSIS OF LIMITED AUTHORITY
MANUAL CONTROL SYSTEMS**

LEE GREGOR HOFMANN

KISHOR V. SHAH

DUNSTAN GRAHAM

Approved for public release; distribution unlimited.

FOREWORD

The research reported here was accomplished for the United States Air Force by Systems Technology, Inc., Hawthorne, California, under Contract No. F33615-70-C-1075. The program was sponsored by the Air Force Flight Dynamics Laboratory, Aeronautical Systems Division, Wright-Patterson Air Force Base, Ohio, under Project No. 8219, Task No. 821904.

This research program was coordinated with a related program conducted by Honeywell, Inc. Results from the latter program are summarized in AFFDL-TR-70-48.

This report has also been issued as Systems Technology, Inc., Technical Report No. 194-1.

The Air Force project engineer was Alonzo J. Connors. The contractor's technical director, project engineer and principal investigator was Dunstan Graham. The research was performed during the period from September 1969 through June 1970. The manuscript was released by the authors for publication in September 1970.

This technical report has been reviewed and is approved.



E. B. WESTBROOK
Chief, Control Criteria Branch
Aeronautical Systems Division
Air Force Flight Dynamics Laboratory

ABSTRACT

Systematic procedures for predicting pilot-vehicle-flight control system performance and proneness to pilot induced oscillations and instabilities are here developed and applied to examples. The systems analyzed have very limited maximum control surface rates and deflections.

Performance analysis is by means of applying random input describing function theory to predict the root-mean-square level of key system variables as a function of the control surface rate and deflection limit levels. Acceptable limit levels are only two to three times the root mean square value of the variable at the point in the system where each limiter nonlinearity occurs.

Pilot induced oscillations and instabilities are predicted by applying sinusoidal input describing function theory. A sinusoidal input describing function is derived for the rate limited integrator having a restricted output range. This is the key element in the model for an actuator having limited maximum rate and deflection. Pilot induced oscillations correspond to a stable limit cycle. Furthermore, pilot induced instabilities may result when conditions derived from the unstable limit cycle solutions are exceeded. A simple design criterion for eliminating pilot induced oscillations and instabilities is

Select the linear system gains and equalization so that the locus of closed-loop system roots as a function of the forward-loop actuator gain over the range from zero to its nominal value, does not exhibit conditional stability.

Results of analyzing three minimum back-up manual flight control system modifications for the F-4C are compared with data from piloted fixed-base simulator experiments for the same system configurations. The analytically determined minimum limits for the three example back-up systems compare favorably with the minimum limits determined in fixed-base simulation. Predicted and measured pilot opinion ratings also compare favorably. Unfortunately, however, predicted and measured performance do not compare favorably. This may be because of inaccurate or incomplete documentation of the measured performance.

CONTENTS

	<u>Page</u>
I. INTRODUCTION	1
A. Background	1
B. Purpose	1
C. The Problem and Objective	2
D. State-Of-The-Art and Approach	3
E. Organization of the Report	4
II. THE PROBLEM AND ANALYTICAL APPROACH	6
A. Problem	6
B. Example Applications	6
C. Analytical Approach	10
D. Nonlinearities	20
III. MINIMUM CONTROL PARAMETER VALUE SELECTION AND SYSTEM PERFORMANCE PREDICTION	26
A. Longitudinal Control	26
B. Lateral Control	31
C. Minimum Control Parameter Value Selection	37
D. Verification of System Performance	40
E. Nonlinear System A	40
F. Nonlinear System B	51
G. Nonlinear System C	56
H. Comparison of Predicted and Measured Pilot Opinion Ratings and Performance	59
IV. DERIVATION OF THE SINUSOIDAL INPUT DESCRIBING FUNCTION FOR THE LIMITING INTEGRATOR	68
A. Validity of the Describing Function	81
B. Applying the Describing Function	81
V. PREDICTION AND AVOIDANCE OF PILOT INDUCED OSCILLATIONS	84
A. System A	86
B. System B	96
C. System C	102

CONTENTS (cont'd)

	<u>Page</u>
D. Comparison of Predicted and Measured Pilot Induced Oscillations Tendency Ratings	104
E. Avoiding Pilot Induced Oscillations by Design	105
VI. SUMMARY	109
REFERENCES	111
APPENDIX I. F-4C STABILITY DERIVATIVES, TRANSFER FUNCTIONS, GUIDANCE SYSTEM GEOMETRY AND DISTURBANCE MODELS	114
APPENDIX II. MANUAL LANDING APPROACH CONTROL FOR BASIC F-4C BACK-UP SYSTEM	123
APPENDIX III. COMPUTER PROGRAM FOR SINUSOIDAL INPUT DESCRIBING FUNCTION FOR LIMITING INTEGRATOR	149
APPENDIX IV. TABULATION OF SINUSOIDAL INPUT DESCRIBING FUNCTION FOR THE LIMITING INTEGRATOR	156
APPENDIX V. SUMMARY OF FACTORED CLOSED-LOOP TRANSFER FUNCTIONS FOR LINEAR AND NONLINEAR, LONGITUDINAL AND LATERAL SYSTEMS A, B AND C	181
APPENDIX VI. MEAN SQUARE PERFORMANCE DATA AND PILOT OPINION RATINGS RESULTING FROM HONEYWELL, INC. FIXED-BASE, PILOTED SIMULATOR EXPERIMENTS (REPRODUCED AND SUMMARIZED FROM REF. 1)	213

LIST OF FIGURES

	<u>Page</u>
1. Equivalent Representations of a Limiter	14
2. Random Input Describing Function for Normalized Limiter . . .	15
3. Equivalent Random Input Describing Function Representations for a Limiter	16
4. Block Diagrams for Direct Manual Control Surface Actuation	21
5. Deflection and Rate Limiting Actuator Model	24
6. Longitudinal F-4C Block Diagram for System A	27
7. Block Diagram Changes for Pitch Control by Means of Stabilator Tab	29
8. Lateral F-4C Block Diagram for System A	32
9. Block Diagram Changes for Roll Control by Means of Spoilers Having Reduced Effectiveness	34
10. Block Diagram Changes for Roll Control by Means of Modified Ailerons	36
11. Solution for the Equivalent Gains for Longitudinal System A Rate Limit Equations	42
12. Solution for the Equivalent Gains for Longitudinal System A Deflection Limit Equations	43
13. Finding Alternate Solutions for which Closed-Loop System Performance is Invariant	46
14. Solution for the Equivalent Gains for Lateral System A Rate Limit Equations	48
15. Solution for the Equivalent Gains for Lateral System A Deflection Limit Equations	49
16. Block Diagram Changes for Pitch Control by Means of Stabilator Tab	51
17. Solution for Equivalent Gain, K_p , for Longitudinal System B .	53
18. Block Diagram Changes for Roll Control by Means of Spoilers Having Reduced Effectiveness	54

LIST OF FIGURES (cont'd)

	<u>Page</u>
19. Solution for Equivalent Gain, K_p , for Lateral System B	55
20. Block Diagram Changes for Roll Control by Means of Modified Ailerons	57
21. Solution for Equivalent Gain, K_p , for Lateral System C	58
22. Mathematical Model of the Limiting Integrator	68
23. Negative Inverse of Normalized Sinusoidal Input Describing Function for a Limiting Integrator	79
24. Loop Structure Containing Nonlinear Actuator	82
25. Sinusoidal Input Describing Function for Normalized Limiter	85
26. Frequency Response for Longitudinal System A Proneness Condition ($\tau_s = 0.2$ sec)	87
27. Frequency Response for Longitudinal System A Sustenance Condition ($\tau_s = 0.0$ sec)	88
28. Determining the Limit Cycles for Longitudinal System A with $\tau_s = 0.2$ sec and $K_\theta = 0.0$ sec	89
29. Determining the Limit Cycles for Longitudinal System A with $\tau_s = 0.0$ sec and $K_\theta = 0.0$ sec	91
30. Frequency Response for Lateral System A. Proneness Condition ($\tau_{sp} = 0.2$ sec) and Sustenance Condition ($\tau_{sp} = 0.0$ sec)	93
31. Determining the Limit Cycles for Lateral System A with $\tau_{sp} = 0.2$ sec and $\tau_{sp} = 0.0$ sec	94
32. Determining the Limit Cycles for Lateral System A with $\tau_{sp} = 0.2$ sec and $\tau_{sp} = 0.0$ sec	97
33. Determining the Limit Cycles for Longitudinal System B with $\tau_s = 0.2$ sec	98
34. Determining the Limit Cycles for Longitudinal System B with $\tau_s = 0.0$ sec	99
35. Determining the Limit Cycles for Lateral System B with $\tau_{sp} = 0.2$ sec and $\tau_{sp} = 0.0$ sec	101
36. Determining the Limit Cycles for Lateral System C with $\tau_a = 0.2$ sec and $\tau_a = 0.0$ sec	103

LIST OF FIGURES (cont'd)

	<u>Page</u>
37. Approach Geometry for Coincident ILS Signal Null and Reference Glide Path ($d_c = y_c = 0$)	120
38. Longitudinal F-4 Block Diagram for System A	129
39. Effect of $u_{AS} \rightarrow \delta_T$ Closure upon the Key Numerator, $N_{\delta_s}^{-hp}$	131
40. Effect of $u_{AS} \rightarrow \delta_T$ Closure upon the $N_{\delta_s}^{\theta}$ Numerator	132
41. Effect of $u_{AS} \rightarrow \delta_T$ Closure upon the Characteristic Polynomial, Δ	133
42. Effect of $\dot{\theta} \rightarrow \delta_s$ Closure upon the Characteristic Polynomial, Δ''	134
43. Effect of $\theta \rightarrow \delta_s$ for Obtaining Favorable Root Locations in the Open-Loop Function Numerator for Final Loop Closure	135
44. Final Loop Closure, $[K_d(s+K_{\bar{d}}/K_d)h_p/(s+K_{\theta}\theta)] \rightarrow \delta_s$, which gives the Closed-Loop System Characteristic Polynomial, Δ'''	136
45. Glide Slope Frequency Response for Closed-Loop System	137
46. Lateral F-4 Block Diagram for System A	143
47. Effect of $\varphi \rightarrow \delta_{sp}$ Closure upon the Characteristic Polynomial, Δ'	145
48. Effect of $\psi \rightarrow \delta_{sp}$ for Obtaining Favorable Root Locations in the Open-Loop Function Numerator for Final Loop Closure	146
49. Final Loop Closure, $[K_y y + K_{\psi} s \psi / (s + \omega_1)] \rightarrow \delta_{sp}$, which gives the Closed-Loop System Characteristic Polynomial, Δ''	147
50. Localizer Frequency Response for Closed-Loop System	148
51. Flow Diagram for Describing Function Computation	150
52. Handling Qualities Rating Scale	226

LIST OF TABLES

	<u>Page</u>
I. Longitudinal Back-Up Systems	7
II. Lateral-Directional Back-Up Systems	8
III. Quantitative Data for Back-Up Systems	9
IV. Parameters for Linear Pilot Loop Closures, System A, Longitudinal	28
V. RMS Responses to ILS Beam Bends and Normal Gusts for Linear Longitudinal System A	29
VI. RMS Responses to ILS Beam Bends and Normal Gusts for Linear Longitudinal Systems B and C	30
VII. Parameters for Linear Pilot Loop Closures, System A, Lateral	33
VIII. RMS Responses to ILS Beam Bends and Side Gusts for Linear Lateral System A	33
IX. RMS Responses to ILS Beam Bends and Side Gusts for Linear Lateral System B	35
X. Parameters for Linear Pilot Loop Closures, System C, Lateral	36
XI. RMS Responses to ILS Beam Bends and Side Gusts for Linear Lateral System C	37
XII. Selection of Minimum Control Parameter Values	39
XIII. RMS Responses to ILS Beam Bends and Normal Gusts for Nonlinear Longitudinal System A	44
XIV. RMS Responses to ILS Beam Bends and Side Gusts for Nonlinear Lateral System A	50
XV. RMS Responses to ILS Beam Bends and Side Gusts for Nonlinear Lateral System B	56
XVI. RMS Responses to ILS Beam Bends and Side Gusts for Nonlinear Lateral System C	59
XVII. Summary of Predicted Pilot Flying Qualities Ratings	61
XVIII. Summary of Mean Square Performance Measures Derived from Analysis for Comparison with Actual Measurements	63

LIST OF TABLES (cont'd)

	<u>Page</u>
XXIX. Maximum Acceptable Levels of Glide Slope Error and Localizer Error	65
XX. Summary of Fourier Coefficients for Output Waveform of the Limiting Integrator	72
XXI. Summary of Predicted Pilot Induced Oscillation Tendency Ratings	105
XXII. F-4C Parameters for Clean Configuration	115
XXIII. Longitudinal Equations of Motion	116
XXIV. Lateral Equations of Motion	117
XXV. Longitudinal Transfer Functions for the F-4C in Clean Configuration	118
XXVI. Lateral Transfer Functions for the F-4C in Clean Configuration	119
XXVII. Power Spectral Densities for Disturbance Environment at R = 3,690 ft	121
XXVIII. Equations for Basic Longitudinal Loop Closures, System A	128
XXIX. Parameters for Linear Pilot Loop Closures, System A, Longitudinal	130
XXX. Equations for Basic Lateral Loop Closures, System A	141
XXXI. Parameters for Linear Pilot Loop Closures, System A, Lateral	144
XXXII. Program Listing for Computation of the Negative Inverse of the Sinusoidal Input Describing Function for the Limiting Integrator	152
XXXIII. Tabulation of the Negative Inverse of the Nondimensionalized Sinusoidal Input Describing Function for a Rate Limited Integrator Having a Restricted Output Range. Cases III, IV-A, IV-B, IV-C	157
XXXIV. Guide to Tables of Closed-Loop Transfer Functions	181
XXXV. Notation Used for Longitudinal Numerator Designations	182

LIST OF TABLES (cont'd)

	<u>Page</u>
XXXVI. Notation Used for Lateral Numerator Designations . . .	182
XXXVII. Closed-Loop Transfer Functions for Longitudinal Linear System A	184
XXXVIII. Closed-Loop Transfer Functions for Lateral Linear System A	188
XXXIX. Closed-Loop Transfer Functions for Longitudinal Nonlinear System A	191
XXXX. Closed-Loop Transfer Functions for Lateral Nonlinear System A	195
XXXI. Closed-Loop Transfer Functions for Longitudinal Linear and Nonlinear Systems B and C	198
XXXII. Closed-Loop Transfer Functions for Lateral Linear System B	201
XXXIII. Closed-Loop Transfer Functions for Lateral Nonlinear System B	204
XXXIV. Closed-Loop Transfer Functions for Lateral Linear System C	207
XXXV. Closed-Loop Transfer Functions for Lateral Nonlinear System C	210
XXXVI. Evaluations - Redundant Actuator/Back-Up Power Systems	214
XXXVII. Evaluations - Mechanical Back-Up System No. 1	218
XXXVIII. Evaluations - Mechanical Back-Up System No. 2	223
XXXIX. PIO Tendency Rating Scale	227
L. Summary of Pilot Opinion From Simulation (Ref. 1)	228

SYMBOLS

A	Fourier cosine coefficient (-)
a_y'	Lateral acceleration perturbation at station l_x, l_z (ft/sec ²)
a_z	Normal acceleration perturbation (ft/sec ²)
B	Fourier sine coefficient (-)
b	Output of limiting integrator
C	Amplitude of c
CL_0	Trim value of lift coefficient
c	Output of linear integrator in limiting integrator model
d	Deviation of aircraft from ideal geometric reference glide path (ft)
d_c	ILS glide slope beam "bends" (ft)
E	Amplitude of e
e	Input to limiting integrator
F_{PR}	Pilot force on rudder pedals (lb)
F_{SL}	Longitudinal pilot force on stick (lb)
F_{SLD}	Lateral pilot force on stick (lb)
G	Gain on linear portion of limiter input-output characteristic
GR	Gear ratio (-)
GS	Angular glide slope deviation (deg)
g	Gravitational acceleration (ft/sec ²)
H_8	Hinge moment gradient (ft-lb/deg)
HP_{max}	Instantaneous peak horsepower required by actuator (550. lb-ft/sec)
h	Altitude perturbation (ft)
I_x, I_y, I_z	Moments of inertia (sl-ft ²)

SYMBOLS (cont'd)

I_{xz}	Product of inertia referred to body axes (sl-ft ²)
j	$\sqrt{-1}$
K	Small signal open-loop gain of actuator (rad/sec)
$K()$	Feedback loop gains
K_{eq}	Normalized random input describing function equivalent gain (-)
K_p	Equivalent gain for normalized output limiter (-)
K_R	Equivalent gain for normalized rate limiter (-)
k	Enforcement gain (rad/sec)
LOC	Angular localizer deviation as measured at a range equal to that to the glide slope transmitter antenna site (deg)
L	Rolling moment applied to aircraft (ft-lb); integral scale length of homogeneous isotropic atmospheric turbulence (ft)
L_i'	$\frac{L_i + \frac{I_{xz}}{I_x} N_i}{1 - \frac{I_{xz}^2}{I_x I_z}} ; i = p, r, \beta, \delta, v$
L_p	$(1/I_x)(\partial L/\partial p)$ (1/sec)
L_r	$(1/I_x)(\partial L/\partial r)$ (1/sec)
L_β	$(1/I_x)(\partial L/\partial \beta)$ (1/sec ²)
L_δ	$(1/I_x)(\partial L/\partial \delta)$ (rad/sec ² /deg)
$l(\cdot)$	Length along (\cdot)-axis (ft)
m	Aircraft mass (sl)
M	Aerodynamic pitching moment applied to aircraft (ft-lb)
M_q	$(1/I_y)(\partial M/\partial q)$ (1/sec)
M_u^*	$(1/I_y)(\partial M/\partial u + Z_j \partial T/\partial u)$ (1/sec-ft)

SYMBOLS (cont'd)

M_w	$(1/I_y)(\partial M/\partial w)$ (1/sec-ft)
M_{α}	$U_0 M_w$ (1/sec ²)
M_{δ}	$(1/I_y)(\partial M/\partial \delta)$ (rad/sec ² /deg)
N	Yawing moment applied to aircraft (ft-lb)
$N(j\omega)$	Sinusoidal input describing function

$$N'_i = \frac{N_i + \frac{I_{xz}}{I_z} L_i}{1 - \frac{I_{xz}^2}{I_x I_z}} ; \quad i = p, r, \beta, \delta, v$$

N_p	$(1/I_z)(\partial N/\partial p)$ (1/sec)
N_r	$(1/I_z)(\partial N/\partial r)$ (1/sec)
N_{β}	$(1/I_z)(\partial N/\partial \beta)$ (1/sec ²)
N_{δ}	$(1/I_z)(\partial N/\partial \delta)$ (rad/sec ² /deg)

$N_{(\cdot)}^{[\cdot]}$ Transfer function numerator polynomial for the $[\cdot]$ output in response to the (\cdot) input

$N_{(3)(4)}^{[1][2]}$ Coupling numerator polynomial, $N_{(3)(4)}^{[1][2]} = (N_{(3)}^{[1]} N_{(4)}^{[2]} - N_{(4)}^{[1]} N_{(3)}^{[2]}) / \Delta$

n_z	Normal acceleration in g's (-)
P	Output limit level (deg); also total body axis roll rate in Ref. 1 (deg/sec)
P_R	Rudder pedal deflection (in)
p	Rolling component of aircraft angular velocity (rad/sec)
Q	Total body-axis pitch rate in Ref. 1 (deg/sec)
q	Pitching component of aircraft angular velocity (rad/sec)
R	Rate limit level (deg/sec); also slant range to glide slope transmitter antenna (ft); also total body-axis yaw rate in Ref. 1 (deg/sec)

SYMBOLS (cont'd)

R_{rwy}	Distance between glide slope and localizer transmitting antenna sites (ft)
r	Yawing component of aircraft angular velocity (rad/sec)
S	Saturation level for hard limiter (units of input variable) Also $[\sin^{-1}(1/E^*)]$ in Table XX only.
S_L	Longitudinal deflection of control stick (in)
S_{LD}	Lateral deflection of control stick (in)
s	Laplace transform variable (rad/sec)
T	Aircraft engine thrust (lb)
T_L	Lead time constant adopted by the human operator (sec)
t	Time (sec)
U_0	Longitudinal (x) component of trim (equilibril) translational velocity of aircraft (ft/sec)
u	Longitudinal (x) component of perturbed translational velocity of aircraft (ft/sec)
V_{T_0}	Total trim (equilibril) translational velocity of aircraft = $\sqrt{U_0^2 + W_0^2}$ (ft/sec)
v	Lateral (y) component of translational velocity of aircraft (ft/sec)
v_g	Side gust velocity (ft/sec)
W	Gross weight (lb)
W_0	Normal (z) component of trim (equilibril) translational velocity of aircraft (ft/sec)
$W(j\omega)$	Frequency response function for linear portion of the system
w	Normal (z) component of perturbed translational velocity of aircraft (ft/sec)
w_g	Normal gust velocity (ft/sec)
X	Aerodynamic longitudinal force applied to controlled element (lb)
X_u^*	$(1/m)(\partial X/\partial u + \cos \xi_0 \partial T/\partial u)$ (1/sec)
X_w	$(1/m)(\partial X/\partial w)$ (1/sec)

SYMBOLS (cont'd)

X_{α}	$U_0 X_w$ (ft/sec ²)
X_{δ}	$(1/m)(\partial X/\partial \delta)$ (ft/sec ² /deg)
x	Vehicle or controlled element position coordinate in the longitudinal direction, positive forward (ft)
Y	Lateral force applied to controlled element (lb)
Y_v	$(1/m)(\partial Y/\partial v)$ (1/sec)
Y_{δ}^*	$(1/mV_{T_0})(\partial Y/\partial \delta)$ (1/sec/deg)
y	Aircraft position coordinate in the lateral direction, positive to right (starboard) with respect to the ideal geometric reference glide path (ft)
y_c	Localizer beam "bends" (ft)
Z	Aerodynamic normal force applied to controlled element (lb)
Z_u^*	$(1/m)(\partial Z/\partial u - \sin \xi_0 \partial T/\partial u)$ (1/sec)
Z_w	$(1/m)(\partial Z/\partial w)$ (1/sec)
Z_{α}	$U_0 Z_w$ (ft/sec ²)
Z_{δ}	$(1/m)(\partial Z/\partial \delta)$ (ft/sec ² /deg)
z	Aircraft position coordinate in the normal direction, positive down (ft)
α	Angle of attack perturbation (deg)
β	Sideslip angle perturbation (rad)
Γ_0	Trim flight path angle (deg)
λ	Lateral flight path angle perturbation (rad)
Δ	Characteristic polynomial and transfer function denominator
δ	Actuator output (deg)
δ^*	Output of linear integration in nonlinear actuator model (deg)
δ_a	Aileron deflection angle (deg)
δ_r	Rudder deflection angle (deg)

SYMBOLS (cont'd)

δ_s	Stabilator deflection angle (deg)
δ_{sp}	Spoiler deflection angle (deg)
δ_T	Engine thrust increment in terms of equivalent throttle deflection (in $X_{\delta_T} \delta_T$ has units of lb thrust)
δ_t	Stabilator tab deflection angle (deg)
δ_{TH}	Throttle deflection (in $X_{\delta_T} \delta_{TH}$ in the steady state has units of lb thrust)
$\zeta(\cdot)$	Damping ratio for mode indicated in (\cdot) , $(-)$
θ	Pitch attitude angle (rad)
σ	Standard deviation
$\overline{\sigma}_P$	Standard deviation of input to normalized output limiter $(-)$
$\overline{\sigma}_R$	Standard deviation of input to normalized rate limiter $(-)$
$\tau(\cdot)$	Time delay associated with control point, (\cdot) (sec)
$\Phi(\omega)$	Power spectral density (units/(rad/sec))
φ	Roll angle (rad)
ψ	Yaw angle perturbation, for $\theta_0 \ll \pi/2$ is approximately heading angle (rad)
ξ_0	Thrust line inclination angle
Ω	Normalized angular frequency, $\omega/(R/P)(-)$
ω	Angular frequency (rad/sec)
ω_1	Wash-out break frequency for heading feedback (rad/sec)
ω_2	Break frequency for jet engine thrust lag in response to throttle (rad/sec)
ω_3	Break frequency for linear stabilator actuator (rad/sec)
ω_4	Break frequency for pitch rate command attenuation (rad/sec)
ω_5	Break frequency for linear spoiler actuator (rad/sec)
ω_6	Break frequency for roll command attenuation (rad/sec)
ω_N	Break frequency for the effective neuromuscular lag of pilot (rad/sec)

SYMBOLS (cont'd)

Special Notation

$(\cdot)_o$	Trim value of (\cdot)
$(\cdot)_\epsilon$	Difference measured at aircraft c.g. station
$(\cdot)_e$	Difference measured at ILS receiving antenna station
$(\cdot)^*$	Normalized variable, (\cdot)
$(\bar{\cdot})$	Normalized value of (\cdot) or average value of (\cdot) depending upon local context
$\dot{(\cdot)}$	Derivative with respect to time of (\cdot)
$(\cdot)_p$	Apparent value of (\cdot) at ILS receiving antenna station (-)
$(\cdot)_{dB}$	$20 \log_{10} (\cdot)$
$(\cdot)_c$	Commanded value of (\cdot)
DC	Value of quantity at zero frequency

SECTION I
INTRODUCTION

A. BACKGROUND

The Vietnam conflict is the first one in which the majority of the aircraft involved have had relatively complex and elaborate primary flight control systems. Operations in a hostile environment have provided the basis for both new design considerations and reevaluation of the relative weightings applied to older design practices. There have, notably, been well-documented cases of aircraft lost due to battle damage to new features of the primary flight control system. For instance, relatively insignificant ground fire has hit vital hydraulic components with consequent loss of primary controls and ultimately the aircraft, which would have otherwise suffered only minor damage. Such occurrences have focused attention on reducing vulnerability to this kind of damage and additionally on providing back-up flight control systems to minimize the consequences of this damage when it is encountered.

Airframe manufacturers have been studying both problem areas for some time and have gone a long way toward indicating what can be done for their specific aircraft. In most situations, however, these studies have been so specific as to give little appreciation for the general requirements for back-up systems. Further, there has been little or no applied research effort directed at minimum system requirements, so the manufacturers have been able to obtain little quantitative guidance from the services. Because of this state of affairs, there is an urgent need for analysis techniques and design guides for the determination of requirements for minimum back-up flight control systems.

B. PURPOSE

The analytical program reported here was coordinated with a related simulation program conducted by Honeywell, Inc. (Ref. 1). Four "minimum" back-up manual flight control system designs were the main result reported in Ref. 1. These back-up systems are "minimum" in the sense that control authorities, surface rates, hinge moments and actuator

horsepower are at the lowest levels for which the pilot can stabilize the aircraft immediately following the occurrence of certain relatively frequently encountered types of battle damage and accomplish an emergency condition landing. The Honeywell, Inc. program determined minimum levels for these control parameters empirically by means of a piloted, fixed-base simulation program. The aircraft simulated was an F-4C.

The purpose of the research program reported herein was to develop analytical techniques for determining minimum levels for the above control parameters. The analytical techniques consisted of a marriage of nonlinear system describing function analysis with pilot-vehicle analysis techniques. These analytical techniques may be applied to quickly narrow the range of minimum control parameter values which can be expected to result in minimum back-up systems having acceptable pilot-vehicle performance capabilities. By first obtaining this range, the piloted simulation effort required for the development of any particular limited authority manual flight control system can be considerably abridged. This economy results because those simulator runs which would otherwise be necessary to determine the ranges in which the minimum levels for the control parameters lie are no longer necessary. Simulator runs for confirming the analytical results and for fine tuning the pilot-vehicle system are the only ones which may be needed.

The particular cases for which the analysis technique is applied in this report correspond to the F-4C minimum back-up system configurations which were simulated in the study reported in Ref. 1. This affords maximum continuity between the two coordinated research programs.

C. THE PROBLEM AND OBJECTIVE

The concept of a minimum back-up flight control system implies severe limitations on performance with particular regard to torque or power available and the values of surface (or other) control deflection and rates available. The introduction of such limitations may make the combination of pilot, control system, and vehicle a strongly nonlinear feedback system which may display undesirable dynamic behavior atypical of a more nearly linear system. In particular, partial or complete loss

of control of the aircraft for certain inputs or initial conditions as well as potentially destructive pilot induced oscillations are likely to occur if the limitations are severe. These questions concerning system performance have been attacked in the piloted simulation effort reported in Ref. 1. The results, however, and this is particularly true of research on systems with nonlinearities, are, strictly speaking, only applicable to the particular forms of nonlinearity, their position in the system, and the types of vehicle dynamics which have been simulated. Without an analytical theory, the attempt to extrapolate the experimental results of simulation to untried conditions is often perilous.

The objective of the research reported here is to assemble just such an analytical theory which may serve as an adjunct to the design and simulation processes for these back-up systems.

D. STATE-OF-THE-ART AND APPROACH

Comparatively recent development of quasi-linear describing function models for the human pilot, (Refs. 2, 3), an improved understanding of the dynamics of aircraft in control engineering terms (Refs. 4, 5, 6), and their combination into an analytical theory of handling qualities (Refs. 7-10, among others) has allowed the prediction, correlation, and confident extrapolation of a very large number of simulator and flight test results. This process, begun under the sponsorship of the Air Force Flight Dynamics Laboratory, has been extended to applications for a variety of sponsors and projects. (See, for example, Refs. 11-13.) While the overwhelming majority of the earliest applications of the analytical theory of handling qualities involved only quasi-linear pilot models and linear systems, it was clear from the beginning that certain problems with nonlinearities in the control system or in the aerodynamics could be handled by means of describing function analysis (Refs. 14, 15). Indeed, Ref. 16 is a discussion of the analysis of a number of types of pilot induced oscillations, primarily by means of the periodic input describing functions appropriate to that class of problems, while Ref. 17 presents a random input describing function analysis of the performance of a pilot in control, in gusty air, of a VTOL vehicle with

aerodynamic hysteresis. At about the same time that these analyses were being prepared, experimental evidence began to be accumulated that, under certain circumstances, the quasi-linear pilot model derived from tracking tests with linear controlled elements could be successfully carried over to the analysis of systems containing control system nonlinearities (Refs. 18, 19). These data have very recently been augmented by a new investigation with very promising results (Ref. 20), and additional background has been accumulated on the connections between pilot opinion and the operation of nonlinearities in aircraft control systems (Ref. 21).

Therefore, an analytical treatment using mathematical models for the pilot, the nonlinear back-up control system, and the vehicle dynamics is an immediate extension of the existing technology. Because of this, new research results can be tied in with previous results, while the validity of the new models can be established by comparison with the simulation results reported in Ref. 1. At the same time, predictions of pilot opinion rating (which has often been shown to be a much more sensitive indicator of favorable or unfavorable changes in the system than any measures of performance) can be correlated with the pilot opinions delivered in connection with the Ref. 1 simulator tests.

It must be appreciated that the analytical techniques illustrated here have broader application than merely for the design of back-up flight control systems. In fact, they will be potentially useful in any closed-loop control situation wherein the control authority may be limited. The analytical techniques may be especially useful for establishing the control requirements for hovering VTOL's with high disc loading, and for landing approach control of lifting body vehicles, for example.

E. ORGANIZATION OF THE REPORT

Section II contains a more detailed statement of the limited authority flight control problem, descriptions of the analytical methods for its solution and of the F-4C back-up flight control system example to which the resulting analytical techniques are applied. A model for the rate limited integrator having a restricted output range is also developed in Section II.

Section III states the method for applying random input describing functions for system performance prediction and for selection of minimum values for control system parameters.

In Section IV, the sinusoidal input describing function for the rate limited integrator having a restricted output range is developed. This is followed in Section V by the method for application of this and other describing functions for the prediction of pilot induced oscillations and instabilities.

General conclusions and conclusions specific to the F-4C example are drawn in Section VI.

Several detailed developments and supporting data summaries which are necessary for completeness but which are peripheral to the main stream of the report are given in Appendices.

SECTION II

THE PROBLEM AND ANALYTICAL APPROACH

A. PROBLEM

Given that flight control systems are to be designed which require the smallest maximum levels of aerodynamic surface (or other) control deflection, rate or torque for given tasks and flight envelopes, find:

- A method for designing a basic linear flight control system for a particular performance level.
- Minimum values for the control parameters which will not result in significant degradation in performance over that for the basic linear flight control system design.
- A method for determining and minimizing the susceptibility of the system to pilot induced oscillations because of the low levels for the control parameters.

B. EXAMPLE APPLICATIONS

In the work which follows, a method for solving the problem posed will be presented by example. The example will involve the design of three alternative longitudinal and lateral back-up systems for the F-4C. The purpose of these back-up systems is to enable the pilot to recover control of the aircraft after sustaining battle damage which may disable the primary flight control system, and then to execute an emergency landing. This research effort is concerned only with those control parameter values set by instrument landing approach control requirements.

It is very unlikely that all control parameter requirements will be set by the manual instrument landing approach task. This qualification must be borne in mind when considering the results of this report, so that one is not deluded into believing that the minimum levels determined by analysis here are necessarily adequate for the recovery transient, for example, or for large maneuvers in this or other flight regimes.

The details of the dynamic description of the standard F-4C (before battle damage, and unmodified for back-up flight control system capability) are given in Appendix I. The data there are for the bare airframe in a clean configuration except for landing gear extension. (Flaps are assumed disabled by hydraulic system damage.) Included in Appendix I are dimensional stability derivatives, geometrical, moment of inertia and pertinent trim data. Longitudinal and lateral transfer functions are also given as is a description of the assumed instrument landing system geometry. Normal and side gust models of the atmospheric turbulence, and a model of the instrument landing system "beam bends" complete the description of the assumed disturbance environment for the manual landing approach task.

The three back-up flight control systems configurations considered are designated Systems A, B and C.

TABLE I
LONGITUDINAL BACK-UP SYSTEMS

<u>System</u>	<u>Limits Resulting from Ref. 1 Simulation Program</u>	<u>Description</u>
A	$ \delta_s \leq 1.5 \text{ deg}$ $ \dot{\delta}_s \leq 1.0 \text{ deg/sec}$ $HP \leq 0.1 \text{ (instantaneous)}$ $ F_{SL} \leq 45 \text{ lb}$	Back-up power supply and redundant actuator for pitch control. Simple spring feel system.
B	$ \delta_t \leq 2.5 \text{ deg}$ $ F_{SL} \leq 85 \text{ lb}$	Manually powered pitch control via 30% tab on stabilator which, with the stabilator locked in trimmed position, is used as an elevator.
C	Same as Back-Up System B	

TABLE II

LATERAL-DIRECTIONAL BACK-UP SYSTEMS

<u>System</u>	<u>Limits Resulting from Ref. 1 Simulation Program</u>	<u>Description</u>
A	$\delta_a \equiv 0 \text{ deg}$ $ \delta_{sp} \leq 10 \text{ deg}$ $ \dot{\delta}_{sp} \leq 15 \text{ deg/sec}$ $ \delta_r \leq 7 \text{ deg}$ $ F_{SLD} \leq 25 \text{ lb}$ $ F_{PR} \leq 300 \text{ lb}$	Back-up power supply and redundant actuators for roll control via spoilers only. Simple spring feel system. Manually powered rudder for yaw control.
B	$\delta_a \equiv 0 \text{ deg}$ $ \delta_{sp}^{(1)} \leq 10 \text{ deg} *$ $ \delta_r \leq 7 \text{ deg}$ $ F_{SLD} \leq 60 \text{ lb}$ $ F_{PR} \leq 300 \text{ lb}$	Manually powered roll control via spoilers redesigned to have 2/3 of the effectiveness and hinge moment of existing design. Manually powered rudder for yaw control. Ailerons not used.
C	$\delta_{sp} \equiv 0 \text{ deg}$ $ \delta_a^{(2)} \leq 10 \text{ deg} *$ $ \delta_r^{(3)} \leq 7 \text{ deg} *$ $ F_{SLD} \leq 60 \text{ lb}$ $ F_{PR} \leq 100 \text{ lb}$	Manually powered roll control via ailerons redesigned to have balanced hinges and tabs. Manually powered rudder using tab. Spoilers not used.

*Superscripted control variables indicate that certain modifications to the basic aircraft have been made. These modifications result in the modified stability derivatives given in the footnotes of Table XXII.

The descriptions of back-up system modifications for longitudinal control are given in Table I, and those for lateral control in Table II.

Certain quantitative data are needed to complete the descriptions of the back-up systems. These are listed below.

TABLE III

QUANTITATIVE DATA FOR BACK-UP SYSTEMS

Longitudinal Systems

System A

$$F_{SL} = 7.5 S_L \quad (\text{lb})$$

$$S_L = -0.3 \delta_s^* \quad (\text{in})$$

Systems B and C

For pitch control by means of the 30% stabilator tab, δ_t , the following control effectiveness derivatives are used.

$$X_{\delta_t} = 2/3 X_{\delta_s} \quad (\text{ft/sec}^2/\text{deg})$$

$$Z_{\delta_t} = 2/3 Z_{\delta_s} \quad (\text{ft/sec}^2/\text{deg})$$

$$M_{\delta_t} = 2/3 M_{\delta_s} \quad (\text{rad/sec}^2/\text{deg})$$

$$F_{SL} = 14.25 S_L \quad (\text{lb})$$

$$S_L = -2.78 \delta_t \dagger \quad (\text{in})$$

Lateral Systems

System A

$$F_{SLD} = 6.25 S_{LD} \quad (\text{lb})$$

$$S_{LD} = -0.0855 \delta_{sp}^* \quad (\text{in})$$

$$F_{PR} = 39.6 \delta_r + 15.6 \beta \ddagger \quad (\text{lb})$$

$$P_R = -0.0877 \delta_r^* \quad (\text{in})$$

System B

For roll control, the spoiler control effectiveness derivatives are 2/3 of the values given in Table XXII, Appendix I.

$$F_{SLD} = 25.0 S_{LD} \quad (\text{lb})$$

$$S_{LD} = -0.0855 \delta_{sp}^* \quad (\text{in})$$

$$F_{PR} = 39.6 \delta_r + 15.6 \beta \ddagger \quad (\text{lb})$$

$$P_R = -0.0877 \delta_r^* \quad (\text{in})$$

(continued)

TABLE III(cont'd)

QUANTITATIVE DATA FOR BACK-UP SYSTEMS

System C

$$F_{SLD} = 15.0 S_{LD} \quad (1b)$$

$$S_{LD} = -0.125 \delta_a^* \quad (in)$$

$$F_{PR} = 13.2 \delta_r + 5.20 \beta^\# \quad (1b)$$

$$P_R = -0.0877 \delta_r^* \quad (in)$$

*Gearing constant assumed to be that for undamaged system given in Ref. 1 in absence of information to the contrary.

†Gearing constant inferred from mean-square data in Ref. 1.

‡ $\delta(\cdot)$ has units of degrees of (\cdot); β is in degrees.

C. ANALYTICAL APPROACH

The analytical approach to solution of this problem consists of three major steps. These steps are:

- Synthesis of a linear pilot-vehicle-flight control system which achieves the minimum acceptable performance level with the least stringent control requirements.
- Selection of minimum control parameter values such as deflection limits, rate limits, etc., and verification that the selected values do not influence the system performance in a significant way.
- Estimation of the susceptibility of the pilot-vehicle-flight control system combination to pilot induced oscillations and possible instabilities for the selected values of the control parameters.

Consider each of the three major steps listed above with respect to the analytical techniques which they involve.

Synthesis of the linear pilot-vehicle-flight control system for a specific minimum performance capability provides the basic system design. This basic design is elaborated in the subsequent steps in such a way

that important nonlinear effects are adequately represented in the system performance analysis.

Initial data required are specification of the aircraft dynamics, the form of the flight control system, and the minimum level of performance. A linearized perturbation description of the aircraft plus the trim values of the control deflections is adequate. The "form of the flight control system" consists of a designation of the control points and motion quantities which are explicitly or implicitly available to the pilot. The minimum level of performance may be specified in terms of maximum root-mean-square (RMS) error tolerable in following the guidance commands or alternatively in terms of a desired bandwidth for closed-loop system in response to guidance commands, and so forth. For the examples to be treated here, the linearized perturbation description of the aircraft is expressed in terms of transfer functions in Tables XXV and XXVI of Appendix I. The only nonzero trim value for a control deflection is for the stabilator, $\delta_{S_0} = -2.815$ deg, (See Table XXII). The control inputs available to the pilot are: stabilator, δ_S , or stabilator tab, δ_t ; throttle, δ_T ; spoilers, δ_{Sp} , or ailerons, δ_a ; and rudder, δ_r . The pilot displays include airspeed, $(V_{T_0} + u_{AS})$; attitude indicator, θ and ϕ ; angle of attack, α ; altitude, h ; sink rate, $-\dot{h}$; radio magnetic indicator, ψ ; glide slope bar, d_e/R ; and localizer bar, $y_e/(R+R_{RWY})$. In addition engine performance instruments and flight director instruments were also available. (The engine instruments are not primary flight instruments, the flight director mechanization equations are not available from Ref. 1. Since all the flight director information is available from other instruments, this omission is not necessarily crucial for the purposes of this analysis.)

The desired level of performance is specified by the closed-loop bandwidths desired for tracking the glide slope and localizer beams. The desired closed-loop bandwidth in each case is 0.30 rad/sec.

These data are used along with the quasi-linear describing function for the human pilot, (Refs. 2 and 3) to arrive at a complete linear description of the pilot-vehicle system. The appropriate system organization, i.e., the association of display information with each control,

and selection of the human pilot describing function parameters are accomplished by applying the analytical theory of handling qualities. (Refs. 7, 8, 9 and 10 for example.) The literature on the analytical theory of handling qualities has now reached a mature state. Because of this, this particular step is regarded as within the state-of-the-art, and therefore detailed consideration of this matter has been relegated to Appendix II.

Equally important to the methods for quantitative pilot-vehicle analysis are the qualitative methods for estimating pilot opinion rating. Pilot opinion rating estimates are formed based on the equalization which the pilot must supply and upon the quality of system performance which can be attained. Pilot opinion assumes an important role because it is usually a considerably more sensitive indicator of system acceptability than are numerical measures of system performance such as root-mean-square error. This is because the pilot can and does introduce equalization as the dynamics of his control task deteriorate. Often the pilot does this in such a way that there is little or no deterioration in the level of system performance. It does require more effort on the part of the pilot, however, because of the additional equalization. This additional effort is reflected by an appropriate degradation in his opinion rating. For minimum back-up flight control system design, it might be argued that any minimum system which is flyable and landable will be adequate. However, this is not necessarily a proper view because other back-up system configurations of similar complexity, cost and weight may result in more favorable pilot opinion even though the system performance levels are comparable. In such a case, more favorable pilot opinion is roughly equivalent to an increased capability to perform other tasks or to cope with additional emergencies. This increased capability will further enhance the survivability of both pilot and aircraft.

Another way in which pilot opinion is important for this study is that it provides a valuable tie-in between the analytical work here and the piloted simulator results reported in Ref. 1. This is because it is often possible to determine qualitative discrepancies between the piloting technique assumed in the analysis and that actually used by the pilots in the experiments by comparison of predicted and actual pilot opinions.

The second major step, selection of minimum control parameter values and verification of performance, is accomplished in the following way. First, all the nonlinearities in the system are modelled in terms of simple nonlinearities (i.e., the saturation, dead zone, etc.) for which the random input describing functions are known or easily calculated. (See Refs. 14 or 15 for example.) In certain cases, it will be necessary to construct the models of the nonlinear effects using combinations of linear dynamic elements and the simple nonlinearities. This is necessary in the case of mechanical hysteresis (Refer to Ref. 22, for example) or in the case of the rate limited integrator having a restricted output range which is important in the minimum back-up system design problem considered here. Next, the variances of the inputs to the nonlinear elements are calculated assuming that the characteristic parameter of the nonlinearity is at the limiting value which renders the nonlinear element linear. The variances of these inputs can be determined using the linear system model of the first step. A trial selection of a permissible value for the characteristic parameter of the nonlinearity can be based upon the magnitude of the input signal variance. The relationship between the input variance and the characteristic parameter of the nonlinearity is established by the random input describing function for the nonlinear element. (Refs. 14 and 15) For the simple nonlinearities, the random input describing function is an equivalent gain which is a function of the input variance and the characteristic parameter of the nonlinearity.

One proceeds by selecting the maximum (or minimum) value of the parameter which will not cause more than a negligible change in the equivalent gain of the nonlinear element in comparison to the equivalent gain value for linear behavior.

An example at this point will help make matters more clear. Consider a hard limiter type of nonlinearity having a gain, G , in the linear region and have the saturation level, S . Figure 1 shows equivalent representations of this limiter. The equivalent gain or random input describing function for the normalized limiter is given in Fig. 2. If σ is the root-mean-square value of the zero-mean Gaussian input signal to the actual limiter, then

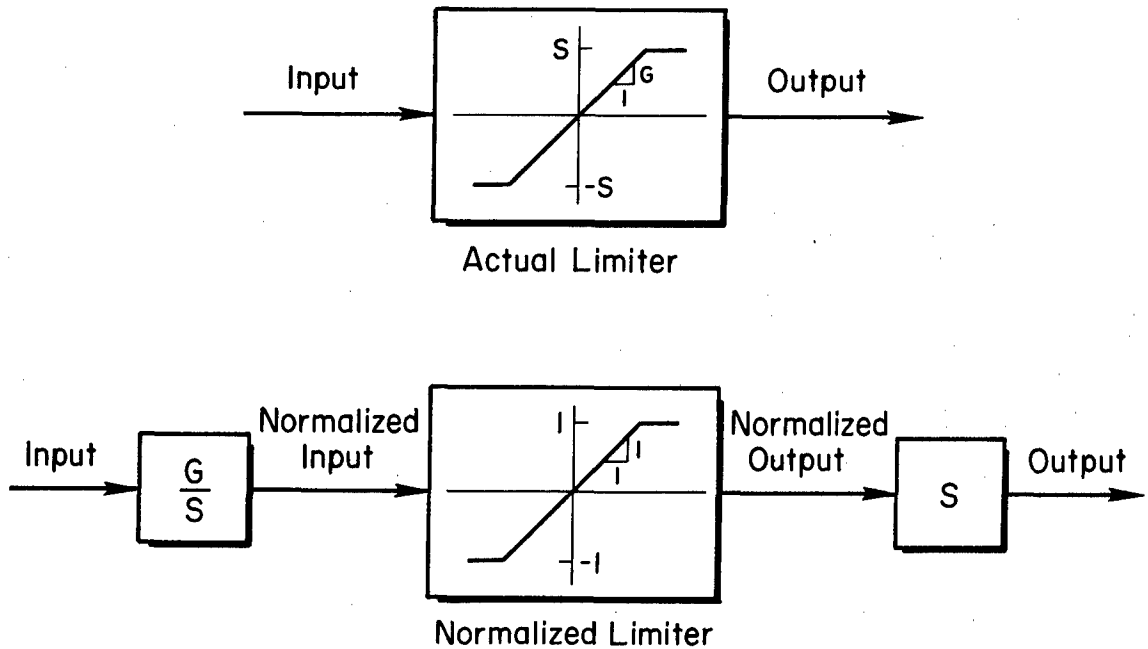


Figure 1. Equivalent Representations of a Limiter

$\bar{\sigma} = \sigma G/S$ is the root-mean-square value of the normalized input to the normalized limiter in Fig. 3. The normalized limiter characteristic is approximated by its equivalent gain, K_{eq} , which is given as a function of $\bar{\sigma}$ in Fig. 2. The random input describing function for the limiter which results is shown in Fig. 3.

In absence of nonlinear effects, S is infinite. This means $\bar{\sigma} = 0$ and $K_{eq} = 1$. It is clear from Fig. 2 that $1.0 \geq K_{eq} > 0.954$ for $0 \leq \bar{\sigma} \leq 0.5$, and that $1.0 \geq K_{eq} > 0.997$ for $0 \leq \bar{\sigma} \leq 0.33$.

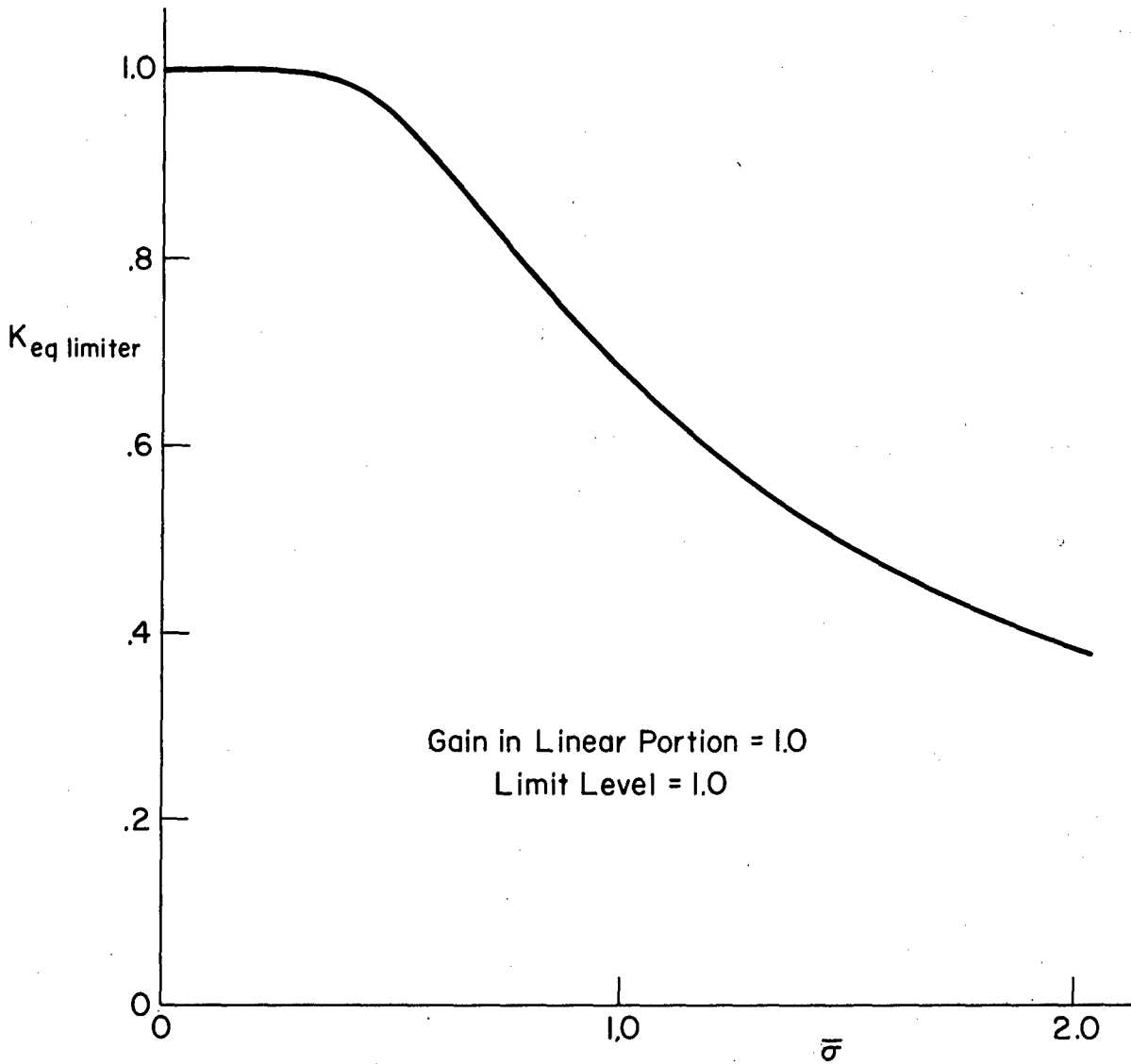


Figure 2. Random Input Describing Function for Normalized Limiter

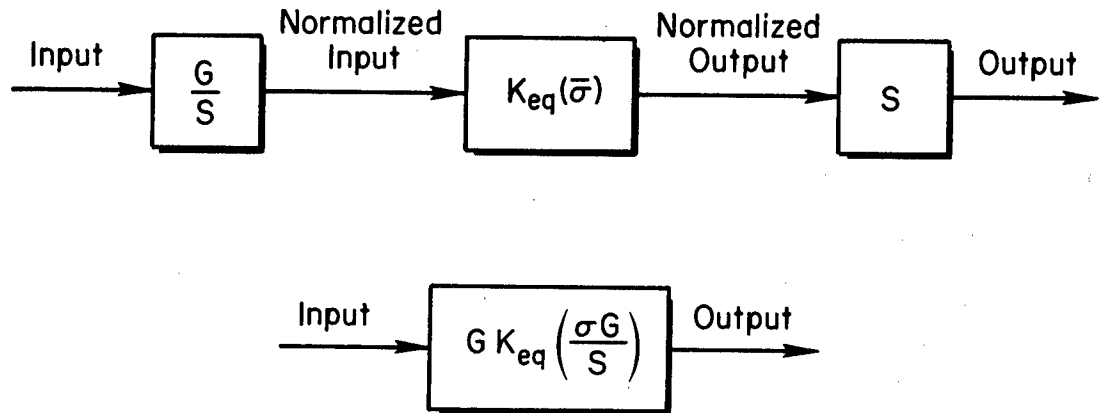


Figure 3. Equivalent Random Input Describing Function Representations for a Limiter

Arbitrarily* designate $0 \leq \bar{\sigma} \leq 0.33$ as defining the range for $\bar{\sigma}$ which causes "no more than a negligible change in the equivalent gain in comparison to the equivalent gain value for linear behavior," $K_{eq} = 1$. Then the "minimum value" of the control parameter, S/G (based upon the

*It is clear that $0 < \bar{\sigma} \leq 0.5$ would result in less than a 5% reduction in gain from the value for linear behavior. Often this is acceptable. In fact, it is considered good engineering practice to size component ranges, capacities, etc., by choosing the maximum $\bar{\sigma}$ such that $0.33 \leq \bar{\sigma}_{max} \leq 0.5$. This choice results in the limit level being encountered less than 5% of the time for the larger value, and less than 0.3% of the time for the smaller value.

above criterion) is

$$\frac{S}{G} = \frac{\sigma}{0.33} \quad (1)$$

The next matter to be considered is that of system performance verification using the trial "minimum value" for characteristic parameter of the nonlinearity. If the nonlinearity enters the system structure in an open-loop way, this is merely a matter of replacing the normalized nonlinearity by its equivalent gain and performing the necessary calculations of root-mean-square value of the variables of interest.

More often the nonlinear element is part of a closed-loop system which may contain still other nonlinear elements. Applications under these circumstances require further explanation. Consider first one nonlinearity in a closed loop. In this case, the input variance to the equivalent gain representation of the normalized nonlinear element will be a function of that equivalent gain. This complicates the matter of determining the equivalent gain value. Solution requires simultaneous satisfaction of both the system equation expressing the root-mean-square value of the input to the normalized nonlinearity as a function of the equivalent gain and the random input describing function equation expressing the equivalent gain for the normalized nonlinearity as a function of the root-mean-square value of the input. Direct algebraic solution is usually out of the question because the equations are very complicated functions of their independent variables. Numerical solution is one alternative, but a graphical method of solution will be discussed here because it makes the matter clear.

The random input describing function equation for the limiter is available as a graph in Fig. 2. The equivalent gain, K_{eq} , may be regarded as the independent variable. A similar graph can be constructed for the system. This would plot $\bar{\sigma}$ as a function of K_{eq} . If these two plots were overlaid, the intersection of the two curves gives the values for K_{eq} and $\bar{\sigma}$ which simultaneously satisfy the two equations. To verify

that the performance of the nonlinear system is not degraded to an unacceptable extent in comparison with the basic linear system performance, the solution value of K_{eq} is used to recompute the root-mean-square value of the variables of interest for the nonlinear system.

When two or more nonlinearities are present, the solution is more complicated but the concepts used to arrive at the solution are the same. Consider the case wherein two nonlinearities are contained in closed loops. Here, two system equations and two random input describing function equations must be simultaneously satisfied. The two system equations express the root-mean-square value of the input to the equivalent gain representations for each nonlinearity as a function of both equivalent gains. That is:

$$\bar{\sigma}_1 = \bar{\sigma}_1(K_{eq1}, K_{eq2}) \quad (2)$$

$$\bar{\sigma}_2 = \bar{\sigma}_2(K_{eq1}, K_{eq2}) \quad (3)$$

The two random input describing function equations each describe one nonlinearity in the manner discussed earlier. Graphical solution of this problem is still reasonable. One proceeds by holding one equivalent gain, say K_{eq2} , constant and plotting the system equation for $\bar{\sigma}_1$ as a function K_{eq1} . This is repeated for several constant values of K_{eq2} . For each constant value of K_{eq2} , an intersection with the random input describing function curve for the first nonlinearity results. Next, the values of $\bar{\sigma}_2$ are computed for the K_{eq1} value at each intersection using the corresponding constant value of K_{eq2} . The resulting data can be used to plot $\bar{\sigma}_2$ versus K_{eq2} as a curve along which K_{eq1} is a parameter. If this curve is overlaid on the random input describing function curve for the second nonlinearity, the intersection of the curves will identify the values of K_{eq1} and K_{eq2} which simultaneously satisfy all four equations.

While it is possible to perform the many computations required for evaluating Eqs. 2 and 3 by hand, efficiency actually dictates machine aided computation of these quantities. When more than two nonlinearities are

involved in closed loops, numerical solution of the system and random input describing function equations on a digital computer is a virtual necessity. For less than five nonlinear elements numerical solution can be quite rapid.

Performance verification is accomplished in the same way as for the single nonlinear element-in-closed-loop case.

The third major step is evaluation of the susceptibility of the pilot-vehicle-flight control system combination to pilot induced oscillations and instabilities. Pilot induced oscillations and instabilities may arise because of one or more conditions. These conditions are:

- Linear instability or neutral stability (Ref. 16)
- Stable limit cycle because of nonlinearity (Ref. 16)
- Oscillatory divergence because of nonlinearity (initial conditions outside of unstable limit cycle boundary)

The first condition is the result of the pilot-vehicle-flight control system combination having an inappropriate structure or gain values for the existing aircraft configuration and flight condition. No nonlinear effects are involved. Pilot induced oscillations because of this reason are often the result of stability augmentation system failures and improper or lack of pilot accommodation to the failure. Linear servo analysis theory can be applied to determine the existence of this condition.

The second condition is the result of unavoidable or intentional nonlinearities such as friction, dead zones and preload in the control system. Control deflection rate limits and control deflection limits are further examples of this type of nonlinearity. Such nonlinearities are the main concern of this study. They may give rise to a pilot induced oscillation which is a neutrally stable oscillation. Sinusoidal input describing function theory may be applied to determine if a neutrally stable oscillation may be sustained, and if so, its amplitude and frequency (Refs. 14 and 15). While the sinusoidal describing function theory can be applied easily for most problems of interest here, it nevertheless is an approximate technique and so the results are approximate

as well. The pilot induced oscillations are the stable limit cycles indicated by the sinusoidal input describing function analysis.

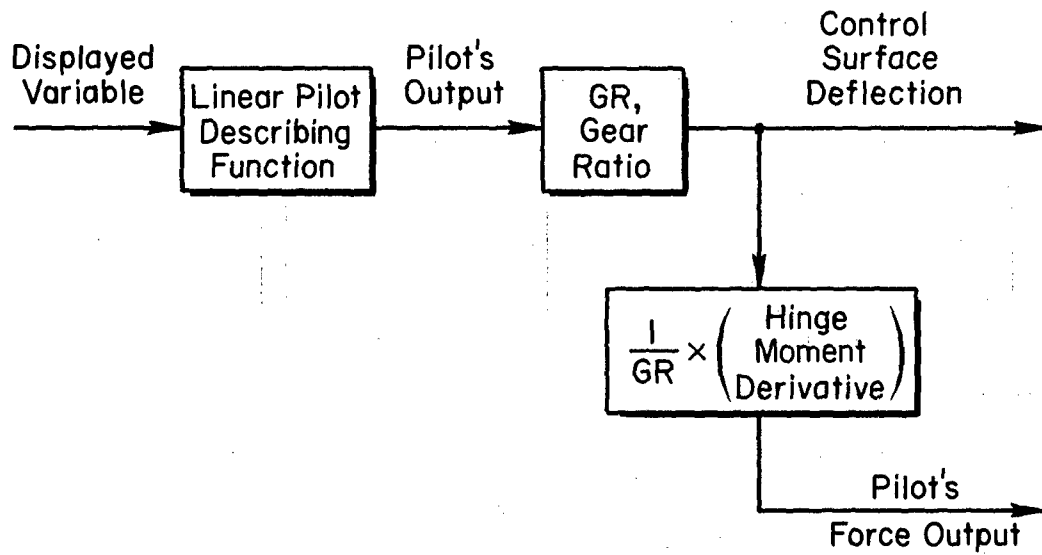
The third condition is also the result of unavoidable or intentional nonlinearities. However, this condition may lead to pilot induced instability. The second condition, above, is usually the result of synchronous behavior on the part of the pilot, and, in this respect, it is distinctly different from the third condition. The third condition may be the result of attempting large maneuvers with very limited control authority. The instability occurs when the state vector at some time passes out of the stable region of the state space for the particular system involved. Exact determination of this stable region in general is not possible for most of the problems of interest in aircraft flight control. However, the sinusoidal input describing function can be of some small help in estimating the size characteristics of maneuvers which may lead to unstable oscillations. This estimate is based upon the parameters which characterize the unstable limit cycle solutions for the system.

D. NONLINEARITIES

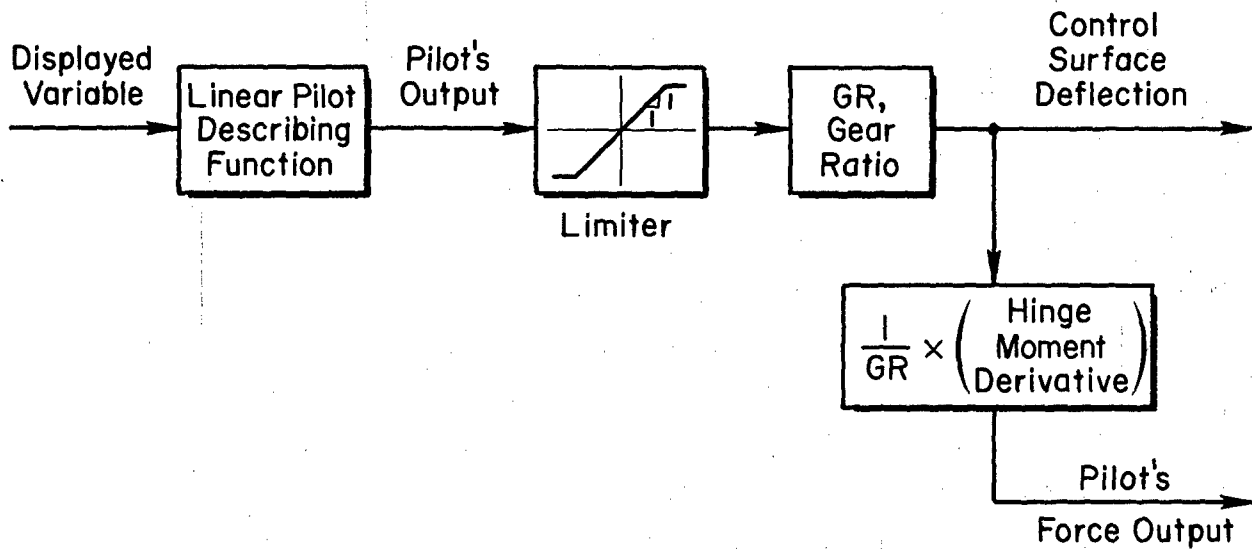
The three minimum back-up flight control system configurations contain two different types of nonlinearities of importance. These are:

- Direct manual control authority limits determined by pilot strength or by control surface travel stops.
- Actuator rate and displacement limits for a fully-powered manual control system.

The first nonlinear effect is modelled by a limiter characteristic which is inserted between the pilot's output and the control surface deflection. The effect is modelled in this way because the pilot's force output is nearly linearly proportional to control surface deflection. While it has not been established that the limiter reflects, in an accurate way, pilot strength limits upon the force developed on his control manipulator, it is clear that the proper qualitative relationship exists. In the absence of a more definitive description, it is necessary to use the above model. The distinction between linear and nonlinear systems, in this respect, is shown by the block diagram in Fig. 4.



a) Linear Direct Manual Control System Model



b) Nonlinear Direct Manual Control System Model

Figure 4. Block Diagrams for Direct Manual Control Surface Actuation

The maximum force levels which are assumed in this study for the longitudinal stick, lateral stick and pedal pilot output modalities are 100 lb, 85 lb and 300 lb, respectively.

It is clear that Fig. 4 can also represent the effect of control surface travel stops insofar as the relationships among the displayed variable, pilot's output and control surface deflection are concerned. However, the pilot's force output is not correctly represented when the travel limits are encountered.

For the three example back-up systems, the control surface travel stops set the deflection limit levels in all cases but one in the landing approach condition. The one exception, longitudinal control by means of a stabilator tab for Systems B and C, is configured in such a way that the control surface travel stops are reached simultaneously with the presumed maximum longitudinal stick force the pilot can develop. In effect, then, all control deflection limits will result from the travel stops in these examples.

The second type of nonlinear effect, actuator rate and deflection limiting in a fully-powered manual control system, requires a more complex model. The key item in the model is the rate limited integrator having a restricted output range. (Henceforth, this is referred to as the limiting integrator for brevity.) The limiting integrator models the power element of the hydraulic actuator. The rate limit arises from the maximum flow limit of the hydraulic valve and the output range limit arises because of the limited stroke length of the power element. This analysis neglects the variation of the hydraulic valve maximum flow limit with (load) pressure. In order for the power element to be a useful positioning actuator, there must be a unity gain feedback of output position, forward-loop amplification and perhaps equalization. It will be assumed here that the feedback and feedforward functions are linear. Furthermore, it will be assumed that the feedforward function is a pure gain, K . (This assumption is not necessary for the analysis techniques that will be used. It is made here for consistency with the actuator description in Ref. 1) If the power element is represented in such a way that the input and output units are the same except for the integration,

then K is the small signal open-loop gain of the actuator. K is also equal to the small signal bandwidth of the actuator. The complete nonlinear actuator model is shown in Fig. 5. The unity gain feedback and pure gain feedforward functions discussed above are evident in the figure. The limiting integrator model of the power element requires additional explanation.

The effect of the flow rate limiting is represented by the path from e^* to a . The flow rate limit limits the output rate to not more than R (units/sec). The output or deflection limit is P (units). When the power element reaches the output range limit, $\pm P$, the output rate, $\dot{\delta}$, must go to zero. This is ensured by the feedback through the enforcement gain, k . In principle, the enforcement should be infinite, but as a practical matter any value which is numerically much greater than the largest system break frequency is adequate. Notice that the enforcement loop is a negative feedback loop around the integrator when $|\delta^*| > P$. Then, a and $\dot{\delta}$ are related by the transfer function:

$$\frac{\dot{\delta}}{a} = \frac{s}{s + k} \quad (4)$$

This makes it clear that $\dot{\delta}$ will go to zero for $|\delta^*| > P$ in the limit as k becomes infinite. For large but finite values of k , $\dot{\delta}$ will become zero very quickly after $|\delta^*| > P$.

The nonlinear actuator model in Fig. 5 will be used in the description of the fully-powered back-up system, System A. When the performance calculations are made, the random input describing function for the normalized limiter will replace each of the normalized limiters in Fig. 5. For this analysis, large values of the enforcement gain, k , will be used. When the pilot induced oscillation investigation is made, the enforcement gain will be infinite and a sinusoidal describing function will be derived for the limiting integrator. The remaining linear feedback and feedforward portions of the actuator model can be lumped with the other linear elements of the pilot-vehicle-flight control

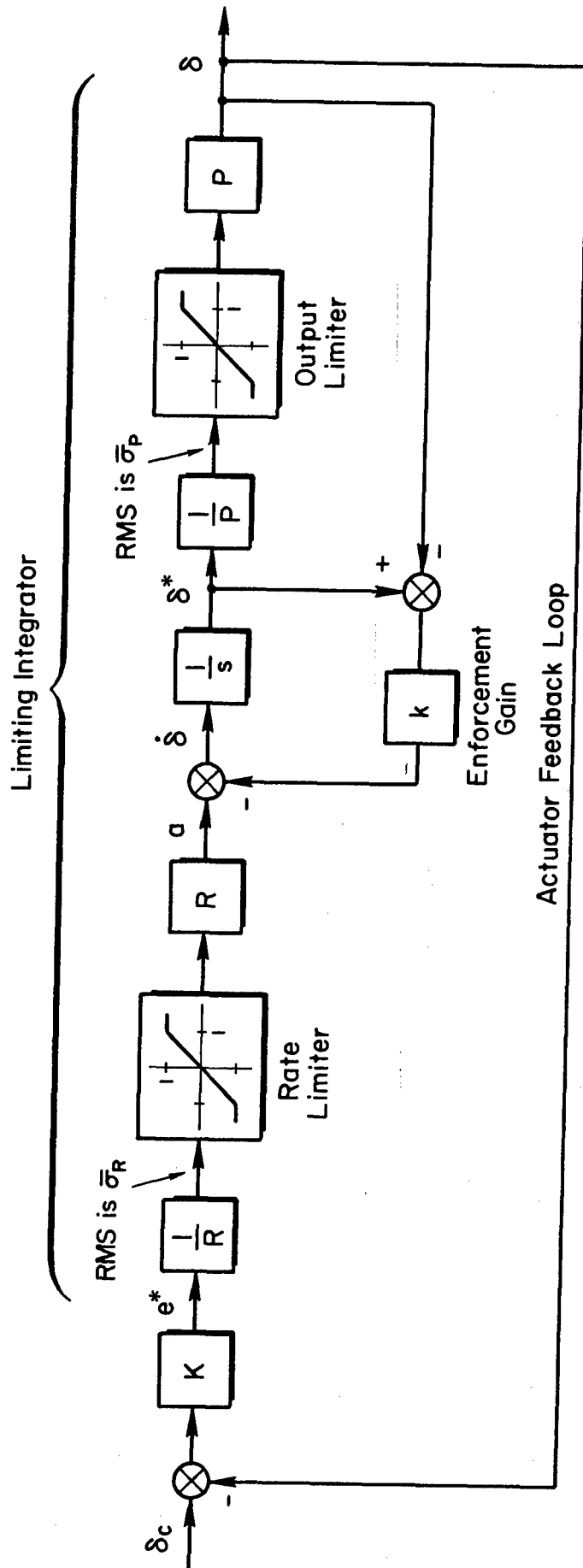


Figure 5. Deflection and Rate Limiting Actuator Model

system model, and the sinusoidal describing function analysis carried out in the usual manner (e.g. Ref. 14).

The next three Sections of the report are concerned with the execution of the analytical approach discussed above for the three F-4C minimum back-up flight control system examples.

SECTION III

MINIMUM CONTROL PARAMETER VALUE SELECTION AND SYSTEM PERFORMANCE PREDICTION

Initial selections of the minimum control parameter values are based upon the linear pilot-vehicle-flight control system analyses carried out in detail for the F-4C back-up System A. (Since back-up systems A, B and C are substantially similar, it is not necessary to perform a detailed linear analysis for each one.) The highlights of the linear back-up System A analysis are summarized below.

A. LONGITUDINAL CONTROL

For longitudinal control of the F-4C, the following feedbacks are necessary. Airspeed error must be fed back to throttle because the trim approach speed is below the minimum power trim airspeed. Feedback of pitch rate to stabilator is required to augment short period damping. Pitch attitude feedback to stabilator provides flight path damping for tracking the reference glide slope. (This is because $\dot{d} \doteq V_{T_0} \theta$.) Finally, deviation with respect to the glide slope reference is compensated by an integral by-pass and fed to stabilator. This provides the "outer" or guidance loop suitable for tracking the glide slope even with wind disturbance inputs. (The integration in the integral by-pass is presumed to be the result of the pilot's use of the pitch trim button.)

A block diagram for the linear longitudinal System A design is shown in Fig. 6.* Notice that actuation dynamics and lag equalization for attenuating the high frequency pitch rate commands are included here.

*A special notation is used in this figure which deserves explanation. First order polynomial factors such as $(s + \omega_1)$ are represented by (ω_1) for compactness. Thus, in particular, $1/(0)$ represents an integrator, while the quadratic factor $(s^2 + 2\zeta\omega_n s + \omega_n^2)$ is represented by the symbol $[\zeta, \omega_n]$. This notation will be used routinely throughout the remainder of the report.

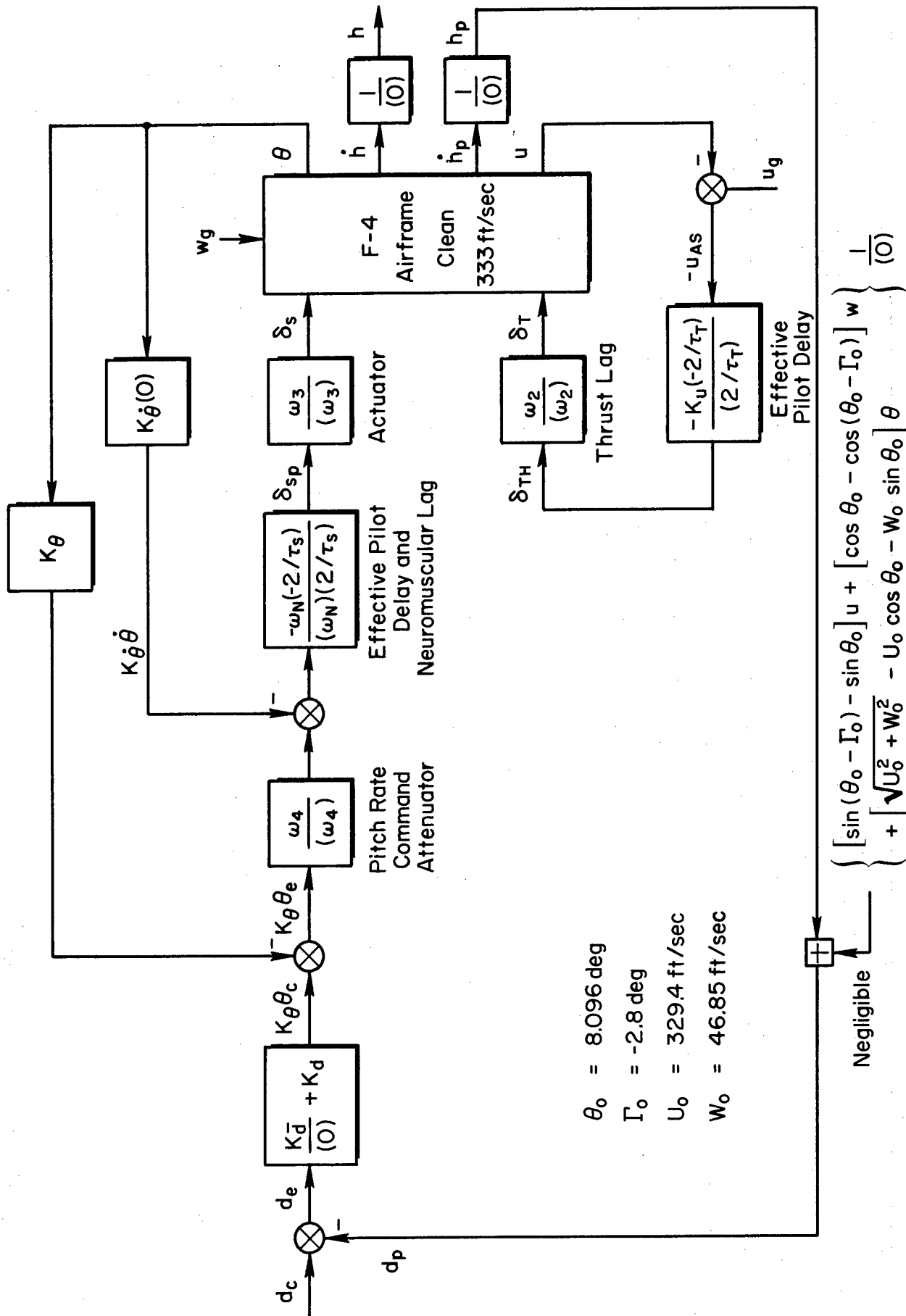


Figure 6. Longitudinal F-4C Block Diagram for System A

The values of the pilot loop gains and equalization break frequencies for System A are given in Table IV. The closures represented here lead to a closed-loop system bandwidth in tracking the glide slope reference of 0.27 rad/sec. The closed-loop root-mean-square performance for linear System A is given in Table V. This table lists the root-mean-square values of the several variables of interest in response to the ILS beam bends and normal gust disturbances.

TABLE IV
PARAMETERS FOR LINEAR PILOT LOOP CLOSURES,
SYSTEM A, LONGITUDINAL

$K_u m X_{\delta_T}$	59.7	lb/(ft/sec)
τ_T	0.33	sec
ω_2	0.50	rad/sec
K_{θ}	-0.244	sec
ω_N	10.0	rad/sec
τ_s	0.2	sec
ω_3	10.0	rad/sec
K_{θ}	-0.393	--
ω_4	2.25	rad/sec
$K_{\dot{d}}$	-0.0015	deg/(ft/sec)
$K_{\ddot{d}}$	-0.03	deg/ft

TABLE V

RMS RESPONSES TO ILS BEAM BENDS AND
NORMAL GUSTS FOR LINEAR LONGITUDINAL SYSTEM A

<u>VARIABLE</u>	<u>RMS RESPONSE</u>		
	<u>ILS Bends</u>	<u>Normal Gusts</u>	<u>Total</u>
Glide slope deviation	3.40	8.79	9.42 ft
Pitch attitude	0.212	0.790	0.82 deg
Pitch rate	0.135	1.318	1.32 deg/sec
Stabilator angle	0.042	0.266	0.270 deg
Stabilator rate	0.061	0.845	0.847 deg/sec
Throttle in equivalent thrust	22.0	143.0	144.0 lb
Airspeed error	0.366	2.38	2.41 ft/sec

The longitudinal portions of Systems B and C are identical, and are, dynamically speaking, similar to System A. The main differences are that Systems B and C are manually powered. This eliminates the actuator dynamics, and the use of a stabilator tab as an elevator (instead of moving the entire stabilator) reduces the control effectiveness derivatives to $2/3$ of their former values. Thus these changes may be represented as shown in Fig. 7.

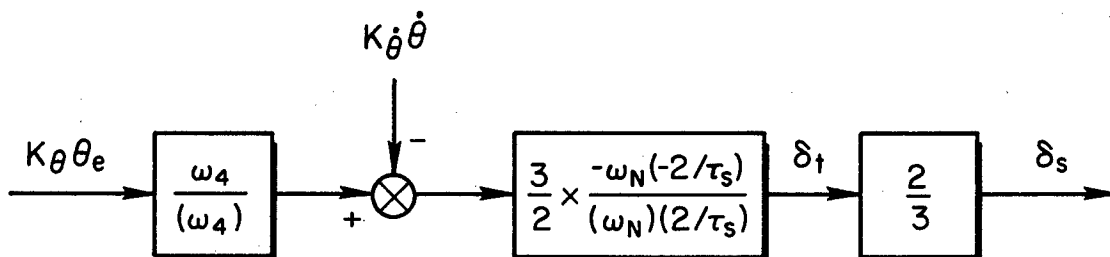


Figure 7. Block Diagram Changes for Pitch Control
by Means of Stabilator Tab

The values of the pilot's loop gains and equalization break frequencies for Systems B and C are the same as for System A (Table IV) except that the actuator break frequency is not relevant.

The root-mean-square values for the Systems B and C variables are, therefore, nearly the same as for System A except for the root-mean-square tab deflection and tab rate. The root-mean-square tab deflection is approximately 1.5 times the root-mean-square stabilator deflection for System A and the root-mean-square tab rate is approximately 1.5 times the root-mean-square stabilator rate for System A. The actual root-mean-square values for linear Systems B and C are given in Table VI.

TABLE VI

RMS RESPONSES TO ILS BEAM BENDS AND
NORMAL GUSTS FOR LINEAR LONGITUDINAL
SYSTEMS B AND C

<u>VARIABLE</u>	<u>RMS RESPONSE</u>		
	<u>ILS Bends</u>	<u>Normal Gusts</u>	<u>Total</u>
Glide slope deviation	3.37	8.70	9.33 ft
Pitch attitude	0.206	0.740	0.768 deg
Pitch rate	0.126	1.23	1.24 deg/sec
Stabilator tab angle	0.0603	0.394	0.399 deg
Stabilator tab rate	0.0900	2.05	2.05 deg/sec
Throttle in equivalent thrust	21.7	142.0	144.0 lb
Airspeed error	0.361	2.37	2.39 ft/sec
Longitudinal stick force	2.39	15.6	15.8 lb
Longitudinal stick displacement	0.168	1.10	1.11 in.

B. LATERAL CONTROL

For lateral-directional control of the F-4C, the following feedbacks are necessary. Roll attitude feedback to spoilers is required for roll stabilization. Feedback of washed-out heading to spoilers provides flight path damping for tracking the localizer reference. (This is because $\dot{y} = V_{T_0} \psi$.) Finally, lateral displacement with respect to the localizer is fed to the spoilers. This provides the "outer" or guidance loop. The following control paths may be useful but are not necessary. Feedback of roll rate to spoilers may be used to increase roll damping, and spoiler-to-rudder crossfeed may be useful in adjusting the ω_ϕ/ω_d ratio so that maximum closed-loop dutch roll damping will result.

A block diagram for the linear lateral System A design is shown in Fig. 8. Notice that actuation dynamics and lag equalization for attenuating the high frequency roll attitude commands are included.

The values for the pilot loop gains and break frequencies for lateral System A are given in Table VII. The closed-loop root-mean-square performance for this system is given in Table VIII. These closures lead to a closed-loop system bandwidth in tracking the localizer reference of 0.247 rad/sec.

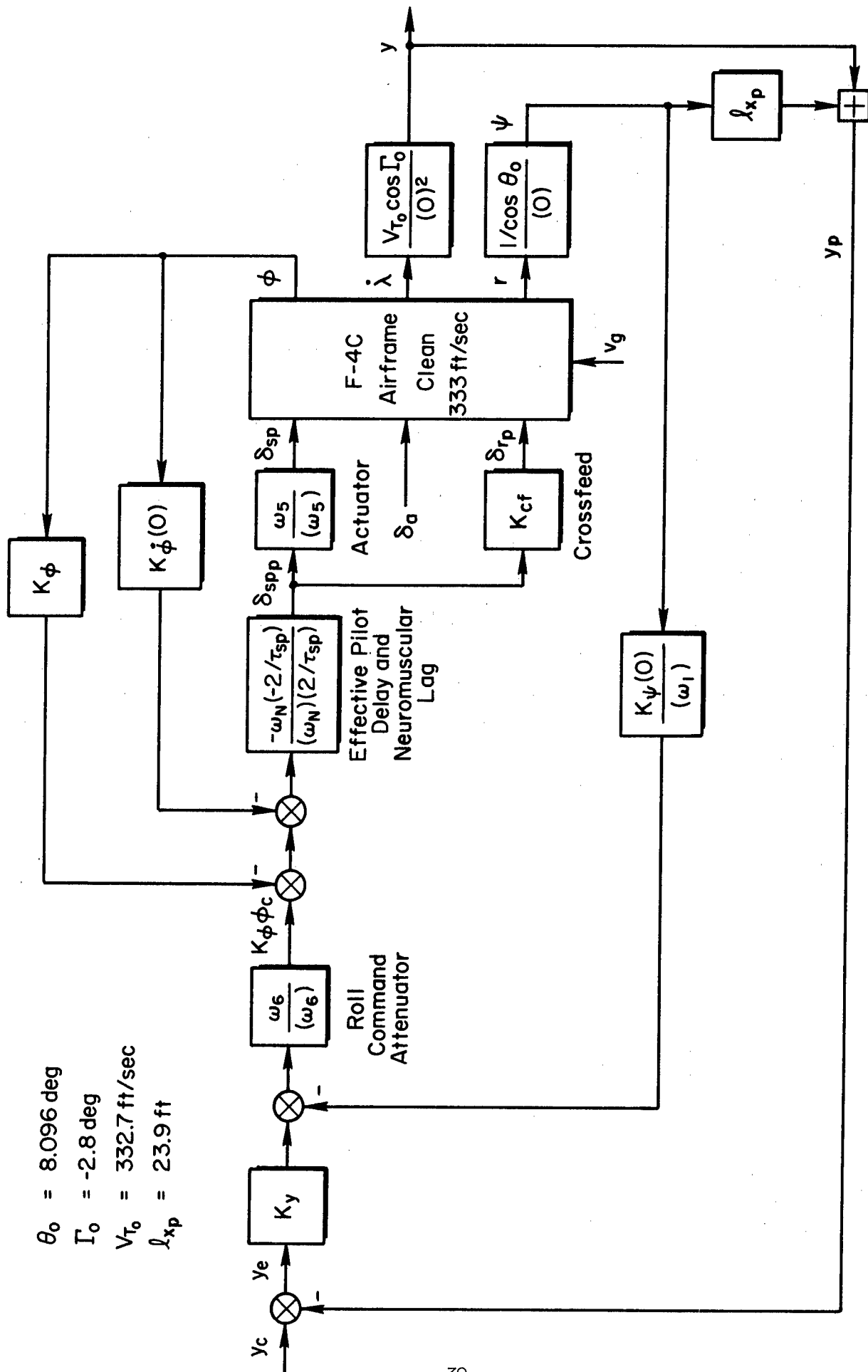


Figure 8. Lateral F-4C Block Diagram for System A

TABLE VII

PARAMETERS FOR LINEAR PILOT LOOP CLOSURES,
SYSTEM A, LATERAL

K_{cf}	0.0	---
$K_{\dot{\phi}}$	0.0	sec
ω_N	10.0	rad/sec
τ_{sp}	0.2	sec
ω_5	10.0	rad/sec
K_{ϕ}	0.629	--
ω_6	0.85	rad/sec
K_{ψ}	1.74	--
ω_7	0.01	rad/sec
K_y	0.03	deg/ft

TABLE VIII

RMS RESPONSES TO ILS BEAM BENDS AND SIDE GUSTS
FOR LINEAR LATERAL SYSTEM A

<u>VARIABLE</u>	<u>RMS RESPONSE</u>		
	<u>ILS Bends</u>	<u>Side Gusts</u>	<u>Total</u>
Localizer deviation	8.68	16.9	19.02 ft
Roll attitude angle	0.203	5.11	5.12 deg
Roll rate	0.0603	9.08	9.09 deg/sec
Sideslip angle	0.00298	1.90	1.90 deg
Heading angle	0.0939	1.22	1.22 deg
Spoiler deflection angle	0.162	3.56	3.57 deg
Spoiler deflection rate	0.122	6.02	6.02 deg/sec
Rudder deflection	0.0	0.0	0.0 deg

Lateral-directional System B is, dynamically speaking, similar to System A. The main differences are that System B is manually powered which eliminates the actuator dynamics, and the spoilers are reduced in effectiveness to $2/3$ of effectiveness for System A. These changes may be represented as in Fig. 9. $\delta_{sp}^{(1)}$ in Fig. 9 is the spoiler deflection for System B.

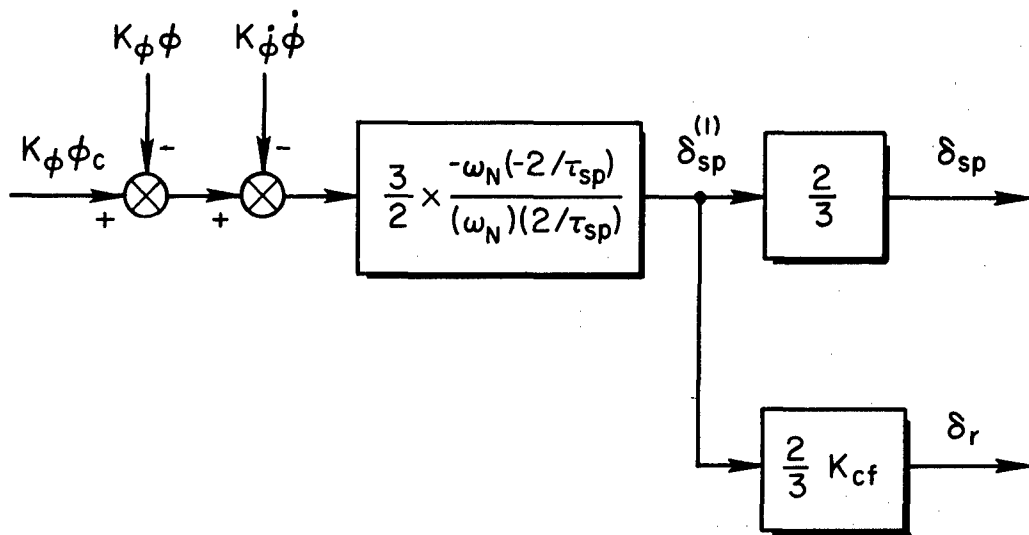


Figure 9. Block Diagram Changes for Roll Control by Means of Spoilers Having Reduced Effectiveness

The values for the pilot loop gain and equalization break frequencies for lateral System B are the same as for System A (Table VII) except that the actuator break frequency is not relevant. The closed-loop root-mean-square performance for this system is given in Table IX.

TABLE IX

RMS RESPONSES TO ILS BEAM BENDS AND SIDE GUSTS
FOR LINEAR LATERAL SYSTEM B

<u>VARIABLE</u>	<u>RMS RESPONSE</u>		
	<u>ILS Bends</u>	<u>Side Gusts</u>	<u>Total</u>
Localizer deviation	8.67	16.8	18.9 ft
Roll attitude angle	0.197	5.04	5.04 deg
Roll rate	0.0585	8.98	8.98 deg/sec
Sideslip angle	0.00287	1.88	1.88 deg
Heading angle	0.0918	1.21	1.22 deg
Mod. spoiler deflection angle	0.236	5.37	5.38 deg
Mod. spoiler deflection rate	0.202	9.15	9.16 deg/sec
Rudder deflection	0.0	0.0	0.0 deg

Lateral-directional System C has a loop structure which is similar to the one for System A. However, since the ailerons are used in place of the spoilers, the numerators of the airframe transfer functions are somewhat changed. Small changes in the pilot's loop gains are necessary to arrive at the best minimum back-up system parameter values. The most noteworthy change in this respect is that the best value of the roll rate feedback gain is no longer zero as it was for Systems A and B. The fact that System C is manually powered results in elimination of the actuation dynamics. These several changes may be represented by Fig. 10.

The values for the pilot loop gains and break frequencies for lateral System C are given in Table X. The closed-loop root-mean-square performance for this system is displayed in Table XI. These loop closures result in a closed-loop bandwidth in following the localizer reference of 0.35 rad/sec.

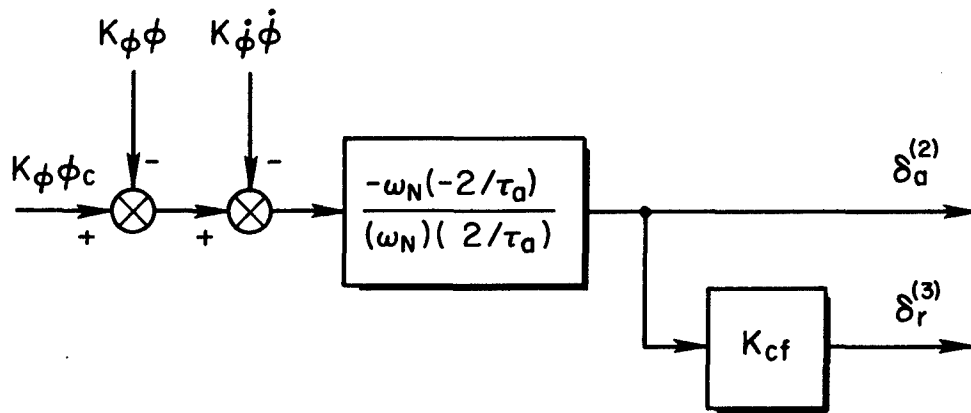


Figure 10. Block Diagram Changes for Roll Control by Means of Modified Ailerons

TABLE X

PARAMETERS FOR LINEAR PILOT LOOP CLOSURES, SYSTEM C, LATERAL

K_{cf}	0.0	--
$K_{\phi\dot{\phi}}$	0.314	sec
ω_N	10.0	rad/sec
τ_a	0.2	sec
K_{ϕ}	0.440	--
ω_G	0.85	rad/sec
K_{ψ}	1.74	--
ω_1	0.01	rad/sec
K_y	0.049	deg/ft

TABLE XI

RMS RESPONSES TO ILS BEAM BENDS AND SIDE GUSTS
FOR LINEAR LATERAL SYSTEM C

<u>VARIABLE</u>	<u>RMS RESPONSE</u>		
	<u>ILS Bends</u>	<u>Side Gusts</u>	<u>Total</u>
Localizer deviation	8.76	13.6	16.2 ft
Roll attitude angle	0.536	3.78	3.81 deg
Roll rate	2.48	6.65	7.09 deg/sec
Sideslip angle	0.0322	1.30	1.30 deg
Heading angle	0.187	1.25	1.26 deg
Aileron deflection angle	0.182	3.09	3.09 deg
Aileron deflection rate	0.229	6.96	6.96 deg/sec
Rudder deflection	0.0	0.0	0.0 deg

C. MINIMUM CONTROL PARAMETER VALUE SELECTION

The results from the preceding estimates of linear system performance are used, in turn, to estimate the "minimum" control parameter values. The approach used is the one described in detail in Section II. Namely, the characteristic parameter for each nonlinearity is selected on the basis of the root-mean-square level of the signal in the linear system model at the point where that nonlinearity occurs. If the characteristic parameter of the nonlinearity is chosen relative to the root-mean-square level of the signal in such a way that the effect of the nonlinearity is very small, then the performance of the linear and nonlinear system will be nearly the same.

All the nonlinearities involved in the back-up system designs are unity-gain limiters. Therefore, all the control parameters considered here are limit levels. If these limit levels are 2 to 3 times the

root-mean-square level of the signals, then the effect of the nonlinearities will indeed be small.

For System A, the root-mean-square values of stabilator deflection and rate are used to determine the minimum values for the stabilator authority and rate limit control parameters for longitudinal control. A similar procedure is employed for lateral-directional control in connection with System A and so on for the other back-up system designs. The 2σ and 3σ values of the minimum control parameter values selected in this manner are summarized in Table XII for each back-up system configuration. The minimum back-up system parameters determined empirically by simulation (Ref. 1) are also included in the Table for comparative purposes.

Several of the empirically determined minimum control parameter values fall within the range recommended on the basis of analysis. This range, of course, is defined by the 2 and 3 times root-mean-square signal levels (2σ and 3σ columns in Table XII). Still others of the empirically determined minimum control parameter values are approximately within a factor of 2 of the extremes of the analytically recommended range. The remaining empirically determined minimum control parameters are vastly different. Minimum values for the latter group are apparently set by considerations apart from those involved with landing approach control. For example, maximum horsepower will most likely be set by the maximum stabilator deflection-rate-hinge moment gradient product required in the back-up system flight envelope for recovery from a battle damage transient. It is most likely that the rudder deflection limits are also set by this consideration. Crosswind landing capability might also set the rudder deflection limits, but this requirement has not been considered in Ref. 1, nor is it considered here.

TABLE XII
SELECTION OF MINIMUM CONTROL PARAMETER VALUES

System Configuration	Variable Associated With Limit	Minimum Control Parameter Value Based Upon		
		3σ	2σ	Ref. 1
A	$\dot{\delta}_s$	2.55	1.7	1.0 deg/sec
	δ_s	0.81	0.54	1.5 deg
	Maximum HP_s^*	0.00275	0.00122	0.1 HP^\dagger
	$\dot{\delta}_{sp}$	18.1	12.04	15.0 deg/sec
	δ_{sp}	10.7	7.14	10.0 deg
	δ_r	0	0	7.0 deg [†]
	Maximum HP_{sp}^*	0.0547	0.0243	--
B	δ_t	1.20	0.80	2.5 deg
	$\delta_{sp}^{(1)}$	16.13	10.75	10.0 deg
	δ_r	0	0	7.0 deg [†]
C	δ_t	1.24	0.80	2.5 deg
	$\delta_a^{(2)}$	9.28	6.184	10.0 deg
	$\delta_r^{(3)}$	0	0	7.0 deg [†]

* Determined at $V_{T_0} = 333.0$ ft/sec. Maximum HP depends upon the δ_s and $\dot{\delta}_s$ control parameter values and upon the stabilator hinge moment gradient.

† These minimum control parameter values would appear to be set by other considerations than landing approach control.

D. VERIFICATION OF SYSTEM PERFORMANCE

Having arrived at recommended levels for the minimum control parameter values based upon linear analysis, one would ordinarily proceed to verify that nonlinear system performance is not appreciably degraded from linear system performance. If this is not the case, or if further reduction in the minimum control parameters perhaps seems warranted, the performance verification calculations would be repeated as an iterative design process. The initial selection of the minimum control parameter values, e.g. Table XII, would provide the starting point for this process. In fact, however, it is very doubtful that the values found at the end of any such iterative procedure will differ to any significant extent from the initial values without violating the performance or other design goals for the back-up system design.

Instead of verifying performance for recommended minimum control parameter values in Table XII, the values from Ref. 1 will be used. This is done in order to obtain quantitative measures of performance by analytical means which are directly comparable with the quantitative measures of performance given in Ref. 1. In doing so, the computational technique used for performance verification will be demonstrated, and at the same time results needed to tie-in the analysis with the experiments will be produced.

E. NONLINEAR SYSTEM A

Performance verification calculations proceed using the longitudinal System A model of Fig. 6 with the linear actuator model, $\omega_3/(s+\omega_3)$, replaced by the nonlinear actuator model of Fig. 5. The values for the actuator rate and deflection limits are obtained from Table XII.

$$R = 1.0 \text{ deg/sec} \quad (5)$$

$$P = 1.5 \text{ deg} \quad (6)$$

The small signal open-loop gain for the nonlinear actuator is:

$$K = \omega_z = 10.0 \text{ rad/sec} \quad (7)$$

Next, $\bar{\sigma}_R$ and $\bar{\sigma}_P$ for the closed-loop system are computed as functions of the equivalent gains for the rate and deflection limiters, K_R and K_P , and the results are overplotted on the random input describing function for the normalized limiter. The result is shown in Figs. 11 and 12.

In Fig. 11, $\bar{\sigma}_R$ for the closed-loop system is plotted versus K_R for two constant values of K_P . For the value of K_R at the intersection of the curves in Fig. 11, $\bar{\sigma}_P$ is plotted versus K_P in Fig. 12. The values of K_R and K_P for which simultaneous intersections (solutions) occur are:

$$K_R = 0.62 \quad (8)$$

$$K_P = 1.0 \quad (9)$$

The above values for the equivalent gains of the nonlinearities permit one to compute the performance for the nonlinear system. That is, the root-mean-square levels for the variables of interest are computed with these equivalent gains substituted for the nonlinear elements in Fig. 5. The results of this performance computation are summarized in Table XIII.

Comparison of the nonlinear system performance values with the linear system performance values (Table V) shows a small but distinct increase in almost all root-mean-square values for the nonlinear system. The performance of the nonlinear system can, nevertheless, be judged acceptable.

It is informative to reflect upon the relation that the minimum values of the control parameters of Ref. 1 bear to the values recommended here, and on the related consequences in terms of effects upon performance. The deflection limit specified in Ref. 1 is generous in comparison to the minimum value range recommended in Table XII. This is also reflected in the solution for the equivalent gains. That is, Fig. 12 shows that $\bar{\sigma}_P$ could indeed be somewhat larger (as the result of making P much smaller) without changing K_P from unity by any significant amount. If indeed the deflection limit, P, is set by landing approach requirements, it may be safely reduced from the Ref. 1 value in the context of this study.

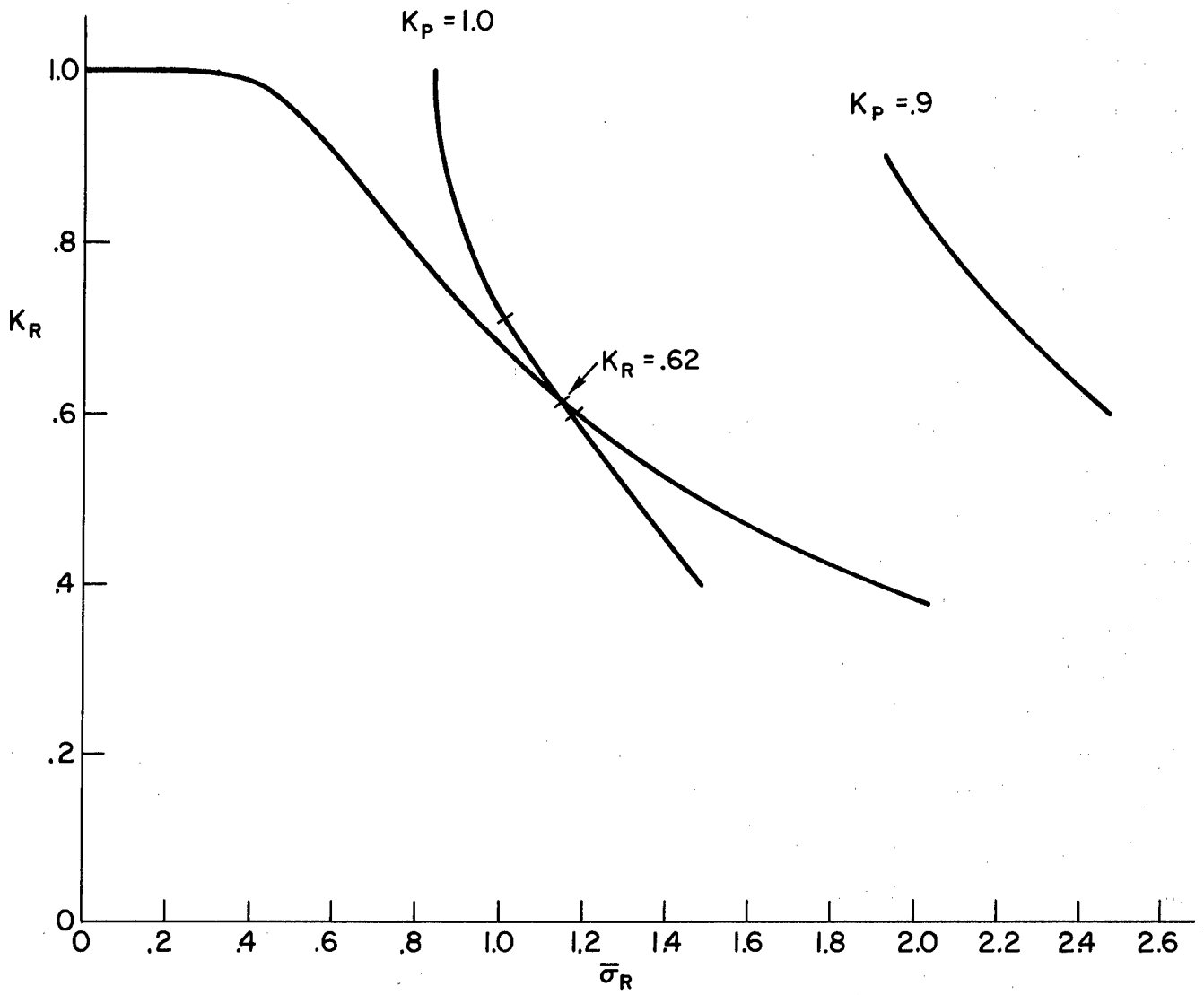


Figure 11. Solution for the Equivalent Gains for Longitudinal System A Rate Limit Equations

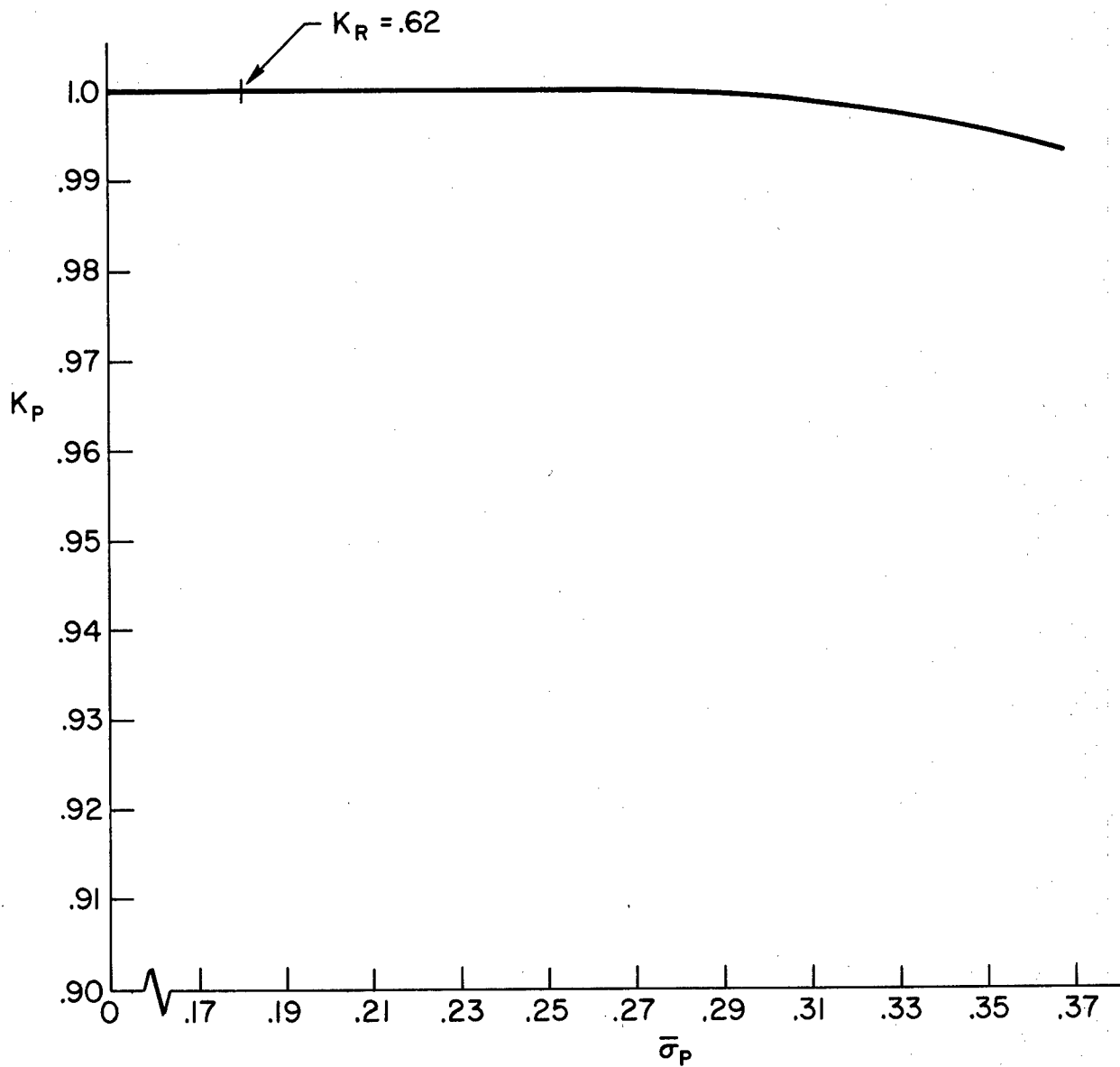


Figure 12. Solution for the Equivalent Gains for Longitudinal System A Deflection Limit Equations

TABLE XIII

RMS RESPONSES TO ILS BEAM BENDS AND NORMAL GUSTS
FOR NONLINEAR LONGITUDINAL SYSTEM A

	<u>RMS RESPONSE*</u>		
	<u>ILS Bends</u>	<u>Normal Gusts</u>	<u>Total</u>
Glide slope deviation	3.42	8.84	9.48 ft
Pitch attitude	0.216	0.827	0.855 deg
Pitch rate	0.140	1.37	1.38 deg/sec
Stabilator angle	0.0288	0.266	0.270 deg
Stabilator rate	0.0605	0.715	0.719 deg/sec
Throttle in equivalent thrust	22.2	143.0	145.0 lb
Airspeed error	0.369	2.39	2.42 ft/sec
$\bar{\sigma}_R$	0.0976	1.15	1.16 --
$\bar{\sigma}_P$	0.0228	0.178	0.180 --
Longitudinal stick force	0.0648	0.599	0.608 lb
Longitudinal stick displacement	0.00864	0.0798	0.081 in.

*Values calculated for enforcement gain, $k = 100$.

The matter of the acceptability of the Ref. 1 rate limit which is less than the recommended range also deserves comment. The effect of the rate limit is to reduce the effective bandwidth of the actuator. This effective bandwidth is $K K_R$. For computation of the recommended minimum control parameter values, the small signal open-loop gain of the actuator, K , was fixed at 10.0/sec. In retrospect, this was a reasonable way to proceed, but a better choice might have been to select this gain in the linear analysis to meet the minimum performance requirement just as the pilot loop closure gains were selected. If this were done, the

nonlinear system performance would not be so tolerant of reductions in K_R from unity. Then if one wished to use a value of the small signal actuator open-loop gain which was larger than this value, say K_2 , it would be an easy matter to determine an appropriate minimum value for the rate limit, R_2 , for use with that gain. This may be done by requiring that

$$K_2 K_{R_2} = K K_R \quad (10)$$

which is the condition for invariance of the closed-loop system, together with the random input describing function equation,

$$K_{R_2} = K_{R_2} \left(\frac{K_2}{R_2} \frac{R}{K} \bar{\sigma}_R \right) \quad (11)$$

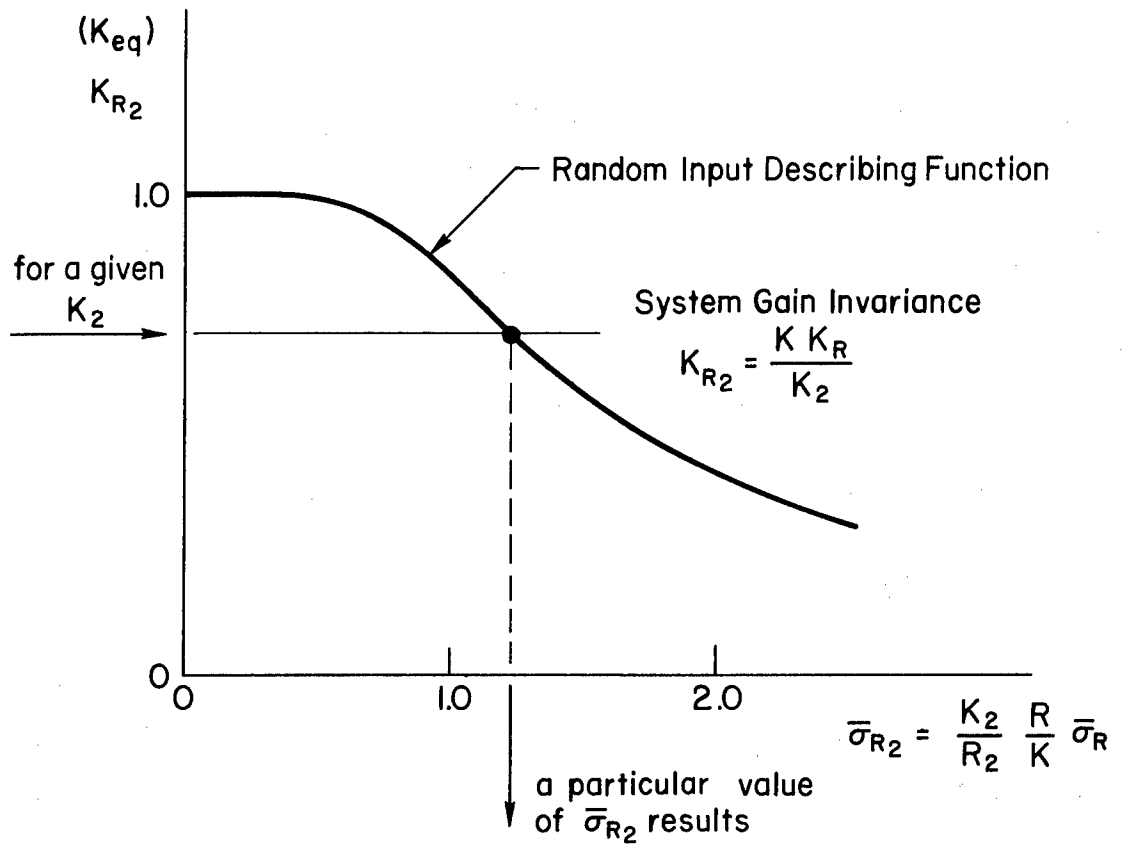
which relates the new equivalent gain, K_{R_2} , to the new normalized root-mean-square input,

$$\bar{\sigma}_{R_2} = \frac{K_2}{R_2} \frac{R}{K} \bar{\sigma}_R \quad (12)$$

The quantity $R \bar{\sigma}_R / K$ is a constant for any one example. The way in which K_{R_2} may be evaluated graphically is illustrated in Fig. 13. For the purpose of illustration it is assumed that the nonlinearity is a rate limiter.

It is apparent in Fig. 13 that an entire family of solutions exist. One must be cautious, however, when using those solutions for which $\bar{\sigma}_{R_2} > 0.5$ because of the approximate nature of the describing function.

Next, consider the lateral nonlinear System A performance. The performance calculations proceed using the lateral System A model of Fig. 8 with the linear actuator model, $\omega_5 / (\omega_5)$, replaced by the nonlinear actuator model of Fig. 5. The values for the actuator rate and deflection limits are then obtained from Table XII.



since K_2 and $R \bar{\sigma}_R / K$ are known, it is a simple matter to compute R_2 from $\bar{\sigma}_{R_2}$

$$R_2 = \frac{K_2}{\bar{\sigma}_{R_2}} \frac{R}{K} \bar{\sigma}_R$$

Figure 13. Finding Alternate Solutions for which Closed-Loop System Performance is Invariant

$$R = 15.0 \text{ deg/sec} \quad (13)$$

$$P = 10.0 \text{ deg} \quad (14)$$

The small signal open-loop gain for the actuator is

$$K = \omega_5 = 10.0 \text{ rad/sec} \quad (15)$$

The solution for the values of the equivalent gains is obtained by the same procedure used for the longitudinal solution. The graphical solution is shown in Figs. 14 and 15. Values of K_R and K_P for which simultaneous intersections (solutions) occur are:

$$K_R = 0.987 \quad (16)$$

$$K_P = 0.996 \quad (17)$$

The above values for the equivalent gains of the nonlinearities lead to the computed performance for the nonlinear system given in Table XIV.

The Ref. 1 minimum control parameter values fall within the recommended range in Table XIII for lateral control with System A. There is good reason to believe in retrospect that both the recommended and Ref. 1 minimum values of the rate limit are larger than is necessary. As far as the recommended value is concerned, this is for the same reason as in the longitudinal case. The linear design was based upon a fixed value of the actuator open-loop gain instead of using as small a value as possible. In simulation, the minimum value of rate limit (Ref. 1) is probably high because the pilot subjects probably felt a high effective open-loop actuator gain (actuator bandwidth) was necessary in order to control the dutch roll. However, the linear analyses in Appendix II show that there can be no effective control over the dutch roll. Had the linear analysis been available to guide the simulation experiments, this hypothesis might perhaps have been confirmed.

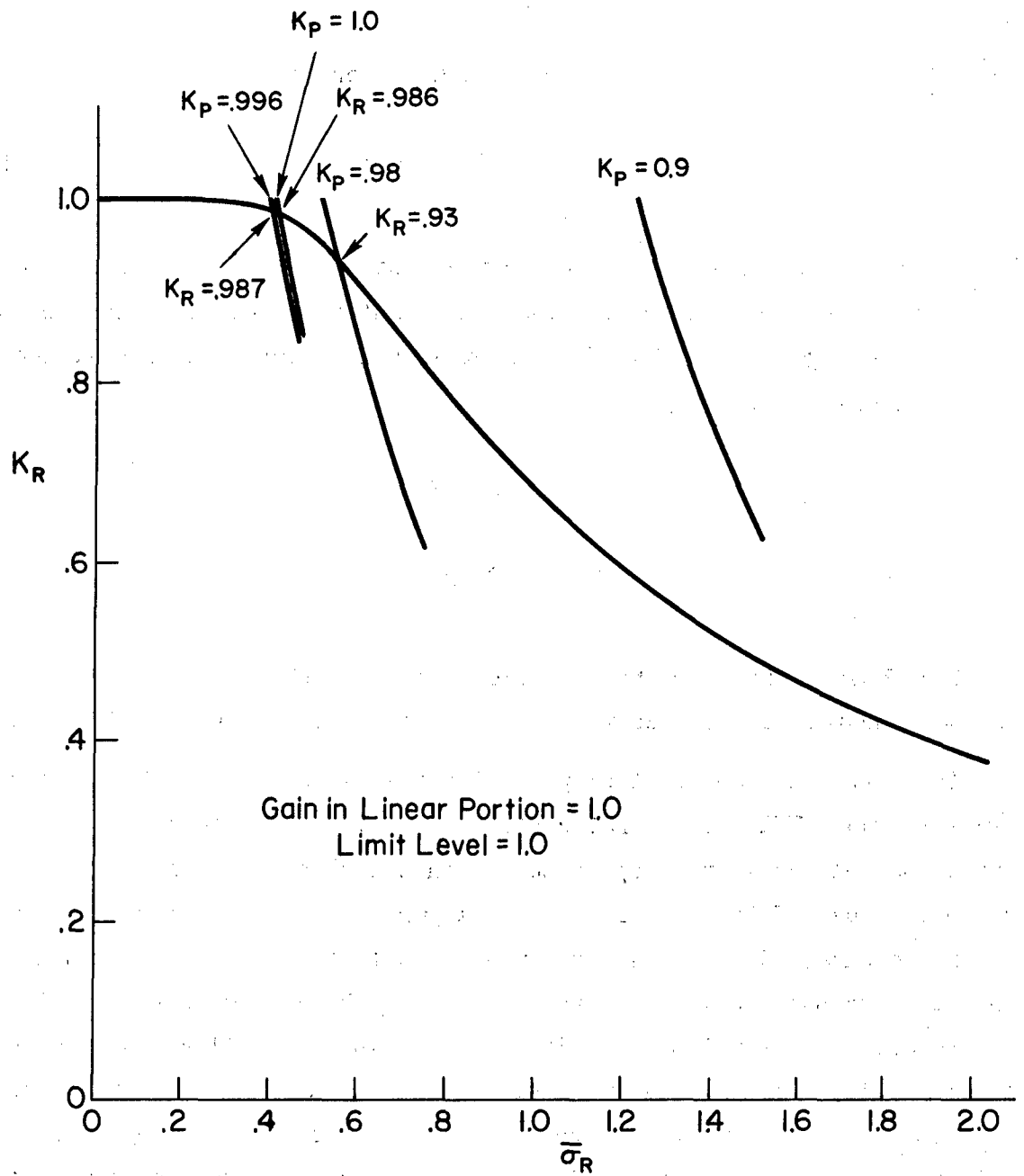


Figure 14. Solution for the Equivalent Gains for Lateral System A Rate Limit Equations

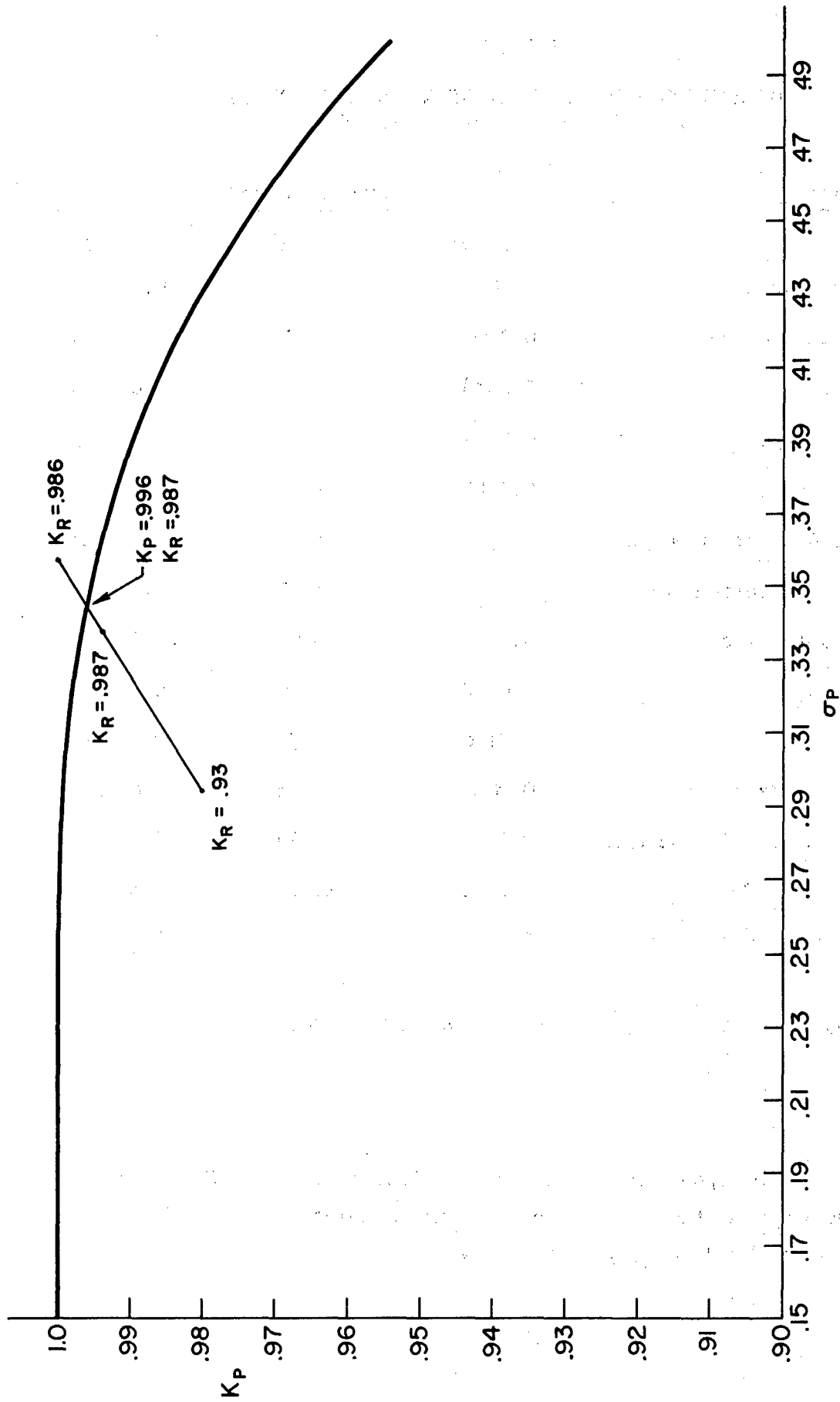


Figure 15. Solution for the Equivalent Gains for Lateral System A
Deflection Limit Equations

TABLE XIV

RMS RESPONSES TO ILS BEAM BENDS AND SIDE GUSTS
FOR NONLINEAR LATERAL SYSTEM A

<u>VARIABLE</u>	<u>RMS RESPONSE*</u>		
	<u>ILS Bends</u>	<u>Side Gusts</u>	<u>Total</u>
Localizer deviation	8.70	17.1	19.2 ft
Roll attitude angle	0.202	5.10	5.10 deg
Roll rate	0.0588	9.06	9.06 deg/sec
Sideslip angle	0.00292	1.90	1.90 deg
Heading angle	0.0945	1.22	1.22 deg
Spoiler deflection angle	0.157	3.42	3.42 deg
Spoiler deflection rate	0.117	5.77	5.77 deg/sec
Rudder deflection	0.0	0.0	0.0 deg
$\bar{\sigma}_R$	0.00902	0.402	0.402 --
$\bar{\sigma}_P$	0.0158	0.343	0.343 --
Lateral stick force	0.0839	1.83	1.83 lb
Lateral stick displacement	0.0134	0.292	0.292 in.
Rudder pedal force	0.0456	29.6	29.6 lb
Rudder pedal displacement	0.0	0.0	0.0 in.

*Values calculated for enforcement gain, $k = 100$.

The peak horsepower required for the stabilator and spoiler actuators in System A during the landing approach is calculated below. The peak horsepower required, HP_{max} , is given by

$$HP_{\max} = \left| \frac{\left(\begin{array}{l} \text{hinge moment gradient} \\ \text{in ft-lb/deg} \end{array} \right) \left(\begin{array}{l} \text{maximum surface} \\ \text{deflection in} \\ \text{deg} \end{array} \right) \left(\begin{array}{l} \text{maximum rate of} \\ \text{surface deflection} \\ \text{in deg/sec} \end{array} \right)}{550 \times 57.3} \right|$$

For the stabilator actuator, $HP_{\max} = 0.0020$ horsepower. This is well within the 0.1 horsepower limit imposed in the simulation experiments. The horsepower limit is doubtless determined by critical battle damage transient conditions where the dynamic pressure and consequently the maximum hinge moment is very much greater than in landing approach. For the spoiler actuator, $HP_{\max} = 0.0424$ horsepower in the landing approach. Notice in each case that the peak horsepower required depends only upon the hinge moment gradient, and the control surface rate and deflection limits. Therefore, it is not really necessary to impose horsepower limits explicitly as was done in the Ref. 1 simulation.

F. NONLINEAR SYSTEM B

Performance verification calculations for longitudinal nonlinear System B are based upon the block diagram of Fig. 6 as modified by Fig. 16 below.

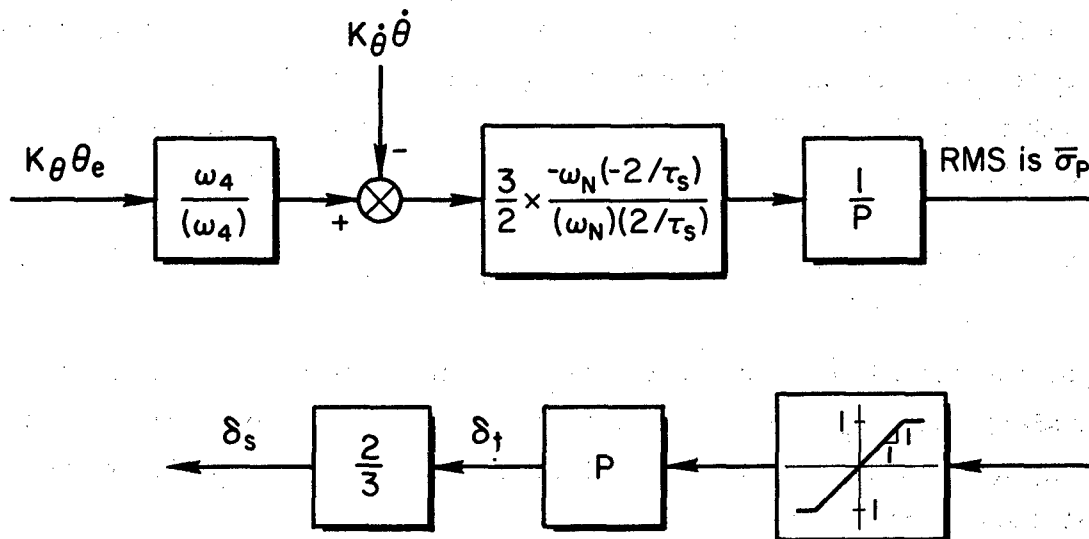


Figure 16. Block Diagram Changes for Pitch Control by Means of Stabilator Tab

The value for the tab deflection limit is obtained from Table XII.

$$P = 2.5 \text{ deg} \quad (18)$$

Here only $\bar{\sigma}_P$ is a function of an equivalent gain, K_P . The result of the calculation of $\bar{\sigma}_P$ is overplotted on the random input describing function for the normalized limiter in Fig. 17. The value of K_P at the intersection is

$$K_P = 1.0 \quad (19)$$

for $\bar{\sigma}_P = 0.16$. The nonlinear system performance is computed using this value of the equivalent gain. The results, however, are the same as for linear longitudinal System B because $K_P = 1.0$. Therefore, the values in Table VI apply here as well.

This result shows that the Ref. 1 value of the minimum tab deflection limit could probably have been reduced to a value within the recommended value range and still have met the landing approach control requirements.

Longitudinal Systems B and C are identical. Therefore, the above results and conclusions apply to System C as well.

Performance verification calculations for lateral nonlinear System B are based upon the block diagram of Fig. 8 as modified by Fig. 18 below. The value for the modified spoiler deflection limit, P , is obtained from Table XII.

$$P = 10.0 \text{ deg} \quad (20)$$

$\bar{\sigma}_P$ for the closed-loop system is then calculated as a function of the equivalent gain, K_P , and the result is overplotted on the random input describing function for the normalized limiter in Fig. 19. The value of K_P at the intersection is:

$$K_P = 0.94 \quad (21)$$

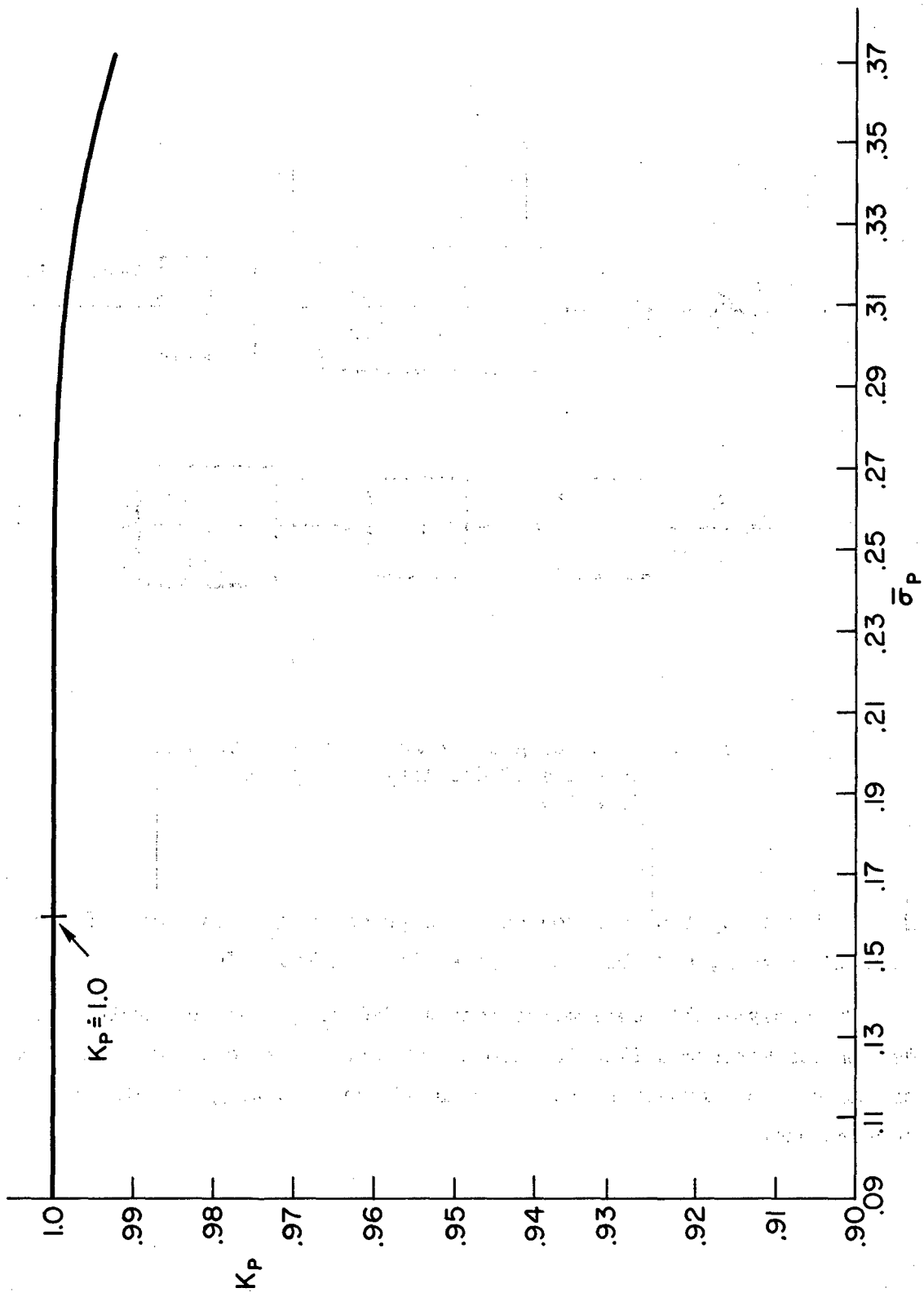


Figure 17. Solution for Equivalent Gain, K_p , for Longitudinal System B

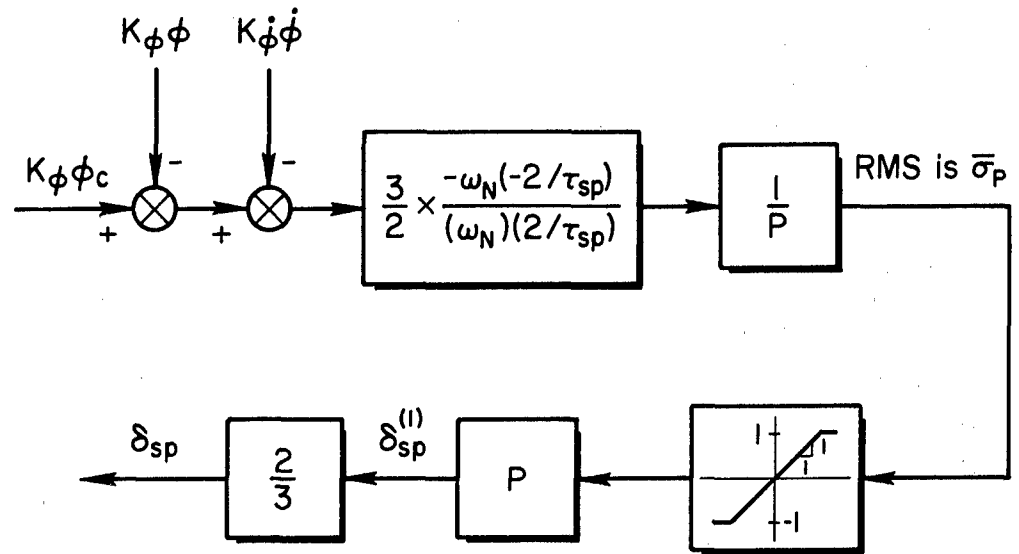


Figure 18. Block Diagram Changes for Roll Control by Means of Spoilers Having Reduced Effectiveness

The nonlinear system performance is computed using this value of the equivalent gain, and the results are given in Table XV.

The analytically determined recommended range and the empirically determined minimum deflection limits of Ref. 1 are consistent in terms of the values themselves and in terms of the resulting effects upon performance.

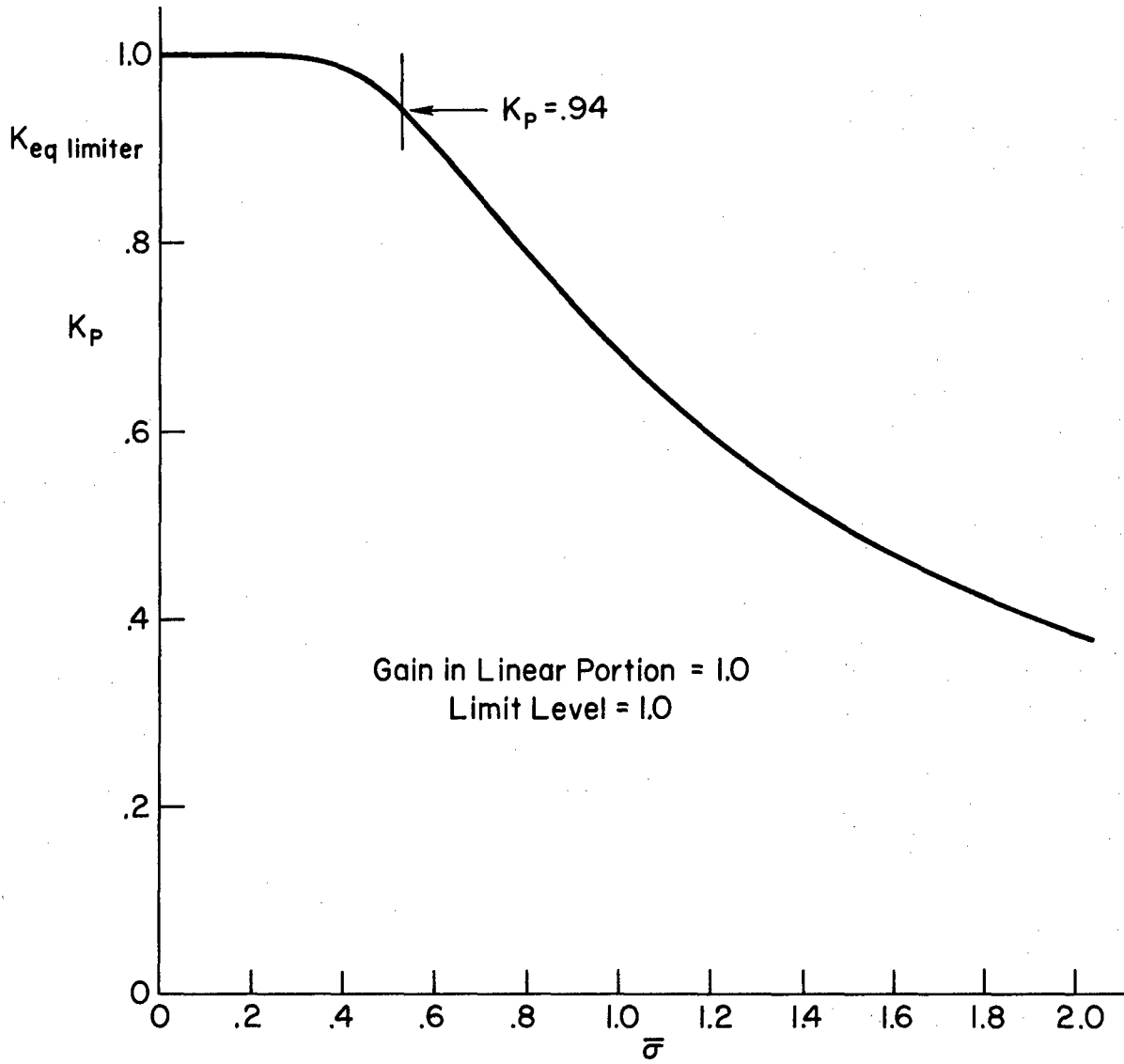


Figure 19. Solution for Equivalent Gain, K_p , for Lateral System B

TABLE XV

RMS RESPONSES TO ILS BEAM BENDS AND SIDE GUSTS
FOR NONLINEAR LATERAL SYSTEM B

<u>VARIABLE</u>	<u>RMS RESPONSE</u>		
	<u>ILS Bends</u>	<u>Side Gusts</u>	<u>Total</u>
Localizer deviation	8.70	17.1	19.2 ft
Roll attitude angle	0.196	5.01	5.01 deg
Roll rate	0.0563	8.94	8.94 deg/sec
Sideslip angle	0.00282	1.88	1.88 deg
Heading angle	0.0934	1.22	1.22 deg
Mod. spoiler deflection angle	0.226	5.02	5.03 deg
Mod. spoiler deflection rate	0.189	8.56	8.57 deg/sec
Rudder deflection	0.0	0.0	0.0 deg
$\bar{\sigma}_P$	0.024	0.534	0.535 --
Lateral stick force	0.483	10.73	10.75 lb
Lateral stick deflection	0.0193	0.429	0.430 in.
Rudder pedal force	0.0440	29.3	29.3 lb
Rudder pedal deflection	0.0	0.0	0.0 in.

G. NONLINEAR SYSTEM C

It has already been pointed out that the longitudinal portion of System C is identical to the longitudinal portion of System B. Therefore, Fig. 6 and 16, and Table VI apply for System C.

Performance verification calculations for the lateral nonlinear System C are based upon Fig. 8 as modified by Fig. 20 below.

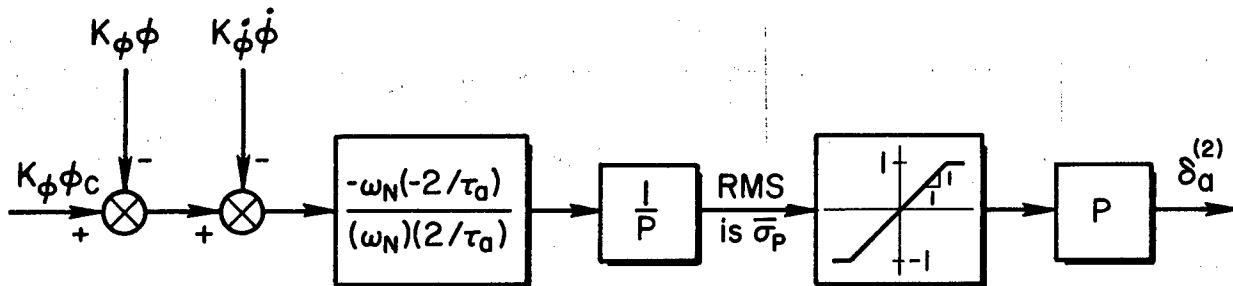


Figure 20. Block Diagram Changes for Roll Control by Means of Modified Ailerons

The value for the modified aileron deflection limit, P , is obtained from Table XII.

$$P = 10.0 \text{ deg} \quad (22)$$

$\bar{\sigma}_p$ for the closed-loop system is calculated as a function of the equivalent gain, K_p , and the result is overplotted on the random input describing function for the normalized limiter in Fig. 21. The value of K_p at the intersection is:

$$K_p = 0.999 \quad (23)$$

The nonlinear system performance is computed using this value of the equivalent gain, and the results are given in Table XVI.

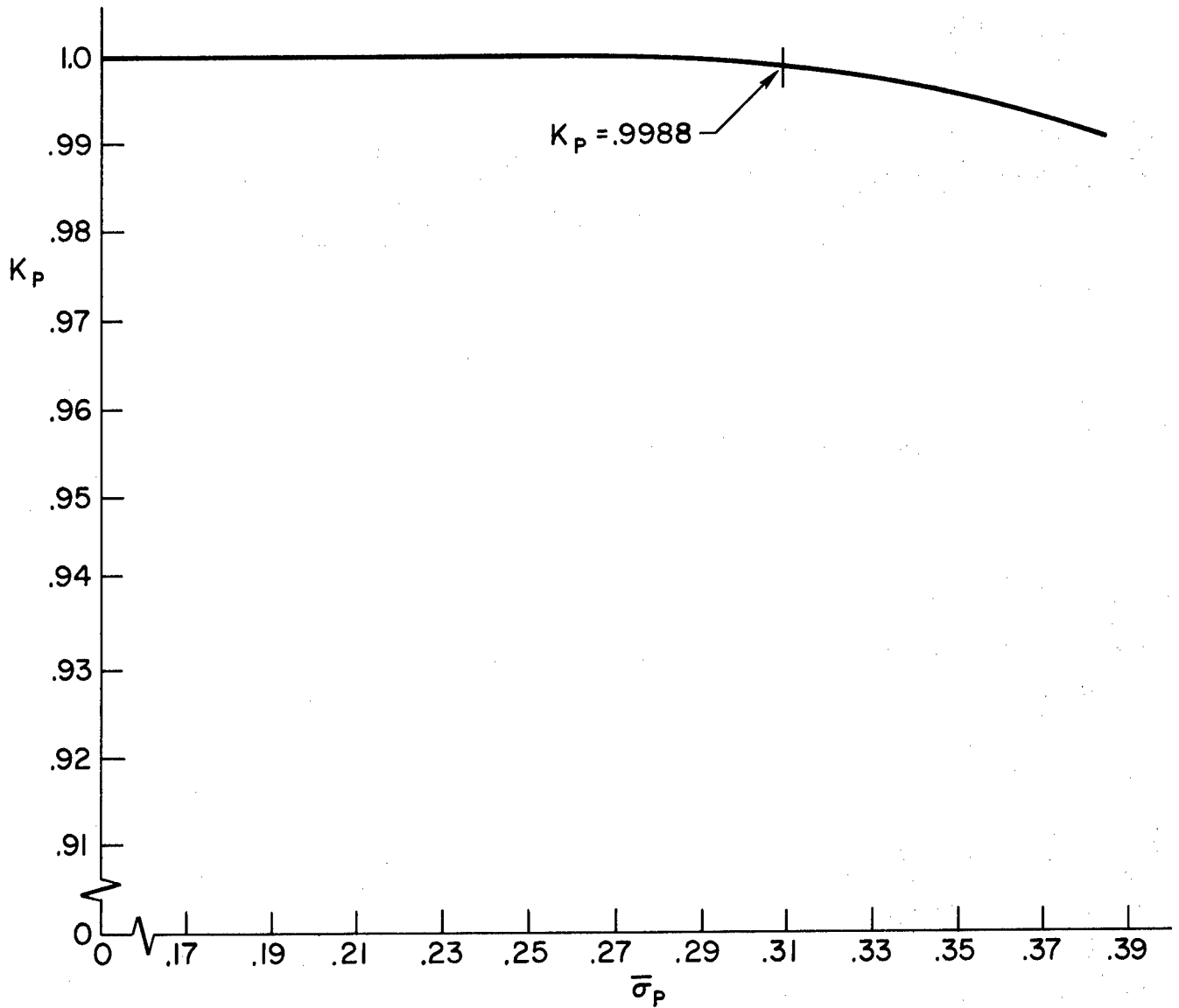


Figure 21. Solution for Equivalent Gain, K_p ,
for Lateral System C

TABLE XVI

RMS RESPONSES TO ILS BEAM BENDS AND SIDE GUSTS
FOR NONLINEAR LATERAL SYSTEM C

<u>VARIABLE</u>	<u>RMS RESPONSE</u>		
	<u>ILS Bends</u>	<u>Side Gusts</u>	<u>Total</u>
Localizer deviation	8.76	13.61	16.2 ft
Roll attitude angle	0.537	3.78	3.81 deg
Roll rate	0.249	6.62	6.63 deg/sec
Sideslip angle	0.0322	1.30	1.30 deg
Heading angle	0.187	1.25	1.26 deg
Mod. aileron deflection angle	0.182	3.08	3.09 deg
Mod. aileron deflection rate	0.229	6.95	6.95 deg/sec
Rudder deflection	0.0	0.0	0.0 deg
$\bar{\sigma}_p$	0.0182	0.309	0.309 --
Lateral stick force	1.05	17.8	17.9 lb
Lateral stick displacement	0.0228	0.385	0.386 in.
Rudder pedal force	0.167	6.76	6.76 lb
Rudder pedal displacement	0.0	0.0	0.0 in.

The analytically determined recommended range and the empirically determined minimum deflection limits of Ref. 1 are consistent in terms of the values themselves and in terms of the resulting effects upon performance.

H. COMPARISON OF PREDICTED AND MEASURED PILOT OPINION RATINGS AND PERFORMANCE

The main determinant of the success of analytical techniques for determining the minimum values of the control parameters is by means of

comparisons of predicted and measured pilot opinion ratings and performance.

Pilot opinion ratings are considered first. Predicted pilot opinion ratings for the three back-up system configurations are given in Table XVII. These predicted opinions are derived on the combined basis of equalization required of the pilot in closing the control loops, performance of the complete closed-loop system, and subsidiary problems exposed in the course of performing the basic loop closures. (See Appendix II.) The numerical rating assignments are made by means of identifying the verbal descriptions given in Fig. 52 of Appendix VI with the equalization requirements, system performance levels, and so forth. Actually only two factors are involved in pilot opinion degradation for the back-up systems which were studied. The first of these factors is the low bandwidth of control for the closed-loop system. This, of course, is a result of the design objective to arrive at a minimum system. While the pilots may not be fond of the control bandwidth limitations that have been employed, the limitations fall at what experience has shown to be a barely acceptable level. The degrading effect of this factor on pilot opinion ratings will, therefore, tend to be small.

The second, and main, factor affecting pilot opinion ratings is a problem of the subsidiary type. For the task and system configurations which were studied, there is no really effective way in which the pilots might damp the dutch roll without using an order of magnitude or more spoiler (or aileron) authority. The result of this problem is a degradation from a predicted pilot opinion rating (POR) of 2, in the absence of side gusts, to 5 in the presence of side gusts for Systems A and B. The pilot cannot increase the closed-loop dutch roll damping ratio beyond 0.12 for these systems. In the presence of side gusts, the predicted pilot opinion rating for System C degrades only to 4 or 5. This is because the pilot can increase the closed-loop dutch roll damping ratio to 0.34 for System C. This difference among the three lateral back-up systems is also evident in the root-mean-square values of the roll attitude angle.* (Refer to Tables XIV, XV and XVI.) As pointed

*This is because the dutch roll motion for these examples is characterized by a high ϕ/β ratio.

TABLE XVII

SUMMARY OF PREDICTED PILOT FLYING QUALITIES RATINGS

System Configuration	Flying Qualities Rating	Factors Causing Rating Degradation
A w/o gusts	2	
A w/ gusts	5	large side gust excitation of dutch roll can only be fixed by a yaw damper.
B w/o gusts	2	
B w/ gusts	5	large side gust excitation of dutch roll can only be fixed by a yaw damper.
C w/o gusts	2	
C w/ gusts	4-5 (see text)	substantial side gust excitation of dutch roll can only be fixed by a yaw damper.

out in Appendix II, what is really needed in these back-up system designs is a back-up yaw damper system. It appears that this back-up possibility was not even given preliminary consideration in Ref. 1 because only those back-up system requirements arising from quasi-static considerations were investigated. Consequently, this may be regarded as a valuable lesson-by-example. Dynamic requirements, too, are capable of generating back-up system requirements.

A comparison of the predicted and measured pilot opinion ratings (Table XVII and Table L of Appendix VI) shows very close agreement between the two. Measured pilot opinion rating for System B, however, appears to have high variability. This is very likely the result of a confusion in the mind of the pilot of the lightly damped dutch roll motions with pilot induced oscillation tendencies. More will be

said about this when the pilot induced oscillation tendency ratings are discussed below.

The quantitative measures of performance for the three back-up systems have been summarized in Table XVIII. The units on all the variables have been converted for agreement with the simulation results summarized in Tables XXXXVI, XXXXVII, XXXXVIII of Appendix VI. It should be noticed in particular that mean-square, in distinction to root-mean-square values, are entered in these tables. Favorable comparisons with the experimental data are indicated by check marks following the entries in Table XVIII. (A comparison has been termed "favorable" whenever the analytically determined root-mean-square value of a variable is within a factor of two of several experimentally determined values.) The agreement is good in general for the δ_s , $\dot{\delta}_s$, δ_{sp} , $\dot{\delta}_{sp}$, δ_a , $\dot{\delta}_a$, β , q , ϕ and p variables. In other words agreement is good for all the "inner loop" variables.

The general lack of agreement for the other variables (airspeed deviation, θ , ψ , δ_p , glide slope deviation, and localizer deviation) deserves special comment. The necessity of comment is because there may be a tendency to doubt analytically derived pilot-vehicle performance results when these are in conflict with experimental results.

Consider the values of $\overline{u_e^2}$. By the definition given in Eq 61 of Appendix VI, the experimental measurements were made about the nominal trim approach speed (198 kts) used for the analysis instead of the mean approach speed for each experiment. A consequence of this is that experimental values of $\overline{u_e^2}$ are much larger than the ones determined analytically. This may be appreciated from the following equation

$$[(U_0 + U_1 + u) - U_0]^2 = U_1^2 + 2U_1u + u^2 \quad (24)$$

where U_1 is the deviation of the mean approach speed for a given experimental run from 198 knots. Instructions to the pilots (Fig. 34 of Ref. 1) dictate a trim speed of 175 kts. Pilot comments indicate trim airspeeds of up to 220 kts (see Tables XXXXVI and XXXXVII). Clearly these deviations in trim speed from the nominal ($U_1^2 \doteq 600 \text{ kts}^2$) would obscure the fluctuations of interest ($\overline{u^2} \doteq 4.0 \text{ kts}^2$). Not only is this the case, but many of the values for $\overline{u_e^2}$ given in Tables XXXXVI, XXXXVII and XXXXVIII exceed 2400 kts^2

TABLE XVIII

SUMMARY OF MEAN-SQUARE PERFORMANCE MEASURES DERIVED
FROM ANALYSIS FOR COMPARISON WITH ACTUAL MEASUREMENTS

	<u>System A</u>	<u>System B</u>	<u>System C</u>
$\overline{u_e^2}$ kts ²	2.05 ×	2.00 ×	2.00 ×
$\overline{\theta_e^2}$ deg ²	0.73 ×	0.590 ×	0.590 ×
$\overline{\delta_{se}^2}$ deg ²	0.073 ×	0.159 ✓	0.159 ✓
$\overline{\dot{\delta}_s^2}$ (deg/sec) ²	0.518 ✓×(See text)	4.20 ✓	4.20
$\overline{GS^2}$ deg ²	0.0217 ×	0.0210 ×	0.0210 ×
$\overline{Q^2}$ (deg/sec) ²	1.91 ✓	1.54 ✓	1.54 ✓
$\overline{\varphi^2}$ deg ²	26.0 ✓	25.1 ✓	14.5 ✓
$\overline{\psi^2}$ deg ²	1.49	1.49	1.59
$\overline{P^2}$ (deg/sec) ²	82.2 ✓	79.9 ✓	44.0 ✓
$\overline{\beta^2}$ deg ²	3.62 ✓	3.53 ✓	1.69 ✓
$\overline{LOC^2}$ deg ²	0.0889 ×	0.0889 ×	0.0633 ×
$\overline{\delta_a^2}$ deg ²	NA	NA	9.55 ✓
$\overline{\dot{\delta}_a^2}$ (deg/sec) ²	NA	NA	48.3 ✓
$\overline{\delta_r^2}$ deg ²	0.0	0.0 ✓	0.0
$\overline{\delta_{sp}^2}$ deg ²	11.7 ✓×	25.3 ✓	NA
$\overline{\dot{\delta}_{sp}^2}$ (deg/sec) ²	33.3 ✓	73.4 ✓	NA

✓ following number indicates reasonable agreement with mean-square value from Ref. 1 simulation.

× following number indicates that the reported experimental results are not reasonable.

and one value is 17,900 kts². These facts cast some doubt upon the validity of the data, the units, or the definition given for $\overline{u_e^2}$ in these tables.

Next consider $\overline{\theta_e^2}$. In Tables XXXXVI, XXXXVII and XXXXVIII many values for $\overline{\theta_e^2}$ exceed 36.0 deg² and there are high values of 691.0 deg² and 10,900 deg². Values acceptable to pilots in the landing approach are on the order of 4.0 deg². The experimental data for $\overline{\theta_e^2}$ therefore does not appear to meet the test for reasonability.

In the case of $\overline{\delta_{se}^2}$ for System A, three mean-square measurements exceed the square of the difference between limit level and trim which is 4.0 deg². In the case of $\overline{\delta_s^2}$ for System A, two mean-square measurements exceed the square of the rate limit values. Two mean-square values of $\overline{\delta_{sp}^2}$ for System A also exceed the square of the deflection limit level. Mean-square values of the output of a symmetric limiter cannot possibly exceed the square of the limit level.

The final remarks on the experimental data concern the mean-square glide slope and localizer deviation data. Both quantities are in units of deg². The localizer transmitting antenna site is presumed (incorrectly) in Ref. 1 to be located at the glide slope transmitting antenna site. The discussion which follows will correct for this error. In all but 9 out of 45 runs the mean-square glide slope deviation exceeds the square of the maximum linear range for actual glide slope deviation indication on the crosspointer instrument which is 0.49 deg². The largest mean-square glide slope deviation measured is 5.95 deg². Results for the localizer must be examined at a particular range because of the previously noted problem. At an altitude of 100 ft on a -2.0 deg reference glide path, the range to the glide slope transmitting antenna site is 2,865.0 ft. This enables the true localizer deviation to be calculated in linear units. The conversion factor to convert LOC in Tables XXXXVI, XXXXVII and XXXXVIII is 50.0 ft/deg. The square of the maximum linear range for localizer deviation on the crosspointer instrument is 6.25 deg² which corresponds to 190,358.0 ft² or (436.3 ft)² for a 10,000 ft range to the localizer transmitting antenna site. When this deviation is expressed in the terms of LOC degree units used in Ref. 1 the result is equivalent to:

$$LOC^2 = (8.726 \text{ deg})^2 = 76.143 \text{ deg}^2 \quad (25)$$

Six mean-square values, $\overline{LOC^2}$, exceed this level. If the linear localizer deviation at 100 ft altitude were to be within ± 100 ft, then $\overline{LOC^2}$ must be less than 4.0 deg^2 . Only 18 out of 45 experiments have values for $\overline{LOC^2}$ which are less than 4.0 deg^2 . The pilot comments indicate that, at most, only three experimental runs (Table XXXVI; DS, 11/21/69, 19 through DS, 11/21/69, 21) were "unsuccessful." These are the runs with the 3 highest values for $\overline{LOC^2}$ which is some small comfort.

The Category II "window" (Refs. 23, 24 and 25) may be used to gauge the order magnitude for acceptable glide slope and localizer deviations for emergency condition landings. This "window" is an FAA specification of maximum permissible glide slope and localizer deviation conditions at 100 ft altitude from which safe landings can be conducted with a high confidence level. The window dimensions are given in Table XIX.

TABLE XIX

MAXIMUM ACCEPTABLE LEVELS OF
GLIDE SLOPE AND LOCALIZER ERROR

<u>Glide Slope Error</u> *	<u>Localizer Error</u> †
12.0 ft‡	72.7 ft
0.686 "dots"	0.333 "dots"
0.240 deg	0.417 deg
51.4 μa	25.0 μa ‡
	1.454 "LOC" deg

*At a range to the transmitting antenna of 2,865.0 ft on a -2.0 reference glide path at $h = 100$ ft.

†At a range to the transmitting antenna of 10,000 ft.

‡Absolute specification.

It must be pointed out that these window dimensions are approximately three times the root-mean-square levels of glide slope and localizer deviations that are acceptable for normal landing approaches. (These, however, might be enlarged by a factor of 1.5 for emergency condition landing approaches.) The root-mean-square deviations must bear this relationship to the window dimensions so that the probability of flying through the window and on to a successful landing will be sufficiently high.

Overall, some of the experimental results do not appear to meet the test of reasonability. Therefore, the comparison between the analytical and experimental results for those variables, u_e , θ_e , GS and LOC, should not be made on the basis of these data.

This still leaves the analytically and experimentally determined mean square values of ψ and δ_r which do not compare favorably in all cases. Because mean-square values of β are small and in agreement for the analytical and experimental results, it can be concluded that the large experimental mean-square values of ψ are the result of lateral flight path angle changes. This in turn could be held responsible for the large experimental mean square values of localizer deviation. This would be confirmed to some extent by the linear analyses which showed that a rather large value of the heading-to-spoiler feedback gain ($K_\psi = 1.74 \text{ deg/deg}$) is necessary in order to obtain adequate lateral flight path damping. In the case of the rudder, it is not clear from the experimental data for ϕ , ψ , β , LOC and δ_r that the pilot subjects found the rudder helpful for stabilizing the aircraft in roll. When rudder was used both good and poor performance resulted. When rudder was not used, the same thing can be said.

In summary then, comparison of the experimental data and the analytical predictions results in the following conclusions.

- Predicted and measured pilot opinion agree closely.
- Predicted and measured control deflections and rates (except for rudder in Systems A and C) as well as pitch rates, roll angles, roll rate, and sideslip angle compare favorably.

- Experimentally measured pitch angle, glide slope deviation and localizer deviation do not meet the test of reasonability. (The reported high mean-square values for these variables did not elicit critical pilot comments.) Comparison of mean square performance in connection with these outer loop variables is not realistically possible.

This concludes the performance analysis of the back-up systems. The next Section develops a sinusoidal input describing function needed for estimating the susceptibility of the back-up systems to pilot induced oscillations and possible instabilities.

SECTION IV

DERIVATION OF THE SINUSOIDAL INPUT DESCRIBING FUNCTION FOR THE LIMITING INTEGRATOR

Back-up System A uses redundant actuators and back-up power systems for actuation of the stabilator and the spoilers. The nature of these actuation devices requires that they be small in size and low in weight and power consumption. This in turn implies minimal authority (deflection) and deflection rates for the actuators. The nonlinearities introduced by these low limits are the central matter here. The problem can be reduced to one of considering a rate limited integrator having a restricted output range. This element can be used as part of the open-loop function for the nonlinear actuator model.

The rate limited integrator having a restricted output range (or the limiting integrator for the sake of brevity) is modeled as shown by the following block diagram.

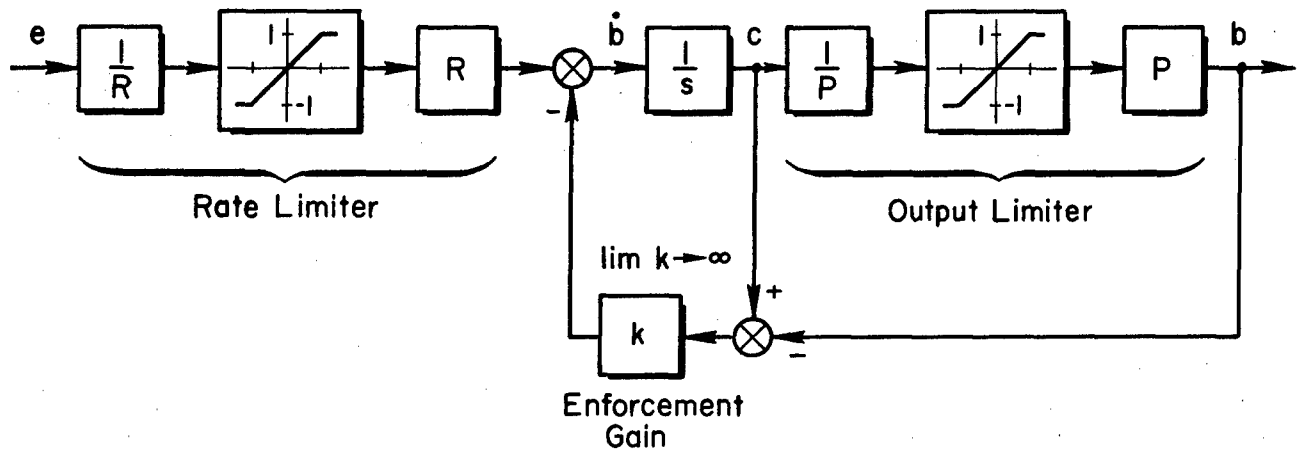


Figure 22. Mathematical Model of the Limiting Integrator

The problem of deriving the sinusoidal input describing function, $\frac{b}{e}(j\omega)$, can be broken down into a number of separate problems. Each of these corresponds to a particular mode of operation for the limiting integrator. There are four primary modes of operation. Letting C be the peak value of c and E be the peak value of e , these modes are:

<u>Mode Designation</u>	<u>Mode of Operation</u>	<u>Conditions</u>
I	Linear	$E/R \leq 1, C/P < 1$
II	Rate Limiting	$E/R > 1, C/P < 1$
III	Output Limiting	$E/R \leq 1, \lim_{k \rightarrow \infty} C/P = 1$
IV	Rate and Output Limiting	$E/R > 1, \lim_{k \rightarrow \infty} C/P = 1$

Mode IV may be further broken down into submodes a through c. Submode a occurs when no constant rate segment appears in the output waveform even though rate limiting occurs. This "masking" of the rate limiting tends to occur when the input frequency is very low and the output limit is small. Submode b occurs when a constant rate segment appears in the output waveform and this segment intersects the output limit level, P . Submode c occurs when a constant rate segment is present in the output waveform, but the constant rate segment does not intersect the output limit level, P .

Algebraic expressions are developed for the output waveforms of the limiting integrator in a table which follows. These expressions, in turn, enable one to compute the Fourier coefficients for the output waveform at the fundamental or input frequency. The output waveform is considered in the steady state, that is, to have a zero mean value and to be repetitive at the fundamental period. It is then sufficient to compute the Fourier coefficients for one-half cycle of the sine wave input. The cosine and sine Fourier coefficients at the fundamental frequency, nondimensionalized by the output limit, P , are then respectively

$$A = \frac{2}{\pi} \int_0^{\pi} \frac{b}{P} \cos(\omega t) d(\omega t) \quad (26)$$

$$B = \frac{2}{\pi} \int_0^{\pi} \frac{b}{P} \sin(\omega t) d(\omega t) \quad (27)$$

where $b = b(\omega t)$ is the expression for the output waveform.

The describing function, N , for the limiting integrator can be computed from Eq 26 and 27 and the expression for the input waveform. The expression for the input waveform when nondimensionalized by the rate limit, R , is

$$\frac{e}{R} = \frac{E}{R} \sin(\omega t) = E^* \sin(\omega t) \quad (28)$$

where E^* is the nondimensionalized amplitude of the input sine wave. However, for application of the describing function, the amplitude ratio in dB units and the phase angle in degrees of the negative inverse of the describing function are the quantities of interest. These are given by:

$$\left| -1/N \right|_{dB} = -10 \log_{10} \frac{A^2 + B^2}{E^{*2}} \quad (29)$$

$$\angle -1/N = -180 - \tan^{-1}(A/B) \text{ deg} \quad (30)$$

The remaining detail is the development of expressions for A and B for the several modes of operation which may characterize the limiting integrator. This is done in summary form in Table XX. In the first column of this table, the algebraic expression for a segment of the output waveform is given, followed in the second column by the range of validity for the expression. The fourth and fifth columns give the contribution of that segment to the Fourier cosine coefficient, A , and Fourier sine coefficient, B , respectively. For completeness, the conditions for existence of the particular mode of operation are given along with

sketches of the output waveform (solid) and the input waveform after rate limiting (dash-dot). In the following table, the nondimensionalizations given below are used.

$$\Omega = \omega/(R/P) \quad (31)$$

$$E^* = E/R \quad (32)$$

$$C^* = C/P \quad (33)$$

The equations of Table XX have been evaluated by means of a simple computer program. This program is given in Appendix III. A numerical listing for the nondimensional negative inverse of the describing function is given in Appendix IV. Those numerical results have also been plotted in a form convenient for use in Fig. 23.

The regions and subregions for the various modes of operation have been marked out in Fig. 23. A series of blank boxes has been supplied across the top of the first part of Fig. 23 so the actual frequencies for each example application may be entered. The ordinate of the plot, the normalized amplitude ratio inverse, may be adjusted to remove the normalizing factor merely shifting the 0 dB line by $|R/P|_{dB}$. The normalized input amplitude is a read-out parameter from the plot and so the actual value of the input amplitude may be computed after the limit cycle solution is found.

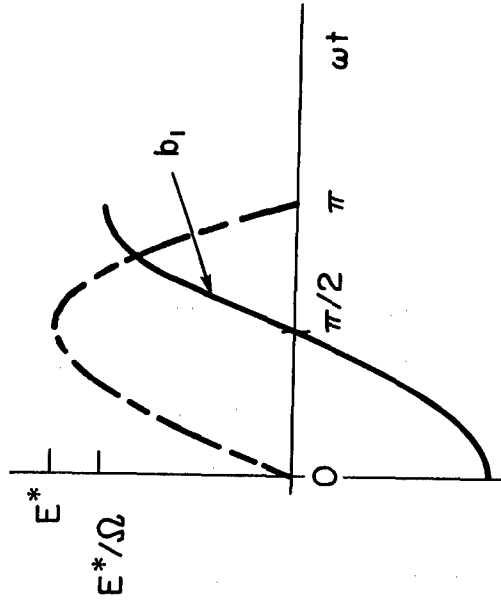
TABLE XX

SUMMARY OF FOURIER COEFFICIENTS FOR OUTPUT WAVEFORM OF THE LIMITING INTEGRATOR

CASE I Linear

Conditions for existence

$$E^* \leq 1 ; \Omega \geq E^*$$



b/P	Range of Validity For ωt	Cosine Coefficient	Sine Coefficient
$-\frac{E^*}{\Omega} \cos \omega t$	≥ 0 $< \pi$	$a_1 = -E^*/\Omega$	$b_1 = 0$

Total cosine and sine coefficients at the fundamental frequency are:

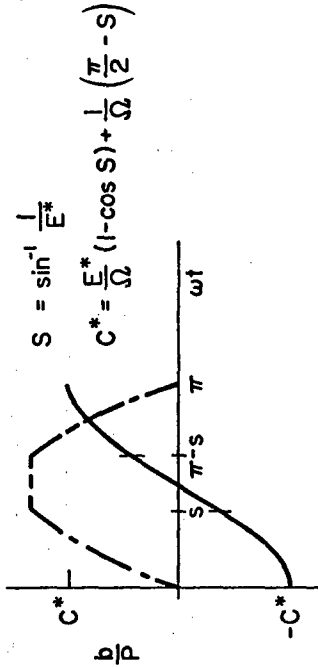
$$A = a_1 ; B = b_1 = 0$$

TABLE XX (cont'd)

CASE II Rate Limiting

Conditions for existence

$$E^* > 1 ; \infty > \Omega \geq E^* [1 - \cos S] + \frac{\pi}{2} - S$$



b/P	Range of Validity FOR ωt	Cosine Coefficient	Sine Coefficient
$\frac{E^*}{\Omega} (1 - \cos \omega t) - C^*$	≥ 0 $< S$	$a_1 = \frac{2}{\pi\Omega} \left(1 - \frac{E^*}{2} S - \frac{1}{2} \sqrt{1 - \frac{1}{E^{*2}}} \right) - \frac{2C^*}{\pi E^*}$	$b_1 = \frac{2E^*}{\pi\Omega} \left(1 - \frac{1}{2E^{*2}} - \sqrt{1 - \frac{1}{E^{*2}}} \right) - \frac{2C^*}{\pi} \left(1 - \sqrt{1 - \frac{1}{E^{*2}}} \right)$
$\frac{E^*}{\Omega} (1 - \cos S) - C^*$ $-\frac{S}{\Omega} + \frac{\omega t}{\Omega}$	$\geq S$ $< \pi - S$	$a_2 = \frac{4}{\pi\Omega E^*} \left(\frac{\pi - S - E^*}{2} \sqrt{1 - \frac{1}{E^{*2}}} \right)$	$b_2 = \frac{4}{\pi} \sqrt{1 - \frac{1}{E^{*2}}} \left\{ \frac{E^*}{\Omega} (1 - \cos S) - C^* - \frac{S}{\Omega} + \frac{\pi}{2\Omega} \right\}$
$\frac{E^*}{\Omega} (1 - \cos S) - C^* - \frac{2S}{\Omega}$ $+ \frac{\pi}{\Omega} - \frac{E^*}{\Omega} (\cos S + \cos \omega t)$	$\geq \pi - S$ $\leq \pi$	$a_3 = -\frac{2}{\pi\Omega E^*} \left\{ \frac{E^*}{\Omega} (1 - \cos S) - C^* - \frac{2S}{\Omega} + \frac{\pi}{\Omega} \right\} - \frac{E^* S}{\pi\Omega} + \frac{\sqrt{1 - \frac{1}{E^{*2}}}}{\pi\Omega}$	$b_3 = \frac{2}{\pi} \left(1 - \sqrt{1 - \frac{1}{E^{*2}}} \right) \left(L_1 - C^* - \frac{2S}{\Omega} + \frac{\pi}{\Omega} \right) - \frac{2E^*}{\pi\Omega} \left(\frac{0.5}{E^{*2}} - 1 + \sqrt{1 - \frac{1}{E^{*2}}} \right)$ where $L_1 = \frac{E^*}{\Omega} \left(1 - \cos \left[\sin^{-1} \left(\frac{1}{E^*} \right) \right] \right)$

Total cosine and sine coefficients at the fundamental frequency are:

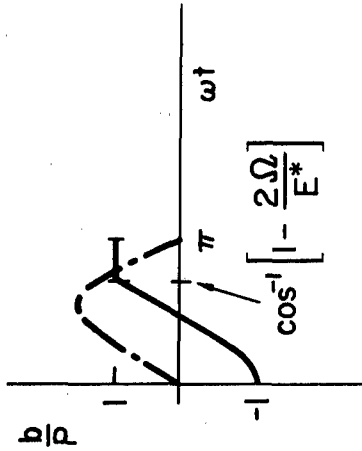
$$A = a_1 + a_2 + a_3 ; B = b_1 + b_2 + b_3$$

TABLE XX (cont'd)

CASE III Output Limiting

Conditions for existence

$$E^* \leq 1 ; E^* > \Omega > 0$$



b/p	Range of Validity For ωt	Cosine Coefficient	Sine Coefficient
$\frac{E^*}{\Omega} (1 - \cos \omega t) - 1$	≥ 0 $< \cos^{-1} \left[1 - \frac{2\Omega}{E^*} \right]$	$a_1 = \frac{2E^*}{\pi\Omega} \left[\frac{4\Omega}{E^*} \left(1 - \frac{\Omega}{E^*} \right) \right]^{1/2} \times$ $\left(\frac{1 + \frac{\Omega}{E^*}}{2} - \frac{\cos^{-1} \left(1 - \frac{2\Omega}{E^*} \right)}{2} \right)$ $- \frac{2}{\pi} \left\{ \frac{4\Omega}{E^*} \left(1 - \frac{\Omega}{E^*} \right) \right\}^{1/2}$	$b_1 = 0$
1	$\geq \cos^{-1} \left[1 - \frac{2\Omega}{E^*} \right]$ $\leq \pi$	$a_2 = - \frac{2}{\pi} \left\{ \frac{4\Omega}{E^*} \left(1 - \frac{\Omega}{E^*} \right) \right\}^{1/2}$	$b_2 = \frac{4}{\pi} \left[1 - \frac{\Omega}{E^*} \right]$

Total cosine and sine coefficients for the fundamental frequency are:

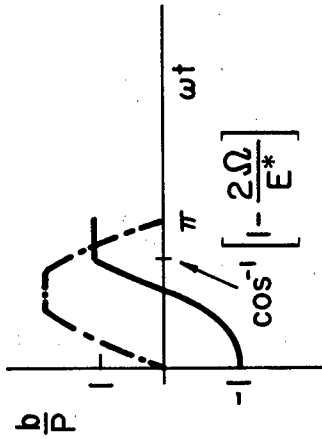
$$A = a_1 + a_2 ; B = b_1 + b_2$$

TABLE XX (cont'd)

CASE IV Rate and Output Limiting

(a) Constant rate segment does not appear in output waveform. Waveform equations and Fourier cosine and sine coefficients are same as for Case III, but conditions for existence are different. These are:

$$E^* > 1 ; \quad \frac{1}{2} E^* \left(1 - \cos \left[\sin^{-1} \frac{1}{E^*} \right] \right) \geq \Omega > 0$$



(b) Constant rate segment of output waveform intersects the output limit level.

Conditions for existence

$$E^* > 1 ; \quad \frac{\pi}{2} - S + \frac{E^*}{2} (1 - \cos S) \geq \Omega > \frac{E^*}{2} (1 - \cos S)$$

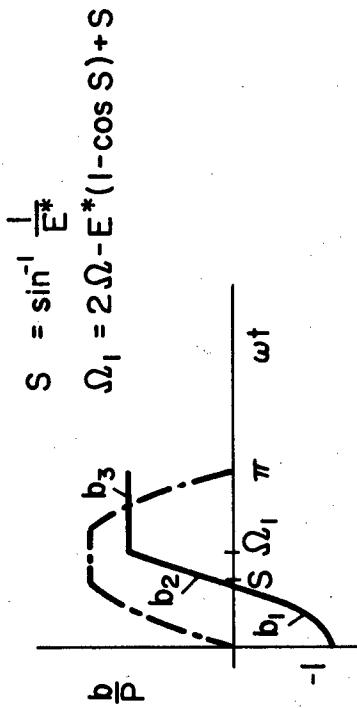


TABLE XX (cont'd)

b/P	Range of Validity For ωt	Cosine Coefficient	Sine Coefficient
$\frac{E^*}{\Omega} (1 - \cos \omega t) - 1$	≥ 0 $< S$	$a_1 = \frac{2}{\pi\Omega} \left(1 - \frac{E^*}{2} S - \frac{1}{2} \sqrt{1 - \frac{1}{E^{*2}}} \right) - \frac{2}{\pi E^*}$	$b_1 = \frac{2E^*}{\pi\Omega} \left(1 - \frac{1}{2E^{*2}} - \sqrt{1 - \frac{1}{E^{*2}}} \right) - \frac{2}{\pi} \left(1 - \sqrt{1 - \frac{1}{E^{*2}}} \right)$
$\frac{E^*}{\Omega} (1 - \cos S) - 1$ $-\frac{S}{\Omega} + \frac{\omega t}{\Omega}$	$\geq S_1$ $< \Omega_1$	$a_2 = \frac{2}{\pi} \left(\sin \Omega_1 - \frac{1}{E^*} \right) \times \left\{ \frac{E^*}{\Omega} (1 - \cos S) - 1 - \frac{S}{\Omega} \right\} + \frac{2}{\pi\Omega} \left(\cos \Omega_1 + \Omega_1 \sin \Omega_1 - \sqrt{1 - \frac{1}{E^{*2}}} - \frac{S}{E^*} \right)$	$b_2 = -\frac{2}{\pi} \left(\cos \Omega_1 - \sqrt{1 - \frac{1}{E^{*2}}} \right) \times \left\{ \frac{E^*}{\Omega} (1 - \cos S) - 1 - \frac{S}{\Omega} \right\} + \frac{2}{\pi\Omega} \left(\sin \Omega_1 - \Omega_1 \cos \Omega_1 - \frac{1}{E^*} + \sqrt{1 - \frac{1}{E^{*2}}} S \right)$
1	$\geq \Omega_1$ $\leq \pi$	$a_3 = -\frac{2}{\pi} \sin \Omega_1$	$b_3 = \frac{2}{\pi} (\cos \Omega_1 + 1)$

Total cosine and sine coefficients at the fundamental frequency are:

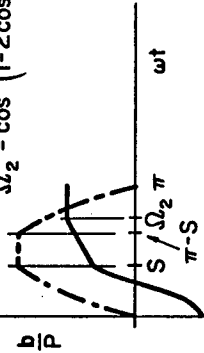
$$A = a_1 + a_2 + a_3 \quad ; \quad B = b_1 + b_2 + b_3$$

TABLE XX (concluded)

(c) Constant rate segment in the output waveform does not intersect the output limit level.

$$S = \sin^{-1} \frac{1}{E^*}$$

$$\Omega_2 = \cos^{-1} \left(1 - 2 \cos S + \frac{\pi}{E^*} - \frac{2S}{E^*} - \frac{2\Omega}{E^*} \right)$$



Conditions for existence

$$E^* > 1 ; E^*(1 - \cos S) + \frac{\pi}{2}$$

$$-S \geq \Omega \geq \frac{E^*}{2} (1 - \cos S) + \frac{\pi}{2} - S$$

b/P	Range of Validity For ωt	Cosine Coefficient	Sine Coefficient
$\frac{E^*}{\Omega} (1 - \cos S) - 1$	≥ 0	$a_1 = \frac{2}{\pi} \left(1 - \frac{E^*}{2} S - \frac{1}{2} \sqrt{1 - \frac{1}{E^{*2}}} \right)$	$b_1 = \frac{2E^*}{\pi} \left(1 - \frac{1}{2E^{*2}} - \sqrt{1 - \frac{1}{E^{*2}}} \right)$
$\frac{E^*}{\Omega} (1 - \cos S) - 1$	$< S$	$-\frac{2}{\pi E^*}$	$-\frac{2}{\pi} \left(1 - \sqrt{1 - \frac{1}{E^{*2}}} \right)$
$\frac{E^*}{\Omega} (1 - \cos S) - 1$	$\geq S$	$a_2 = \frac{1}{\pi \Omega E^*} \left(\frac{\pi}{2} - S - E^* \sqrt{1 - \frac{1}{E^{*2}}} \right)$	$b_2 = \frac{1}{\pi} \sqrt{1 - \frac{1}{E^{*2}}} \left\{ \frac{E^*}{\Omega} (1 - \cos S) - 1 - \frac{S}{\Omega} + \frac{\pi}{2\Omega} \right\}$
$-R1 + \frac{\omega t}{\Omega}$	$< \pi - S$		$-1 - \frac{S}{\Omega} + \frac{\pi}{2\Omega}$
$\frac{E^*}{\Omega} (1 - \cos S) - 1$	$\geq \pi - S$	$a_3 = \frac{2}{\pi} \left(\sin \Omega_2 - \frac{1}{E^*} \right) \times$	$b_3 = -\frac{2}{\pi} \left(\cos \Omega_2 + \sqrt{1 - \frac{1}{E^{*2}}} \right)$
$-\frac{E^*}{\Omega} (\cos S + \cos \omega t)$	$< \Omega_2$	$\left\{ \frac{E^*}{\Omega} (1 - \cos S) - 1 - \frac{2S}{\Omega} + \frac{\pi}{\Omega} \right\}$ $-\frac{2E^*}{\pi} \left\{ \sqrt{1 - \frac{1}{E^{*2}}} \left(\sin \Omega_2 - \frac{0.5}{E^*} \right) + \frac{\Omega_2}{2} \frac{\sin 2 \Omega_2}{4} - \frac{\pi + S}{2} \right\}$	$\left\{ \frac{E^*}{\Omega} (1 - \cos S) - 1 - \frac{2S}{\Omega} + \frac{\pi}{\Omega} \right\}$ $-\frac{E^*}{\pi} \left\{ -2 \sqrt{1 - \frac{1}{E^{*2}}} \cos \Omega_2 - \frac{2}{\cos 2 \Omega_2} + \frac{1}{E^{*2}} \right\}$
1	$\geq \Omega_2$	$a_4 = -\frac{2}{\pi} \sin \Omega_2$	$b_4 = \frac{2}{\pi} (\cos \Omega_2 + 1)$
	$\leq \pi$		

Total cosine and sine coefficients at the fundamental frequency are:

$$A = a_1 + a_2 + a_3 + a_4 ; B = b_1 + b_2 + b_3 + b_4$$

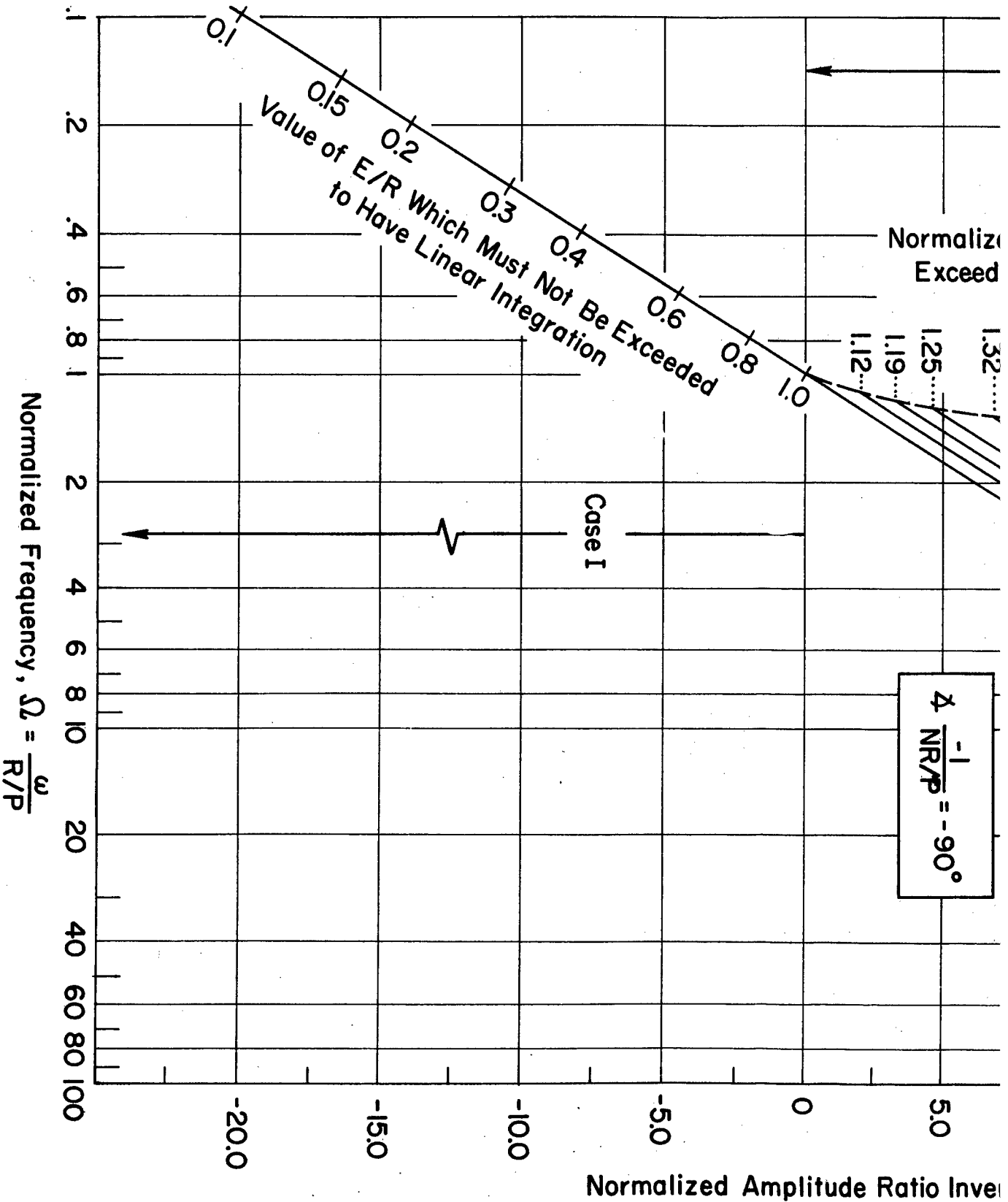
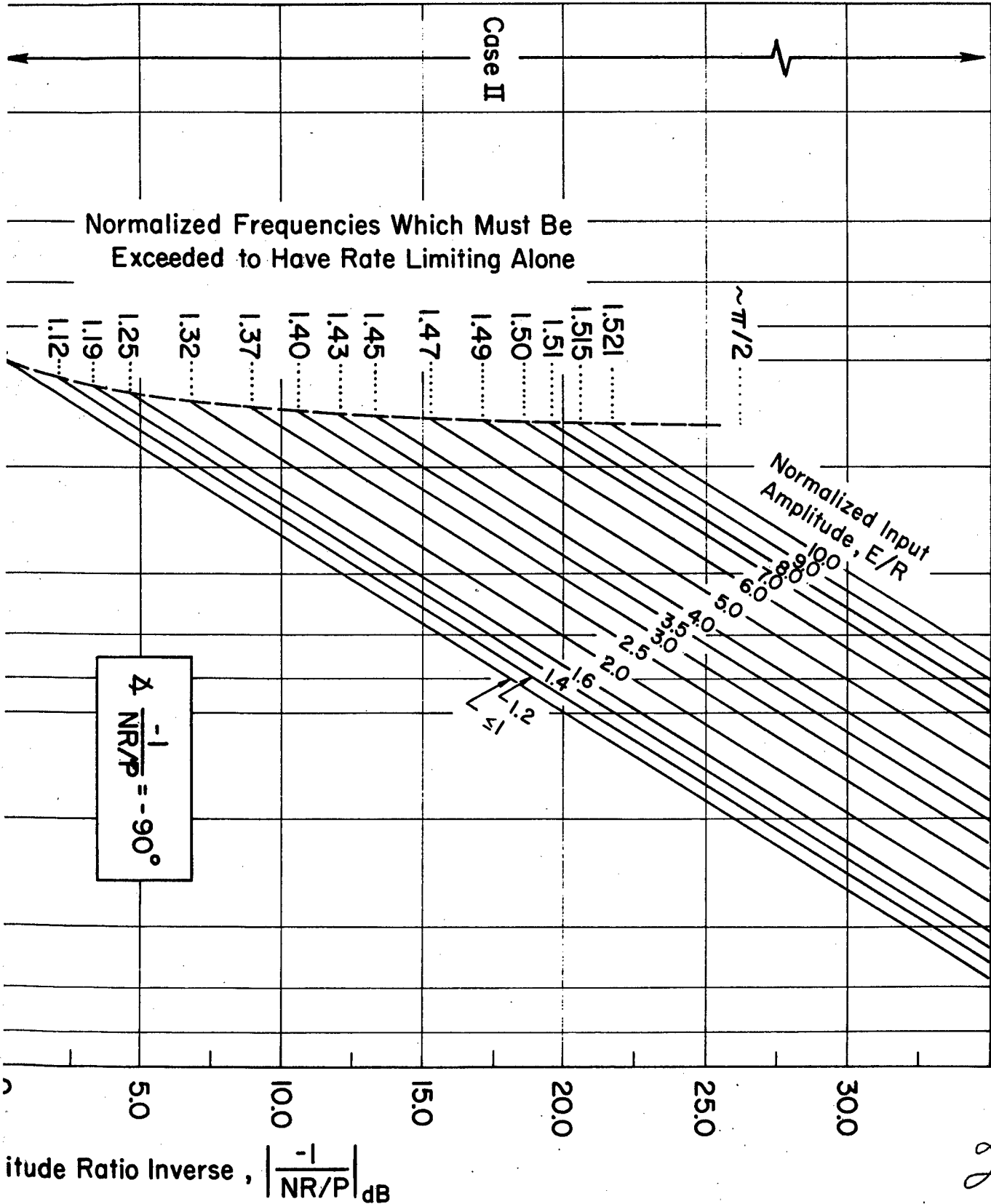


Figure 23. Negative Inverse of Normalized Sinusoidal Input Describing Function for a Limiting Integrator (Two pages)



2

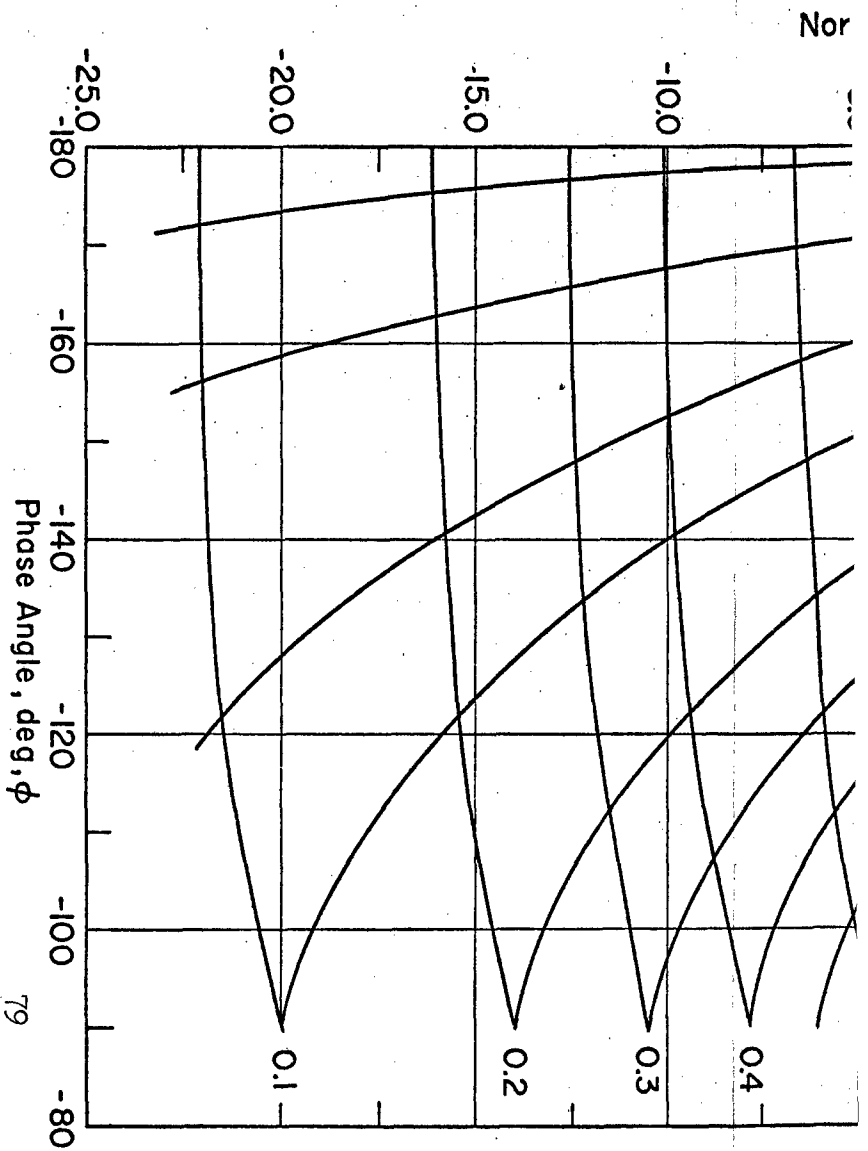
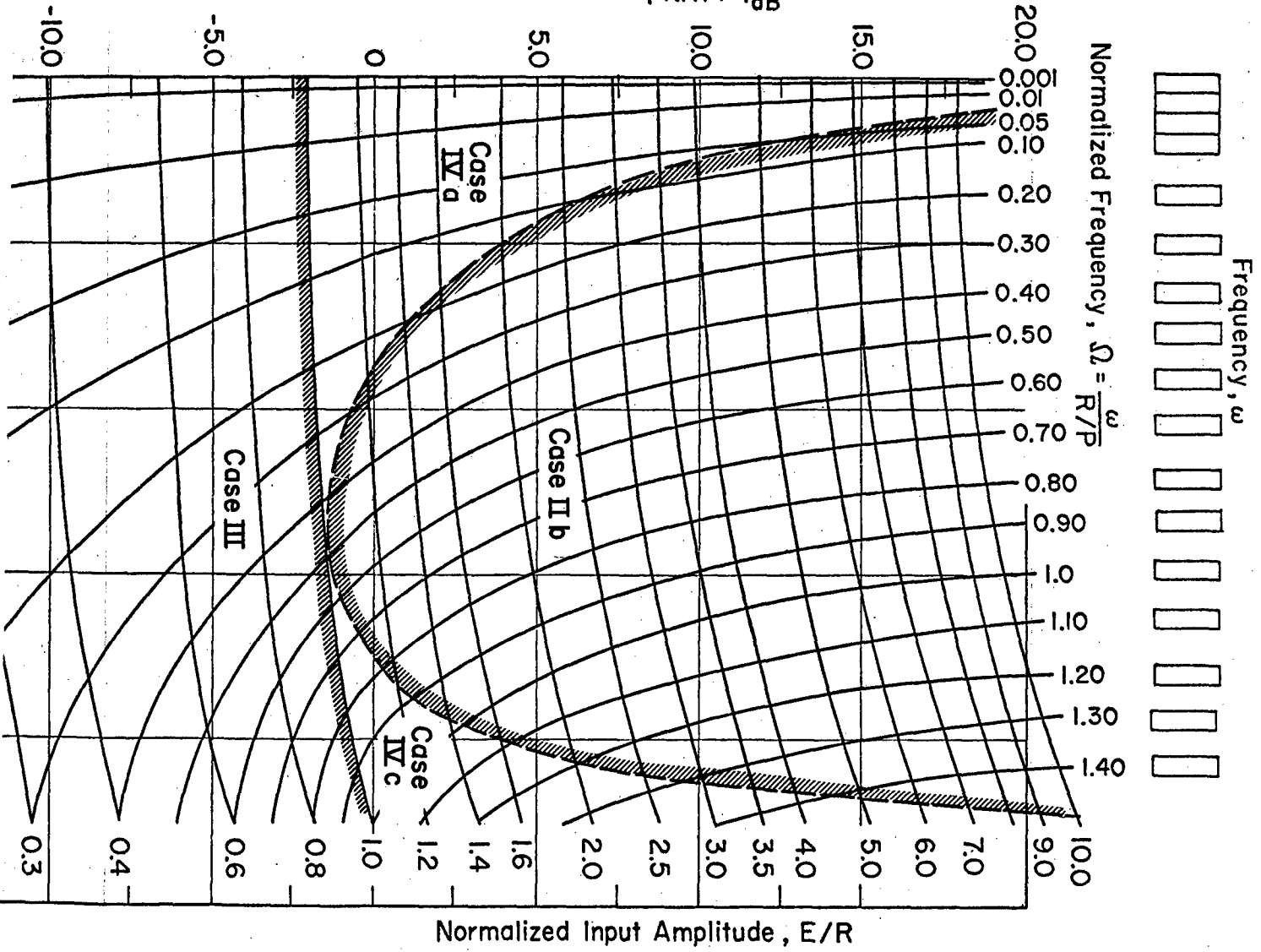


Figure 25 (concluded)

Normalized Amplitude Ratio Inverse, $\left| \frac{-1}{NR/P} \right|_{dB}$



A. VALIDITY OF THE DESCRIBING FUNCTION

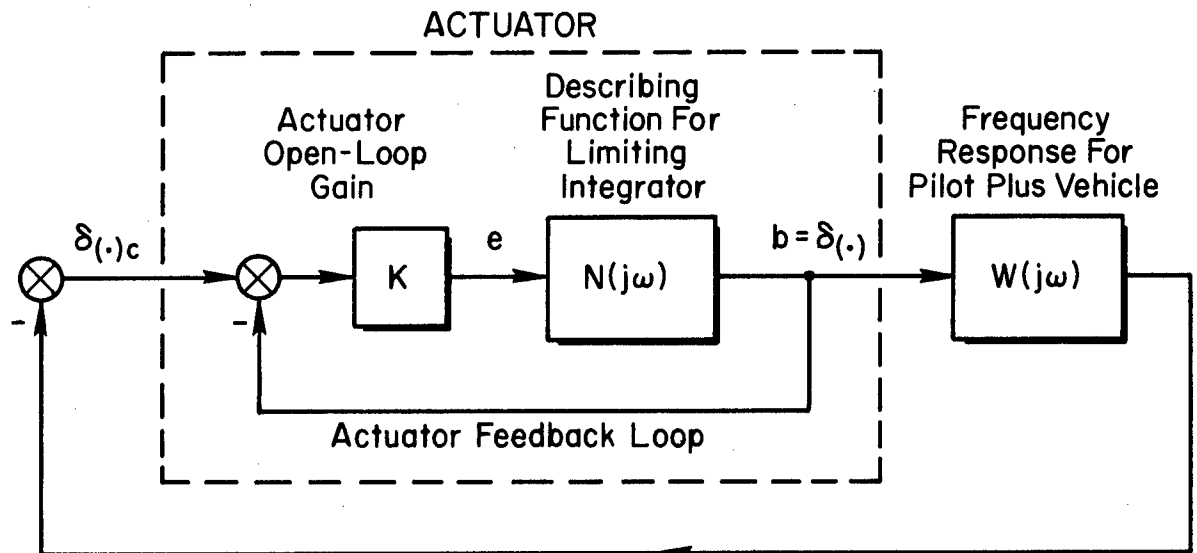
Validity of the sinusoidal input describing function technique is often tied to the requirement that linear portion of the loop containing the nonlinear element have a low pass nature. This is to insure that the higher harmonics of the fundamental or limit cycle frequency are sufficiently attenuated in traversing the loop that they do not cause the input waveform to the nonlinear element to be appreciably non-sinusoidal.

When the limiting integrator is part of the open-loop function for an actuator having unity gain feedback, it is quite clear that the linear frequency response function will not have a low pass nature. (Refer to Fig. 24.) The question is, "How will this unusual feature affect the validity of the results?" The answer is, "Not at all." This is because the nonlinear element itself contains an integration which, of course, is of a low pass nature. Furthermore, except in the presence of severe output limiting the nonlinear element output waveform tends to be reasonably sine-like. This may be appreciated from the sketches in Table XX. Consequently, the describing function for the limiting integrator can be expected to be valid for applications in which the frequency response amplitude ratio for the linear portion of the loop remains finite as the frequency becomes infinite.

B. APPLYING THE DESCRIBING FUNCTION

Application of the describing function requires a frequency response plot (amplitude ratio in dB versus phase angle with frequency as a parameter) for the remaining linear part of the system under investigation, $K[1+W(j\omega)]$. Refer to Fig. 24. This frequency response is for the portion of the system which has as its input, the output of the limiting integrator, and has as its output the input to the limiting integrator. This frequency response is overplotted on the describing function of Fig. 23 after the nondimensionalizing factors have been accounted for. This in effect solves the equation:

$$K[1 + W(j\omega)] = -1/N(j\omega) \quad (34)$$



$\delta(\cdot)_c$ = Commanded Actuator Deflection

$\delta(\cdot)$ = Actuator Deflection

Figure 24. Loop Structure Containing Nonlinear Actuator

Limit cycle solutions are indicated by intersections of the frequency response curve with the describing function which have identical amplitude ratio, phase and frequency. Since amplitude ratio and phase are made identical by overplotting, one need only inspect for possible frequency intersections. If a frequency intersection is found, the corresponding value of the normalized input amplitude is noted. When the limit cycle found is a stable one, the frequency at that intersection and the corresponding input amplitude can be used along with various frequency response functions for the linear portion of the system to determine the amplitudes of the various system variables in the limit cycle condition. It is evident from Fig. 23 that limit cycles are possible only if the phase

angle of the frequency response enters the closed interval, -90 deg to -180 deg. In applications where a unity gain feedback loop is closed around the limiting integrator, the phase angle is asymptotic to 0 deg at high frequencies. This means that it will often be possible to avoid limit cycles in such cases through proper design of the lower frequency portion of the frequency response function.

The stability of the limit cycles indicated by the intersections can be determined using the conventional rule of thumb applied to plots on the coordinates of the Nichols' chart, i.e. amplitude in dB vs. phase angle in deg. To paraphrase Ref. 14 on this rule of thumb,

If the frequency response curve and the describing function are assigned a direction sense, so that the frequency response curve is "pointing" in the direction of increasing frequency and the describing function, with phase held constant in the direction of increasing amplitude, then a convergent situation will occur when the describing function in the direction of increasing amplitude appears to an observer on the frequency response curve facing in the direction of increasing frequency, to cross from left to right. When the opposite of these equivalent conditions occurs, the state of the system is divergent and the limit cycle is unstable.

An unstable limit cycle means that the system is divergent from the indicated limit cycle condition. From an unstable limit cycle, oscillations of the system will either increase or decrease in amplitude depending upon the direction of disturbance from the limit cycle condition. The unstable limit cycles for the examples at hand, can be used to form estimates of those regions of the state space where recovery to a stable condition is not possible with a given nonlinear controller.

Stable limit cycle solutions for the examples at hand correspond to pilot induced oscillations.

The next Section will cover applications of the sinusoidal describing function for the prediction and avoidance of pilot induced oscillations.

SECTION V

PREDICTION AND AVOIDANCE OF PILOT INDUCED OSCILLATIONS

Prediction and avoidance of pilot induced oscillations and instabilities is accomplished by applying linear servo analysis and sinusoidal input describing function techniques. The linear servo analysis is used to identify pilot induced oscillations or instabilities arising because of neutrally stable or unstable linear pilot-vehicle-flight control system behavior. The sinusoidal input describing function technique is used to identify stable limit cycles arising because of nonlinearities in the pilot-vehicle-flight control system. The sinusoidal input describing function technique can also be used to identify unstable limit cycles. These, in turn, may be used to estimate initial conditions from which convergent control with a given nonlinear system is not possible.

Two different nonlinear elements must be considered in analyzing the three back-up system configurations. These are the limiting integrator for which the describing function was derived in Section IV, and the simple limiter. The negative inverse describing function for the normalized limiter is plotted in Fig. 25. The data for Fig. 25 is from p. 132 of Ref. 14.

The limiting integrator forms part of the actuator model in System A. The limiter alone represents the control surface stops or pilot strength limitations in Systems B and C.

When investigating pilot induced oscillations, two different conditions should be considered. These represent susceptibility to initiating the oscillation and the ability to sustain the oscillation. The susceptibility is evaluated by assuming that the pilot controls in the normal way except that the amount of lead equalization he supplies is reduced. To investigate whether or not the oscillation is sustained it is assumed that the pilot is behaving in a synchronous way, that is, that his effective time delay is zero; and that the amount of lead equalization he supplies is reduced. Given these modes of pilot behavior which are characteristic of the pilot's role in inducing oscillations, it is an easy matter to evaluate,

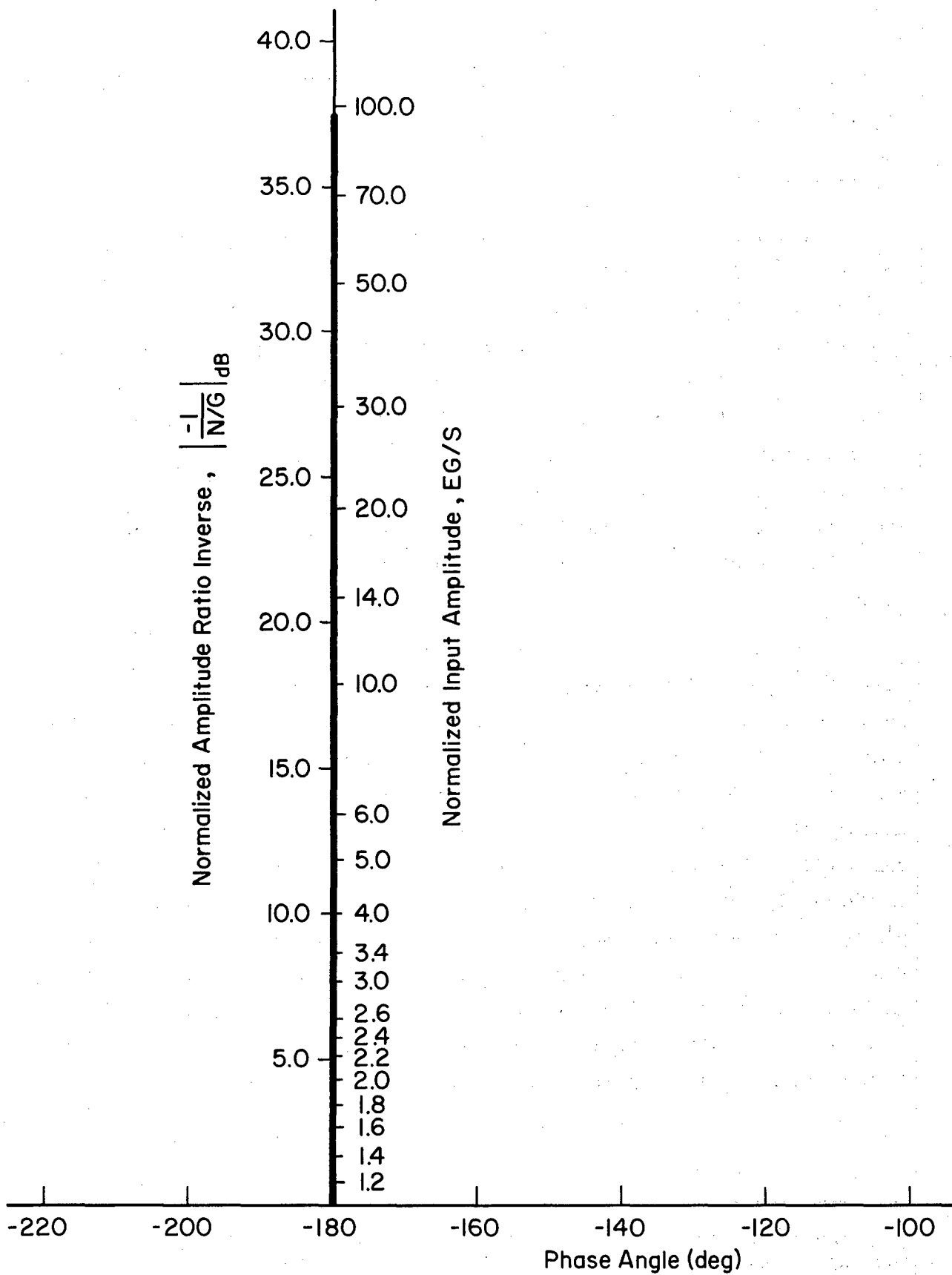


Figure 25. Sinusoidal Input Describing Function for Normalized Limiter

using the describing function technique, the propensity of the system to produce these oscillations.

A. SYSTEM A

Application of the describing function for the limiting integrator for System A will be considered first. The portions of the frequency response for which the phase angle is between -90 deg and -180 deg for longitudinal System A are given in Fig. 26 and 27. Figure 26 is for the proneness condition, that is, with normal effective delay for the pilot and degraded lead equalization. Figure 27 is for the condition for continuing, that is, with zero effective delay for the pilot and degraded lead equalization. The two figures show that fairly substantial lead degradation is required before the phase angle enters the -90 deg to -180 deg region wherein the conditions for a limit cycle may be satisfied.

In the case of Fig. 26 for $K_0 = 0.0$ sec, the frequencies for which the phase angle is in the -90 deg to -180 deg range preclude limit cycles involving output limiting. This is because those frequencies are greater than the maximum frequency for which output limiting is possible, $\pi/2 \times R/P = 1.048$ rad/sec. Since this is the case, only the frequency characteristics at a phase angle of -90 deg are of interest. That is, only point (A) in Fig. 26 is of interest. The amplitude ratio at point (A) is 20.25 dB, and the frequency is 1.075 rad/sec. This is overplotted on the appropriate part of the normalized limiting integrator describing function plot in Fig. 28. The point is again labeled (A). This point falls on the curve for $E/R = 12.3$.* Since $R = 1.0$ deg/sec, $E = 12.3$ deg/sec also. The describing function crosses the frequency response curve from left to right indicating the limit cycle is a stable one.

*The range for E/R in the "standard" describing function plot only goes up to 10.0. This value for E/R was hand computed.

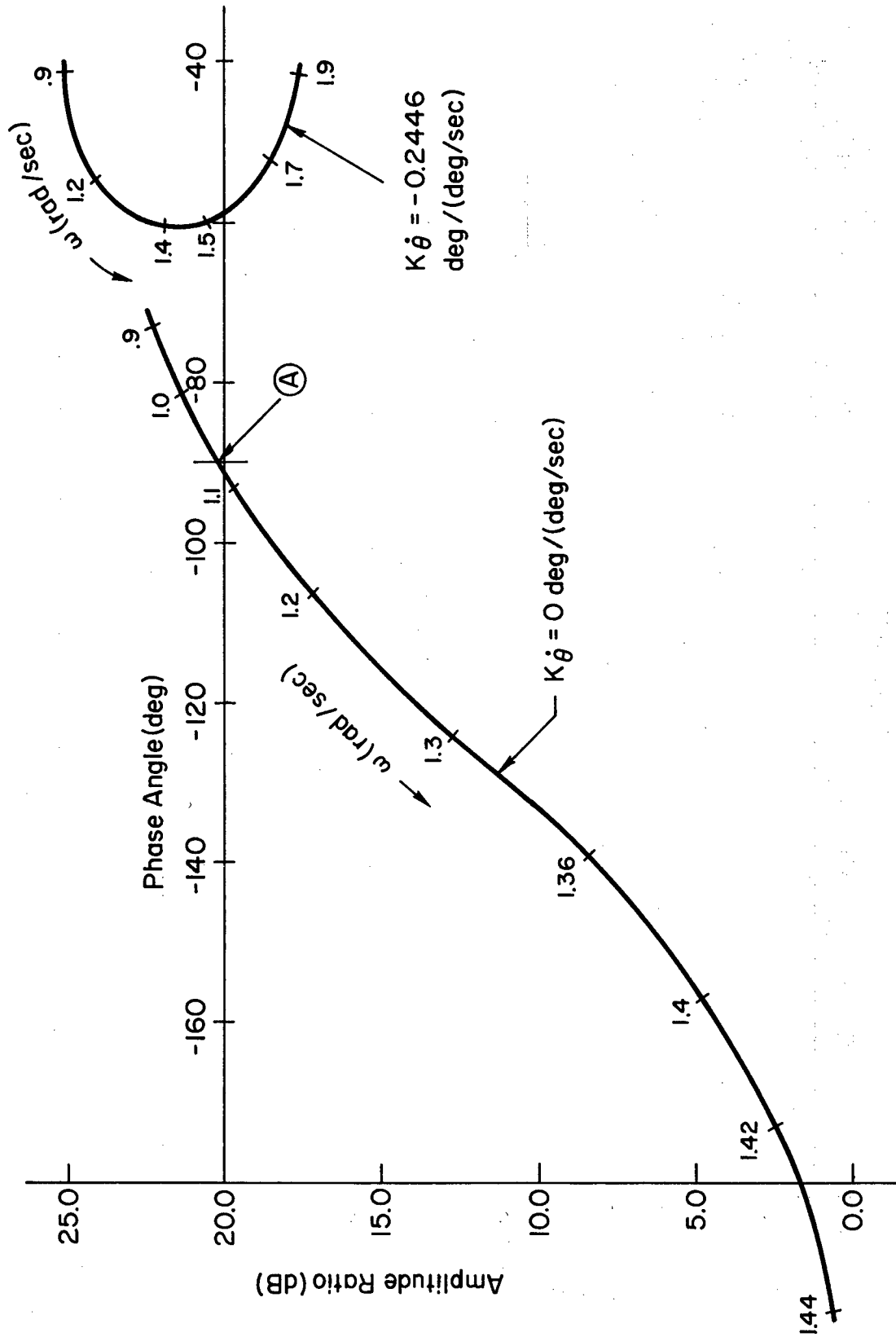


Figure 26. Frequency Response for Longitudinal System A
Proneness Condition ($\tau_s = 0.2 \text{ sec}$)

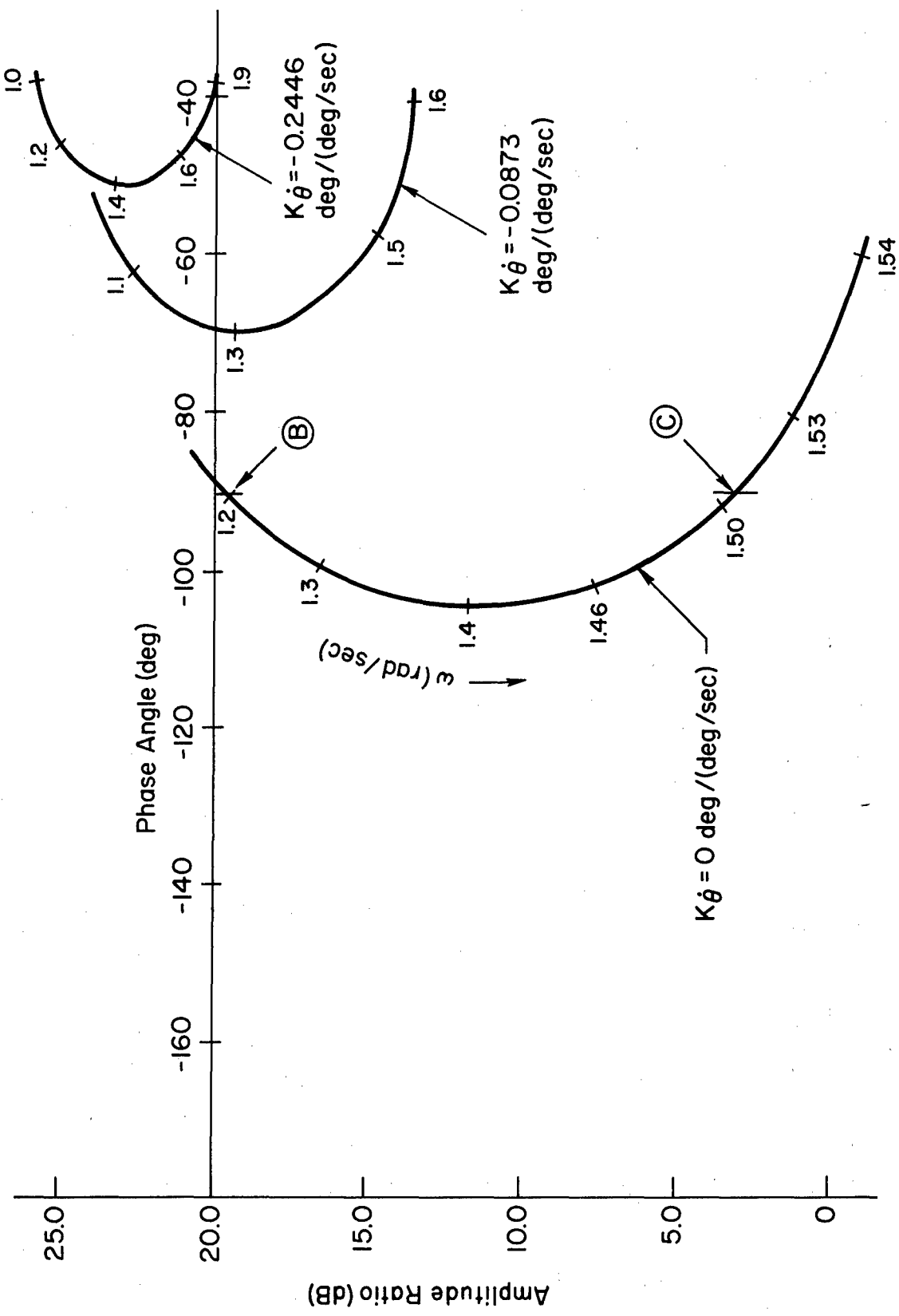


Figure 27. Frequency Response for Longitudinal System A
Sustenance Condition ($\tau_s = 0.0 \text{ sec}$)

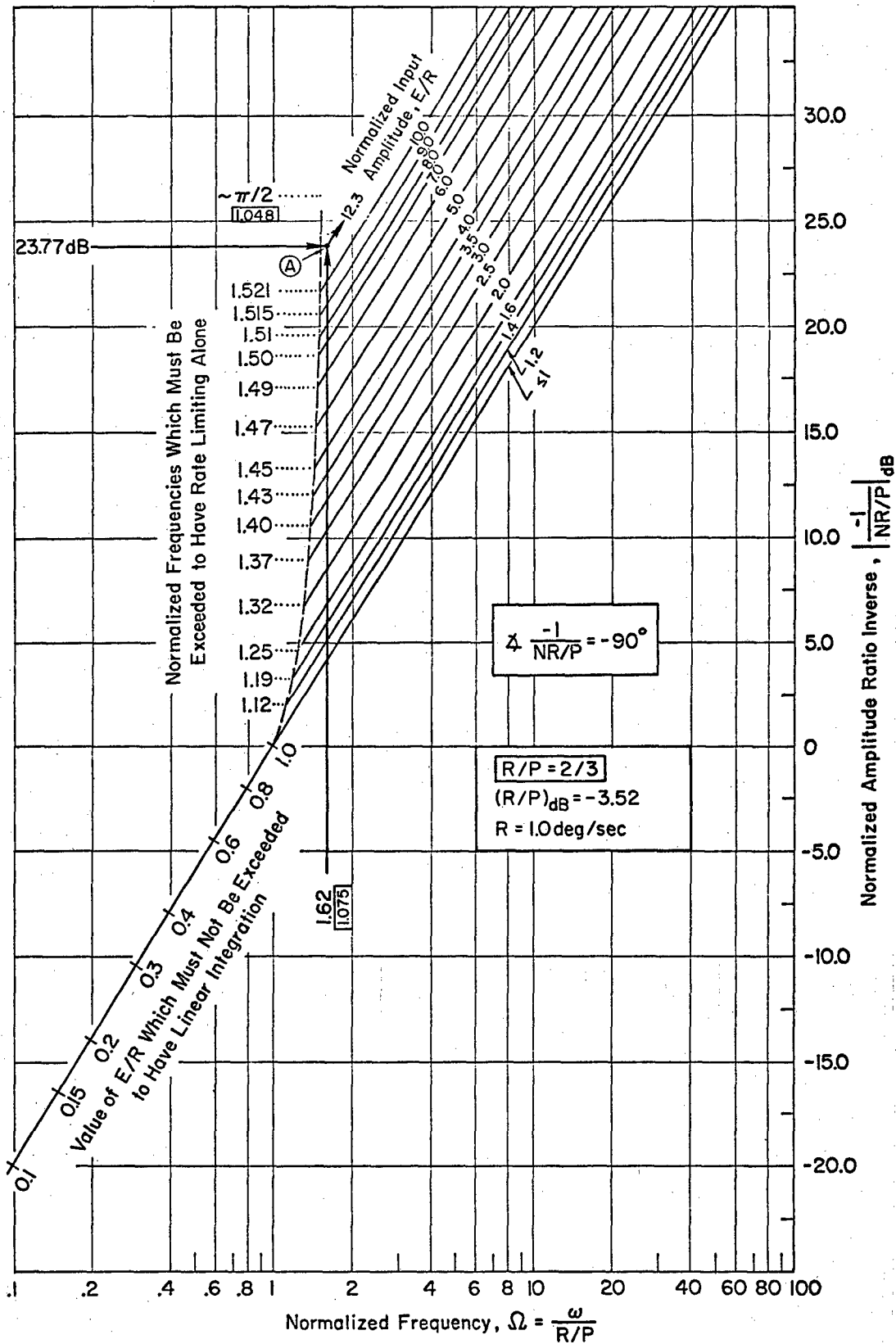


Figure 28. Determining the Limit Cycles for Longitudinal System A with $\tau_s = 0.2 \text{ sec}$ and $K_{\theta} = 0.0 \text{ sec}$

The amplitude, $E = 12.3$ deg/sec, and the frequency, $\omega = 1.075$ rad/sec, of the signal at the input to the limiting integrator may then be used to compute the limit cycle amplitudes of other variables. For example, the amplitude of δ_s is:

$$\text{amplitude of } \delta_s = |N| E = \frac{1}{10.3} \times 12.3 = 1.19 \text{ deg} \quad (35)$$

where $|N|$ is the amplitude ratio of the describing function at point (A). That is, $|N|$ is computed from $|-1/(NR/P)|_{dB} = 23.77$, the value at point (A) in Fig. 28. The values for R and P are obtained from Table I. These are $R = 1.0$ deg/sec and $P = 1.5$ deg. It is also possible to compute the limit cycle amplitude for θ and $n_z = a_z/g$ using the transfer functions in Table XXV of Appendix I and the expressions in Table XXVII of Appendix II. Factored expressions for $N_{\delta_s}^{\theta'}$ and Δ' are available in Figs. 40 and 41 of Appendix II.

$$\begin{aligned} \text{amplitude of } \theta &= \left| \frac{N_{\delta_s}^{\theta'}}{\Delta'} \right|_{s=j 1.075} |N| E \\ &= 57.3 \times 0.0807 \times 1.19 = 5.54 \text{ deg} \end{aligned} \quad (36)$$

$$\begin{aligned} \text{amplitude of } n_z &= \frac{1}{g} \left| \frac{N_{\delta_s}^{a_z'}}{\Delta'} \right|_{s=j 1.075} |N| E \\ &= \frac{1}{32.2} \times 11.82 \times 1.19 = 0.438 \text{ g's} \end{aligned} \quad (37)$$

In the case of Fig. 27 for $K_0^* = 0.0$ sec, the frequencies for which the phase angle is in the -90 deg to -180 deg range also preclude limit cycles involving output limiting for the same reason as is given above. Since this is the case, only the frequency characteristics at a phase angle of -90 deg are of interest. That is, only points (B) and (C) in Fig. 27 are of interest. At point (B), the amplitude ratio is 19.5 dB and the frequency is 1.20 rad/sec. At point (C), the amplitude ratio is 3.25 dB and the frequency is 1.505 rad/sec. Points (B) and (C) are overplotted on the appropriate part of the normalized limiting integrator describing function

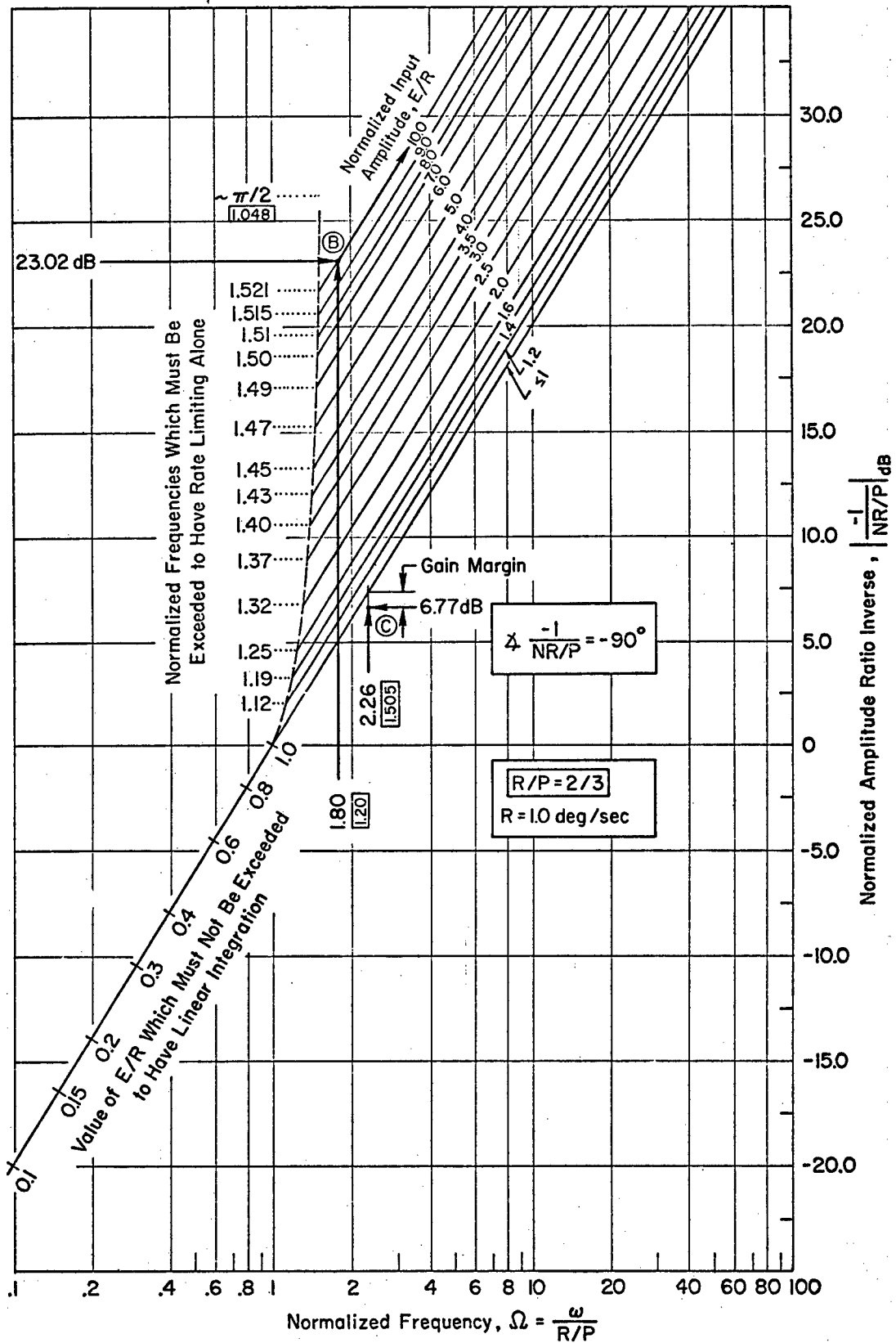


Figure 29. Determining the Limit Cycles for Longitudinal System A with $\tau_s = 0.0 \text{ sec}$ and $K_\theta = 0.0 \text{ sec}$

plot in Fig. 29. Point (B) falls on the curve for $E/R = 10.0$. Since $R = 1.0$ deg/sec, $E = 10.0$ deg/sec. The describing function crosses the frequency response curve at point (B) from left to right, indicating that the limit cycle is a stable one.

Point (C) does not intersect the describing function. A gain margin of 0.65 dB exists so that no limit cycle is indicated at point (C).

The portions of the frequency response for which the phase angle is between -90 deg and -180 deg for lateral System A are given in Fig. 30. Both the proneness ($\tau_{sp} = 0.2$ sec) and the continuation ($\tau_{sp} = 0.0$ sec) conditions are shown in this figure. For lateral control with System A, the pilot does not supply lead equalization (K_{ϕ} is zero) and so the degradation of lead equalization cannot be a factor in possible lateral pilot induced oscillations.

The frequency responses are overplotted on the describing function for the limiting integrator. Intersections with the describing function occur in region (D) and possibly in region (E) of Fig. 31. Region (D) corresponds to an approximate frequency of 0.14 rad/sec and an approximate normalized input amplitude, $E/R = 15.0$. Since $R = 15.0$ deg/sec, $E = 225.0$ deg/sec. The describing function crosses the frequency response curves from right to left indicating an unstable limit cycle. By the location of the intersection on the describing function plot, it is evident that both rate and output limiting are involved in the nonlinear behavior.

These results can be used to estimate conditions from which it would be impossible to track the localizer reference in a stable manner with the existing nonlinear control. This estimate is made by determining those combinations of localizer deviation and deviation rate which exceed the unstable limit cycle values. The unstable limit cycle values for these variables may be determined using frequency response techniques. These steps are performed below.

If conditions occur such that

$$y^2 + (\dot{y}/\omega)^2 > \left(\begin{array}{l} \text{amplitude squared of } y \\ \text{for unstable limit cycle} \end{array} \right) \quad (38)$$

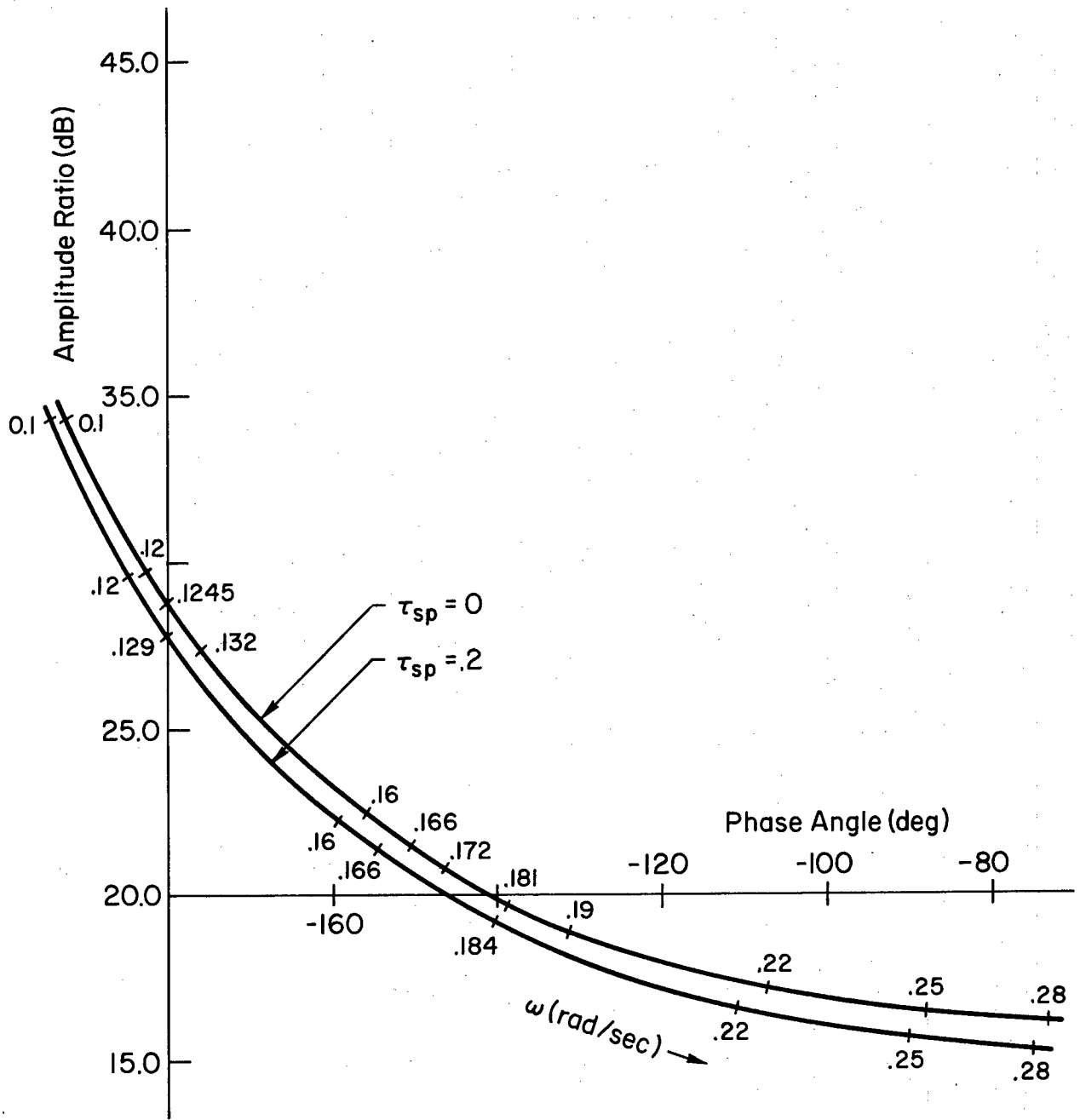


Figure 30. Frequency Response for Lateral System A. Proneness Condition ($\tau_{sp} = 0.2$ sec) and Sustenance Condition ($\tau_{sp} = 0.0$ sec)

then it will not be possible to track the localizer reference in a stable manner. The amplitude of the localizer deviation, y , for the unstable limit cycle is:

$$\begin{aligned} \text{amplitude of } y &= \left| \frac{N_{\delta_{sp}}^y}{\Delta'} \right|_{s=j 0.14} |N| E \\ &= 77.80 \times \frac{1}{20.0} \times 225.0 = 875.0 \text{ ft} \end{aligned} \quad (39)$$

At an altitude of 100.0 ft, $y = 875.0$ ft corresponds to 17.5 deg in "LOC" units (mean-square for an oscillation would be $(17.5)^2/2 = 154.5$ (deg LOC) 2). Since

$$\dot{y} = s y \doteq V_{T_0} \psi \quad (40)$$

the amplitude may alternately be stated in terms of ψ .

$$\begin{aligned} \text{amplitude of } \psi &= \frac{\omega}{V_{T_0} \cos \Gamma_0} \times (\text{amplitude of } y) \times 57.3 \\ &= \frac{0.14}{332.5} 875.0 \times 57.3 = 21.1 \text{ deg} \end{aligned} \quad (41)$$

The corresponding mean square for an oscillation would be $(21.1)^2/2 = 223.0$ deg 2 .

Measured mean-square values in excess of those cited above might indicate that conditions were encountered from which it was not possible to track the localizer reference in a stable manner with the nonlinear control. Indeed, the three runs (DS, 11/21/69, 19 through DS, 11/21/69, 21 in Table XXXXVI of Appendix VI) which the pilot subject termed "unsuccessful" very nearly satisfy this criterion. It must also be borne in mind, however, that the measurements were made in what may possibly have been a transient situation of short duration while the theory being used here rests upon the presumption of steady state condition.

Region (E) must be projected on the constant phase portion of the describing function plot for the limiting integrator, Fig. 32. This is necessary in order to determine if an intersection actually exists. Region (E), when projected, does not intersect the describing function. A gain margin of 28.2 dB exists so that no limit cycle is indicated for region (E).

To summarize the results, for longitudinal control, System A can be said to be slightly to modestly prone to pilot induced oscillations. However, to develop and sustain the oscillation requires virtually complete neglect of the pitch rate feedback task by the pilot. This may be judged unlikely. A longitudinal pilot induced oscillation, if encountered, would be characterized by moderate frequency, low g, and moderate pitch angle. No stable pilot induced oscillations are indicated for lateral control using System A. However, it is possible for large deviations from the localizer reference, large rates of deviation, or combinations of both to present conditions under which stable tracking of the localizer reference is not possible for the given nonlinear control system. These conditions are indicated by the unstable limit cycle in lateral control by means of System A.

B. SYSTEM B

Next, the longitudinal portion of System B will be evaluated for proneness to pilot induced oscillations.

The portions of the frequency response for the linear part of the system for which the phase angle is approximately -180 deg are overplotted on the normalized describing function for the limiter in Fig. 33 and 34. The proneness conditions ($\tau_s = 0.2$ sec) are in Fig. 33, while the conditions for continuing the oscillation ($\tau_s = 0.0$ sec) are in Fig. 34. It turns out that an almost complete degradation of the lead equalization ($K_\theta \rightarrow 0.0$) is necessary before longitudinal System B becomes prone to pilot induced oscillations. Refer to point (F) in Fig. 33. However, even in this case the conditions for continuing the oscillations are not met. That is, in the vicinity of 0 dB and -180 deg in Fig. 34 the frequency response curve for $K_\theta = 0.0$ passes close by the describing function curve but does not intersect it.

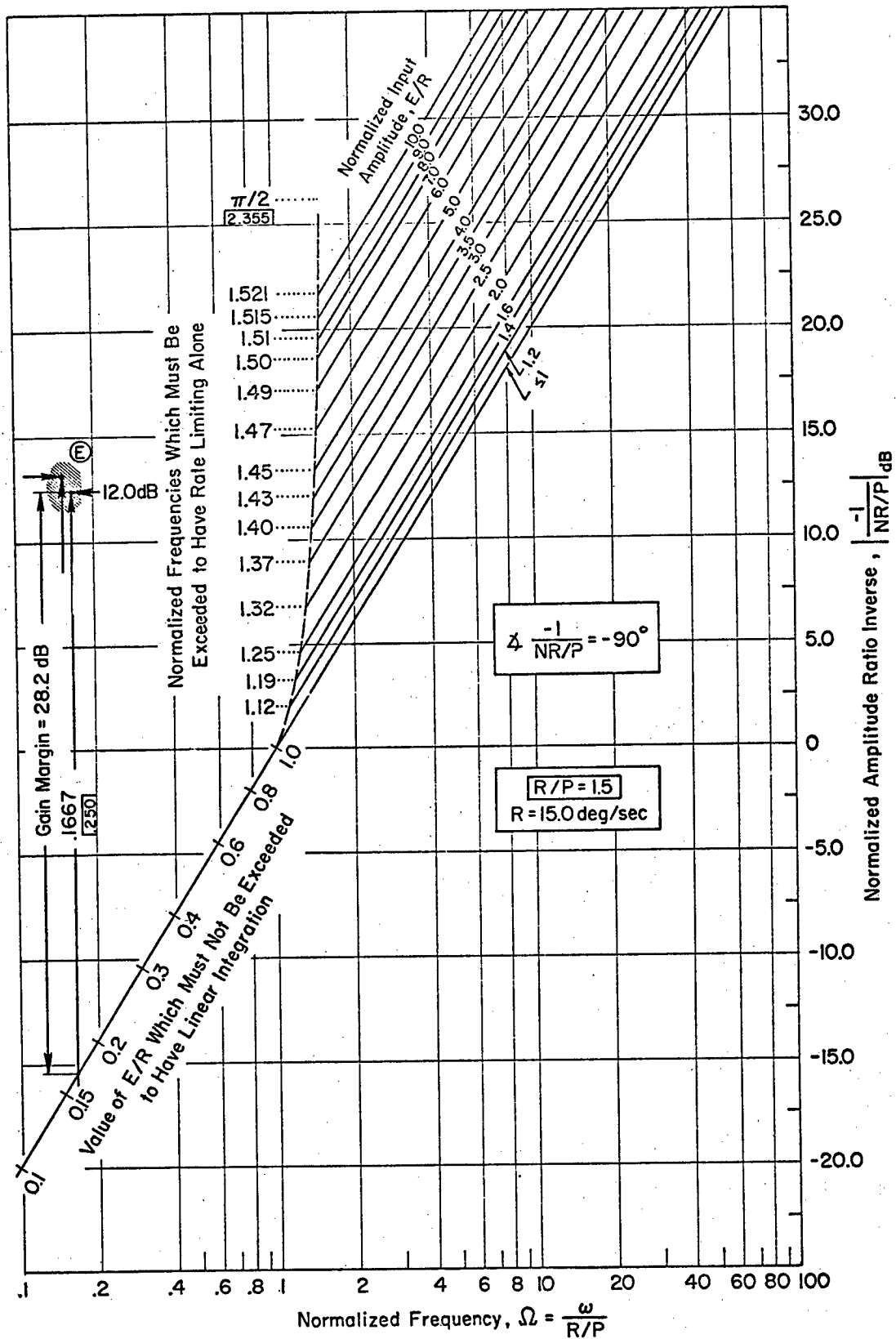


Figure 32. Determining the Limit Cycles for Lateral System A with $\tau_{sp} = 0.2$ sec and $\tau_{sp} = 0.0$ sec

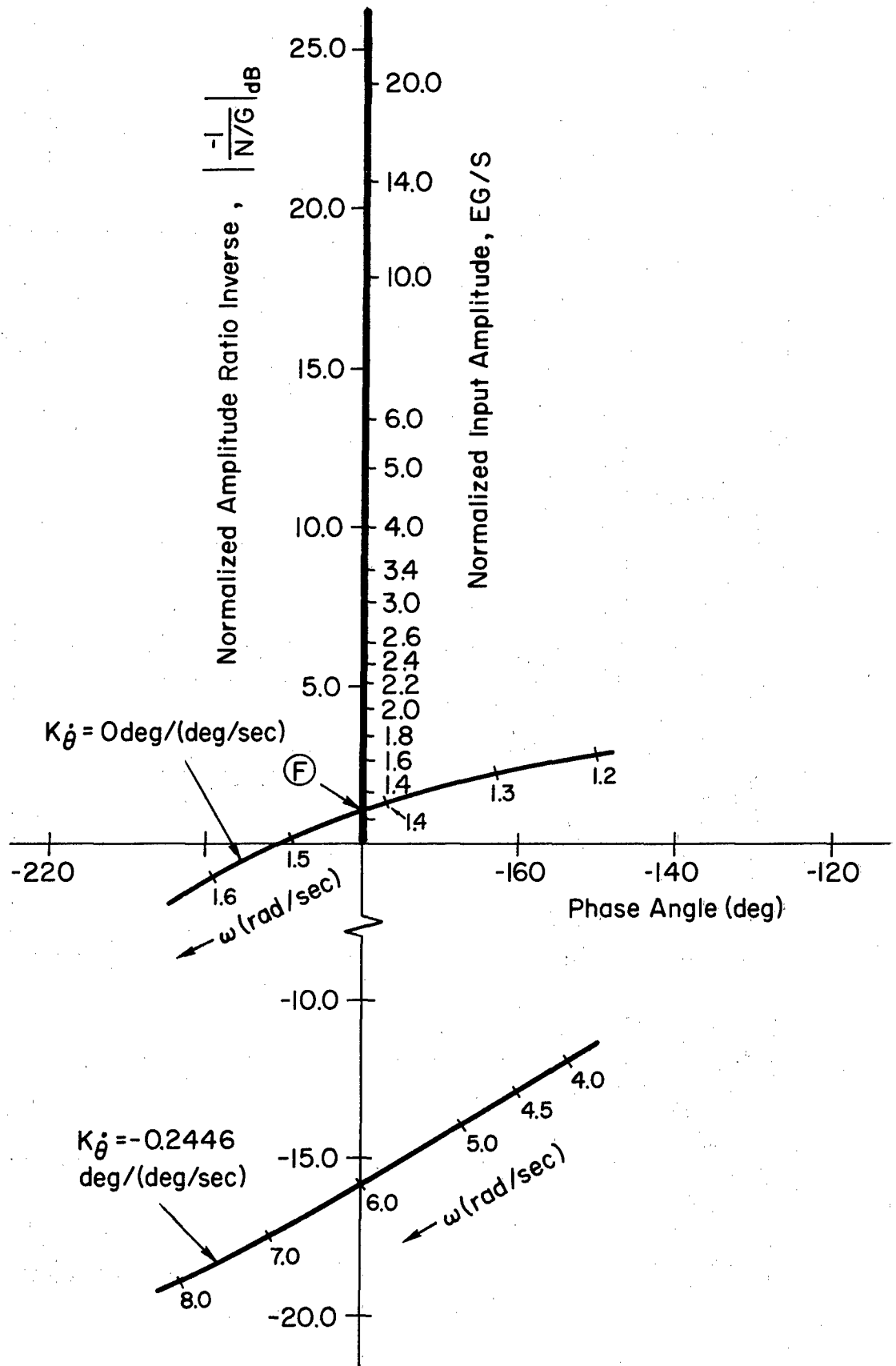


Figure 33. Determining the Limit Cycles for Longitudinal System B with $\tau_s = 0.2 \text{ sec}$

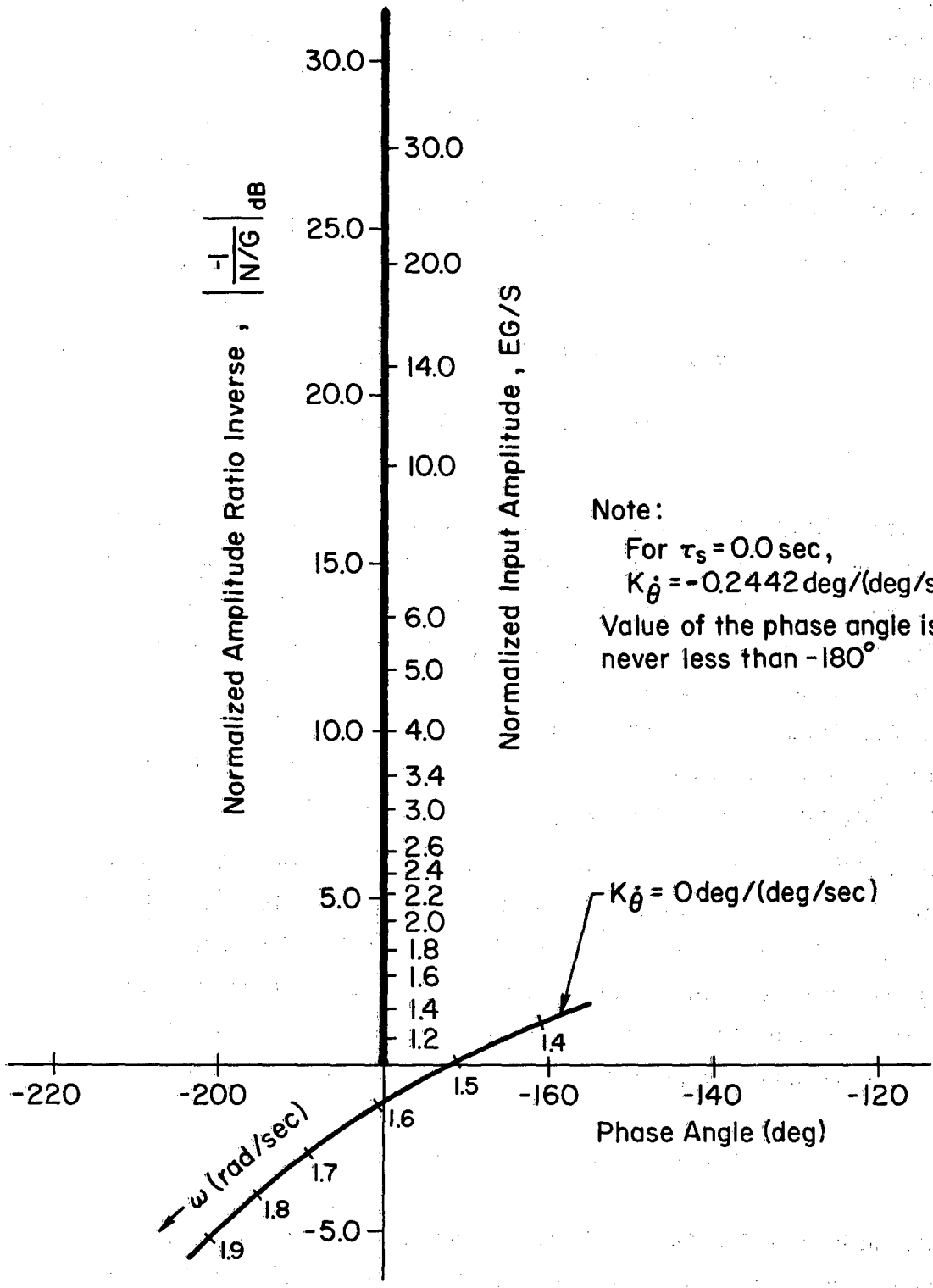


Figure 34. Determining the Limit Cycles for Longit+ System B with $\tau_s = 0.0 \text{ sec}$

The describing function crosses the frequency response curve from left to right in Fig. 33 indicating that a stable limit cycle exists. Its parameters are $\omega = 1.43$ rad/sec and (amplitude of input to normalized limiter) = 1.30. These parameters, the limit level, the normalized describing function gain and the vehicle transfer functions can be used to compute the limit cycle amplitudes for other variables of interest.

$$\text{amplitude of } \delta_t = 2.84 \text{ deg} \quad (42)$$

$$\text{amplitude of } \theta = 9.57 \text{ deg} \quad (43)$$

$$\text{amplitude of } n_z = 0.815 \text{ g's} \quad (44)$$

The possibility of lateral pilot induced oscillations for System B will now be considered. The portions of the frequency response for which the phase angle is approximately -180 deg are overplotted on the normalized describing function for the limiter in Fig. 35. Both the proneness ($\tau_{sp} = 0.2$ sec) and the continuation ($\tau_{sp} = 0.0$ sec) conditions are shown in this figure. For lateral control with System B, the pilot does not supply lead equalization and so degradation of lead equalization cannot be a factor in any lateral pilot induced oscillations.

Intersections with the describing function occur for both curves at approximately $\omega = 0.126$ rad/sec and $E G/S = 4.25$ in region (G). Since $G = 1$ and $S = 10.0$ deg, $E = 42.5$ deg. The describing function crosses the frequency response curves from right to left indicating an unstable limit cycle. The unstable limit cycle values for y and ψ can be determined in the manner used previously for System A. The results are:

$$\text{amplitude of } y = 842.0 \text{ ft} \quad (45)$$

At an altitude of 100.0 ft, $y = 842.0$ ft corresponds to 16.8 deg in "LOC" units (The mean square for an oscillation would be $(16.8)^2/2 = 142.0$ (deg LOC)²).

$$\text{amplitude of } \psi = 18.3 \text{ deg} \quad (46)$$

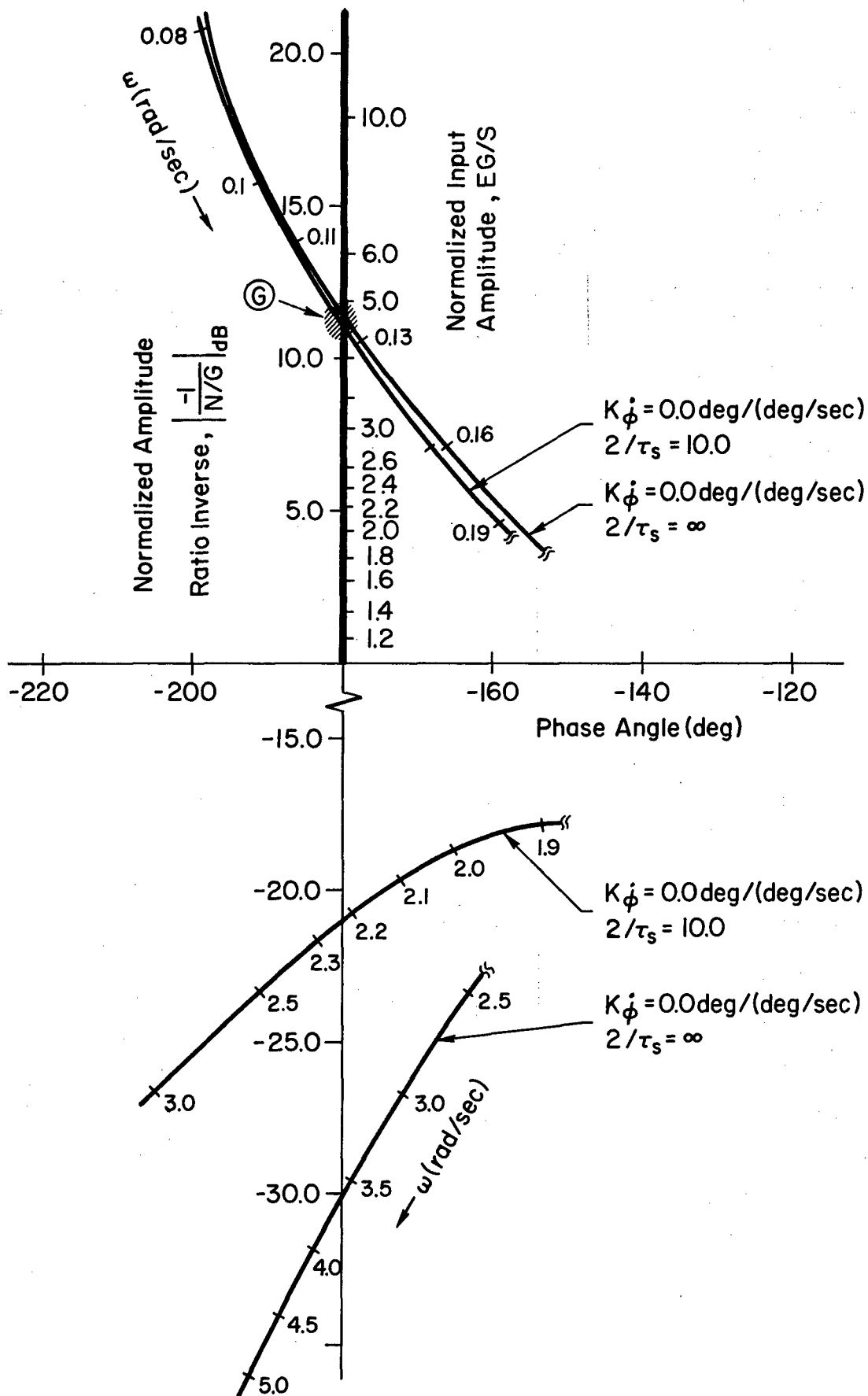


Figure 35. Determining the Limit Cycles for Lateral System B with $\tau_{sp} = 0.2$ sec and $\tau_{sp} = 0.0$ sec

The corresponding mean square value for an oscillation would be $(18.3)^2/2 = 334.0 \text{ deg}^2$.

To summarize these results, for longitudinal control, System B can be said to be slightly prone to pilot induced oscillations. However, to develop the oscillation requires virtually complete neglect of the pitch rate feedback task by the pilot. This may be judged unlikely. A longitudinal pilot induced oscillation, if encountered, would be characterized by moderate frequency, moderate g's and large pitch angle. No stable pilot induced oscillations are indicated for lateral control using System B. However, it is possible for large deviations from the localizer reference, large rates of deviation, or combinations of both to present conditions under which stable tracking of the localizer reference is not possible for the given nonlinear control system. These conditions are indicated by the unstable limit cycle indicated for lateral control by means of System B.

C. SYSTEM C

The longitudinal portion of System C is identical to the longitudinal portion of System B. Therefore, the same data and conclusions with respect to pilot induced oscillations apply to both systems.

The possibility of lateral pilot induced oscillations for System C will be considered next. The portions of the frequency responses for which the phase angle is -180 deg are overplotted on the normalized describing function for the limiter in Fig. 36. Intersections with the describing function occur in region (H) of Fig. 36. This corresponds to an approximate frequency of $\omega = 0.26 \text{ rad/sec}$ and an approximate normalized input amplitude, $E G/S = 5.0$. Since $G = 1.0$ and $S = 10.0 \text{ deg}$, $E = 50.0 \text{ deg}$. The describing function crosses the frequency response curves from right to left indicating an unstable limit cycle. The unstable limit cycle values for y and ψ can be determined in the manner used previously for System A. The results are:

$$\text{amplitude of } y = 103.0 \text{ ft} \quad (47)$$

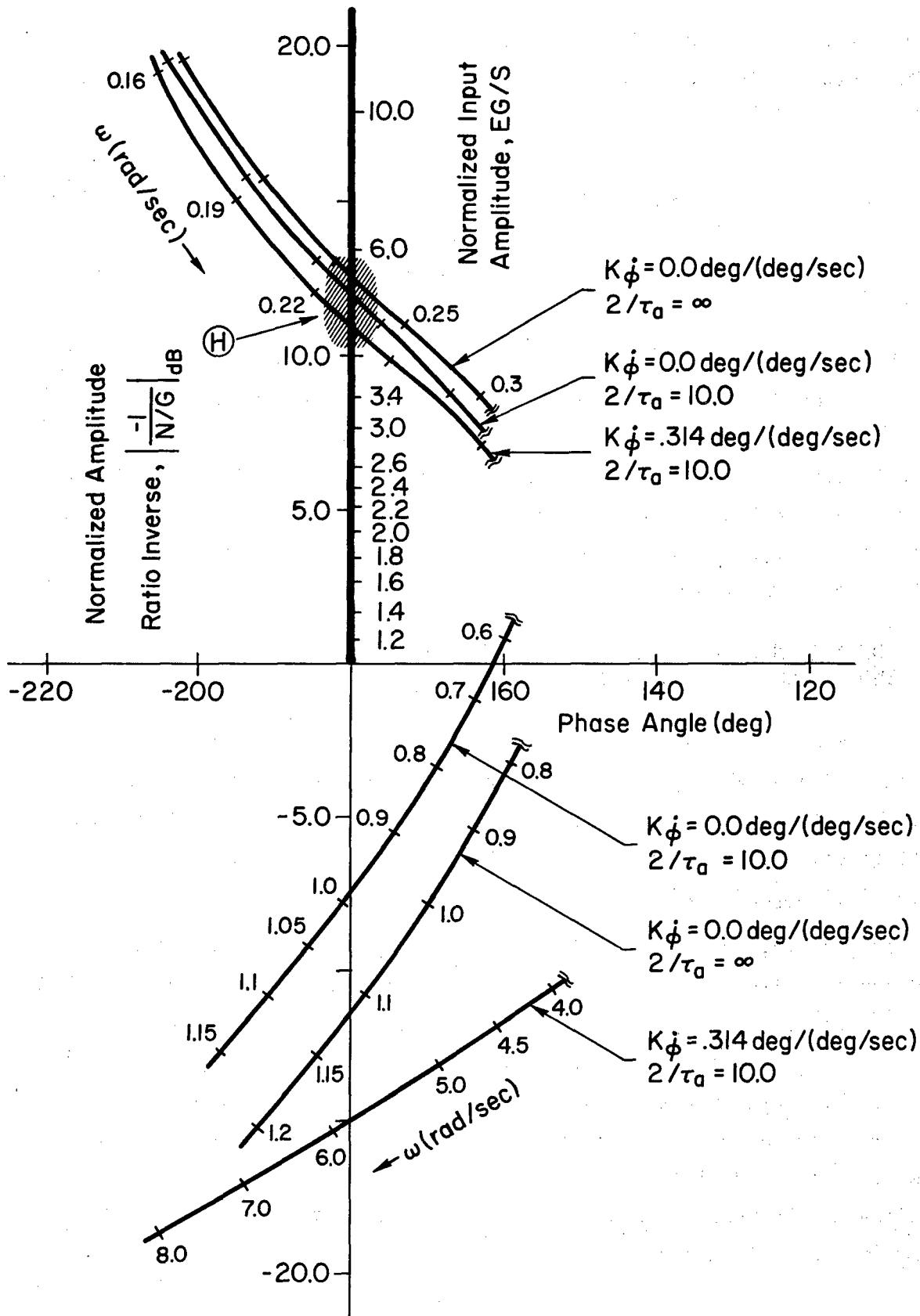


Figure 36. Determining the Limit Cycles for Lateral System C with $\tau_a = 0.2 \text{ sec}$ and $\tau_a = 0.0 \text{ sec}$

At an altitude of 100.0 ft, $y = 103.0$ ft corresponds to 2.06 deg in "LOC" units. (The mean square for an oscillation would be $(2.06)^2/2 = 2.11$ (deg LOC)²).

$$\text{amplitude of } \psi = 4.61 \text{ deg} \quad (48)$$

The corresponding mean square for an oscillation would be $(4.61)^2/2 = 10.6$ deg².

No stable pilot induced oscillations are indicated for lateral control using System C. However, it is possible for moderate deviations from the localizer reference, moderate rates of deviation, combinations of both to present conditions under which stable tracking of the localizer reference is not possible for the given nonlinear control system. These conditions are indicated by the unstable limit cycle indicated for lateral control by means of System C.

D. COMPARISON OF PREDICTED AND MEASURED PILOT INDUCED OSCILLATION TENDENCY RATINGS

A summary of predicted pilot induced oscillation tendency ratings is given in Table XXI. These ratings are based upon the verbal descriptions for the rating numbers given in Table XXXIX of Appendix VI. The predicted ratings compare very favorably with the measured ratings summarized in Table L of Appendix VI.

It appears, in the case of System A with gust inputs, that the considerable variability in measured pilot ratings (see Table L Appendix VI) may be due to the large side gust excitation of the dutch roll. This arises because of low closed-loop dutch roll damping. Consequently, it is possible that the pilot subjects regard the lightly damped dutch roll mode response as being somewhat similar to pilot induced oscillation onset. The analytical results, however, indicate a pilot induced oscillation (either because of actuator nonlinearities or because of ω_p/ω_d effects) is improbable.

TABLE XXI

SUMMARY OF PREDICTED PILOT INDUCED
OSCILLATION TENDENCY RATINGS

System Configuration	Rating	Factors Causing Rating Degradation
A w/o gusts	3	modest pitch lead required to prevent pilot induced oscillation
A w/ gusts	3	same as w/o gusts
B w/o gusts	2	only very small pitch lead required to prevent pilot induced oscillation
B w/ gusts	2	same as w/o gusts
C w/o gusts	2	only very small pitch lead required to avoid pilot induced oscillation
C w/ gusts	2	same as w/o gusts

E. AVOIDING PILOT INDUCED OSCILLATIONS BY DESIGN

While the ability to predict pilot induced oscillations and instabilities by analytical means is of considerable value, it is, ultimately, the ability to avoid them by means of prudent design which is the engineer's objective. In this subsection, techniques for avoiding pilot induced oscillation arising from rate limiting, output limiting or both which appear to be applicable in general will be summarized. These techniques have been inferred from the example applications made earlier in this Section.

The first rule for avoiding pilot induced oscillations and instabilities is almost trivial.

- The closed-loop pilot-vehicle-flight control system must exhibit linear stability for small perturbations in the absence of command and disturbance inputs.

The next rule is:

- Pilot induced oscillations and instabilities arising from actuator rate limits, actuator deflection limits, or both will not exist when the locus of closed-loop roots for the linear pilot-vehicle-flight control system as a function of the forward-loop actuator gain from zero up to its nominal value does not indicate conditional system stability.

A variant of this rule applies when the pilot exercises direct manual control of the control surface.

- Pilot induced oscillations and instabilities arising from pilot strength limitations or control surface deflection limits will not exist when the locus of closed-loop roots for the linear pilot-vehicle-flight control system as a function of the gain at the point where the nonlinearity occurs, does not indicate conditional system stability for any lesser magnitude of the open-loop gain.

Conditional stability can be avoided in fully powered systems by selecting or changing the design parameters in the manner suggested below. The design parameters, in this case are

K	actuator open-loop gain
R	actuator rate limit
R/P	actuator rate limit-to-deflection limit ratio

A way for accomplishing this is suggested by the normalizing factors for the limiting integrator describing function. Refer to Fig. 23. The following observations can be made. The frequency response curve can be shifted vertically with respect to the describing function by changing the actuator open-loop gain, K. This shift can also be made by changing the rate limit-to-deflection limit ratio, R/P. However, R/P also shifts the contours of constant frequency for the describing function at the same time. These two parameters can be used to control the location of the intersection of the describing function and the frequency response

curves, or to prevent intersections from occurring. The rate limit parameter, R , controls the amplitude of the limit cycle when intersections exist.

The design approach, then, is as follows. $K/(R/P)$ is held constant. (The describing function and the frequency response curves are not shifted relative to one another.) Then R/P is adjusted so that no intersections occur at phase angles between -90 deg and -180 deg. (This generally occurs when the lines of constant describing function frequency in this phase interval are always to the left of the corresponding frequency points on the frequency response curve.)

In order to avoid intersections with the portion of the describing function for which the phase is -90 deg, it may be necessary to further adjust R/P until a positive gain margin is indicated.

This process can be repeated for several different constant values of $K/(R/P)$ to develop a family of conditions all of which will not result in limit cycles.

The approach described above may be overly conservative, however. This is because the existence of unstable limit cycle solutions does not necessarily lead to undesirable consequences. It is only when the maneuver size which precludes stable recovery is small that unstable limit cycle solutions have unfavorable implications. Consequently, if the above design criteria and procedures for avoiding all limit cycle solutions are applied only for avoiding stable limit cycle solutions, a less restrictive design will usually result. The unstable limit cycle solutions which may remain must be checked to determine if the upper limit on maneuver size which still permits stable recovery is acceptable.

The above design technique has not considered the possibility of altering the shape of the frequency response curve by means of introducing equalization (e.g. by changing flight director gains). In some situations, changes in equalization will also be a distinct possibility. However, this is essentially a linear servo analysis design technique which is already well-known. Therefore it is not appropriate to discuss it here.

Conditional stability itself can be avoided in systems wherein the pilot exercises direct manual control by a similar approach. The techniques are somewhat simpler, however, because of the more elementary nature of the describing function for the limiter and the smaller number of parameters which characterize that describing function. The design parameters for the system in this case are:

G gain for linear segment of the limiter characteristic

G/S ratio of limiter gain to limit level

In this application, the limiter gain, G , is interpreted as a gain factor which alters the loop gains for the linear portion of the system rather than as the linear segment gain of the limiter characteristic. This is because the limiter gain in the physical system model has been fixed at unity by assumption.

A way to avoid limit cycles is suggested by the normalizing factors of the limiter describing function. Refer to Fig. 25. The following observations can be made. The frequency response curve can be shifted vertically with respect to the describing function by changing the gain, G . The ratio of limiter gain to limit level, G/S , controls the amplitude of the limit cycles when intersections exist.

Design is merely a matter of selecting a value of G (that is altering the gain in all paths leading to the nonlinearity by the factor G) such that at points on the frequency response curve for which the phase is -180 deg the amplitude ratio is less than 0 dB.

This design approach can be overly conservative for the same reason as in the previous case. That is, unstable limit cycle solutions do not necessarily lead to undesirable consequences as has already been pointed out above.

Again the possibility of altering the shape of the frequency response curve by means of equalization has not been considered. As noted before this is essentially a linear servo analysis design problem which is already well-known and need not be elaborated.

SECTION VI

SUMMARY

Analytical procedures have been developed for predicting the performance and proneness to pilot induced oscillations and instabilities which may result in systems wherein actuator rate limits, deflection limits or both are the principal nonlinear effects. The analytical procedures are applied to three minimum back-up flight control system designs for the F-4C which were evolved in a piloted fixed-base simulation program. Analyses of the three back-up systems produced results which were qualitatively similar to the ones measured experimentally. Namely, predicted and measured pilot opinion agree closely. Pilot comments indicated that opinion ratings were degraded for the reasons exposed by analysis. The minimum rate and deflection limits which the pilots found acceptable for emergency landing conditions were also in qualitative agreement with the minimum values determined by the analytical methods. Agreement between the analytically predicted performance and the measured performance was, quantitatively, reasonably good for most of the inner loop variables. Agreement between the analytically predicted performance and the measured performance was not at all good for the outer loop variables. There is, however, reason to suspect the validity of the reported experimental data since the mean-square values in several cases are unreasonably large, and, furthermore, these large values are not supported in any way by suitably degraded pilot opinion ratings.

The analytical procedures rest upon the application of random input describing function theory for performance prediction, and upon the application of sinusoidal input describing function theory for prediction of system susceptibility to pilot induced oscillations and instabilities. The applications of these theories is very much along the lines of traditional engineering practice for analyzing nonlinear systems. Key developments, however, which were made were a new model for the rate and deflection limited actuator, guidelines for choosing minimum values of the rate and deflection limits, and a design technique for avoiding pilot induced oscillations and instabilities arising from rate and deflection limit nonlinearities.

The most important element of the actuator model is the limiting integrator (more accurately, the rate limited integrator having a restricted output range). A nondimensionalized sinusoidal input describing function for the limiting integrator has been computed. Availability of this nondimensionalized describing function will substantially facilitate future analyses of the type performed for the example applications.

The guidelines for choosing the rate and deflection limits are that the limit levels should be set at 2 to 3 times the root-mean-square values of the signal in the counterpart linear system at the point where the nonlinearity would occur.

Pilot induced oscillations and instabilities arising from actuation limits can be avoided by satisfying conditions which pertain only to the linear portion of the system. Namely, the locus of closed-loop roots for the linear system should not be conditionally stable for values of the open-loop actuator gain over the range from zero up to its maximum value. When the pilot exercises direct manual control over the control surfaces, the actuator is replaced by a gain. As this gain ranges from zero up to its nominal value of unity, the same criterion applies.

Unstable limit cycle solutions have been interpreted as approximate boundaries for regions of the state space from which stable recovery to the reference flight path is not possible. This consideration introduces additional constraints upon the minimum permissible actuator limits. However, it is not necessary or even desirable to eliminate all unstable limit cycle solutions in order to arrive at a good system design. Unstable limit cycle solutions need only be eliminated when the maximum size maneuver for which stable recovery is possible is too restrictive.

The approach to the analytical design of low authority flight control systems described in this report is an amalgamation of state-of-the-art engineering techniques. The procedure should be readily understood and easily applied by engineers already knowledgeable in the areas of

- Linear servo analysis
- Analytical theory of handling qualities
- Random and sinusoidal input describing function theory

REFERENCES

1. Yore, E. E., Requirements for Minimum Backup Flight Control Systems, AFFDL-TR-70-48, June 1970 (also as Honeywell Report 12140-FR, January 1970).
2. McRuer, D., D. Graham, E. Krendel, and W. Reisener, Jr., Human Pilot Dynamics in Compensatory Systems -- Theory, Models, and Experiments with Controlled Element and Forcing Function Variations, AFFDL-TR-65-15, July 1965.
3. McRuer, D., and H. R. Jex, "A Review of Quasi-Linear Pilot Models," IEEE Trans., Vol. HFE-8, No. 3, September 1967, pp. 231-249.
4. Ashkenas, I. L., and D. T. McRuer, Approximate Airframe Transfer Functions and Application to Single Sensor Control Systems, WADC-TR-58-82, June 1958.
5. Wolkovitch, J., and R. P. Walton, VTOL and Helicopter Approximate Transfer Functions and Closed-Loop Handling Qualities, STI TR-128-1, June 1965.
6. McRuer, D., I. L. Ashkenas, and D. Graham, Aircraft Dynamics and Automatic Control, STI TR-129-1, August 1968.
7. Ashkenas, I. L., A Study of Conventional Airplane Handling Qualities, AFFDL-TR-65-138, Part I, November 1965, Part II, October 1965.
8. Ashkenas, I. L., and D. T. McRuer, "A Theory of Handling Qualities Derived from Pilot-Vehicle System Considerations," Aerospace Eng., Vol. 21, No. 2, February 1962, pp. 60-61, 83-102.
9. McRuer, D. T., and I. L. Ashkenas, Applied Pilot-Aircraft Control Theory, paper presented to the AGARD Symposium on the Human Operator and Aircraft and Missile Control, Paris, France, 5-6 September 1966.
10. Stapleford, R. L., I. L. Ashkenas, D. Graham, J. J. Best, and J. A. Tennant, Analysis of Several Handling Quality Topics Pertinent to Advanced Manned Aircraft, AFFDL-TR-67-2, June 1967.
11. Durand, T. S., and G. L. Teper, An Analysis of Terminal Flight Path Control in Carrier Landing, STI TR-137-1, August 1964.
12. Denery, D. G., and B. Y. Creer, Evaluation of a Pilot Describing Function Method Applied to the Manual Control Analysis of a Large Flexible Booster, NASA TN D-5149, April 1969.
13. Briggs, P., and L. G. Hofmann, The Application of Human Operator Describing Function Theory to the Prediction of Tracking Performance in the Cheyenne Swiveling Gunner's Station, paper presented at the Fifth Annual NASA-University Conference on Manual Control, Cambridge, Mass., 27-29 March 1969.

REFERENCES (cont'd)

14. Graham, D., and D. McRuer, Analysis of Nonlinear Control Systems, John Wiley and Sons, New York, 1961.
15. Gelb, A., and W. E. VanderVelde, Multiple-Input Describing Functions and Nonlinear System Design, McGraw-Hill Book Co., New York, 1968.
16. Ashkenas, I. L., H. R. Jex, and D. T. McRuer, Pilot Induced Oscillations: Their Cause and Analysis, Norair Rept. NOR 64-143, 20 June 1964.
17. Graham, D., and L. G. Hofmann, Investigations of Describing Function Technique, AFFDL-TR-65-137, February 1966.
18. Bergeron, H. P., J. K. Kincaid, and J. J. Adams, Measured Human Transfer Functions in Simulated Single-Degree of Freedom Systems, NASA TN D-2569, January 1965.
19. Graham, D., Research on the Effect of Nonlinearities on Tracking Performance, AMRL-TR-67-9, July 1967.
20. Duggar, L. C., J. T. Mannen, and R. A. Hannen, "Pilot Describing Function Models for Nonlinear Controlled Elements," Fifth Annual NASA-University Conference, NASA SP-215, March 1969, pp. 107-110.
21. Garren, J. F., Jr., D. J. DiCarlo, and N. R. Driscoll, Flight Investigation of an On-Off Control for V/STOL Aircraft Under Visual Conditions, NASA TN D-3436, June 1966; See also: Garren, J. F., Jr., and J. R. Kelly, "Flight Study of On-Off Control for V/STOL Aircraft," Conference on V/STOL and STOL Aircraft, NASA SP-116, April 1966, pp. 269-279.
22. Leland, H. R., "Input-Output Cross-Correlation Functions for Some Memory Type Nonlinear Systems with Gaussian Input," Applications and Industry, AIEE, No. 49, July 1960.
23. Anonymous, Criteria for Approval of Category II Landing Weather Minima, FAA AC No. 120-20, 6 June 1966.
24. Johnson, W. A., and D. T. McRuer, Development of a Category II Approach System Model, STI TR-182-1, December 1969.
25. Graham, D., W. F. Clement, and L. G. Hofmann, Investigation of Measuring System Requirements for Instrument Low-Approach, AFFDL-TR-70-102, August 1970.
26. Jex, H. R., and C. H. Cromwell, III, Theoretical and Experimental Investigation of Some New Longitudinal Handling Qualities Parameters, ASD-TR-61-26, June 1962.

REFERENCES (cont'd)

27. Ashkenas, I. L., and D. T. McRuer, The Determination of Lateral Handling Quality Requirements from Airframe-Human Pilot System Studies, WADC TR-59-135, June 1959.
28. Durand, T. S., and H. R. Jex, Handling Qualities in Single-Loop Roll Tracking Tasks: Theory and Simulator Experiments, ASD-TDR-62-507, November 1962.
29. McRuer, D. T., I. L. Ashkenas, and H. R. Pass, Analysis of Multiloop Vehicular Control Systems, ASD-TDR-62-1014, March 1964.
30. Anonymous, Super Basic, Tymshare Manuals Reference Series, April 1969.
31. Anonymous, User's Bulletin No. 6, Tymshare, Inc., March 1970.

APPENDIX I

F-4C STABILITY DERIVATIVES, TRANSFER FUNCTIONS, GUIDANCE SYSTEM GEOMETRY AND DISTURBANCE MODELS

This Appendix summarizes the basic data for the F-4C aircraft used for example applications of the analysis techniques. The aircraft is in a clean configuration (except for the extended landing gear), and is making a manually controlled instrument approach on a 2.8 deg glide slope of ILS quality. The aircraft is in a clean configuration for landing because it is assumed that the hydraulic system is not functioning as a result of battle damage. The disturbance environment includes ILS glide slope and localizer beam "bends" and normal and side gusts. No steady winds, wind shears, or longitudinal gusts are included in the disturbance environment since these were not included in the Ref. 1 simulation. Complete representation of the disturbance environment is, of course, necessary for actual design calculations, but is not necessary in order to demonstrate application of the analytical techniques.

Dimensional stability derivative data on the F-4C is given in Table XXII along with pertinent data on the geometry, inertias and trim conditions. Tables XXIII and XXIV give the equations of motion upon which the longitudinal transfer functions in Table XXV and the lateral transfer functions in Table XXVI are based. Gust response transfer functions are not given because these are not required for developing the basic control loops.

The longitudinal and lateral approach geometry is shown in Fig. 37. The system is analyzed at a particular point on the approach ($R = 3,690.0$ ft) because the proper measure of performance in tracking the ILS beam is linear measure (in distinction to angular measure) of aircraft deviation from the beam null.

Power spectral densities used for the disturbance environment are given in Table XXVII.

The pilot control inputs consist of stick, rudder pedals, throttles, trim switches, and the pilot displays included airspeed, angle of attack, altitude, sink rate, engine performance, attitude indicator, flight director, radio magnetic indicator, and glide slope-localizer cross pointer instrument.

TABLE XXII

F-4C PARAMETERS FOR CLEAN CONFIGURATION

GEOMETRY & INERTIA		LONGITUDINAL BODY AXES		LATERAL BODY AXES, PRIMED DERIVATIVES	
C_{L_0}	0.4897	X_u^*	(1/sec)	Y_v	(1/sec)
h_0 (ft)	2,000.0	X_w	(1/sec)	$Y_{\delta_{sp}}^*$	(1/sec/deg)
M	0.300	X_{δ_s}	(ft/sec ² /deg)	$Y_{\delta_a}^*$	(1/sec/deg)
V_{T_0}	332.7	X_{δ_T}	(ft/sec ² /unit thrust)	$Y_{\delta_r}^*$	(1/sec/deg)
U_0 (ft/sec)	329.4	Z_u^*	(1/sec)	L_{β}^*	(1/sec ²)
W_0 (ft/sec)	46.85	Z_w	(1/sec)	$L_{\dot{\beta}}$	(1/sec)
Γ_0 (deg)	-2.8	Z_{δ_s}	(ft/sec ² /deg)	$L_{\dot{\gamma}}$	(1/sec)
q	124.7	Z_{δ_T}	(ft/sec ² /unit thrust)	$L_{\delta_{sp}}^*$	(rad/sec ² /deg)
S	530.0	$M_{\dot{\gamma}}^*$	(1/sec-ft)	$L_{\delta_a}^*$	(rad/sec ² /deg)
b	38.66	M_w	(1/sec-ft)	$L_{\delta_r}^*$	(rad/sec ² /deg)
c	16.04	$M_{\dot{\gamma}}$	(1/sec)	$N_{\dot{\beta}}$	(1/sec ²)
W	32,000.0	M_{δ_s}	(rad/sec ² /deg)	$N_{\dot{\gamma}}$	(1/sec)
m	993.8	M_{δ_T}	(1/sec ² /unit thrust)	$N_{\dot{\delta}_{sp}}^*$	(rad/sec ² /deg)
I_x (slug-ft ²)	0.219×10^5	$M_{\dot{\gamma}}$	(1/sec ²)	$N_{\delta_{sp}}^*$	(rad/sec ² /deg)
I_y (slug-ft ²)	1.210×10^5	M_{δ_t}	$= 2/3 X_{\delta_s}$	$N_{\delta_a}^*$	(rad/sec ² /deg)
I_z (slug-ft ²)	1.370×10^5	Z_{δ_t}	$= 2/3 Z_{\delta_s}$	$N_{\delta_r}^*$	(rad/sec ² /deg)
I_{xz} (slug-ft ²)	0.360×10^4	M_{δ_t}	$= 2/3 M_{\delta_s}$	$H_{\delta_{sp}}$	(ft-lb/deg)
X_{CG} (% c)	31.6	H_{δ_s}	(ft-lb/deg)	H_{δ_r}	(ft-lb/deg)
δ_{F_0} (deg)	0.0	H_{δ_t}	(ft-lb/deg)	$H_{\dot{\beta}}$	(ft-lb/deg)
α_0 (deg)	11.911			$H_{\dot{\gamma}}$	(ft-lb/deg)
θ_0 (deg)	8.096			H_{δ_a}	(ft-lb/deg)
δ_{S_0} (deg)	-2.815				
L_{x_p} (ft)	23.9				

Derivatives not listed are assumed zero.

- (1) Values of δ_{sp} derivatives for System B are 2/3 of those values given.
- (2) Allerons are redesigned to have balanced hinges and tabs. Stability derivatives are assumed to be unchanged, but hinge moment derivatives are reduced to 1/3 of values given for unmodified surfaces.
- (3) For System C, rudder is tab actuated. Stability derivatives are assumed to be unchanged, but hinge moment derivatives are reduced to 1/3 of values given for unmodified surfaces.

TABLE XXIII

LONGITUDINAL EQUATIONS OF MOTION

$s - X_u^*$	$-X_w$	$W_0 s + g \cos \theta_0$				u	X_{δ_1}	\dots	X_{δ_n}	$-X_w$	δ_1
$-Z_u^*$	$(1 - Z_w) s - Z_w$	$-U_0 s + g \sin \theta_0$				w	Z_{δ_1}	\dots	Z_{δ_n}	$-Z_w^* s - Z_w$	\vdots
$-M_u^*$	$-M_w^* s - M_w$	$s^2 - M_q s$				θ	M_{δ_1}	\dots	M_{δ_n}	$-M_w^* s + \frac{M_q}{U_0} s - M_w$	δ_n
$-\sin \theta_0$	$\cos \theta_0$	$-U_0 \cos \theta_0 - W_0 \sin \theta_0$	1			\dot{h}					$u g$
	$-s$	$U_0 s - g \sin \theta_0$		1		a_z					$w g$
	$-s$	$l_{x_a} s^2 + U_0 s - g \sin \theta_0$			1	a_z'					
$-\sin \theta_0$	$\cos \theta_0$	$-l_{x_p} s - U_0 \cos \theta_0 - W_0 \sin \theta_0$				\dot{h}_p					

\dot{h} may be replaced by \dot{d} or \dot{h}_p by \dot{d}_p , if θ_0 is replaced by $(\theta_0 - \Gamma_0)$ in the respective equations for \dot{h} or \dot{h}_p . See the list of symbols for the definition of constants and variables appearing in the table.

TABLE XXIV
LATERAL EQUATIONS OF MOTION

$s - Y_V$	$\frac{-W_0}{V_{T0}}$	$\frac{U_0}{V_{T0}}$	$\frac{-g \cos \theta_0}{V_{T0}}$						$Y_{\delta_1}^*$	$Y_{\delta_n}^*$	$-Y_V$		δ_1
$-L'_\beta$	$s - L'_p$	$-L'_r$							L'_{δ_1}	L'_{δ_n}	$-L'_\beta$		\vdots
$-N'_\beta$	$-N'_p$	$s - N'_r$							N'_{δ_1}	N'_{δ_n}	$-N'_p$		δ_n
	-1	$-\tan \theta_0$	s										βg
$-V_{T0} s$	$l_z s + W_0$	$-l_x s - U_0$	$g \cos \theta_0$	1									$p g$
$\frac{-V_{T0} s}{U_0 \epsilon_0}$	$\frac{W_0}{U_0 \epsilon_0}$	$-\frac{1}{\epsilon_0}$			1								
	$-\sin \alpha_G$	$-\cos \alpha_G$											

=

β	p	r	φ	$a_y^{(1)}$	λ	r_G
---------	-----	-----	-----------	-------------	-----------	-------

λ = heading of aircraft velocity vector (measured in horizontal plane)

$\epsilon_0 = \cos \theta_0 + (W_0/U_0) \sin \theta_0$

See the list of symbols for other definitions of constants and variables appearing in the table.

TABLE XXV

LONGITUDINAL TRANSFER FUNCTIONS FOR THE F-4C IN CLEAN CONFIGURATION

Abbreviated notation is used for polynomial factors in root locus form:

Real factor (λ) means $(s + \lambda)$

Quadratic factor $[\zeta, \omega]$ means $[s^2 + 2\zeta\omega s + \omega^2]$

Denominator

$$\Delta = [0.104, 0.159][0.377, 1.309]$$

Thrust Numerators

$$N_{\delta_T}^u = 0.00200(0.027)[0.445, 1.358]$$

$$N_{\delta_T}^{\dot{h}_p} = 0.000228(3.972)[-0.461, 1.021]$$

Stabilator Numerators

$$N_{\delta_S}^{\theta} = -0.0861(0.030)(0.479)$$

$$N_{\delta_S}^{\dot{h}_p} = -1.605(-0.023)[0.091, 2.896]$$

$$N_{\delta_S}^{\dot{h}_q} = 0.4529(-0.023)(-5.173)(5.724)$$

Thrust and Stabilator Coupling Numerators

$$N_{\delta_S \delta_T}^{\theta u} = -0.000172(0.495)$$

$$N_{\delta_S \delta_T}^{\dot{h}_p u} = -0.003232[0.168, 3.02]$$

$$N_{\delta_S \delta_T}^{\dot{h}_q u} = 0.000878(-6.54)(5.132)$$

$$N_{\delta_S \delta_T}^{\dot{h}_p \theta} = 0.0000355(1.268)$$

TABLE XXVI

LATERAL TRANSFER FUNCTIONS FOR THE F-4C IN CLEAN CONFIGURATION

Abbreviated notation is used for polynomial factors in root locus form:

Real factor (λ) means $(s + \lambda)$

Quadratic factor $[\zeta, \omega]$ means $[s^2 + 2\zeta\omega s + \omega^2]$

Denominator

$$\Delta = (0.043)(1.392)[0.114, 1.725]$$

Spoiler Numerators (For System A)

$$N_{\delta_{sp}}^{\phi} = 0.0122[0.120, 1.56]$$

$$N_{\delta_{sp}}^{\lambda} = -0.0000110(-9.158)(10.57)[0.091, 1.617]$$

$$N_{\delta_{sp}}^r = 0.000907(0.683)[0.020, 2.109]$$

$$N_{\delta_{sp}}^{\ddot{y}} = 3.076(0.011)(0.10)(0.571)[0.02, 2.12]$$

Rudder Numerators

$$N_{\delta_r}^{\phi} = 0.0109(4.275)(-4.875)$$

$$N_{\delta_r}^{\lambda} = 0.000419(-2.673)(3.104)[0.256, 2.490]$$

$$N_{\delta_r}^r = -0.0242(1.043)[0.302, 0.920]$$

Aileron Numerators (For System C)

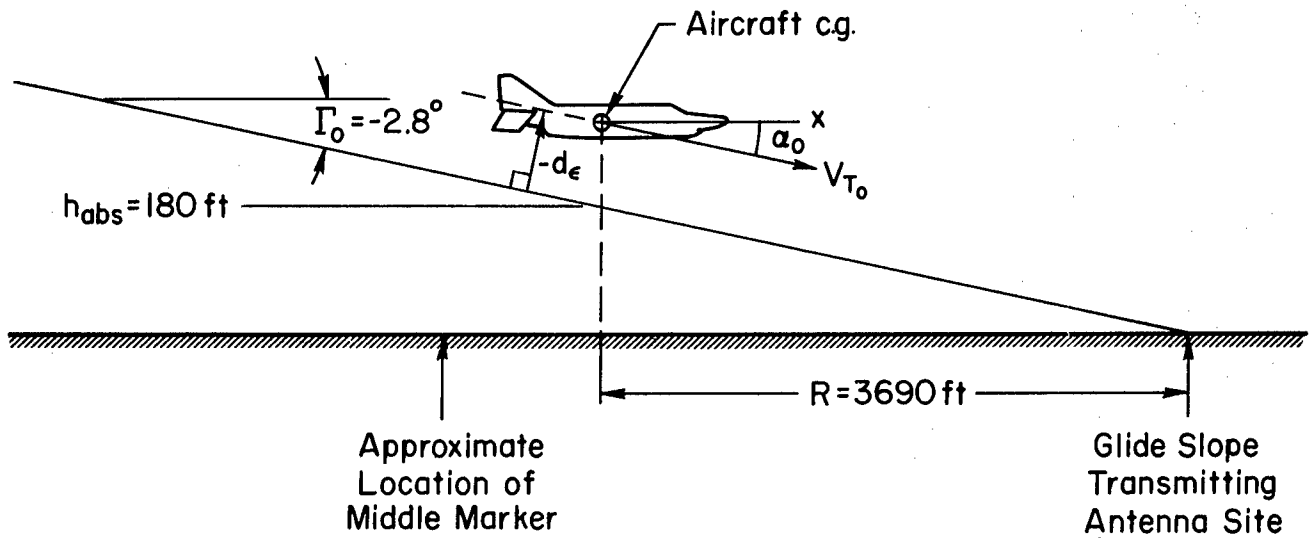
$$N_{\delta_a}^{\phi} = 0.0647[0.132, 1.341]$$

$$N_{\delta_a}^{\lambda} = -0.000033(-11.78)(13.32)[0.056, 1.456]$$

$$N_{\delta_a}^r = 0.000837(0.621)[-0.412, 4.575]$$

$$d_e = d_c - d_p \quad \text{at ILS antenna station}$$

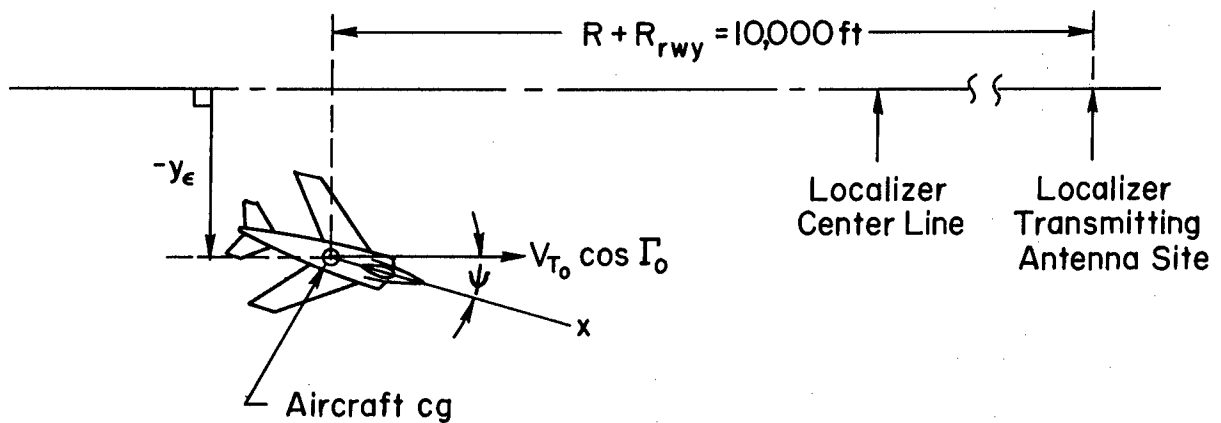
$$d_\epsilon = d_c - d \quad \text{at A/C cg station}$$



a) Longitudinal Approach Geometry

$$y_e = y_c - y_p \quad \text{at ILS antenna station}$$

$$y_\epsilon = y_c - y \quad \text{at A/C cg station}$$



b) Lateral Approach Geometry

Figure 37. Approach Geometry for Coincident ILS Signal Null and Reference Glide Path ($d_c = y_c = 0$)

TABLE XXVII

POWER SPECTRAL DENSITIES FOR DISTURBANCE
ENVIRONMENT AT R = 3,690 FT

SOURCE	VARIABLE, (.)	RMS OF VARIABLE, σ (.)	POWER SPECTRAL DENSITY, Φ (.)(.)
Glide slope "bends"	d_c	3.0 ft	$\frac{(1.20)^2}{\omega^2 + (0.25)^2}$
Localizer "bends"	y_c	8.0 ft	$\frac{(16.0)^2[\omega^2 + (1.5)^2]}{[\omega^2 + (0.35)^2][\omega^2 + (10.0)^2]}$
Normal gusts	w_g	10.0 ft/sec	$\frac{(19.3)^2}{\omega^2 + (5.88)^2}$
Side gusts	v_g	10.0 ft/sec	$\frac{(19.3)^2}{\omega^2 + (5.88)^2}$

The definition of power spectral density used is such that:

$$\sigma^2(.) \triangleq \int_0^{\infty} \Phi(.)(.) (\omega) d\omega$$

Linear control surface actuator dynamics are represented by a unity DC gain first order lag with a break frequency of 10 rad/sec. The lag between throttle displacement and engine thrust build-up is represented conservatively by a unity DC gain first order lag with a break frequency of 0.5 rad/sec.

APPENDIX II

MANUAL LANDING APPROACH CONTROL FOR BASIC F-4C BACK-UP SYSTEM

This Appendix summarizes the results of an analysis of the pilot-vehicle system wherein the system is completely linear. Control activity is kept to the bare minimum required for adequate performance in tracking the ILS beam null in the presence of disturbances. This process leads to an estimate of the basic loop closures and gains the pilot must use for successful performance of the task. These estimates of linear system performance provide the basis for estimating nonlinear system performance in Section III. The techniques used are those reported in Refs. 7, 10, 26, 27 and 28 for example.

Simply stated, this process consists of the following steps

- Examine the key aircraft transfer functions given in Tables XXV and XXVI to discover handling qualities deficiencies.
- Evolve control strategies from among those possible which are capable of overcoming the handling qualities deficiencies and accomplishing the outer loop control objective.
- Find that control strategy which, among those possible, results in both adequate bandwidth tracking of the ILS beam and favorable pilot opinion.

Consider the longitudinal and lateral systems in turn with respect to these steps.

A. LONGITUDINAL

Examination of the key longitudinal transfer functions in Table XXV reveals:

- Additional short period damping is required.
- Additional short period stiffening would be advantageous but is not required.
- A non-minimum phase zero will be characteristic of the stabilator-to-glide slope deviation numerator because the trim

speed is below the minimum power speed for the clean aircraft configuration.

The first finding is the result of observing for $N_{\delta_s}^{\theta}/\Delta$ that closure of a pitch attitude-to-stabilator ($\theta \rightarrow \delta_s$) loop at even moderate gain will result in a considerable decrease in short period damping. The second finding results from the fact that while the short period stiffness (frequency) is adequate by handling qualities standards, it could be increased. If the stiffness were increased, then larger values of gain in the outer (glide slope deviation) loop could be used. The third finding is a consequence of the following. The stabilator-to-glide slope deviation numerator is closely approximated by the stabilator-to-altitude deviation* numerator, $N_{\delta_s}^{h_p}$. $N_{\delta_s}^{h_p}$ (in Table XXV), however, has a zero in the right hand half of the complex plane. This zero will attract a closed-loop pole into the right hand half of the complex plane† for any reasonable value of open-loop gain unless the zero itself can be moved into left hand half of the complex plane.

The control strategies which are capable of fixing the handling qualities deficiencies within the constraint of the cockpit displays available to the pilot are:

- Feedback of pitch attitude rate to stabilator ($\theta \rightarrow \delta_s$) will increase short period damping.
- Feedback of angle of attack or pitch attitude to stabilator ($\alpha \rightarrow \delta_s$ or $\theta \rightarrow \delta_s$) will increase the short period stiffness. $\theta \rightarrow \delta_s$ is the favored choice, however.
- Feedback of airspeed to throttle ($u_{AS} \rightarrow \delta_T$), pitch attitude to throttle ($\theta \rightarrow \delta_T$), or crossfeed of stabilator to throttle ($\delta_s \rightarrow \delta_T$) can move the right half plane zero of $N_{\delta_s}^{h_p}$ into the left hand half of the complex plane.

*Measured at the glide slope receiving antenna station which is taken to be $l_{x_p} = 23.9$ ft for this study.

†Recall that a closed-loop pole in the right hand half of the complex plane means the closed-loop system is unstable.

Additional elements of control strategy necessary to accomplish the outer-loop control objective (tracking the glide slope) are:

- Feedback of glide slope deviation, d_p , at the ILS receiving antenna station to stabilator to obtain adequate bandwidth in following the glide slope.
- Feedback of pitch attitude to stabilator to obtain adequate path damping in following the glide slope. (Recall that $\dot{d} \doteq \dot{h} \doteq V_{T_0} \theta$.)
- Feedback of integral of glide slope deviation, $\int d_p dt$, to stabilator for the purpose of eliminating DC values of glide slope deviation arising from DC values of pitch attitude.

The only part of the control strategy requiring further explanation is the one for moving the right half plane zero of $N_{\delta_s}^{\dot{h}_p}$ into the left hand half of the complex plane. Multiloop analysis results (Ref. 29) state that the only way in which this may be done is by feeding some variable other than h to some control point other than δ_s . Since δ_T is the only other longitudinal control point, its use is mandatory. A survey of the possibilities for modifying the numerator characteristics for the three candidates given by

$u_{AS} \rightarrow \delta_T$

$$N_{\delta_s}^{\dot{h}_p'} = N_{\delta_s}^{\dot{h}_p} + K_u \frac{0.5}{s+0.5} N_{\delta_s \delta_T}^{\dot{h}_p u} \quad (48)$$

$\theta \rightarrow \delta_T$

$$N_{\delta_s}^{\dot{h}_p'} = N_{\delta_s}^{\dot{h}_p} + K_{\theta TH} \frac{0.5}{s+0.5} N_{\delta_s \delta_T}^{\dot{h}_p \theta} \quad (49)$$

$\delta_s \rightarrow \delta_T$

$$N_{\delta_s}^{\dot{h}_p} = N_{\delta_s}^{\dot{h}_p} + K_{STH} \frac{0.5}{s+0.5} N_{\delta_T}^{\dot{h}_p} \quad (50)$$

shows that the first alternative is superior. This is because the resulting two pairs of complex zeros of $N_{\delta_s}^{\dot{h}_p'}$ have the most favorable locations for closure of the outer loops. This can be verified by

sketching the locus of zeros for each case (as a function of K_u , $K_{\theta_{TH}}$ or $K_{S_{TH}}$ as is appropriate) using the transfer functions in Table XXV.

The final step consists of completing the loop closures in numerical detail. This is done using the describing function model for the pilot given in Refs. 2 and 3.

$$Y_{P(\cdot)}(j\omega) = K(\cdot)e^{-j\omega \tau[\cdot]}(1 + j\omega T_L(\cdot)) \quad (51)$$

$$\doteq \frac{-K(\cdot)(j\omega - 2/\tau[\cdot])(1 + j\omega K(\cdot)/K(\cdot))}{(j\omega + 2/\tau[\cdot])} \quad (52)$$

$$\doteq \frac{-K(\cdot)\omega_N(j\omega - 2/\tau\{\cdot\})(1 + j\omega K(\cdot)/K(\cdot))}{(j\omega + \omega_N)(j\omega + 2/\tau\{\cdot\})} \quad (53)$$

The pilots' effective delay, $\tau[\cdot]$, is 0.33 sec to be conservative. The lead, T_L , that may be used must satisfy

$$0 \leq T_L(\cdot) = K(\cdot)/K(\cdot) \leq 5.0 \text{ sec} \quad (54)$$

When the alternate form is used, $\omega_N = 10.0$ rad/sec and $\tau\{\cdot\} = 0.2$ sec. The $[\cdot]$ or $\{\cdot\}$ subscripts contain notation reflecting the control point with which the delay is associated. The (\cdot) subscripts contain notation reflecting the feedback variable associated with the gain.

The loop closures are made with as low values of gain as are consistent with attaining about 0.30 rad/sec bandwidth in tracking the glide slope. This is to keep the required control deflections and rates as small as possible. The loop closure process is routine. The $u_{AS} \rightarrow \delta_T$ loop is closed first to move the right half plane zero of $N_{\delta_S}^{h_p}$ into the left hand half of the complex plane. Next, the $\dot{\theta} \rightarrow \delta_S$ loop is closed to damp the short period. Then the h_p and θ feedback paths are combined. In this key step, a favorable location of the zeros in the numerator of the open-loop function for the outer-loop closure (of glide slope deviation plus pitch attitude to stabilator) is obtained. These zeros, in turn, determine

the approximate location of the closed-loop system poles of the final loop closure which are dominant in the glide slope bend-following response of the pilot-vehicle system. Low-pass pilot equalization is included in the outer loop to serve as a "pitch rate command attenuator." This equalization attenuates the high frequency portion of the effective pitch rate command which is of little help in following the glide slope. This results in a small reduction of the stabilator rate and deflection. The equations for these closures are given in Table XXVIII. The block diagram for the pilot-vehicle system (System A) is given in Fig. 38. Values for the loop closure parameters are given in Table XXIX.

A series of Bode root locus diagrams (refer to Ref. 6), Figs. 39 through 44, show the development of the closed-loop transfer functions quantitatively. The order of presentation of these figures parallels the order of the qualitative development given above.

The resulting closed-loop glide slope following transfer function is:

$$\frac{d}{d_c} = \frac{3.053(0.0464)(0.05)(0.416)(5.632)(6.035)(-5.18)(-10.0)}{(0.423)(6.011)[0.876,0.0446][0.263,0.365]**} \quad (55)$$

** [0.268,1.716][0.776,3.613][0.936,14.17]

The frequency response for d/d_c is plotted in Fig. 45.

The resulting closed-loop bandwidth for glide slope bend-following based upon ± 3 dB is 0.27 rad/sec. However, the closed-loop frequency response is within ± 5.0 dB out to 0.55 rad/sec. This is more than adequate for longitudinal performance.

TABLE XXVIII

EQUATIONS FOR BASIC LONGITUDINAL LOOP
CLOSURES, SYSTEM A

CLOSURES	NAME	EXPRESSION
$u_{AS} \rightarrow \delta_T$	Δ'	$(2/\tau_T)(\omega_2)\Delta - K_u\omega_2(-2/\tau_T)N_{\delta_T}^u$
	$N_{\delta_S}^{\dot{h}'_p}$	$(2/\tau_T)(\omega_2)N_{\delta_S}^{\dot{h}'_p} - K_u\omega_2(-2/\tau_T)N_{\delta_S}^{\dot{h}'_p}u_{\delta_T}$
	$N_{\delta_S}^{\dot{h}'}$	$(2/\tau_T)(\omega_2)N_{\delta_S}^{\dot{h}'}$ $- K_u\omega_2(-2/\tau_T)N_{\delta_S}^{\dot{h}'}$ u_{δ_T}
	$N_{\delta_S}^{\theta'}$	$(2/\tau_T)(\omega_2)N_{\delta_S}^{\theta'}$ $- K_u\omega_2(-2/\tau_T)N_{\delta_S}^{\theta'}$ u_{δ_T}
$u_{AS} \rightarrow \delta_T$ and $\dot{\theta} \rightarrow \delta_S$	Δ''	$(2/\tau_S)(\omega_N)(\omega_3)\Delta' - K_\theta\omega_N\omega_3(0)(-2/\tau_S)N_{\delta_S}^{\theta'}$
	$N_{\delta_S}^{\theta''}$	$(2/\tau_S)(\omega_N)(\omega_3)N_{\delta_S}^{\theta''}$
	$N_{\delta_S}^{\dot{h}''_p}$	$(2/\tau_S)(\omega_N)(\omega_3)N_{\delta_S}^{\dot{h}''_p}$
	$N_{\delta_S}^{\dot{h}''}$	$(2/\tau_S)(\omega_N)(\omega_3)N_{\delta_S}^{\dot{h}''}$
$u_{AS} \rightarrow \delta_T$ $\dot{\theta} \rightarrow \delta_S$ $\theta \rightarrow \delta_S$ and $h_p \rightarrow \delta_S$	Δ'''	$(\omega_4)(0)^2\Delta'' - K_d\omega_N\omega_3\omega_4$ $(-2/\tau_S)\left[(K_{\dot{T}}/K_d)N_{\delta_S}^{\dot{h}'_p} + K_\theta/K_d(0)^2N_{\delta_S}^{\theta'}\right]$ $(\omega_4)(0)^2N_{\delta_S}^{\dot{h}''} = (\omega_4)(0)^2(2/\tau_S)(\omega_N)(\omega_3)N_{\delta_S}^{\dot{h}'}$

$$\frac{d}{d_c} = \frac{h}{h_c} = \frac{-K_d\omega_N\omega_3\omega_4(-2/\tau_S)(K_{\dot{T}}/K_d)N_{\delta_S}^{\dot{h}''}}{(0)^2(\omega_N)(\omega_3)(\omega_4)(2/\tau_S)\Delta''}$$

$$= \frac{-K_d\omega_N\omega_3\omega_4(-2/\tau_S)(K_{\dot{T}}/K_d)N_{\delta_S}^{\dot{h}'}}{\Delta''}$$

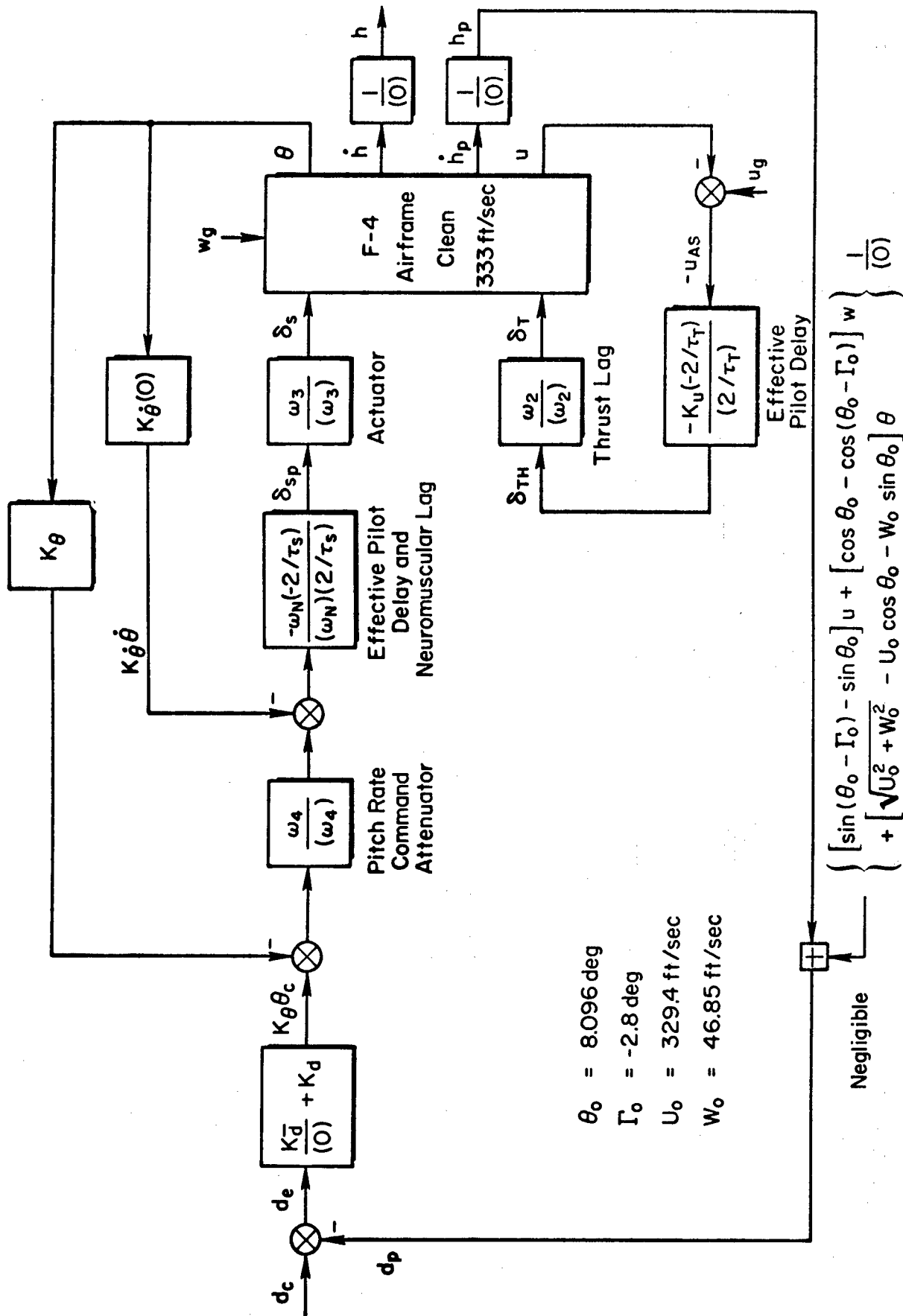
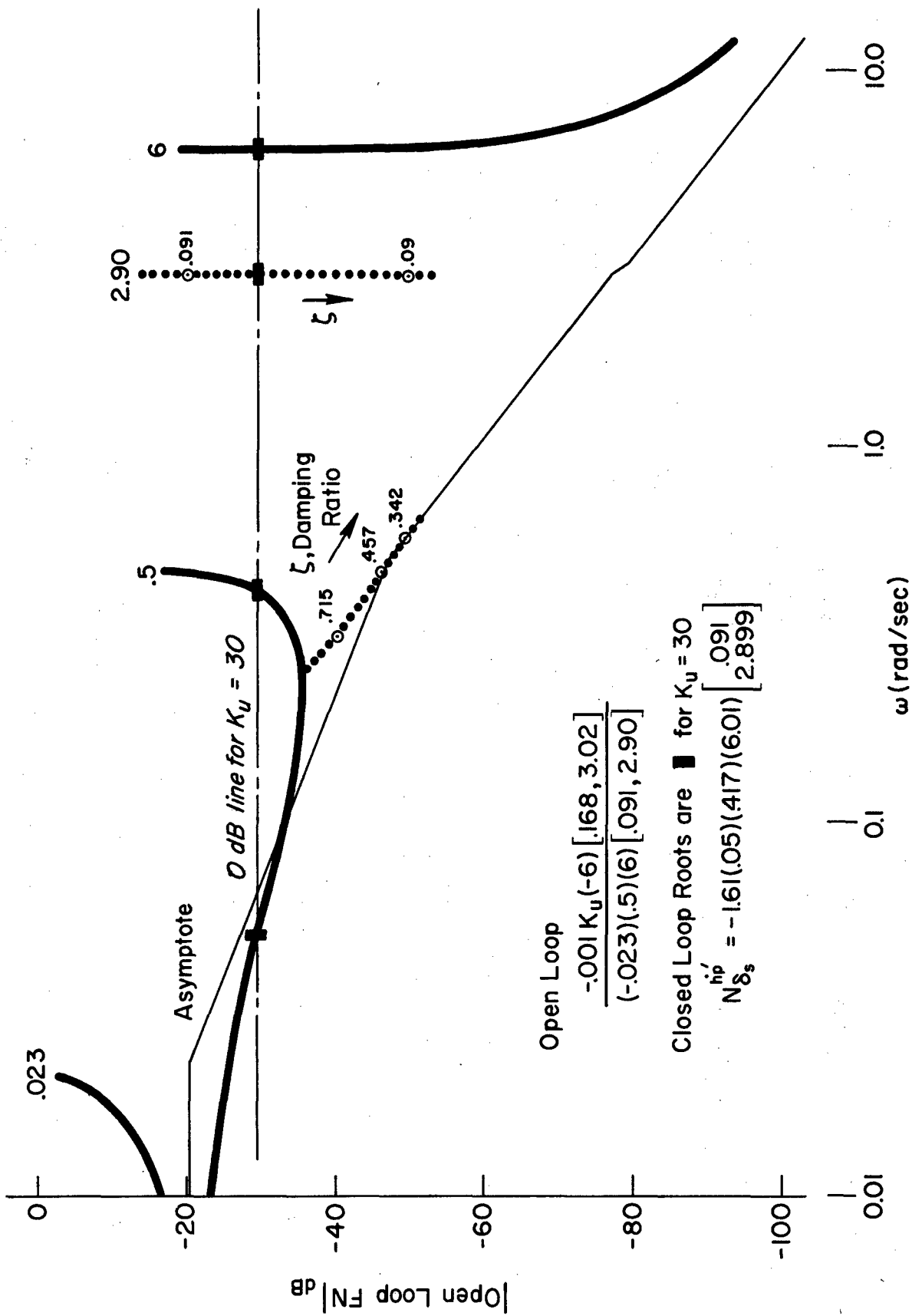


Figure 38. Longitudinal F-4 Block Diagram for System A

TABLE XXIX
 PARAMETERS FOR LINEAR PILOT LOOP CLOSURES,
 SYSTEM A, LONGITUDINAL

$K_u m X_{\delta_T}$	59.7	lb/(ft/sec)
τ_T	0.33	sec
ω_2	0.50	rad/sec
K_{θ}	-0.244	sec
ω_N	10.0	rad/sec
τ_S	0.2	sec
ω_3	10.0	rad/sec
K_{θ}	-0.393	—
ω_4	2.25	rad/sec
K_d	-0.0015	deg/(ft/sec)
K_d	-0.03	deg/ft



Open Loop

$$\frac{-0.01 K_u (-6) [0.168, 3.02]}{(-0.23)(.5)(6) [0.091, 2.90]}$$

Closed Loop Roots are ■ for $K_u = 30$

$$N_{\delta_s}^{hp} = -1.61(.05)(.417)(6.01) \begin{bmatrix} 0.091 \\ 2.899 \end{bmatrix}$$

Figure 39. Effect of $\nu_{AS} \rightarrow \delta_T$ Closure upon the Key Numerator, $N_{\delta_s}^{hp}$

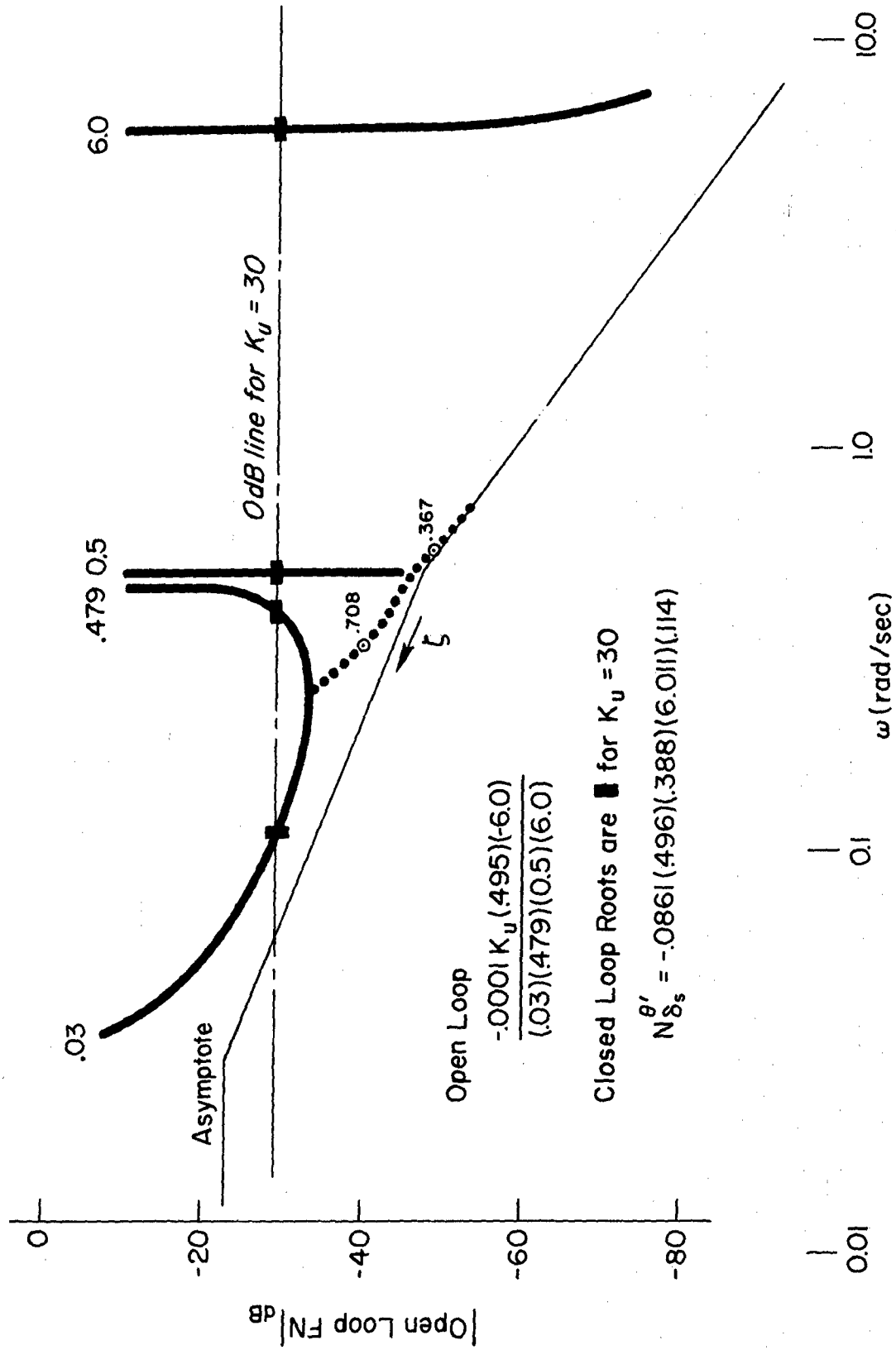


Figure 40. Effect of $u_{AS} \rightarrow \delta_T$ Closure upon the N'_S Numerator

Closed Loop Roots are ■ for $K_u = 30$

$$\text{Open Loop} = \frac{-0.01 K_u (0.27)(-6.0) [445, 1.36]}{(0.5)(6.0) [104, 1.59] [377, 1.31]}$$

$$\Delta' = (427)(6.01) \begin{bmatrix} .376 \\ 1.308 \end{bmatrix} \begin{bmatrix} .279 \\ .178 \end{bmatrix}$$

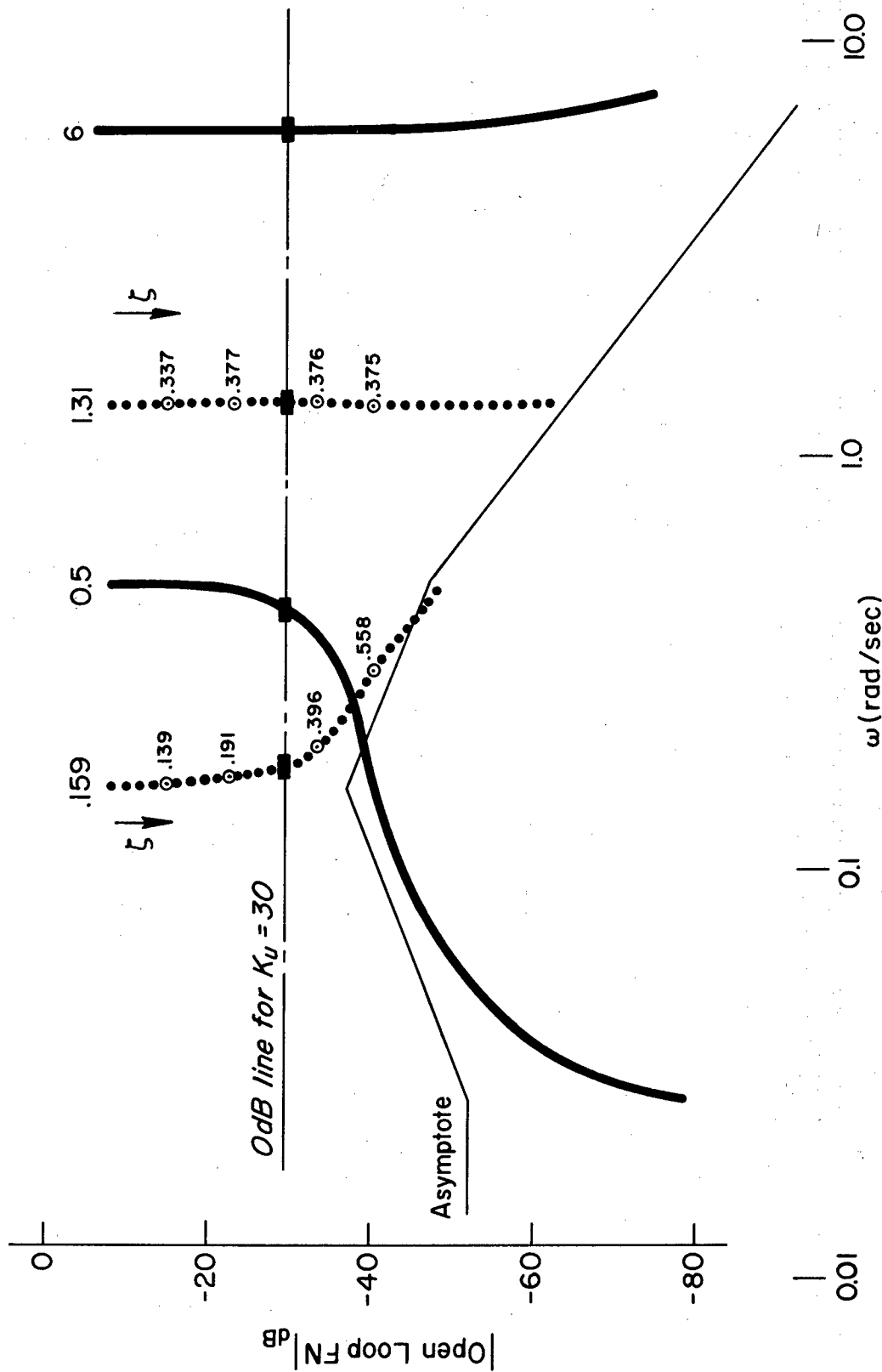


Figure 41. Effect of $u_{AG} \rightarrow \delta_T$ Closure upon the Characteristic Polynomial, Δ

Closed Loop Roots are ■ for $K_{\theta} = -14$

$$\text{Open Loop} = \frac{8.61K_{\theta}(0)(.114)(.388)(496)(6.01)(-10.0)}{(100)^3(6.01)(427)[.376, 1.31][.279, .178]}$$

$$\Delta'' = (.425)(1.65)(6.011) \begin{bmatrix} .306 \\ .154 \end{bmatrix} \begin{bmatrix} .545 \\ 2.648 \end{bmatrix} \begin{bmatrix} .936 \\ 14.13 \end{bmatrix}$$

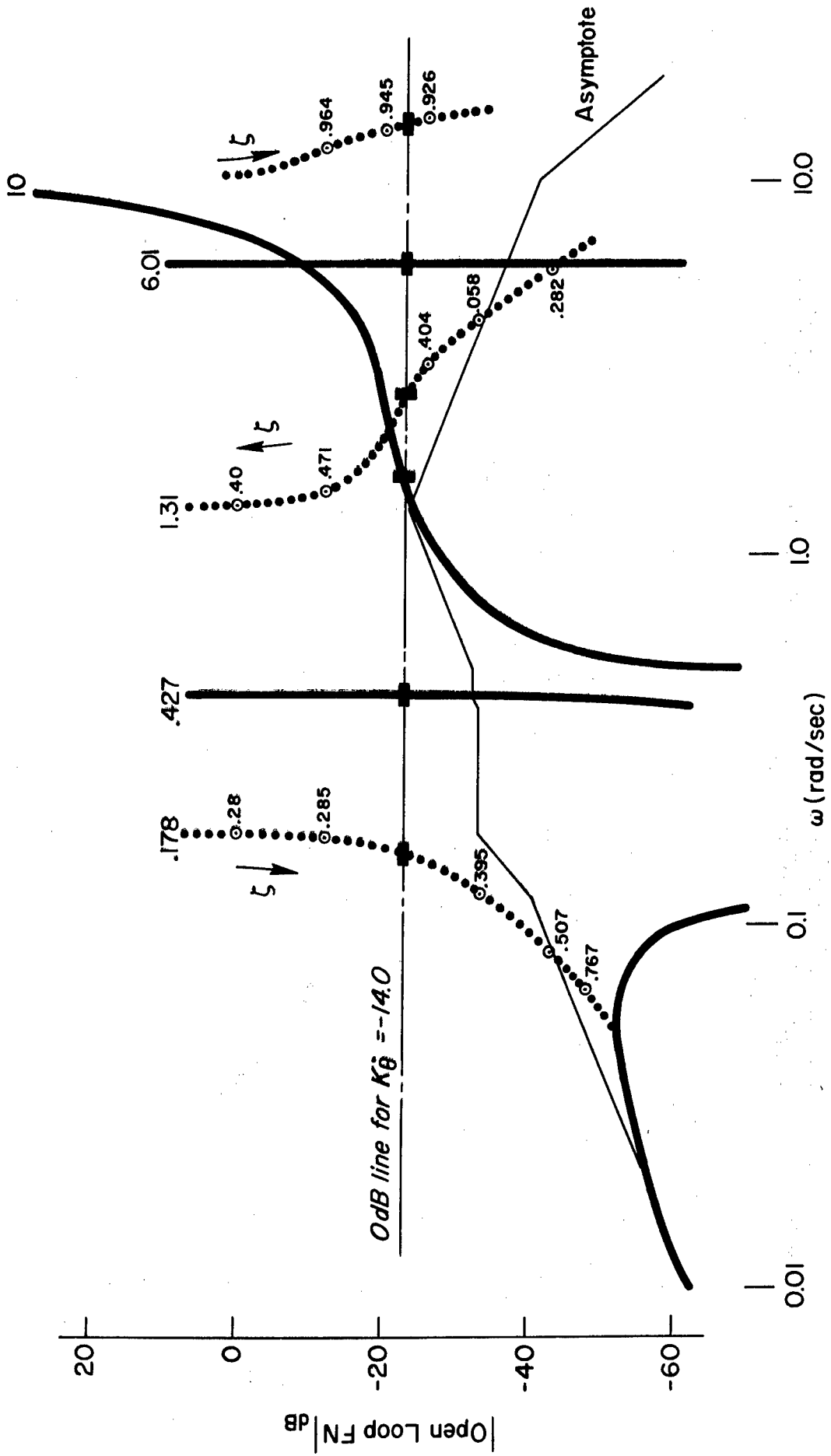
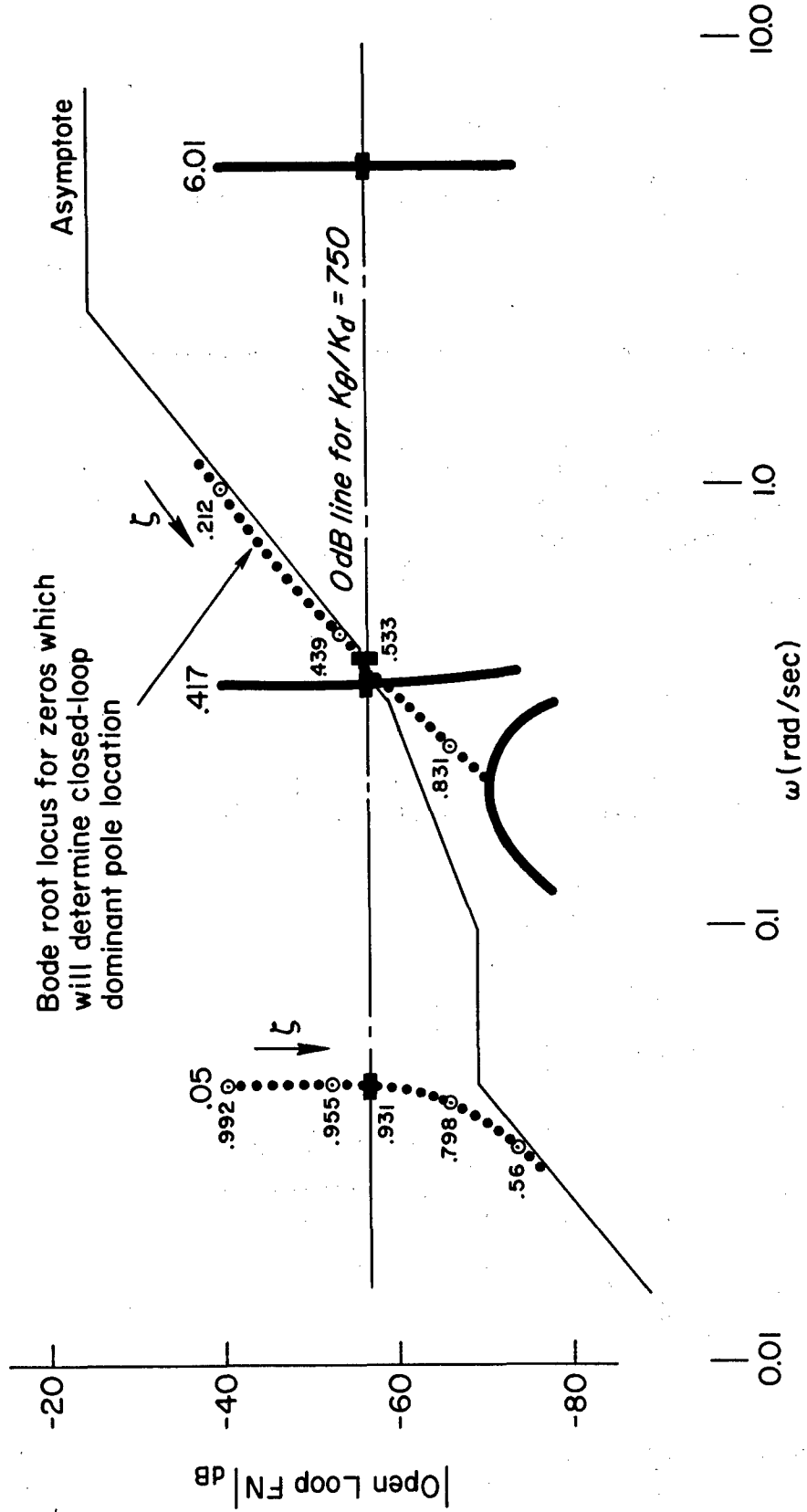


Figure 42. Effect of $\theta \rightarrow \delta_s$ Closure upon the Characteristic Polynomial, Δ''

Closed Loop Roots are ■ for $K_\theta / K_d = 750$

$$\left(s + \frac{K_d}{K_d}\right) N_{\delta s}^{hp'} + \frac{K_\theta}{K_d} s^2 N_{\delta s}^{\theta'} = -66.20(422)(6.011) \begin{bmatrix} .931 \\ .049 \end{bmatrix} \begin{bmatrix} .533 \\ .456 \end{bmatrix}$$

Open Loop =
$$\frac{.0535 K_\theta / K_d (0)^2 (.114)(.388)(496)(6.011)}{(.05)^2 (.417)(6.011) [.091, 2.899]}$$



Bode root locus for zeros which will determine closed-loop dominant pole location

Figure 43. Effect of $\theta \rightarrow \delta_s$ for Obtaining Favorable Root Locations in the Open-Loop Function Numerator for Final Loop Closure

Closed Loop Roots are ■ for $K_d = -.03$
 $\Delta''' = (423)(6.011) \begin{bmatrix} .876 \\ .0446 \end{bmatrix} \begin{bmatrix} .263 \\ .365 \end{bmatrix} \begin{bmatrix} .776 \\ 3.613 \end{bmatrix} \begin{bmatrix} .936 \\ 14.172 \end{bmatrix}$

$$\text{Open Loop} = \frac{14895 K_d (422)(6.011)(-10.0) \begin{bmatrix} .931 \\ .049 \end{bmatrix} \begin{bmatrix} .533 \\ 4.56 \end{bmatrix}}{(0)^2 (425)(1.65)(2.25)(6.011) \begin{bmatrix} .306 \\ .154 \end{bmatrix} \begin{bmatrix} .545 \\ 2.648 \end{bmatrix} \begin{bmatrix} .936 \\ 14.132 \end{bmatrix}}$$

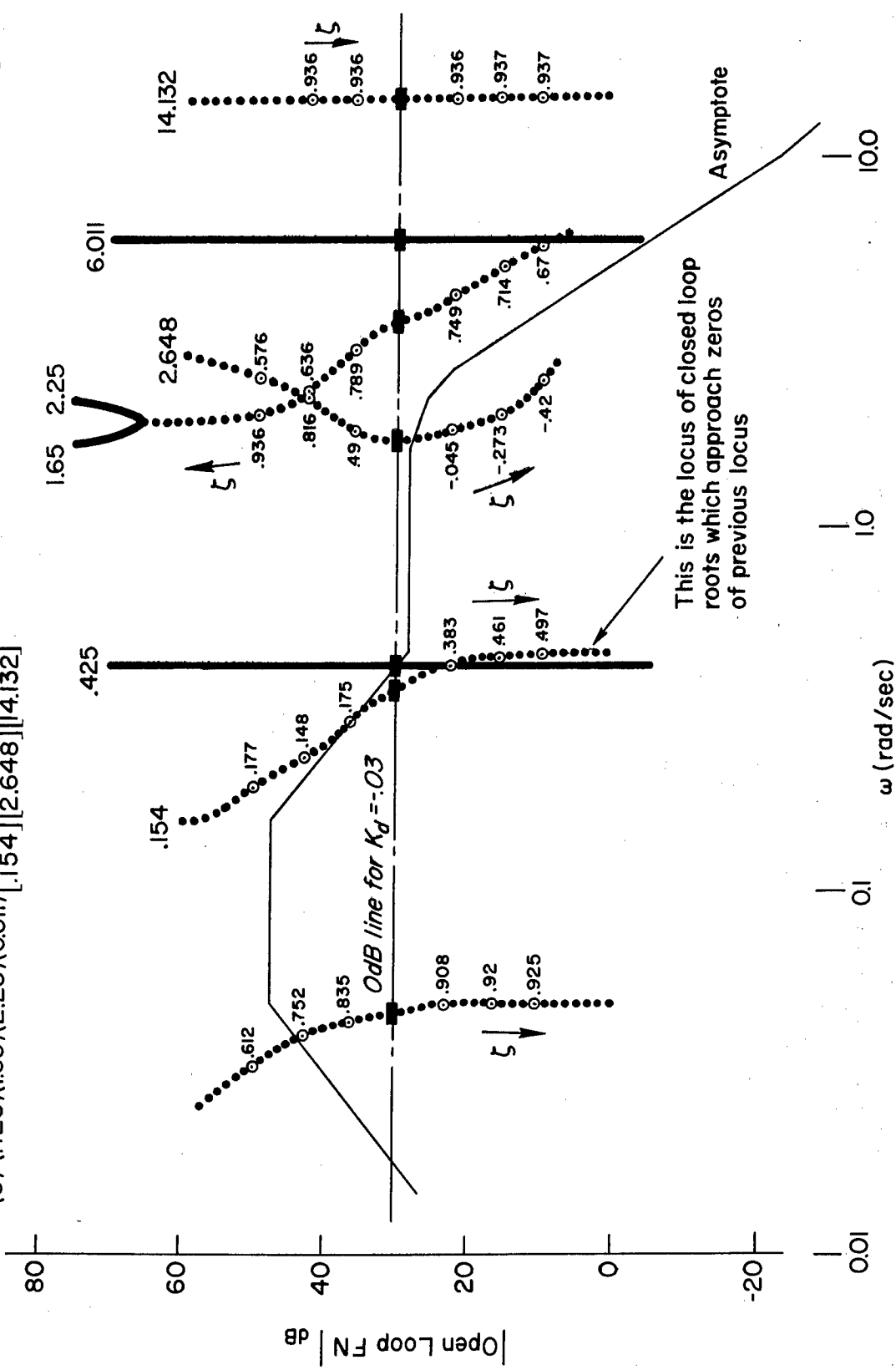


Figure 44. Final Loop Closure, $[K_d(s+K_d/K_d)h_p/(s+K_d\theta)] \rightarrow \delta_s$, which gives the Closed-Loop System Characteristic Polynomial, Δ'''

$$\frac{d}{d_c} = \frac{3.053(0.0464)(.05)(416)(5.632)(6.035)(-5.18)(-10.0)}{(4.23)(6.011) \begin{bmatrix} .876 \\ .0446 \end{bmatrix} \begin{bmatrix} .263 \\ .365 \end{bmatrix} \begin{bmatrix} .268 \\ 1.716 \end{bmatrix} \begin{bmatrix} .776 \\ 3.613 \end{bmatrix} \begin{bmatrix} .936 \\ 14.172 \end{bmatrix}}$$

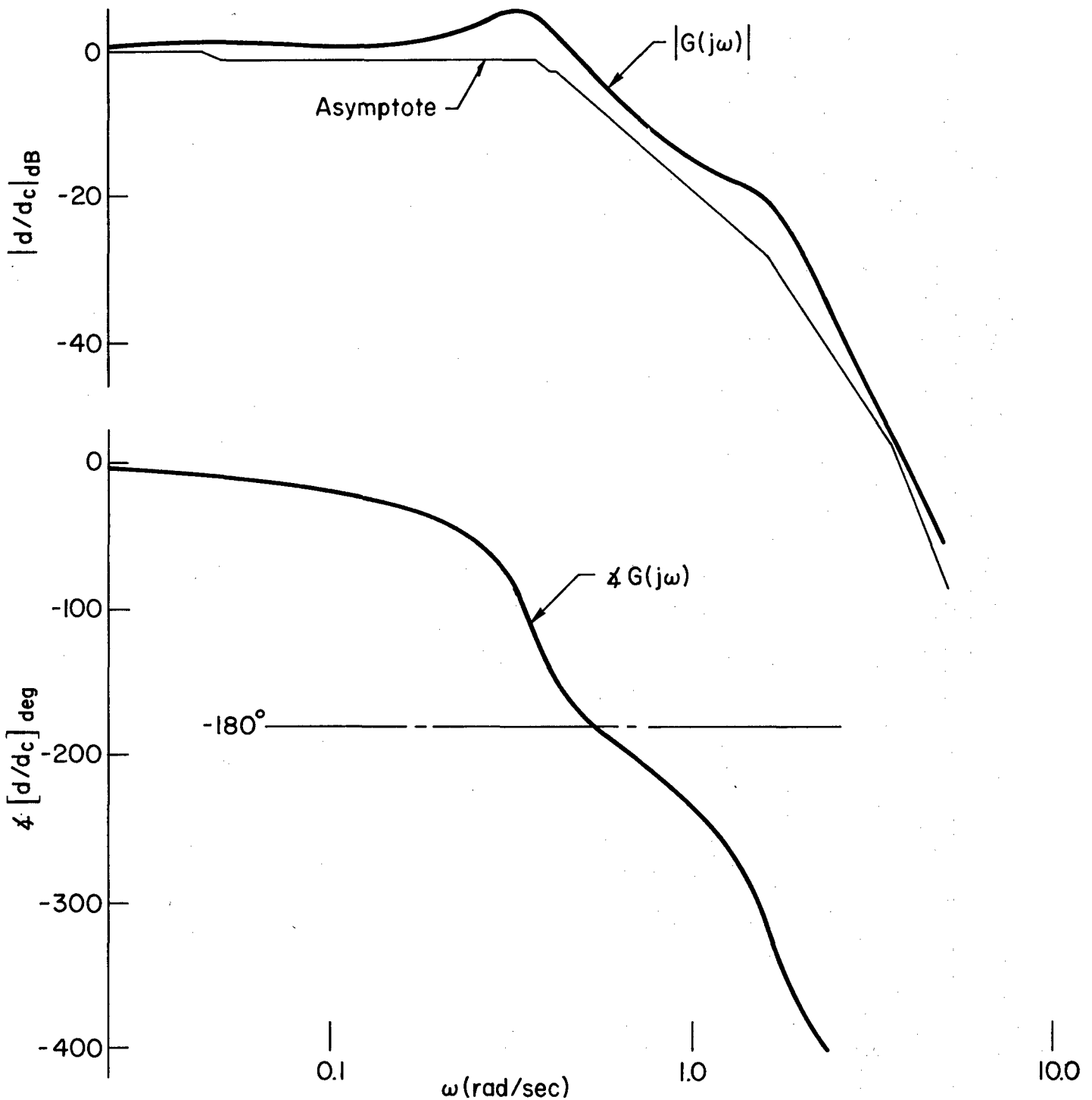


Figure 45. Glide Slope Frequency Response for Closed-Loop System

B. LATERAL

Examination of the key lateral transfer functions in Table XXVI results in three findings.

- Additional dutch roll damping is required.
- $\omega_{\phi}/\omega_d = 1.560/1.725 \doteq 0.9 \doteq 1.0$
- Spoiler roll effectiveness is very low.

All three findings involve the $N_{\delta_{sp}}^{\phi}/\Delta$ transfer function.

The control strategies which are capable of fixing the handling qualities deficiencies are:

- Feedback of yaw rate to rudder ($r \rightarrow \delta_r$) or high-pass filtered lateral acceleration to rudder ($a_y' \rightarrow \delta_r$) would be ideal for increasing the damping of those factors in Δ and $N_{\delta_{sp}}^{\phi}$ which are associated with the dutch roll.

Constraints imposed by the cockpit displays make either loop closure by the pilot improbable. Hence yaw damping stability augmentation is in order. The ground rules for this minimum back-up system study, however, do not permit stability augmentation.* Therefore, feasible alternatives must be found. Alternatives are:

- Accept the low dutch roll damping and the large gust excitation of dutch roll that will result
- Crossfeed spoiler to rudder ($\delta_{sp} \rightarrow \delta_r$) in such a way that the ω_{ϕ}/ω_d ratio will be decreased. Then the pilot's roll-to-spoiler loop closure ($\phi \rightarrow \delta_{sp}$) will result in a modest increase in closed-loop dutch roll damping. Closure of a roll rate-to-spoiler loop ($\dot{\phi} \rightarrow \delta_{sp}$) will allow still another small increase in closed-loop dutch roll damping.

*Furthermore, there is no back-up rudder actuator. However, the performance gains which would result if a back-up rudder tab actuator and yaw rate gyro in an integral package were installed might well justify the additional complexity.

Additional elements of control strategy necessary to accomplish the outer-loop control objective (tracking the localizer) are:

- Feedback of roll to spoiler ($\phi \rightarrow \delta_{sp}$) for roll stabilization. (This loop closure was also cited above in connection with its effect upon closed-loop dutch roll damping.)
- Feedback of localizer deviation, y_p , at the ILS receiving antenna station to spoiler to obtain adequate bandwidth in following the localizer.
- Feedback of washed-out heading angle to spoiler to obtain adequate path damping in following the localizer. (Recall that $\dot{y} = V_T \psi$.) The wash-out is necessary so that DC values of heading angle (such as might arise in countering a crosswind) do not result in DC values of localizer deviation.

The final step consists of completing the loop closures in numerical detail. This is done using the describing function model for the pilot given in Refs. 2 and 3 and which has been summarized very briefly in the previous subsection.

The ultimate objective of the loop closures is that the final, outer-loop closure have a bandwidth of about 0.3 rad/sec. Furthermore, this should be achieved with a minimum of spoiler authority. This last consideration leads to system designs for which the roll angle-to-spoiler loop gain is so low that no additional dutch roll damping can be induced by increasing $\omega_{\phi}/\omega_{\beta}$ by means of spoiler-to-rudder crossfeed. Similarly, the low values of the roll angle-to-spoiler loop gains are such that the natural roll damping of the aircraft, $-L'_p$, is sufficient. Consequently, the gains in the crossfeed and roll rate-to-spoiler are zero.

From this point, the loop closure process is routine. Closure of the $\phi \rightarrow \delta_a$ loop results in a small increase in dutch roll damping as well as providing roll stabilization. Next, the y_p and washed-out ψ feedback paths are combined. In this key step, a favorable location of the zeros in the numerator of the open-loop function for the outer loop closure (of localizer plus heading angle-to-spoiler) is obtained. These zeros, in turn, determine the approximate location of those closed-loop system

poles which are dominant in localizer following response of the pilot-vehicle system.

Low pass pilot equalization is included in the outer loop to serve as a "roll command attenuator." This equalization attenuates the high frequency portion of the effective roll command which is of little help in following the localizer. This results in a small reduction of the spoiler rate and deflection.

The equations for these closures are given in Table XXX. The block diagram for the pilot-vehicle system (System A) is given in Fig. 46. Values for the loop closure parameters are given in Table XXXI.

A series of Bode root locus diagrams, Figs. 47 through 49, show the development of the closed-loop transfer functions quantitatively. The order of presentation of these figures parallels the order of the qualitative development discussion given above.

The resulting closed-loop localizer following transfer function is:

$$\frac{y}{y_c} = \frac{0.00933(0.0)(0.01)(-9.07)(-10.0)(10.68)[0.0911, 1.617]}{(0.0112)(0.239)(0.528)(1.122)(11.96)[0.400, 0.215] **} \quad (56)$$

** [0.113, 1.751][0.976, 9.357]

The frequency response for y/y_c is plotted in Fig. 50.

The resulting closed-loop bandwidth for localizer bend-following based upon ± 3 dB is 0.25 rad/sec. This is possibly adequate for lateral performance.

TABLE XXX

EQUATIONS FOR BASIC LATERAL LOOP
CLOSURES, SYSTEM A

CLOSURES	NAME	EXPRESSION
$\delta_{spp} \rightarrow \delta_r$	Δ_p	$(\omega_5)(\omega_6)\Delta$
	$N_{\delta_{spp}}^{\ddot{y}}$	$V_{T_0} \cos \Gamma_0 \left[\omega_5(\omega_6) N_{\delta_{sp}}^{\dot{\lambda}} + K_{cf}(0)(\omega_5) N_{\delta_r}^{\dot{\lambda}} \right]$
	$N_{\delta_{spp}}^{\Phi}$	$\omega_5(\omega_6) N_{\delta_{sp}}^{\Phi} + K_{cf}(0)(\omega_5) N_{\delta_r}^{\Phi}$
	$N_{\delta_{spp}}^r$	$\omega_5(\omega_6) N_{\delta_{sp}}^r + K_{cf}(0)(\omega_5) N_{\delta_r}^r$
	$N_{\delta_{spp}}^{\ddot{y}_p}$	$N_{\delta_{spp}}^{\ddot{y}} + \ell_{x_p} / \cos \theta_0(0) N_{\delta_{spp}}^r$
$\delta_{spp} \rightarrow \delta_r$	Δ'	$(2/\tau_{sp})(\omega_N)\Delta_p - K_{\phi} \omega_N (K_{\phi}/K_{\dot{\phi}}) (-2/\tau_{sp}) N_{\delta_{spp}}^{\Phi}$
$\dot{\phi} \rightarrow \delta_{spp}$	$N_{\delta_{spp}}^{\Phi'}$	$(2/\tau_{sp})(\omega_N) N_{\delta_{spp}}^{\Phi}$
and		
$\phi \rightarrow \delta_{spp}$	$N_{\delta_{spp}}^{\ddot{y}'_p}$	$(2/\tau_{sp})(\omega_N) N_{\delta_{spp}}^{\ddot{y}_p}$
	$N_{\delta_{spp}}^{\ddot{y}'}$	$(2/\tau_{sp})(\omega_N) N_{\delta_{spp}}^{\ddot{y}}$
	$N_{\delta_{spp}}^{r'}$	$(2/\tau_{sp})(\omega_N) N_{\delta_{spp}}^r$

(cont'd)

TABLE XXX (cont'd)

EQUATIONS FOR BASIC LATERAL LOOP
CLOSURES, SYSTEM A

CLOSURES	NAME	EXPRESSION
$\delta_{spp} \rightarrow \delta_r$	Δ''	$(0)^2(\omega_1)\Delta' - K_y\omega_N(-2/\tau_{sp})\left[(\omega_1)N_{\delta_{spp}}^{\dot{y}_p} + \frac{K\psi}{K_y\cos\theta_o}(0)^2N_{\delta_{spp}}^r\right]$
$\phi \rightarrow \delta_{spp}$		
$\varphi \rightarrow \delta_{spp}$		
$\psi \rightarrow \delta_{spp}$		
$y_p \rightarrow \delta_{spp}$		
	$N_{\delta_{spp}}^{\dot{y}''}$	$(0)^2(\omega_1)N_{\delta_{spp}}^{\dot{y}'} = (0)^2(\omega_1)(2/\tau_{sp})(\omega_N)N_{\delta_{spp}}^{\dot{y}}$

$$\frac{y}{y_c} = \frac{-K_y\omega_N(-2/\tau_{sp})N_{\delta_{spp}}^{\dot{y}''}}{(0)^2(\omega_N)(2/\tau_{sp})\Delta''}$$

$$= \frac{-K_y\omega_N(-2/\tau_{sp})(\omega_1)N_{\delta_{spp}}^{\dot{y}}}{\Delta''}$$

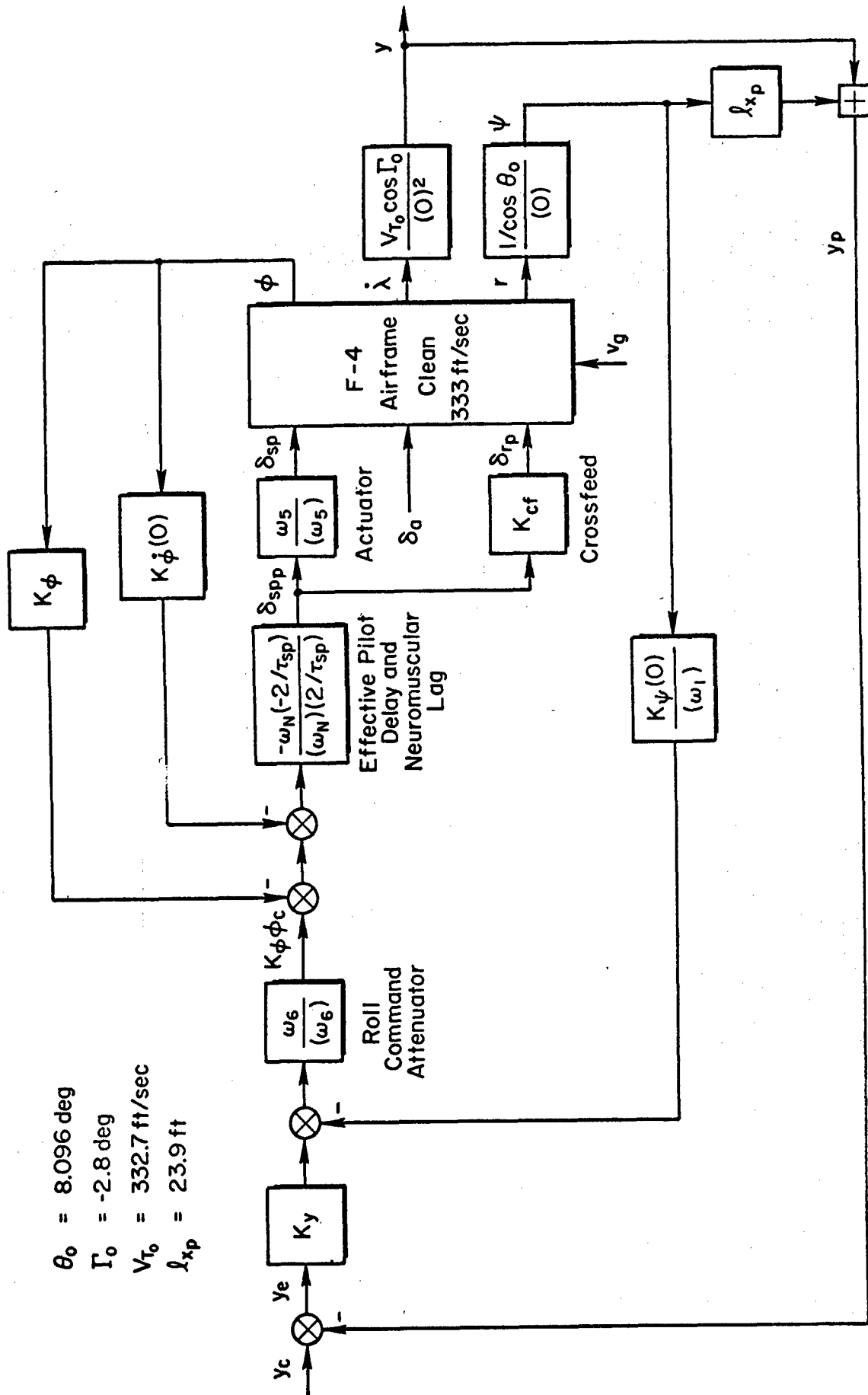


Figure 46. Lateral F-4 Block Diagram for System A

TABLE XXXI

PARAMETERS FOR LINEAR PILOT LOOP CLOSURES,
SYSTEM A, LATERAL

K_{cf}	0	--
K_{ϕ}	0	deg/(rad/sec)
ω_N	10.0	rad/sec
τ_{sp}	0.2	sec
ω_5	10.0	rad/sec
K_{ϕ}	36.0	deg/rad
ω_6	0.85	rad/sec
K_{ψ}	100.0	deg/rad
ω_1	0.01	sec
K_y	0.03	deg/ft

Closed Loop Roots are ■ for $K_\phi = 36$

$$\text{Open Loop} = \frac{-1.215 K_\phi (-10.0) [1.2, 1.556]}{(10.0)^3 (0.43)(1.392) [0.114, 1.725]}$$

$$\Delta' = (11.966) \begin{bmatrix} .111 & .977 \\ 1.747 & .622 \end{bmatrix} \begin{bmatrix} .975 \\ 9.361 \end{bmatrix}$$

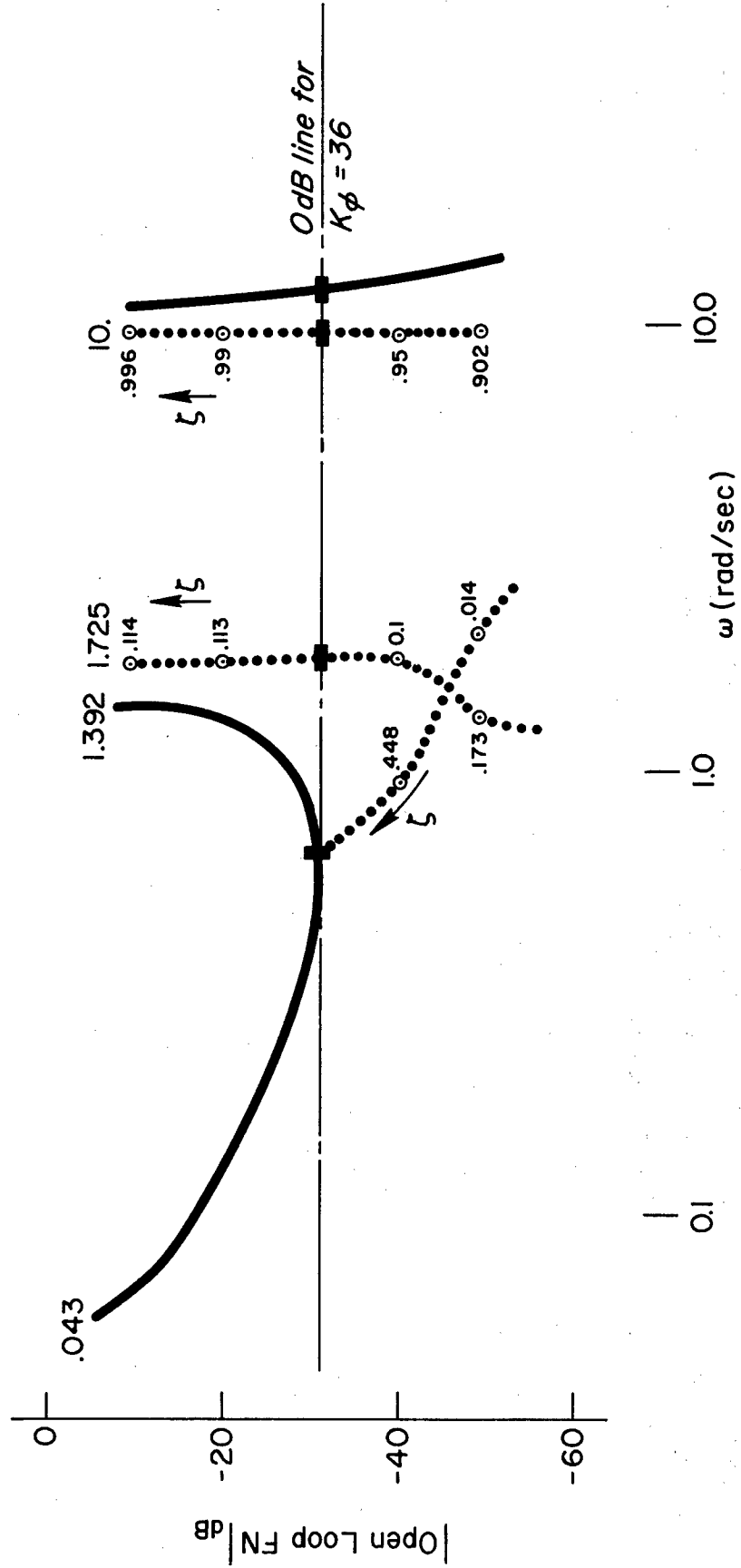


Figure 47. Effect of $\phi \rightarrow \delta_{sp}$ Closure upon the Characteristic Polynomial, Δ'

Closed Loop Roots are ■ for $\frac{K_\psi}{K_y} = 3333$

$$\text{Open Loop} = \frac{.0524 K_\psi / K_y (0)^2 (.683) [.020, 2.109]}{(.01) [.122, 1.526] [.022, 4.672]}$$

$$(\omega_1) N_{\delta_{sp}} + \frac{K_\psi}{K_y} \frac{(0)^2}{\cos \theta_0} N_{\delta_{sp}} = 3.0757 (0.11) (0.10) (0.571) \begin{bmatrix} .02 \\ 2.12 \end{bmatrix}$$

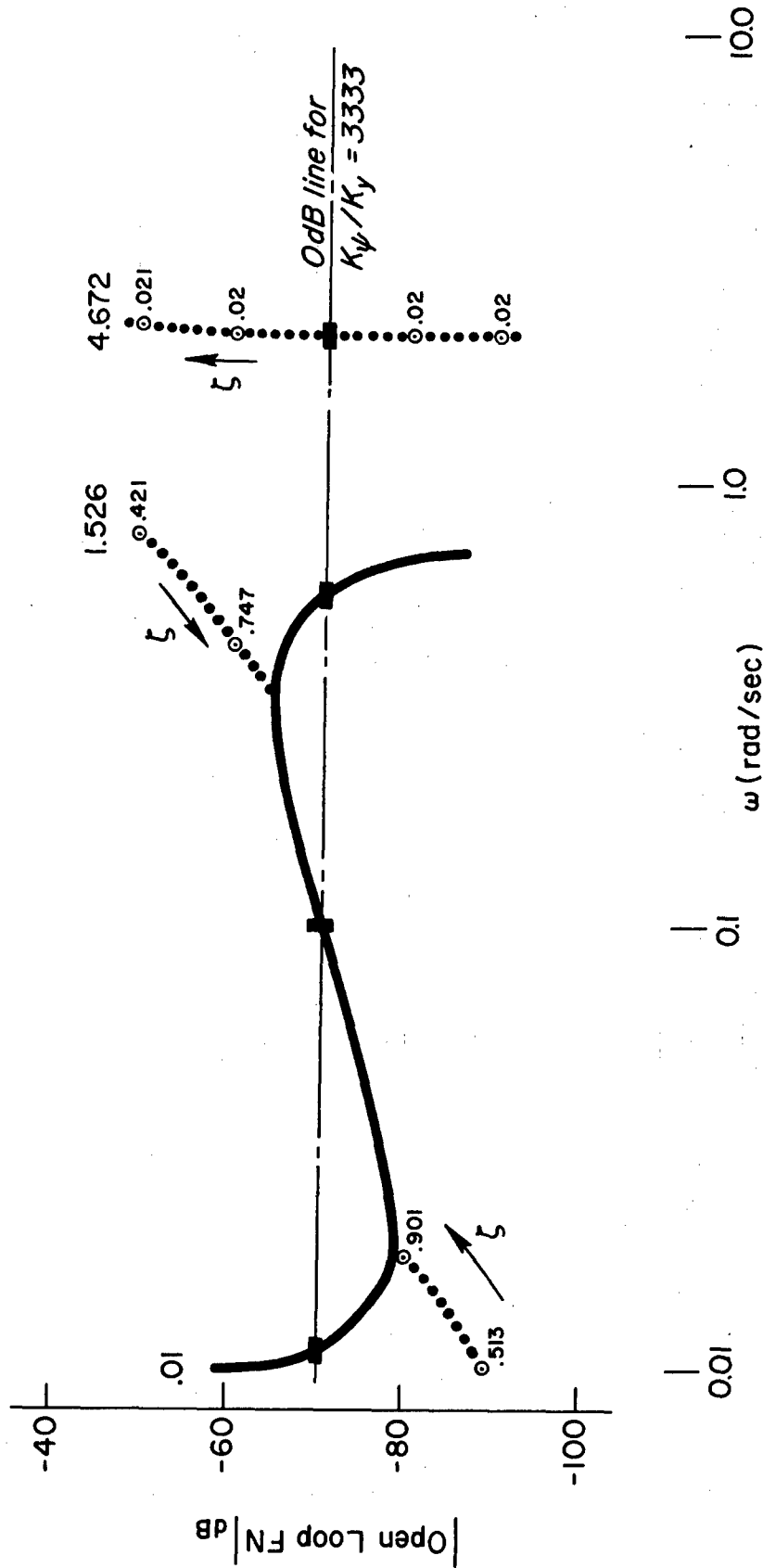


Figure 48. Effect of $\psi \rightarrow \delta_{sp}$ for Obtaining Favorable Root Locations in the Open-Loop Function Numerator for Final Loop Closure

Closed Loop Roots are ■ for $K_y = .03$

$$\text{Open Loop} = \frac{-261.434 K_y (-10.0)(.011)(.571) \begin{bmatrix} .02 \\ 2.12 \end{bmatrix}}{(0)^2 (.01)(.85)(11.97) \begin{bmatrix} .111 \\ 1.747 \end{bmatrix} \begin{bmatrix} .977 \\ .622 \end{bmatrix} \begin{bmatrix} .975 \\ 9.361 \end{bmatrix}}$$

$$\Delta'' = (.011)(.219)(.538)(1.122)(11.956) \begin{bmatrix} .423 \\ .218 \end{bmatrix} \begin{bmatrix} .114 \\ 1.751 \end{bmatrix} \begin{bmatrix} .975 \\ 9.358 \end{bmatrix}$$

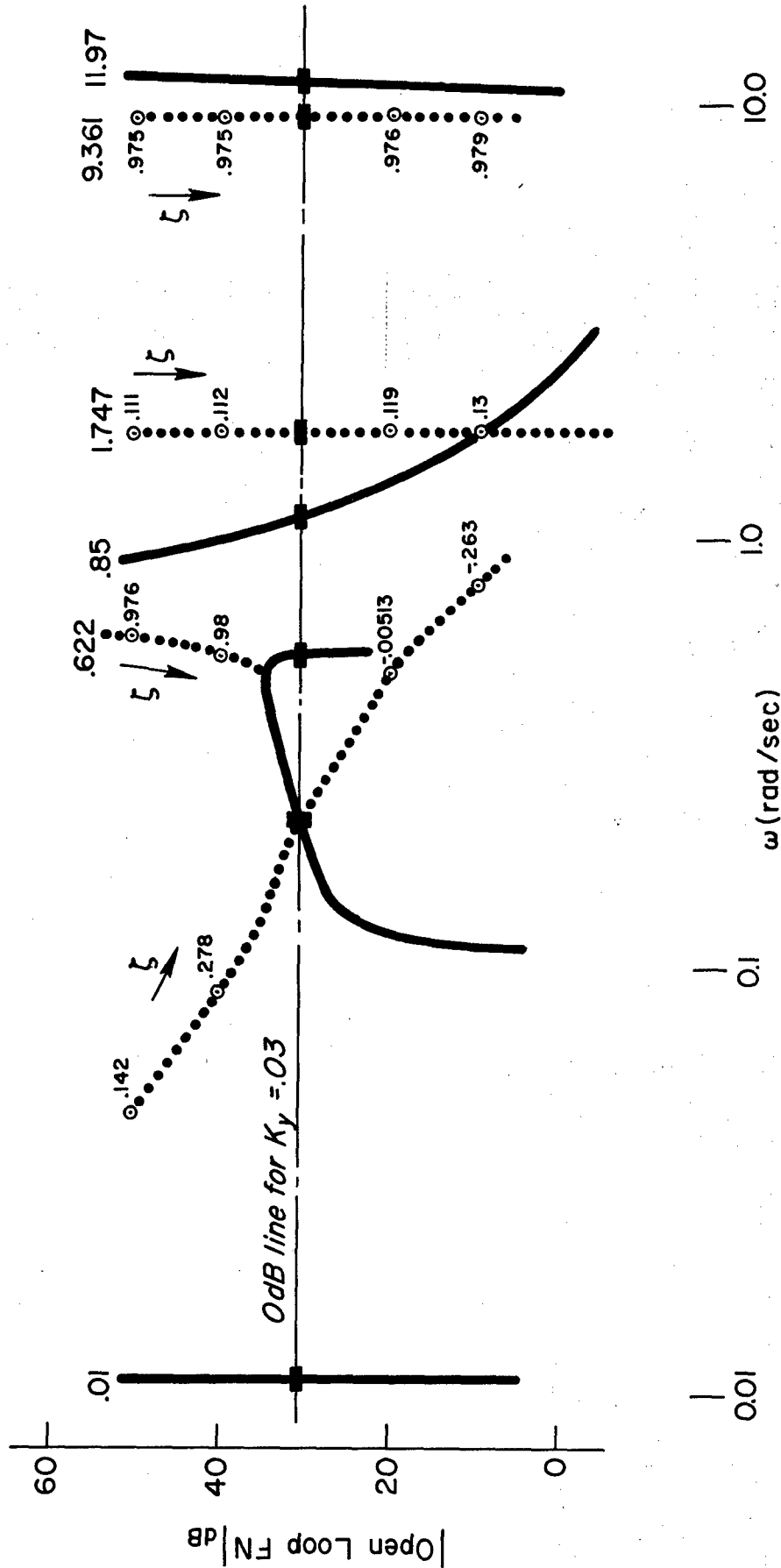


Figure 49. Final Loop Closure, $[K_y y + K_{1y} s \psi / (s + \omega_1)] \rightarrow \delta_{sp}$, which gives the Closed-Loop System Characteristic Polynomial, Δ''

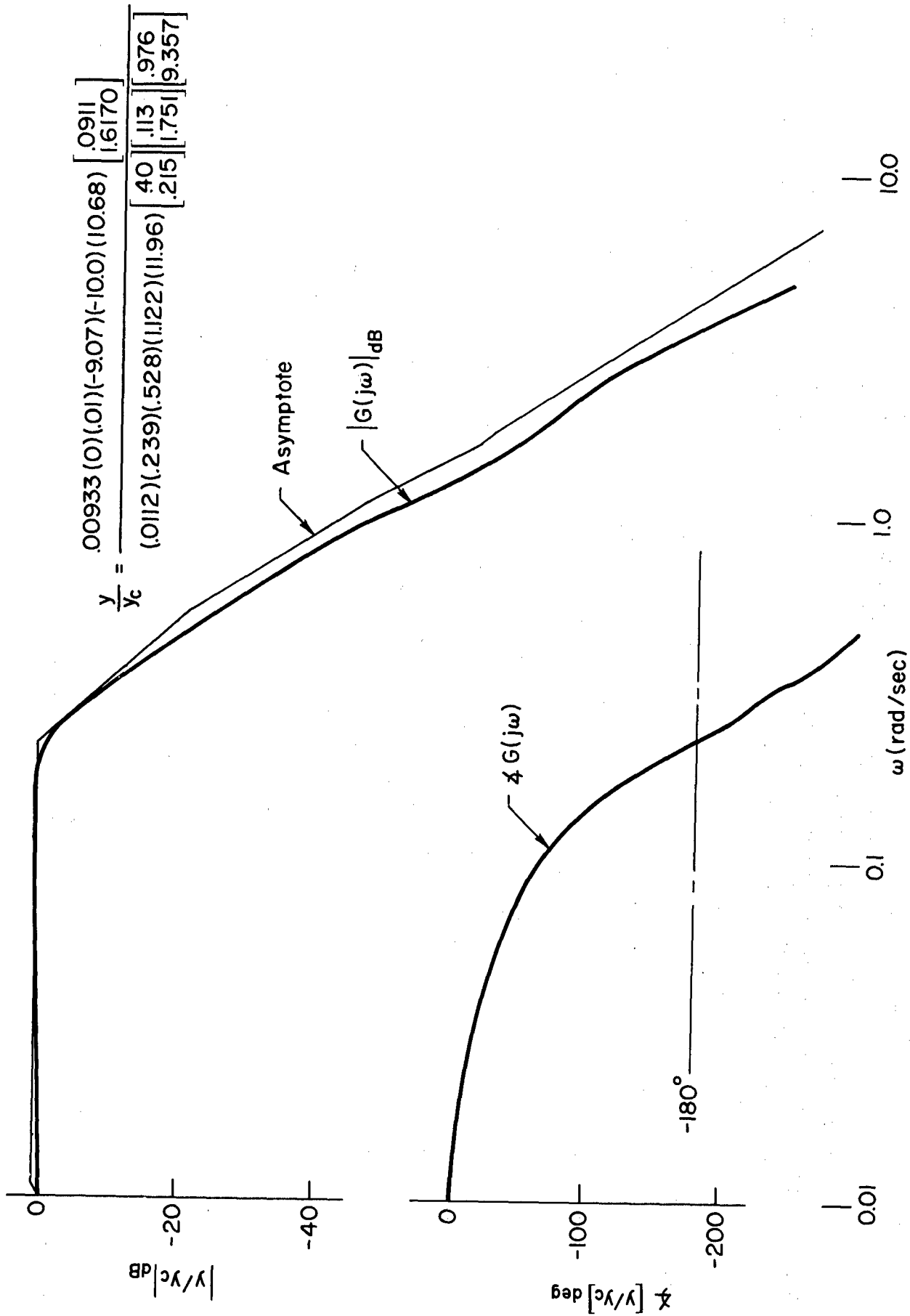


Figure 50. Localizer Frequency Response for Closed-Loop System

APPENDIX III

COMPUTER PROGRAM FOR SINUSOIDAL INPUT DESCRIBING FUNCTION FOR LIMITING INTEGRATOR

A simple computer program has been prepared to compute the negative inverse of the sinusoidal input describing function, Eq 29 and 30, as a function of normalized frequency and rate amplitude. This program uses the Super Basic language as available on the Tymshare Computer System (Refs. 30, 31).

A flow diagram for this program is given in Fig. 51. The program listing is displayed in Table XXXII.

A. PROGRAM USE

In this program, input data are contained in statements, 40, 70, 95, 140, 200, 450. The combination of "FOR" and "NEXT" statements is operationally equivalent to what is conventionally known as a "DO LOOP." Different input amplitudes and frequencies then require appropriate changes in these "FOR" statements.

After logging in, one has to call Super Basic language from Executive by typing "SBA." Then to execute the program, it is loaded by typing "LOAD/DF/" and then given the "RUN" command. (The symbolic version of this program is here assumed to be stored in the file named /DF/.)

Case III will be computed for all rate (i.e. input) amplitudes and then for each particular rate amplitude, Cases IVA, IVB, IVC will be computed in turn.

The format of the print out is as follows.

First, the case number is printed, then rate amplitude is printed. Under this there are three columns for frequency, negative inverse of the sinusoidal describing function in dB, and phase angle. A tabulation of the describing function itself is given in Appendix IV.

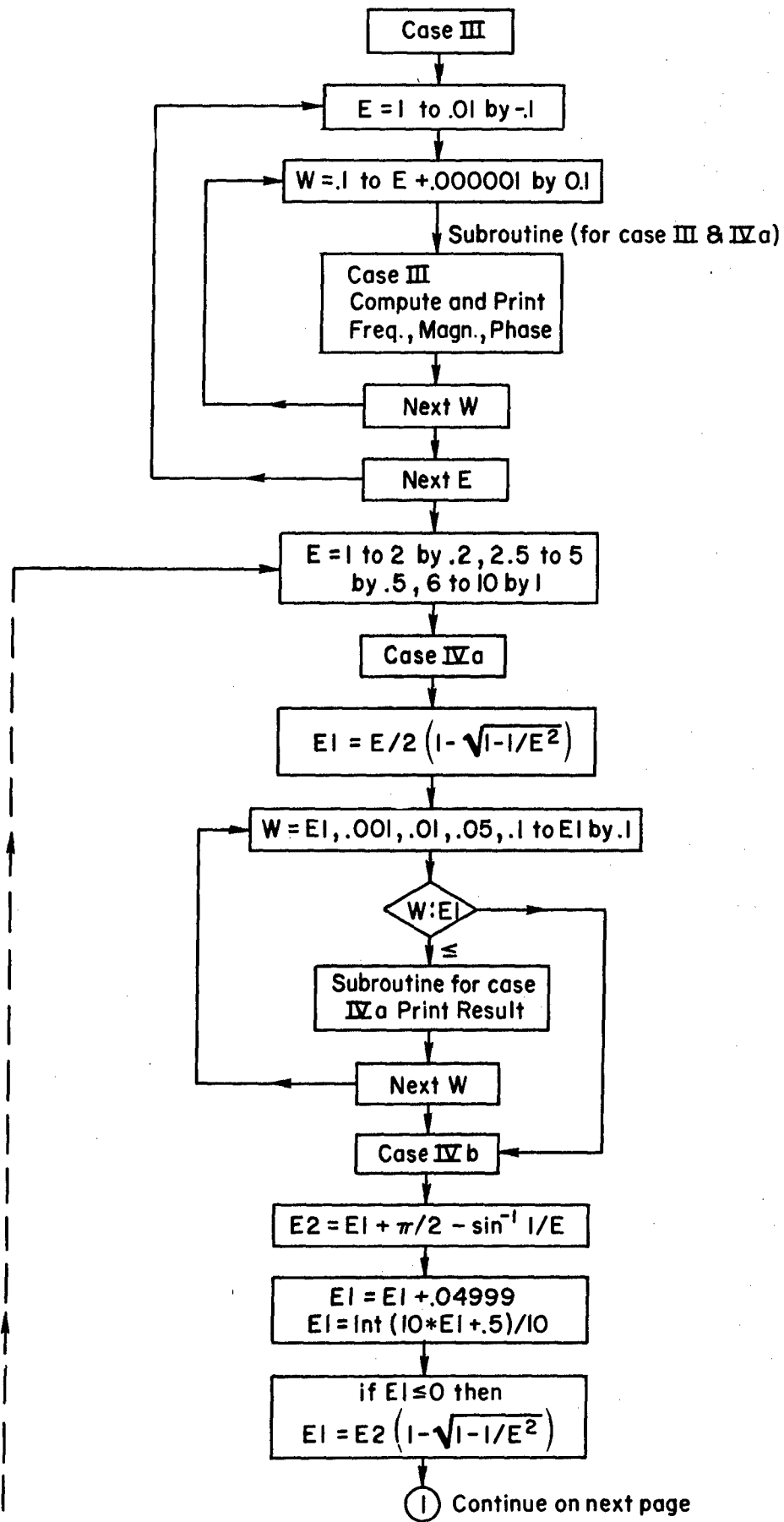


Figure 51. Flow Diagram for Describing Function Computation

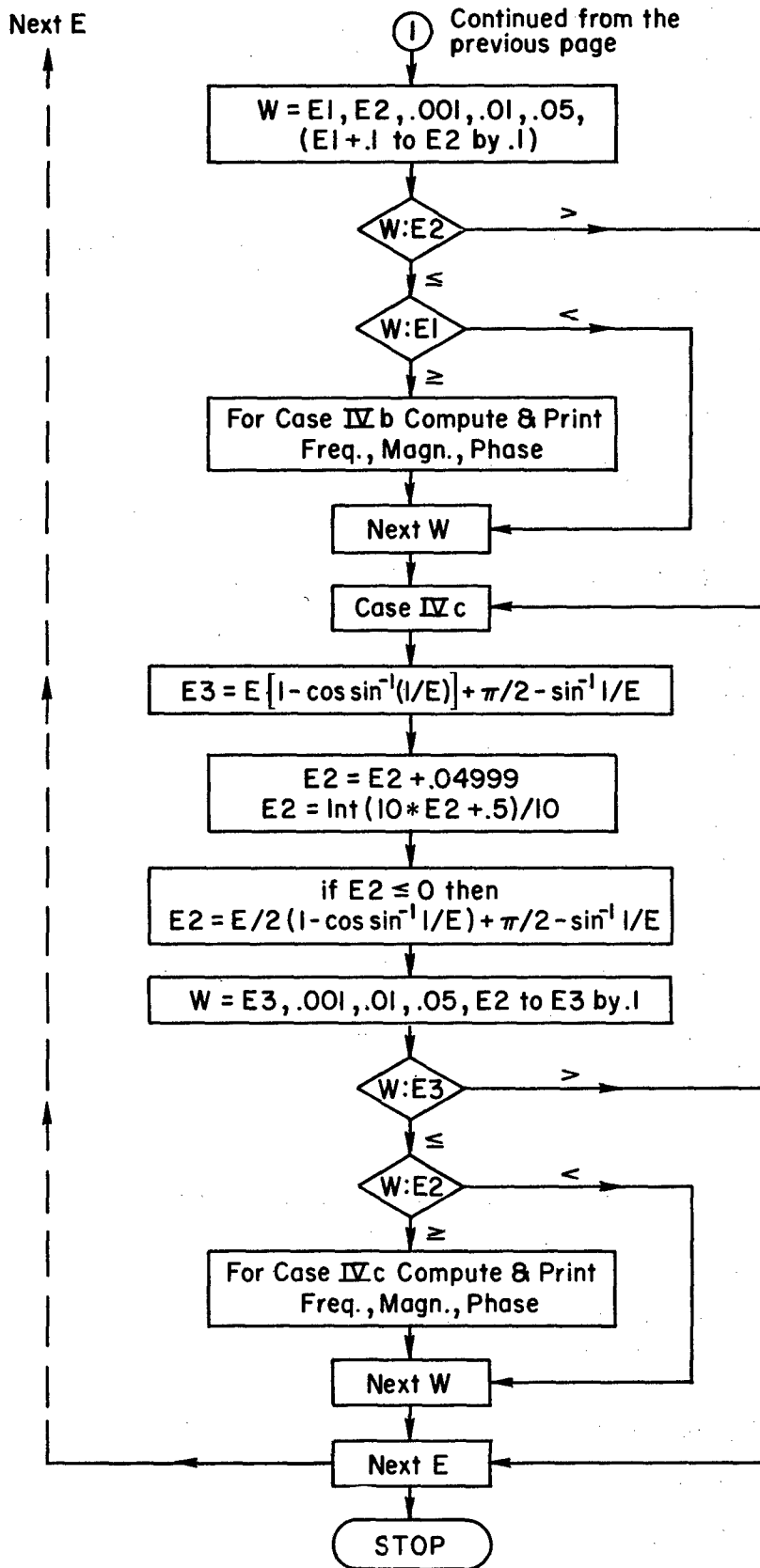


Figure 51. (concluded) Flow Diagram for Describing Function Computation

TABLE XXXII

PROGRAM LISTING FOR COMPUTATION OF THE NEGATIVE INVERSE OF
 THE SINUSOIDAL INPUT DESCRIBING FUNCTION
 FOR THE LIMITING INTEGRATOR

```

10 PRINT
20 PRINT
21PRINT"* 'RATE AMPLITUDE' HAS BEEN NORMALIZED BY DIVIDING BY THE"
22PRINT" RATE LIMIT LEVEL,K."
23PRINT"* 'FREQ' HAS BEEN NORMALIZED BY DIVIDING BY THE RATE-TO-"
24PRINT" POSITION LIMIT RATIO,R/P.
25PRINT"* 'AR DB' IS THE NEGATIVE INVERSE OF THE NORMALIZED"
26PRINT" DESCRIBING FUNCTION,NR/P, IN DB. N HAS BEEN NORMALIZED"
27PRINT" BY MULTIPLYING BY THE RATE-TO-POSITION RATIO, R/P."
28PRINT"* 'PHI', PHASE ANGLE IN DEGREES OF THE NEGATIVE INVERSE"
29PRINT" OF THE NORMALIZED DESCRIBING FUNCTION,HAS NOT BEEN NORMALIZED"
31PRINT IN FORM "' IN ANY WAY *****'/"
38 PRINT IN FORM "25B'CASE III'/"
40 FOR E= 1. TO .01 BY -.1
45 PRINT IN FORM"25B'RATE AMP = '9#//":E
50 PRINT IN FORM "10B'FREQ'8B'AR-DB'8B'PHI'/"
70 FOR W=.001,.01,.05,.1 TO (E+.000001) BY .1
80 GOSUB 900
90 NEXT W,E
95 FOR E=1 TO 2 BY .2,2.5 TO 5 BY .5,6 TO 10 BY 1
97 PRINT IN FORM "25B'RATE AMP = '9#//":E
100PRINT IN FORM "25B'CASE IVA'/"
102 S= ATAN(1/SQR(E*E-1))
104 C=ATAN(SQR(E*E-1))
106 P=SQR(1-1/(E*E))
108 Q=2/PI
120 PRINT IN FORM "10B'FREQ'8B'AR-DB'8B'PHI'/"
130 E1=.5*E*(1-P)

```

```

370 B=B1-B2+B5+B6+B7
380M=-10.*LOG 10((A*A+B*B)/(E*E))
390P$=-180-ATAN(A/B)*180/PI
393 PRINT IN FORM"6B3(1B9#2B)//":W,M,P$
396 NEXT W
400 PRINT IN FORM"25B'CASE IVC'///"
410 E3=E*(1-P)+PI/2-S
420 E2=E2+.04999
430 E2=INT(10*E2+.5)/10
440 IF E2<=0 THEN E2=.5*E*(1-P)+PI/2-S
450 FOR W=E3,.001,.01,.05,E2 TO E3 BY .1
460 IF W>E3 THEN 700
470 IF W<E2 THEN 700
480 A1=Q/W*(1-E/2*S-.5*P)
490 A2=Q/E
500 A6=4/(PI*W*E)*(PI/2-E*P-S)
510 F=1-2*P+PI/E-2/E*S-2*W/E
512 IF (ABS(F)-1)<.00001 THEN 514 ELSE 520
514 W2=PI/2-ATAN(F/SQR(ABS(1-F*F)))
516 GO TO 521
520 W2=PI/2-ATAN(F/SQR(1-F*F)) !W2=ARCCOS(F)
521 L1=E/W*(1-P)
522 R1=1/W*S
530 G=SIN(W2)-1/E
535 V=2*L1/PI-2/PI-4*R1/PI+2/W
540 A$=G*V
550 A8=Q*E/W*(P*(SIN(W2)-.5/E)+W2/2+.25*SIN(2*W2)-1/Q+.5*S)
560 A9=-2/PI*SIN(W2)

```

TABLE XXXII(cont'd)

```

140 FOR W=E1,.001,.01,.05,.1 TO E1 BY .1
145 IF W>E1 THEN 165
150 GOSUB 900
160 NEXT W
165 PRINT IN FORM"25B'CASE IVB'///"
170 E2 = E1+PI/2-S
180 E1=E1+.04999
190 E1=INT(10*E1+.5)/10
195 IF E1<=0 THEN E1=.5*E*(1-P)
200 FOR W=E1,E2,.001,.01,.05,(E1+.1) TO E2 BY .1
205 IF W>E2 THEN 400
206 IF W<E1 THEN 396
210 A1=Q/W*(1-E/2*S-.5*P)
220 A2=2/(PI*E)
230 W1=2*W-E*(1-P)+S
240 L1=E/W*(1-P)
250 R1=1/W*S
260 Z=SIN(W1)-1/E
270 A5=Z*(2*L1/PI-2/PI-2*R1/PI)
280 A6=Q/W*(COS(W1)+W1*SIN(W1)-P-1/E*S)
290 A7=-2/PI*SIN(W1)
300 A=A1-A2+A5+A6+A7
310 B1=2/PI*E/W*(1-P-.5/(E*E))
320 B2=Q*(1-P)
330 Y=COS(W1)-P
340 B5=Y*(-2*L1/PI+2/PI+2*R1/PI)
350 B6=Q/W*(SIN(W1)-W1*COS(W1)-1/E+P*S)
360 B7=Q*(COS(W1)+1)

```

TABLE XXXII (concluded)

```

570 A=A1-A2+A6+A5-A8+A9
580 B1=Q*E/W*(1-P-.5/(E*E))
590 B2=Q*(1-P)
600 B5=P*4/PI*(L1-1-R1)
610 B4=2/W*P
620 U=COS(W2)+P
630 B5=-U*V
640 B6=E/(PI*W)*(-2*P*COS(W2)-.5*COS(2*W2)-1.5+1/(E*E))
650 B7=Q*(COS(W2)+1)
660 B=B1-B2+B5+B4+B5-B6+B7
670 M=-10*LOG 10((A*A+B*B)/(E*E))
680 P5=-180-ATAN(A/B)*180/PI
690 PRINT IN FORM"6B3(1B9#2B)///":W,M,P5
700 NEXT W,E
710 STOP
900 X=1-2*W/E
905 X1=4*W/E*(1-W/E)
910 A1=2*E/(PI*W)*(SQR(ABS(X1))*(0.5+W/E)-PI/4+.5*ATAN(X/SQR(ABS(1-X*X))))
915 A2=2/PI*SQR(ABS(X1))
920 A1=A1-2*A2
925 B3=4/PI*(1-W/E)
930 M=-10.*LOG 10((A1*A1+B3*B3)/(E*E))
935 P5=-180-ATAN(A1/B3)*180/PI
940 PRINT IN FORM"6B3(1B9#2B)///":W,M,P5
945 RETURN

```

APPENDIX IV

TABULATION OF SINUSOIDAL INPUT DESCRIBING FUNCTION FOR THE LIMITING INTEGRATOR

The amplitude in dB and phase angle of the negative inverse of the nondimensionalized describing function derived in Section IV is tabulated as a function of the input amplitude-to-rate limit ratio, $E^* = E/R$, and the normalized frequency, $\Omega = \omega/(R/P)$ in Table XXXIII. The program for computing these results is listed in Appendix III where instructions for its use are also given.

This tabulation includes only Cases III, IVA, IVB and IVC, because a simple graphical construction can be used to obtain the results for Cases I and II from the following tabulated values for which the phase angle of the negative inverse describing function is -90 deg.

The amplitude ratio for the negative inverse describing function for Cases I and II "starts" at the normalized frequency for which the phase angle of the tabulated negative inverse describing function is -90 deg and increases 20 dB per normalized frequency decade for normalized frequencies larger than the "starting" value. The phase angle for Cases I and II is a constant, -90 deg. This graphical construction has been carried out to develop the portion of the limiting integrator describing function plot (Fig. 23) on page 78.

The nomenclature for Table XXXIII is as follows:

$$\text{RATE AMP} = E^* \triangleq E/R \quad (57)$$

$$\text{FREQ} = \Omega \triangleq \omega/(R/P) \quad (58)$$

$$\text{AR-DB} \triangleq \left| -1/(N R/P) \right|_{\text{dB}} \quad (59)$$

$$\text{PHI} \triangleq \angle -1/(N R/P) \quad (60)$$

TABLE XXXIII

TABULATION OF THE NEGATIVE INVERSE OF THE NONDIMENSIONALIZED
SINUSOIDAL INPUT DESCRIBING FUNCTION FOR A RATE LIMITED
INTEGRATOR HAVING A RESTRICTED OUTPUT RANGE.
CASES III, IV-A, IV-B, IV-C

RUN

- * 'RATE AMPLITUDE' HAS BEEN NORMALIZED BY DIVIDING BY THE RATE LIMIT LEVEL, R.
- * 'FREQ' HAS BEEN NORMALIZED BY DIVIDING BY THE RATE-TO-POSITION LIMIT RATIO, R/P.
- * 'AR-DB' IS THE NEGATIVE INVERSE OF THE NORMALIZED DESCRIBING FUNCTION, NR/P, IN DB. N HAS BEEN NORMALIZED BY MULTIPLYING BY THE RATE-TO-POSITION RATIO, R/P.
- * 'PHI', PHASE ANGLE IN DEGREES OF THE NEGATIVE INVERSE OF THE NORMALIZED DESCRIBING FUNCTION, HAS NOT BEEN NORMALIZED IN ANY WAY *****

TABLE XXXIII(cont'd)

CASE III (RATE AMP ≤ 1.0)

RATE AMP = .100E+01

FREQ	AR-DB	PHI
.100E-02	-.210E+01	-.178E+03
.100E-01	-.209E+01	-.172E+03
.500E-01	-.205E+01	-.163E+03
.100E+00	-.200E+01	-.156E+03
.200E+00	-.189E+01	-.145E+03
.300E+00	-.177E+01	-.137E+03
.400E+00	-.163E+01	-.129E+03
.500E+00	-.148E+01	-.122E+03
.600E+00	-.130E+01	-.116E+03
.700E+00	-.110E+01	-.110E+03
.800E+00	-.842E+00	-.103E+03
.900E+00	-.514E+00	-.969E+02
.100E+01	-.283E-05	-.900E+02

(MAXIMUM FREQ IN CASE III
FOR THIS VALUE OF RATE AMP)

TABLE XXXIII(cont'd)

RATE AMP = .900E+00

FREQ	AR-DB	PHI
.100E-02	-.301E+01	-.177E+03
.100E-01	-.300E+01	-.172E+03
.500E-01	-.296E+01	-.162E+03
.100E+00	-.290E+01	-.154E+03
.200E+00	-.278E+01	-.143E+03
.300E+00	-.264E+01	-.134E+03
.400E+00	-.248E+01	-.126E+03
.500E+00	-.230E+01	-.119E+03
.600E+00	-.208E+01	-.112E+03
.700E+00	-.182E+01	-.105E+03
.800E+00	-.147E+01	-.976E+02
.900E+00	-.915E+00	-.900E+02

TABLE XXXIII(cont'd)

RATE AMP = .800E+00

FREQ	AR-DB	PHI
.100E-02	-.404E+01	-.177E+03
.100E-01	-.402E+01	-.171E+03
.500E-01	-.397E+01	-.161E+03
.100E+00	-.391E+01	-.153E+03
.200E+00	-.377E+01	-.141E+03
.300E+00	-.360E+01	-.131E+03
.400E+00	-.342E+01	-.122E+03
.500E+00	-.319E+01	-.114E+03
.600E+00	-.291E+01	-.107E+03
.700E+00	-.254E+01	-.985E+02
.800E+00	-.194E+01	-.900E+02

RATE AMP = .700E+00

FREQ	AR-DB	PHI
.100E-02	-.519E+01	-.177E+03
.100E-01	-.518E+01	-.171E+03
.500E-01	-.513E+01	-.159E+03
.100E+00	-.505E+01	-.151E+03
.200E+00	-.488E+01	-.138E+03
.300E+00	-.469E+01	-.127E+03
.400E+00	-.445E+01	-.118E+03
.500E+00	-.416E+01	-.109E+03
.600E+00	-.377E+01	-.997E+02
.700E+00	-.310E+01	-.900E+02

TABLE XXXIII(cont'd)

RATE AMP = .600E+00

FREQ	AR-DB	PHI
.100E-02	-.653E+01	-.177E+03
.100E-01	-.652E+01	-.170E+03
.500E-01	-.645E+01	-.158E+03
.100E+00	-.636E+01	-.148E+03
.200E+00	-.616E+01	-.134E+03
.300E+00	-.591E+01	-.122E+03
.400E+00	-.561E+01	-.112E+03
.500E+00	-.518E+01	-.101E+03
.600E+00	-.444E+01	-.270E+03

RATE AMP = .500E+00

FREQ	AR-DB	PHI
.100E-02	-.812E+01	-.177E+03
.100E-01	-.810E+01	-.169E+03
.500E-01	-.802E+01	-.156E+03
.100E+00	-.791E+01	-.145E+03
.200E+00	-.765E+01	-.129E+03
.300E+00	-.732E+01	-.116E+03
.400E+00	-.686E+01	-.103E+03
.500E+00	-.602E+01	-.270E+03

TABLE XXXIII(cont'd)

RATE AMP = .200E+00

FREQ	AR-DB	PHI
.100E-02	-.161E+02	-.175E+03
.100E-01	-.160E+02	-.163E+03
.500E-01	-.158E+02	-.141E+03
.100E+00	-.155E+02	-.122E+03
.200E+00	-.140E+02	-.270E+03

RATE AMP = .100E+00

FREQ	AR-DB	PHI
.100E-02	-.221E+02	-.172E+03
.100E-01	-.220E+02	-.156E+03
.500E-01	-.215E+02	-.122E+03
.100E+00	-.200E+02	-.270E+03

TABLE XXXIII(cont'd)

RATE AMP = .400E+00

FREQ	AR-DB	PHI
.100E-02	-.101E+02	-.176E+03
.100E-01	-.100E+02	-.168E+03
.500E-01	-.993E+01	-.153E+03
.100E+00	-.979E+01	-.141E+03
.200E+00	-.944E+01	-.122E+03
.300E+00	-.893E+01	-.107E+03
.400E+00	-.796E+01	-.270E+03

RATE AMP = .300E+00

FREQ	AR-DB	PHI
.100E-02	-.126E+02	-.176E+03
.100E-01	-.125E+02	-.166E+03
.500E-01	-.124E+02	-.148E+03
.100E+00	-.122E+02	-.134E+03
.200E+00	-.116E+02	-.112E+03
.300E+00	-.105E+02	-.270E+03

TABLE XXXIII(cont'd)

CASE IV (RATE AMP ≥ 1.0)

RATE AMP = .100E+02

CASE IVA

FREQ	AR-DB	PHI	
.251E-01	.179E+02	-.176E+03	(MAXIMUM FREQ IN CASE IVA FOR THIS VALUE OF RATE AMP)
.100E-02	.179E+02	-.179E+03	
.100E-01	.179E+02	-.178E+03	

CASE IVB

.100E+00	.179E+02	-.172E+03	(MAXIMUM FREQ IN CASE IVA ROUNDED TO NEXT HIGHEST 0.1)
.150E+01	.214E+02	-.914E+02	(MAXIMUM FREQ IN CASE IVB FOR THIS VALUE OF RATE AMP)
.200E+00	.180E+02	-.166E+03	
.300E+00	.180E+02	-.160E+03	
.400E+00	.181E+02	-.154E+03	
.500E+00	.183E+02	-.149E+03	
.600E+00	.184E+02	-.143E+03	
.700E+00	.186E+02	-.137E+03	
.800E+00	.189E+02	-.131E+03	
.900E+00	.191E+02	-.126E+03	
.100E+01	.194E+02	-.120E+03	
.110E+01	.197E+02	-.114E+03	
.120E+01	.201E+02	-.108E+03	
.130E+01	.205E+02	-.103E+03	
.140E+01	.210E+02	-.969E+02	

CASE IVC

.152E+01	.216E+02	-.900E+02	
.150E+01	.214E+02	-.912E+02	(MAXIMUM FREQ IN CASE IVC FOR THIS VALUE OF RATE AMP)

TABLE XXXIII(cont'd)

RATE AMP = .900E+01

CASE IVA

FREQ	AR-DB	PHI
.279E-01	.170E+02	-.176E+03
.100E-02	.170E+02	-.179E+03
.100E-01	.170E+02	-.177E+03

CASE IVB

.100E+00	.170E+02	-.171E+03
.149E+01	.205E+02	-.916E+02
.200E+00	.170E+02	-.165E+03
.300E+00	.171E+02	-.160E+03
.400E+00	.172E+02	-.154E+03
.500E+00	.174E+02	-.148E+03
.600E+00	.175E+02	-.142E+03
.700E+00	.177E+02	-.137E+03
.800E+00	.179E+02	-.131E+03
.900E+00	.182E+02	-.125E+03
.100E+01	.185E+02	-.120E+03
.110E+01	.188E+02	-.114E+03
.120E+01	.192E+02	-.108E+03
.130E+01	.196E+02	-.102E+03
.140E+01	.200E+02	-.966E+02

CASE IVC

.152E+01	.206E+02	-.900E+02
.150E+01	.205E+02	-.909E+02

TABLE XXXIII(cont'd)

RATE AMP = .800E+01

CASE IVA

FREQ	AR-DB	PHI
.314E-01	.160E+02	-.175E+03
.100E-02	.160E+02	-.179E+03
.100E-01	.160E+02	-.177E+03

CASE IVB

.100E+00	.160E+02	-.171E+03
.148E+01	.194E+02	-.918E+02
.200E+00	.160E+02	-.165E+03
.300E+00	.161E+02	-.159E+03
.400E+00	.162E+02	-.154E+03
.500E+00	.163E+02	-.148E+03
.600E+00	.165E+02	-.142E+03
.700E+00	.167E+02	-.136E+03
.800E+00	.169E+02	-.131E+03
.900E+00	.172E+02	-.125E+03
.100E+01	.175E+02	-.119E+03
.110E+01	.178E+02	-.113E+03
.120E+01	.182E+02	-.108E+03
.130E+01	.186E+02	-.102E+03
.140E+01	.190E+02	-.962E+02

CASE IVC

.151E+01	.196E+02	-.900E+02
.150E+01	.195E+02	-.905E+02

TABLE XXXIII(cont'd)

RATE AMP = .700E+01

CASE IVA

FREQ	AR-DB	PHI
.359E-01	.148E+02	-.175E+03
.100E-02	.148E+02	-.179E+03
.100E-01	.148E+02	-.177E+03

CASE IVB

.100E+00	.148E+02	-.170E+03
.146E+01	.182E+02	-.921E+02
.200E+00	.149E+02	-.165E+03
.300E+00	.149E+02	-.159E+03
.400E+00	.150E+02	-.153E+03
.500E+00	.152E+02	-.147E+03
.600E+00	.153E+02	-.142E+03
.700E+00	.155E+02	-.136E+03
.800E+00	.158E+02	-.130E+03
.900E+00	.160E+02	-.124E+03
.100E+01	.163E+02	-.119E+03
.110E+01	.166E+02	-.113E+03
.120E+01	.170E+02	-.107E+03
.130E+01	.174E+02	-.101E+03
.140E+01	.179E+02	-.957E+02

CASE IVC

TABLE XXXIII(cont'd)

RATE AMP = .600E+01

CASE IVA

FREQ	AR-DB	PHI
.420E-01	.135E+02	-.174E+03
.100E-02	.135E+02	-.179E+03
.100E-01	.135E+02	-.177E+03

CASE IVB

.100E+00	.135E+02	-.170E+03
.145E+01	.167E+02	-.924E+02
.200E+00	.135E+02	-.164E+03
.300E+00	.136E+02	-.158E+03
.400E+00	.137E+02	-.152E+03
.500E+00	.138E+02	-.147E+03
.600E+00	.140E+02	-.141E+03
.700E+00	.142E+02	-.135E+03
.800E+00	.144E+02	-.129E+03
.900E+00	.147E+02	-.124E+03
.100E+01	.150E+02	-.118E+03
.110E+01	.153E+02	-.112E+03
.120E+01	.157E+02	-.106E+03
.130E+01	.161E+02	-.101E+03
.140E+01	.165E+02	-.950E+02

CASE IVC

TABLE XXXIII(cont'd)

RATE AMP = .500E+01

CASE IVA

FREQ	AR-DB	PHI
.505E-01	.119E+02	-.172E+03
.100E-02	.119E+02	-.179E+03
.100E-01	.119E+02	-.177E+03
.500E-01	.119E+02	-.172E+03

CASE IVB

.100E+00	.119E+02	-.169E+03
.142E+01	.150E+02	-.929E+02
.200E+00	.119E+02	-.163E+03
.300E+00	.120E+02	-.157E+03
.400E+00	.121E+02	-.151E+03
.500E+00	.123E+02	-.146E+03
.600E+00	.124E+02	-.140E+03
.700E+00	.126E+02	-.134E+03
.800E+00	.128E+02	-.128E+03
.900E+00	.131E+02	-.123E+03
.100E+01	.134E+02	-.117E+03
.110E+01	.137E+02	-.111E+03
.120E+01	.141E+02	-.106E+03
.130E+01	.145E+02	-.998E+02
.140E+01	.149E+02	-.940E+02

CASE IVC

TABLE XXXIII(cont'd)

RATE AMP = .450E+01

CASE IVA

FREQ	AR-DB	PHI
.563E-01	.110E+02	-.171E+03
.100E-02	.110E+02	-.179E+03
.100E-01	.110E+02	-.176E+03
.500E-01	.110E+02	-.172E+03

CASE IVB

.100E+00	.110E+02	-.168E+03
.140E+01	.140E+02	-.932E+02
.200E+00	.110E+02	-.162E+03
.300E+00	.111E+02	-.157E+03
.400E+00	.112E+02	-.151E+03
.500E+00	.113E+02	-.145E+03
.600E+00	.115E+02	-.139E+03
.700E+00	.117E+02	-.134E+03
.800E+00	.119E+02	-.128E+03
.900E+00	.122E+02	-.122E+03
.100E+01	.125E+02	-.116E+03
.110E+01	.128E+02	-.111E+03
.120E+01	.132E+02	-.105E+03
.130E+01	.136E+02	-.991E+02
.140E+01	.140E+02	-.934E+02

CASE IVC

TABLE XXXIII(cont'd)

RATE AMP = .400E+01

CASE IVA

FREQ	AR-DB	PHI
.635E-01	.996E+01	-.170E+03
.100E-02	.994E+01	-.179E+03
.100E-01	.995E+01	-.176E+03
.500E-01	.996E+01	-.171E+03

CASE IVB

.100E+00	.997E+01	-.168E+03
.138E+01	.129E+02	-.937E+02
.200E+00	.100E+02	-.162E+03
.300E+00	.101E+02	-.156E+03
.400E+00	.102E+02	-.150E+03
.500E+00	.103E+02	-.144E+03
.600E+00	.105E+02	-.139E+03
.700E+00	.107E+02	-.133E+03
.800E+00	.109E+02	-.127E+03
.900E+00	.112E+02	-.121E+03
.100E+01	.115E+02	-.116E+03
.110E+01	.118E+02	-.110E+03
.120E+01	.121E+02	-.104E+03
.130E+01	.126E+02	-.983E+02

CASE IVC

.145E+01	.132E+02	-.270E+03
.140E+01	.130E+02	-.926E+02

TABLE XXXIII(cont'd)

RATE AMP = .350E+01

CASE IVA

FREQ	AR-DB	PHI
.729E-01	.880E+01	-.169E+03
.100E-02	.878E+01	-.179E+03
.100E-01	.879E+01	-.176E+03
.500E-01	.880E+01	-.171E+03

CASE IVB

.100E+00	.881E+01	-.167E+03
.135E+01	.116E+02	-.942E+02
.200E+00	.886E+01	-.161E+03
.300E+00	.893E+01	-.155E+03
.400E+00	.903E+01	-.149E+03
.500E+00	.916E+01	-.143E+03
.600E+00	.933E+01	-.138E+03
.700E+00	.952E+01	-.132E+03
.800E+00	.975E+01	-.126E+03
.900E+00	.100E+02	-.120E+03
.100E+01	.103E+02	-.115E+03
.110E+01	.106E+02	-.109E+03
.120E+01	.110E+02	-.103E+03
.130E+01	.114E+02	-.973E+02

CASE IVC

.143E+01	.120E+02	-.270E+03
.140E+01	.119E+02	-.916E+02

TABLE XXXIII(cont'd)

RATE AMP = .300E+01

CASE IVA

FREQ	AR-DB	PHI
.858E-01	.747E+01	-.167E+03
.100E-02	.744E+01	-.179E+03
.100E-01	.745E+01	-.176E+03
.500E-01	.746E+01	-.170E+03

CASE IVB

.100E+00	.748E+01	-.166E+03
.132E+01	.101E+02	-.950E+02
.200E+00	.752E+01	-.160E+03
.300E+00	.760E+01	-.154E+03
.400E+00	.770E+01	-.148E+03
.500E+00	.783E+01	-.142E+03
.600E+00	.799E+01	-.136E+03
.700E+00	.819E+01	-.130E+03
.800E+00	.841E+01	-.125E+03
.900E+00	.867E+01	-.119E+03
.100E+01	.896E+01	-.113E+03
.110E+01	.929E+01	-.107E+03
.120E+01	.966E+01	-.102E+03
.130E+01	.101E+02	-.959E+02

CASE IVC

.140E+01	.105E+02	-.270E+03
.140E+01	.105E+02	-.901E+02

TABLE XXXIII(cont'd)

RATE AMP = .250E+01

CASE IVA

FREQ	AR-DB	PHI
.104E+00	.590E+01	-.164E+03
.100E-02	.586E+01	-.178E+03
.100E-01	.586E+01	-.175E+03
.500E-01	.588E+01	-.169E+03
.100E+00	.590E+01	-.165E+03

CASE IVB

.200E+00	.595E+01	-.158E+03
.126E+01	.834E+01	-.960E+02
.300E+00	.602E+01	-.152E+03
.400E+00	.612E+01	-.146E+03
.500E+00	.626E+01	-.140E+03
.600E+00	.642E+01	-.134E+03
.700E+00	.661E+01	-.129E+03
.800E+00	.684E+01	-.123E+03
.900E+00	.710E+01	-.117E+03
.100E+01	.739E+01	-.111E+03
.110E+01	.772E+01	-.105E+03
.120E+01	.809E+01	-.997E+02

CASE IVC

.137E+01	.882E+01	-.270E+03
.130E+01	.849E+01	-.940E+02

TABLE XXXIII(cont'd)

RATE AMP = .200E+01

CASE IVA

FREQ	AR-DB	PHI
.134E+00	.399E+01	-.160E+03
.100E-02	.392E+01	-.178E+03
.100E-01	.393E+01	-.175E+03
.500E-01	.395E+01	-.168E+03
.100E+00	.397E+01	-.163E+03

CASE IVB

.200E+00	.403E+01	-.155E+03
.118E+01	.609E+01	-.978E+02
.300E+00	.410E+01	-.149E+03
.400E+00	.420E+01	-.143E+03
.500E+00	.434E+01	-.137E+03
.600E+00	.450E+01	-.131E+03
.700E+00	.469E+01	-.126E+03
.800E+00	.492E+01	-.120E+03
.900E+00	.518E+01	-.114E+03
.100E+01	.547E+01	-.108E+03
.110E+01	.580E+01	-.102E+03

CASE IVC

.132E+01	.669E+01	-.900E+02
.120E+01	.617E+01	-.967E+02
.130E+01	.660E+01	-.909E+02

TABLE XXXIII(cont'd)

RATE AMP = .180E+01

CASE IVA

FREQ	AR-DB	PHI
.152E+00	.309E+01	-.158E+03
.100E-02	.301E+01	-.178E+03
.100E-01	.301E+01	-.174E+03
.500E-01	.303E+01	-.167E+03
.100E+00	.306E+01	-.162E+03

CASE IVB

.200E+00	.312E+01	-.154E+03
.113E+01	.502E+01	-.989E+02
.300E+00	.320E+01	-.148E+03
.400E+00	.330E+01	-.142E+03
.500E+00	.343E+01	-.136E+03
.600E+00	.360E+01	-.130E+03
.700E+00	.379E+01	-.124E+03
.800E+00	.402E+01	-.118E+03
.900E+00	.427E+01	-.112E+03
.100E+01	.457E+01	-.107E+03
.110E+01	.490E+01	-.101E+03

CASE IVC

.129E+01	.567E+01	-.270E+03
.120E+01	.527E+01	-.950E+02

TABLE XXXIII(cont'd)

RATE AMP = .160E+01

CASE IVA

FREQ	AR-DB	PHI
.176E+00	.210E+01	-.154E+03
.100E-02	.198E+01	-.178E+03
.100E-01	.199E+01	-.174E+03
.500E-01	.201E+01	-.166E+03
.100E+00	.205E+01	-.161E+03

CASE IVB

.200E+00	.211E+01	-.153E+03
.107E+01	.379E+01	-.100E+03
.300E+00	.219E+01	-.146E+03
.400E+00	.229E+01	-.140E+03
.500E+00	.243E+01	-.134E+03
.600E+00	.259E+01	-.128E+03
.700E+00	.279E+01	-.122E+03
.800E+00	.301E+01	-.116E+03
.900E+00	.327E+01	-.110E+03
.100E+01	.356E+01	-.104E+03

CASE IVC

.125E+01	.453E+01	-.270E+03
.110E+01	.389E+01	-.987E+02
.120E+01	.428E+01	-.928E+02

TABLE XXXIII(cont'd)

RATE AMP = .140E+01

CASE IVA

FREQ	AR-DB	PHI
.210E+00	.979E+00	-.150E+03
.100E-02	.825E+00	-.178E+03
.100E-01	.831E+00	-.174E+03
.500E-01	.859E+00	-.166E+03
.100E+00	.895E+00	-.159E+03
.200E+00	.971E+00	-.151E+03

CASE IVB

.300E+00	.106E+01	-.144E+03
.985E+00	.239E+01	-.103E+03
.400E+00	.116E+01	-.137E+03
.500E+00	.130E+01	-.131E+03
.600E+00	.146E+01	-.125E+03
.700E+00	.165E+01	-.119E+03
.800E+00	.188E+01	-.113E+03
.900E+00	.214E+01	-.108E+03

CASE IVC

.120E+01	.322E+01	-.270E+03
.100E+01	.243E+01	-.102E+03
.110E+01	.277E+01	-.958E+02

TABLE XXXIII(cont'd)

RATE AMP = .120E+01

CASE IVA

FREQ	AR-DB	PHI
.268E+00	-.276E+00	-.143E+03
.100E-02	-.514E+00	-.178E+03
.100E-01	-.507E+00	-.173E+03
.500E-01	-.474E+00	-.164E+03
.100E+00	-.431E+00	-.158E+03
.200E+00	-.342E+00	-.148E+03

CASE IVB

.300E+00	-.244E+00	-.141E+03
.854E+00	.730E+00	-.106E+03
.400E+00	-.132E+00	-.134E+03
.500E+00	.508E-02	-.128E+03
.600E+00	.171E+00	-.122E+03
.700E+00	.366E+00	-.116E+03
.800E+00	.593E+00	-.110E+03

CASE IVC

.112E+01	.172E+01	-.270E+03
.900E+00	.854E+00	-.104E+03
.100E+01	.116E+01	-.977E+02
.110E+01	.159E+01	-.915E+02

TABLE XXXIII(concluded)

RATE AMP = .100E+01

CASE IVA

FREQ	AR-DB	PHI
.500E+00	-.148E+01	-.122E+03
.100E-02	-.210E+01	-.178E+03
.100E-01	-.209E+01	-.172E+03
.500E-01	-.205E+01	-.163E+03
.100E+00	-.200E+01	-.156E+03
.200E+00	-.189E+01	-.145E+03
.300E+00	-.177E+01	-.137E+03
.400E+00	-.163E+01	-.129E+03
.500E+00	-.148E+01	-.122E+03

CASE IVB

.500E+00	-.148E+01	-.122E+03
.500E+00	-.148E+01	-.122E+03

CASE IVC

.100E+01	-.657E-09	-.900E+02
.500E+00	-.148E+01	-.122E+03
.600E+00	-.130E+01	-.116E+03
.700E+00	-.110E+01	-.110E+03
.800E+00	-.842E+00	-.103E+03
.900E+00	-.514E+00	-.969E+02
.100E+01	-.723E-09	-.900E+02

APPENDIX V

SUMMARY OF FACTORED CLOSED-LOOP TRANSFER FUNCTIONS
FOR LINEAR AND NONLINEAR, LONGITUDINAL AND LATERAL
SYSTEMS A, B AND C

Closed-loop numerators and denominators for the linear and nonlinear back-up system configurations are given in a series of tables. A guide to these tables is given below.

TABLE XXXIV

GUIDE TO TABLES OF CLOSED-LOOP TRANSFER FUNCTIONS

<u>Table No.</u>	<u>System Configuration</u>	<u>Longitudinal</u>	<u>Lateral</u>	<u>Linear</u>	<u>Nonlinear</u>
XXXVII	A	✓		✓	
XXXVIII	↓		✓	✓	
XXXIX		✓			✓
XXXX	↓		✓		✓
XXXXI	B	✓		✓	
XXXXII	↓		✓	✓	
XXXXI		✓			✓
XXXXIII	↓		✓		✓
XXXXI	C	✓		✓	
XXXXIV	↓		✓	✓	
XXXXI		✓			✓
XXXXV	↓		✓		✓

The factors of each numerator or denominator are printed following its descriptive title. Each numerator can be related to the corresponding transfer function expressed in the usual notation using Tables XXXV and XXXVI.

TABLE XXXV

NOTATION USED FOR LONGITUDINAL NUMERATOR DESIGNATIONS

Print Out Description	Description in Usual Notation	Print Out Description	Description in Usual Notation
U/DC	u/d_c	U/WG	u/w_g
THE/DC	θ/d_c	THE/WG	θ/w_g
DD/DS	\dot{d}/d_c	DD/WG	\dot{d}/w_g
DS/DC	δ_s/d_c	DS/WG	δ_s/w_g
DT/DC	δ_T/d_c	DT/WG	δ_T/w_g
DED/DC	\dot{d}_e/d_c	DED/WG	\dot{d}_e/w_g

TABLE XXXVI

NOTATION USED FOR LATERAL NUMERATOR DESIGNATIONS

Print Out Description	Description in Usual Notation	Print Out Description	Description in Usual Notation
B/YC	β/y_c	B/VG	β/v_g
PSD/YC	$\dot{\psi}/y_c$	PSD/VG	$\dot{\psi}/v_g$
PHI/YC	ϕ/y_c	PHI/VG	ϕ/v_g
DS/YC	δ_{sp}/y_c	DS/VG	δ_{sp}/v_g
YE/YC	y_e/y_c	YE/VG	y_e/v_g
YP/YC	y_p/y_c	YP/VG	y_p/v_g

The printing format for the numerators and denominators is as follows.

The coefficient of the highest power of s in the numerator or denominator is printed on the first line. Next, all the first order factors are printed as single numbers each enclosed in parentheses, e.g. $(s+a)$ is printed as (a) . Second order factors are then printed one to a line. There are four quantities enclosed in parentheses for each second order factor. These designate the damping ratio, undamped natural frequency, real part and imaginary part respectively, e.g. $s^2 + 2\zeta\omega_n s + \omega_n^2$ is printed as $(\zeta, \omega_n, \zeta\omega_n, \omega_n \sqrt{1-\zeta^2})$. For example, the quadratic factor, $[s^2 + 2(.268)1.72s + (1.72)^2]$ would be listed on a single line in the output as $(.268E 0, .172E 1, .459E 0, .165E 1)$. On the final line, the coefficient of the lowest power of s in the numerator or denominator is printed enclosed within $< >$ marks.

TABLE XXXVII
 CLOSED-LOOP TRANSFER FUNCTIONS FOR
 LONGITUDINAL LINEAR SYSTEM A

PROJECT: L F-4 VTO 333F/S F UP

DENOMINATOR:

```
.30000E- 1
( .50000E- 1) ( .42262E  0) ( .60110E  1)
( .87632E  0, .44574E- 1 , .39061E- 1, .21473E- 1)
( .26298E  0, .36517E  0 , .96031E- 1, .35231E  0)
( .77647E  0, .36130E  1 , .28054E  1, .22768E  1)
( .26778E  0, .17156E  1 , .45942E  0, .16530E  1)
( .93619E  0, .14172E  2 , .13268E  2, .49815E  1)
< .77914E- 2>
```

NUMERATOR: U /DC FILE NAME? /1/
 OLD FILE

```
.12915E- 1
( .50000E- 1) ( .50000E- 1) ( .50000E  0) ( .00000E  0) ( .60000E  1)
(-.10000E  2) ( .63069E  2)
( .71355E  0, .58729E  0 , .41906E  0, .41146E  0)
<-.21071E- 1>
```

NUMERATOR: THE/DC FILE NAME? /2/
 OLD FILE

```
-.17439E- 1
( .50000E- 1) ( .11421E  0) ( .50000E- 1) ( .38717E  0) ( .00000E  0)
( .49620E  0) ( .60109E  1) (-.10000E  2)
< .57497E- 4>
```

NUMERATOR: DD /DC FILE NAME? /3/
 OLD FILE

```
.91600E- 1
( .46432E- 1) ( .50000E- 1) ( .50000E- 1) ( .41635E  0) ( .00000E  0)
( .60350E  1) ( .56321E  1) (-.51783E  1) (-.10000E  2)
< .77919E- 2>
```

TABLE XXXVII(cont'd)
 CLOSED-LOOP TRANSFER FUNCTIONS FOR
 LONGITUDINAL LINEAR SYSTEM A

NUMERATOR: DS /DC FILE NAME? /4/
 OLD FILE

.20250E 0
 (.50000E- 1) (.50000E- 1) (.00000E 0) (.42669E 0) (.60105E 1)
 (-.10000E 2)
 (.27836E 0, .17834E 0 , .49642E- 1, .17129E 0)
 (.37636E 0, .13063E 1 , .49162E 0, .12102E 1)
 <-.70457E- 3>

NUMERATOR: DT /DC FILE NAME? /5/
 OLD FILE

.19373E 0
 (.50000E- 1) (.50000E- 1) (.00000E 0) (-.60000E 1) (-.10000E 2)
 (.63069E 2)
 (.71355E 0, .58729E 0 , .41906E 0, .41146E 0)
 < .63213E 0>

NUMERATOR: DED/DC FILE NAME? /6/
 OLD FILE

.30000E- 1
 (.50000E- 1) (-.58337E- 3) (.57814E- 3) (.00000E 0) (.43474E 0)
 (.60110E 1)
 (.87329E 0, .21252E 0 , .18559E 0, .10354E 0)
 (.25051E 0, .17048E 1 , .42707E 0, .16504E 1)
 (.77484E 0, .35906E 1 , .27822E 1, .22699E 1)
 (.93619E 0, .14172E 2 , .13267E 2, .49813E 1)
 <-.44931E- 6>

NUMERATOR: U /WG FILE NAME? /7/
 OLD FILE

.53572E- 3
 (.50000E- 1) (.49385E- 1) (.50000E 0) (.60000E 1) (.16016E 2)
 (-.10293E 2)
 (.97744E 0, .12978E 1 , .12685E 1, .27410E 0)
 (-.11233E 0, .46384E 0 , -.52103E- 1, .46091E 0)
 (.76877E 0, .93423E 1 , .71820E 1, .59746E 1)
 <-.20691E- 1>

TABLE XXXVII(cont'd)
 CLOSED-LOOP TRANSFER FUNCTIONS FOR
 LONGITUDINAL LINEAR SYSTEM A

NUMERATOR: THE/WG FILE NAME? /8/
 OLD FILE

-.44406E- 4
 (.50000E- 1) (.41665E 0) (.10210E 0) (.49953E- 1) (.92274E 1)
 (.60107E 1) (.24314E 1) (-.24592E 1)
 (-.18035E 0, .57839E 0 , -.10432E 0, .56891E 0)
 (.99858E 0, .10385E 2 , .10371E 2, .55302E 0)
 < .56460E- 4>

NUMERATOR: DD /WG FILE NAME? /9/
 NEW FILE

-.15669E- 1
 (.50000E- 1) (.14580E- 2) (-.46588E- 3) (.40525E 0) (.15588E 0)
 (.60106E 1)
 (.27073E 0, .11989E 1 , .32458E 0, .11541E 1)
 (.76569E 0, .40150E 1 , .30743E 1, .25825E 1)
 (.94575E 0, .13931E 2 , .13175E 2, .45263E 1)
 < .90869E- 6>

NUMERATOR: DS /WG FILE NAME? /10/
 NEW FILE

.62168E- 1
 (.50048E- 1) (.50000E- 1) (.42942E 0) (-.42505E 0) (-.22452E 1)
 (.60107E 1) (-.10000E 2)
 (.45697E 0, .22934E 0 , .10480E 0, .20400E 0)
 (.61587E 0, .18527E 1 , .11410E 1, .14597E 1)
 <-.69186E- 3>

NUMERATOR: DT /WG FILE NAME? /11/
 OLD FILE

.80358E- 2
 (.50000E- 1) (.49385E- 1) (-.60000E 1) (.16016E 2) (-.10293E 2)
 (.97744E 0, .12978E 1 , .12685E 1, .27410E 0)
 (-.11233E 0, .46384E 0 , -.52103E- 1, .46091E 0)
 (.76877E 0, .93423E 1 , .71820E 1, .59746E 1)
 < .62073E 0>

TABLE XXXVII(concluded)
 CLOSED-LOOP TRANSFER FUNCTIONS FOR
 LONGITUDINAL LINEAR SYSTEM A

NUMERATOR: DED/WG FILE NAME? /12/
 OLD FILE

```

.10613E- 2
( .50000E- 1) ( .82506E- 3) (-.84200E- 3) ( .40448E  0) ( .15740E  0)
( .60106E  1) ( .17095E  2)
( .30914E  0, .13031E  1 , .40284E  0, .12393E  1)
( .62155E  0, .35812E  1 , .22259E  1, .28054E  1)
( .84198E  0, .13154E  2 , .11075E  2, .70966E  1)
<-.90869E- 6>

```

TABLE XXXVIII

CLOSED-LOOP TRANSFER FUNCTIONS FOR LATERAL LINEAR SYSTEM A

DENOMINATOR:

-.44639E 0
 (.11240E- 1) (.23967E 0) (.52795E 0) (.10000E 2) (.11224E 1)
 (.11957E 2)
 (.39987E 0, .21468E 0 , .85841E- 1, .19677E 0)
 (.11293E 0, .17508E 1 , .19772E 0, .17396E 1)
 (.97575E 0, .93574E 1 , .91305E 1, .20481E 1)
 <-.10539E 1>

NUMERATOR: B /YC FILE NAME? /1/ OLD FILE

-.12521E- 4
 (.00000E 0) (.10000E- 1) (.00000E 0) (.74542E 0) (.48557E 0)
 (.10000E 2) (-.10000E 2) (-.71764E 2)
 <-.32524E- 3>

NUMERATOR: PSD/YC FILE NAME? /2/ OLD FILE

.10429E- 2
 (.00000E 0) (.10000E- 1) (.00000E 0) (.68273E 0) (.10000E 2)
 (-.10000E 2)
 (.20363E- 1, .21093E 1 , .42952E- 1, .21089E 1)
 <-.31679E- 2>

NUMERATOR: PHI/YC FILE NAME? /3/ OLD FILE

.13829E- 1
 (.00000E 0) (.10000E- 1) (.00000E 0) (.10000E 2) (-.10000E 2)
 (.12027E 0, .15562E 1 , .18718E 0, .15449E 1)
 <-.33493E- 1>

NUMERATOR: DS /YC FILE NAME? /4/ OLD FILE

.11383E 1
 (.42665E- 1) (.00000E 0) (.10000E- 1) (.00000E 0) (.13917E 1)
 (.10000E 2) (-.10000E 2)
 (.11356E 0, .17249E 1 , .19588E 0, .17138E 1)
 <-.20109E 0>

TABLE XXXVIII(cont'd)

CLOSED-LOOP TRANSFER FUNCTIONS FOR LATERAL LINEAR SYSTEM A

NUMERATOR: YE /YC FILE NAME? /5/ NEW FILE

```

-.44639E 0
( .00000E 0) ( .00000E 0) ( .66509E 0) ( .10000E 2) ( .10977E 1)
( .11957E 2)
( .47786E 0, .32475E 0, .15518E 0, .28527E 0)
( .11287E 0, .17507E 1, .19761E 0, .17396E 1)
( .97575E 0, .93575E 1, .91305E 1, .20482E 1)
<-.11029E 4>
    
```

NUMERATOR: YP /YC FILE NAME? /6/ NEW FILE

```

.20759E- 1
( .10000E- 1) ( .10000E 2) (-.10000E 2)
( .12215E 0, .15252E 1, .18631E 0, .15138E 1)
( .18026E- 1, .46718E 1, .84213E- 1, .46711E 1)
<-.10539E 1>
    
```

NUMERATOR: B /VG FILE NAME? /7/ NEW FILE

```

-.16097E- 3
( .11239E- 1) ( .53004E 0) ( .25152E 0) ( .11263E 1) ( .10000E 2)
( .11603E 2) ( .25638E 2)
( .40914E 0, .20964E 0, .85774E- 1, .19129E 0)
( .98303E 0, .94364E 1, .92762E 1, .17312E 1)
<-.31625E- 2>
    
```

NUMERATOR: PSD/VG FILE NAME? /8/ NEW FILE

```

.21955E- 2
( .00000E 0) ( .10000E- 1) ( .10234E 1) ( .10000E 2) ( .12235E 2)
(-.28227E 0, .14738E 0, -.41601E- 1, .14139E 0)
( .90225E 0, .77627E 0, .70039E 0, .33474E 0)
( .96655E 0, .93763E 1, .90626E 1, .24048E 1)
< .31636E- 2>
    
```

TABLE XXXVIII(concluded)

CLOSED-LOOP TRANSFER FUNCTIONS FOR LATERAL LINEAR SYSTEM A

NUMERATOR: PHI/VG FILE NAME? /9/ NEW FILE

-.13349E- 1
 (-.91657E- 2) (.91091E 1) (.11912E 1) (.10000E 2)
 (.70296E 0, .55468E- 2, .38991E- 2, .39450E- 2)
 (-.12658E 0, .46250E 0, -.58545E- 1, .45878E 0)
 (.99800E 0, .10453E 2, .10432E 2, .66133E 0)
 < .95464E- 5>

NUMERATOR: DS /VG FILE NAME? /10/ NEW FILE

-.48057E 2
 (.52327E- 1) (.16977E- 1) (.13402E- 1) (-.16597E 0) (.11516E 1)
 (.10000E 2) (-.41126E 0) (-.10000E 2)
 < .44973E- 2>

NUMERATOR: YE /VG FILE NAME? /11/ NEW FILE

.10761E- 2
 (.14968E- 3) (.10000E 2) (.11940E 1) (.68180E 1)
 (-.10960E 0, .45780E 0, -.50176E- 1, .45504E 0)
 (.97425E 0, .11894E 2, .11583E 2, .26818E 1)
 (-.15587E 0, .20373E 2, -.31756E 1, .20124E 2)
 < .16137E 0>

NUMERATOR: YP /VG FILE NAME? /12/ NEW FILE

-.10761E- 2
 (.14968E- 3) (.11940E 1) (.10000E 2) (.68180E 1)
 (-.10960E 0, .45780E 0, -.50176E- 1, .45504E 0)
 (.97425E 0, .11894E 2, .11583E 2, .26818E 1)
 (-.15587E 0, .20373E 2, -.31756E 1, .20124E 2)
 <-.16137E 0>

TABLE XXXIX

CLOSED-LOOP TRANSFER FUNCTIONS FOR LONGITUDINAL NONLINEAR SYSTEM A

PROJECT: L F-4 VTO 333F/S F UP

DENOMINATOR:

.45000E- 1
 (.50000E- 1) (.42258E 0) (.60109E 1)
 (.87640E 0, .44587E- 1 , .39076E- 1, .21472E- 1)
 (.25968E 0, .36614E 0 , .95077E- 1, .35358E 0)
 (.75798E 0, .32251E 1 , .24446E 1, .21036E 1)
 (.24108E 0, .17140E 1 , .41320E 0, .16634E 1)
 (.94377E 0, .12478E 2 , .11776E 2, .41252E 1)
 < .72460E- 2>

NUMERATOR: U /DC FILE NAME? /1/
 NEW FILE

.12011E- 1
 (.50000E- 1) (.50000E- 1) (.50000E 0) (.00000E 0) (.60000E 1)
 (-.10000E 2) (.63069E 2)
 (.71355E 0, .58729E 0 , .41906E 0, .41146E 0)
 <-.19596E- 1>

NUMERATOR: THE/DC FILE NAME? /2/
 NEW FILE

-.16219E- 1
 (.50000E- 1) (.11421E 0) (.50000E- 1) (.38717E 0) (.00000E 0)
 (.49620E 0) (.60109E 1) (-.10000E 2)
 < .53473E- 4>

NUMERATOR: DD /DC FILE NAME? /3/
 NEW FILE

.85188E- 1
 (.46432E- 1) (.50000E- 1) (.50000E- 1) (.41635E 0) (.00000E 0)
 (.60350E 1) (.56321E 1) (-.51783E 1) (-.10000E 2)
 < .72464E- 2>

TABLE XXXIX(cont'd)

CLOSED-LOOP TRANSFER FUNCTIONS FOR LONGITUDINAL NONLINEAR SYSTEM A

NUMERATOR: DT /DC FILE NAME? /4/
NEW FILE

.18017E 0
(.50000E- 1) (.50000E- 1) (.00000E 0) (-.60000E 1) (-.10000E 2)
(.63069E 2)
(.71355E 0, .58729E 0 , .41906E 0, .41146E 0)
< .58788E 0>

NUMERATOR: DED/DC FILE NAME? /5/
NEW FILE

.45000E- 1
(.50000E- 1) (-.58337E- 3) (.57815E- 3) (.00000E 0) (.43497E 0)
(.60109E 1)
(.87588E 0, .21330E 0 , .18683E 0, .10292E 0)
(.75520E 0, .32021E 1 , .24182E 1, .20990E 1)
(.22418E 0, .17030E 1 , .38177E 0, .16596E 1)
(.94377E 0, .12477E 2 , .11775E 2, .41250E 1)
<-.41786E- 6>

NUMERATOR: U /WG FILE NAME? /6/
NEW FILE

.80358E- 3
(.50000E- 1) (.49386E- 1) (.50000E 0) (.60000E 1) (.14243E 2)
(-.10296E 2)
(.96656E 0, .12845E 1 , .12416E 1, .32939E 0)
(-.12187E 0, .46380E 0 , -.56526E- 1, .46035E 0)
(.78694E 0, .78808E 1 , .62017E 1, .48626E 1)
<-.19243E- 1>

NUMERATOR: THE/WG FILE NAME? /7/
NEW FILE

-.66609E- 4
(.50000E- 1) (.41658E 0) (.10212E 0) (.49953E- 1) (.60107E 1)
(.61062E 1) (.24722E 1) (-.24562E 1)
(-.19517E 0, .57581E 0 , -.11238E 0, .56474E 0)
(.99973E 0, .10020E 2 , .10017E 2, .23333E 0)
< .52508E- 4>

TABLE XXXIX(cont'd)

CLOSED-LOOP TRANSFER FUNCTIONS FOR LONGITUDINAL NONLINEAR SYSTEM A

NUMERATOR: DD /WG FILE NAME? /8/
NEW FILE

-.23503E- 1
 (.50000E- 1) (.14581E- 2) (-.46588E- 3) (.40550E 0) (.15537E 0)
 (.60107E 1)
 (.24028E 0, .11970E 1 , .28761E 0, .11619E 1)
 (.74292E 0, .35865E 1 , .26645E 1, .24007E 1)
 (.95176E 0, .12316E 2 , .11722E 2, .37793E 1)
 < .84508E- 6>

NUMERATOR: DT /WG FILE NAME? /9/ NEW FILE

.12054E- 1
 (.50000E- 1) (.49386E- 1) (-.60000E 1) (.14243E 2) (-.10296E 2)
 (.96656E 0, .12845E 1 , .12416E 1, .32939E 0)
 (-.12187E 0, .46380E 0 , -.56526E- 1, .46035E 0)
 (.78694E 0, .78808E 1 , .62017E 1, .48626E 1)
 < .57728E 0>

NUMERATOR: DED/WG FILE NAME? /10/
NEW FILE

.15920E- 2
 (.50000E- 1) (.82507E- 3) (-.84200E- 3) (.40476E 0) (.15686E 0)
 (.60107E 1) (.15701E 2)
 (.27526E 0, .13026E 1 , .35857E 0, .12523E 1)
 (.62006E 0, .32690E 1 , .20270E 1, .25647E 1)
 (.85293E 0, .11860E 2 , .10115E 2, .61911E 1)
 <-.84508E- 6>

TABLE XXXIX(concluded)

CLOSED-LOOP TRANSFER FUNCTIONS FOR LONGITUDINAL NONLINEAR SYSTEM A

NUMERATOR: SBP/DC FILE NAME? /1/
 OLD FILE

.12555E 0
 (.50000E- 1) (.50000E- 1) (.00000E 0) (.42669E 0) (.60105E 1)
 (-.10000E 2)
 (.27836E 0, .17834E 0 , .49642E- 1, .17129E 0)
 (.37636E 0, .13063E 1 , .49162E 0, .12102E 1)
 <-.43683E- 3>

NUMERATOR: SBP/WG FILE NAME? /2/
 OLD FILE

.38544E- 1
 (.50048E- 1) (.50000E- 1) (.42942E 0) (-.42505E 0) (-.22452E 1)
 (.60107E 1) (-.10000E 2)
 (.45697E 0, .22934E 0 , .10480E 0, .20400E 0)
 (.61587E 0, .18527E 1 , .11410E 1, .14597E 1)
 <-.42895E- 3>

TABLE XXXX

CLOSED-LOOP TRANSFER FUNCTIONS FOR LATERAL NONLINEAR SYSTEM A

PROJECT: LD F-4 VT0333F/S F UP

DENOMINATOR:

-.44639E 0
 (.22358E 0) (.11240E- 1) (.56007E 0) (.10000E 2) (.11292E 1)
 (.12020E 2)
 (.37398E 0, .21127E 0, .79010E- 1, .19594E 0)
 (.11305E 0, .17497E 1, .19781E 0, .17385E 1)
 (.97670E 0, .94291E 1, .92094E 1, .20234E 1)
 <-.10361E 1>

NUMERATOR: B /YC FILE NAME? /1/ OLD FILE

-.12309E- 4
 (.00000E 0) (.10000E- 1) (.00000E 0) (.74542E 0) (.48557E 0)
 (.10000E 2) (-.10000E 2) (-.71764E 2)
 <-.31973E- 3>

NUMERATOR: PSD/YC FILE NAME? /2/ OLD FILE

.10252E- 2
 (.00000E 0) (.10000E- 1) (.00000E 0) (.68273E 0) (.10000E 2)
 (-.10000E 2)
 (.20363E- 1, .21093E 1, .42952E- 1, .21089E 1)
 <-.31142E- 2>

NUMERATOR: PHI/YC FILE NAME? /3/ OLD FILE

.13595E- 1
 (.00000E 0) (.10000E- 1) (.00000E 0) (.10000E 2) (-.10000E 2)
 (.12027E 0, .15562E 1, .18718E 0, .15449E 1)
 <-.32925E- 1>

TABLE XXXX(cont'd)

CLOSED-LOOP TRANSFER FUNCTIONS FOR LATERAL NONLINEAR SYSTEM A

NUMERATOR: DS /YC FILE NAME? /4/ OLD FILE

.11190E 1
 (.42665E- 1) (.00000E 0) (.10000E- 1) (.00000E 0) (.13917E 1)
 (.10000E 2) (-.10000E 2)
 (.11356E 0, .17249E 1 , .19588E 0, .17138E 1)
 <-.19769E 0>

NUMERATOR: YE /YC FILE NAME? /5/ OLD FILE

-.44639E 0
 (.00000E 0) (.00000E 0) (.67875E 0) (.10000E 2) (.11056E 1)
 (.12020E 2)
 (.47359E 0, .31457E 0 , .14898E 0, .27706E 0)
 (.11300E 0, .17497E 1 , .19771E 0, .17385E 1)
 (.97670E 0, .94291E 1 , .92094E 1, .20236E 1)
 <-.10844E 4>

NUMERATOR: YP /YC FILE NAME? /6/ OLD FILE

.20407E- 1
 (.10000E- 1) (.10000E 2) (-.10000E 2)
 (.12215E 0, .15252E 1 , .18631E 0, .15138E 1)
 (.18026E- 1, .46718E 1 , .84213E- 1, .46711E 1)
 <-.10361E 1>

NUMERATOR: B /VG FILE NAME? /7/ NEW FILE

-.16097E- 3
 (.11239E- 1) (.56270E 0) (.23307E 0) (.11323E 1) (.10000E 2)
 (.11668E 2) (.25638E 2)
 (.38306E 0, .20682E 0 , .79224E- 1, .19105E 0)
 (.98375E 0, .95102E 1 , .93557E 1, .17074E 1)
 <-.31089E- 2>

TABLE XXXX(concluded)

CLOSED-LOOP TRANSFER FUNCTIONS FOR LATERAL NONLINEAR SYSTEM A

NUMERATOR: PSD/VG FILE NAME? /8/ NEW FILE

```

.21955E- 2
( .00000E 0) ( .10000E- 1) ( .10495E 1) ( .10000E 2) ( .12296E 2)
(-.28719E 0, .14666E 0, -.42120E- 1, .14048E 0)
( .91936E 0, .75646E 0, .69546E 0, .29761E 0)
( .96782E 0, .94438E 1, .91399E 1, .23766E 1)
< .31100E- 2>

```

NUMERATOR: PHI/VG FILE NAME? /9/ NEW FILE

```

-.13349E- 1
(-.91586E- 2) ( .11815E 1) ( .91917E 1) ( .10000E 2)
( .70302E 0, .55465E- 2, .38996E- 2, .39442E- 2)
(-.11943E 0, .45537E 0, -.54387E- 1, .45211E 0)
( .99811E 0, .10526E 2, .10506E 2, .64747E 0)
< .93846E- 5>

```

NUMERATOR: DS /VG FILE NAME? /10/ NEW FILE

```

-.47242E 2
( .52327E- 1) ( .16977E- 1) ( .13402E- 1) (-.16597E 0) ( .11516E1)
( .10000E 2) (-.41126E 0) (-.10000E 2)
< .44211E- 2>

```

NUMERATOR: YE /VG FILE NAME? /11/ NEW FILE

```

.10761E- 2
( .45521E- 3) ( .10000E 2) ( .11834E 1) ( .69133E 1)
(-.10274E 0, .45058E 0, -.46292E- 1, .44820E 0)
( .97436E 0, .11957E 2, .11656E 2, .26641E 1)
(-.15584E 0, .20373E 2, -.31749E 1, .20124E 2)
< .16463E 0>

```

NUMERATOR: YP /VG FILE NAME? /12/ NEW FILE

```

-.10761E- 2
( .15521E- 3) ( .11834E 1) ( .10000E 2) ( .69133E 1)
(-.10274E 0, .45058E 0, -.46292E- 1, .44820E 0)
( .97436E 0, .11957E 2, .11656E 2, .26641E 1)
(-.15584E 0, .20373E 2, -.31749E 1, .20124E 2)
<-.16463E 0>

```

TABLE XXXXI
 CLOSED-LOOP TRANSFER FUNCTIONS FOR
 LONGITUDINAL LINEAR AND NONLINEAR SYSTEMS B AND C

PROJECT: L F-4 VTO 333F/S F UP

DENOMINATOR:

-.30000E- 1
 (.50000E- 1) (.42269E 0) (.60111E 1) (.14617E 2)
 (.87618E 0, .44555E- 1 , .39038E- 1, .21475E- 1)
 (.26818E 0, .36357E 0 , .97501E- 1, .35025E 0)
 (.30484E 0, .16979E 1 , .51757E 0, .16171E 1)
 (.86176E 0, .42999E 1 , .37055E 1, .21815E 1)
 <-.77914E- 3>

NUMERATOR: U /DC FILE NAME? /1/ OLD FILE

-.12915E- 2
 (.50000E- 1) (.50000E- 1) (.00000E 0) (.50000E 0) (.60000E 1)
 (-.10000E 2) (.63069E 2)
 (.71355E 0, .58729E 0 , .41906E 0, .41146E 0)
 < .21071E- 2>

NUMERATOR: THE/DC FILE NAME? /2/ OLD FILE

.17439E- 2
 (.50000E- 1) (.50000E- 1) (.11421E 0) (.00000E 0) (.49620E 0)
 (.38717E 0) (.60109E 1) (-.10000E 2)
 <-.57497E- 5>

NUMERATOR: DD /DC FILE NAME? /3/ NEW FILE

-.91600E- 2
 (.50000E- 1) (.50000E- 1) (.46432E- 1) (.00000E 0) (.41635E 0)
 (.60350E 1) (.56321E 1) (-.51783E 1) (-.10000E 2)
 <-.77919E- 3>

TABLE XXXXI(cont'd)

CLOSED-LOOP TRANSFER FUNCTIONS FOR
LONGITUDINAL LINEAR AND NONLINEAR SYSTEMS B AND C

NUMERATOR: DT /DC FILE NAME? /4/ NEW FILE

-.19373E- 1
(.50000E- 1) (.50000E- 1) (.00000E 0) (-.60000E 1) (-.10000E 2)
(.63069E 2)
(.71355E 0, .58729E 0 , .41906E 0, .41146E 0)
<-.63213E- 1>

NUMERATOR: DED/DC FILE NAME? /5/ NEW FILE

-.30000E- 1
(.50000E- 1) (-.58338E- 3) (.57814E- 3) (.00000E 0) (.43438E 0)
(.60112E 1) (.14616E 2)
(.86916E 0, .21129E 0 , .18364E 0, .10449E 0)
(.28720E 0, .16883E 1 , .48486E 0, .16171E 1)
(.86185E 0, .42766E 1 , .36858E 1, .21689E 1)
< .44931E- 7>

NUMERATOR: SBP/DC FILE NAME? /2/ NEW FILE

-.12150E- 1
(.50000E- 1) (.50000E- 1) (.00000E 0) (.42669E 0) (.60105E 1)
(-.10000E 2)
(.27836E 0, .17834E 0 , .49642E- 1, .17129E 0)
(.37636E 0, .13063E 1 , .49162E 0, .12102E 1)
< .42274E- 4>

NUMERATOR: U /WG FILE NAME? /6/ NEW FILE

-.53572E- 3
(.50000E- 1) (.49384E- 1) (.50000E 0) (.60000E 1) (-.10280E 2)
(.99355E 0, .13140E 1 , .13055E 1, .14901E 0)
(-.96761E- 1, .46350E 0 , -.44849E- 1, .46133E 0)
(.89874E 0, .11693E 2 , .10509E 2, .51273E 1)
< .20691E- 2>

NUMERATOR: THE/WG FILE NAME? /7/ NEW FILE

.44406E- 4
(.50000E- 1) (.10208E 0) (.49953E- 1) (.41676E 0) (.23912E 1)
(.98087E 1) (.10178E 2) (.60107E 1) (-.24660E 1)
(-.15497E 0, .58151E 0 , -.90116E- 1, .57449E 0)
<-.56460E- 5>

TABLE XXXXI(concluded)
 CLOSED-LOOP TRANSFER FUNCTIONS FOR
 LONGITUDINAL LINEAR AND NONLINEAR SYSTEMS B AND C

NUMERATOR: DD /WG FILE NAME? /8/ NEW FILE

```
.15669E- 1
( .50000E- 1) ( .15673E  0) ( .14580E- 2) (-.46588E- 3) ( .40484E  0)
( .60106E  1) ( .14100E  2)
( .31731E  0, .11925E  1 , .37839E  0, .11309E  1)
( .85829E  0, .47256E  1 , .40559E  1, .24250E  1)
<-.90869E- 7>
```

NUMERATOR: DT /WG FILE NAME? K/9/ NEW FILE

```
-.80358E- 2
( .50000E- 1) ( .49384E- 1) (-.60000E  1) (-.10280E  2)
( .99355E  0, .13140E  1 , .13055E  1, .14901E  0)
(-.96761E- 1, .46350E  0 , -.44849E- 1, .46133E  0)
( .89874E  0, .11693E  2 , .10509E  2, .51273E  1)
<-.62073E- 1>
```

NUMERATOR: DED/WG FILE NAME? /10/ NEW FILE

```
-.10613E- 2
( .50000E- 1) ( .82505E- 3) ( .15830E  0) (-.84202E- 3) ( .40401E  0)
( .60106E  1)
( .35889E  0, .12917E  1 , .46359E  0, .12057E  1)
( .67506E  0, .41714E  1 , .28159E  1, .30775E  1)
( .94014E  0, .14861E  2 , .13972E  2, .50647E  1)
< .90869E- 7>
```

NUMERATOR: SBP/WG FILE NAME? /1/

```
NEW FILE
-.37301E- 2
( .50048E- 1) ( .50000E- 1) ( .42942E  0) (-.42505E  0) ( .60107E  1)
(-.22452E  1) (-.10000E  2)
( .45697E  0, .22934E  0 , .10480E  0, .20400E  0)
( .61587E  0, .18527E  1 , .11410E  1, .14597E  1)
< .41512E- 4>
```

TABLE XXXXII

CLOSED-LOOP TRANSFER FUNCTIONS FOR LATERAL LINEAR SYSTEM B

PROJECT: LD F-4 VTC333F/S F UP

DENOMINATOR:

-.29759E- 1
 (.11240E- 1) (.57202E 0) (.22982E 0) (.11419E 1) (.10000E 2)
 (.40090E 0, .21101E 0 , .84594E- 1, .19331E 0)
 (.99526E 0, .10126E 2 , .10078E 2, .98434E 0)
 (.11577E 0, .17506E 1 , .20267E 0, .17388E 1)
 <-.70263E- 2>

NUMERATOR: B /YC FILE NAME? /1/ OLD FILE

-.83475E- 7
 (.00000E 0) (.10000E- 1) (.00000E 0) (.74542E 0) (.48557E 0)
 (.10000E 2) (-.10000E 2) (-.71764E 2)
 <-.21683E- 5>

NUMERATOR: PSD/YC FILE NAME? /111/ NEW FILE

.69524E- 5
 (.00000E 0) (.10000E- 1) (.00000E 0) (.68273E 0) (.10000E 2)
 (-.10000E 2)
 (.20363E- 1, .21093E 1 , .42952E- 1, .21089E 1)
 <-.21119E- 4>

NUMERATOR: PHI/YC FILE NAME? /3/ OLD FILE

.92196E- 4
 (.00000E 0) (.10000E- 1) (.00000E 0) (.10000E 2) (-.10000E 2)
 (.12027E 0, .15562E 1 , .18718E 0, .15449E 1)
 <-.22329E- 3>

TABLE XXXXII(cont'd)

CLOSED-LOOP TRANSFER FUNCTIONS FOR LATERAL LINEAR SYSTEM B

NUMERATOR: DS /YC FILE NAME? /4/ OLD FILE

.75886E- 2
 (.42665E- 1) (.00000E 0) (.10000E- 1) (.00000E 0) (.13917E 1)
 (.10000E 2) (-.10000E 2)
 (.11356E 0, .17249E 1 , .19588E 0, .17138E 1)
 <-.13406E- 2>

NUMERATOR: YE /YC FILE NAME? /5/ OLD FILE

-.29759E- 1
 (.00000E 0) (.00000E 0) (.11199E 1) (.68786E 0) (.10000E 2)
 (.49559E 0, .31947E 0 , .15833E 0, .27748E 0)
 (.99526E 0, .10126E 2 , .10078E 2, .98441E 0)
 (.11571E 0, .17506E 1 , .20257E 0, .17389E 1)
 <-.73524E 1>

NUMERATOR: YP /YC FILE NAME? /6/ OLD FILE

.13839E- 3
 (.10000E- 1) (.10000E 2) (-.10000E 2)
 (.12215E 0, .15252E 1 , .18631E 0, .15138E 1)
 (.18026E- 1, .46718E 1 , .84213E- 1, .46711E 1)
 <-.70263E- 2>

NUMERATOR: B /VG FILE NAME? /7/ NEW FILE

-.10731E- 4
 (.11239E- 1) (.23973E 0) (.11433E 1) (.57492E 0) (.10000E 2)
 (.25626E 2)
 (.40887E 0, .20624E 0 , .84326E- 1, .18821E 0)
 (.99722E 0, .10089E 2 , .10061E 2, .75111E 0)
 <-.21083E- 4>

TABLE XXXXII(concluded)

CLOSED-LOOP TRANSFER FUNCTIONS FOR LATERAL LINEAR SYSTEM B

NUMERATOR: PSD/VG FILE NAME? /8/ NEW FILE

.14637E- 3
 (.00000E 0) (.10000E- 1) (.11026E 1) (.10000E 2)
 (-.28012E 0, .14719E 0 , -.41232E- 1, .14130E 0)
 (.93809E 0, .76147E 0 , .71432E 0, .26378E 0)
 (.99281E 0, .10200E 2 , .10126E 2, .12213E 1)
 < .21091E- 4>

NUMERATOR: PHI/VG FILE NAME? /9/ NEW FILE

-.88994E- 3
 (-.91658E- 2) (.10000E 2) (.11636E 1) (.10228E 2) (.97571E 1)
 (.70296E 0, .55468E- 2 , .38991E- 2, .39450E- 2)
 (-.10957E 0, .46730E 0 , -.51201E- 1, .46449E 0)
 < .63643E- 7>

NUMERATOR: DS /VG FILE NAME? /10/ NEW FILE

-.32038E 0
 (.52327E- 1) (.16977E- 1) (.13402E- 1) (.11516E 1) (-.16597E 0)
 (-.41126E 0) (.10000E 2) (-.10000E 2)
 < .29982E- 4>

NUMERATOR: YE /VG FILE NAME? /11/ OLD FILE

.71741E- 4
 (.14968E- 3) (.11644E 1) (.82271E 1) (.11735E 2) (.10000E 2)
 (-.92113E- 1, .46221E 0 , -.42576E- 1, .46025E 0)
 (-.15437E 0, .20424E 2 , -.31527E 1, .20179E 2)
 < .10758E- 2>

NUMERATOR: YP /VG FILE NAME? /12/ OLD FILE

-.71741E- 4
 (.14968E- 3) (.82271E 1) (.11644E 1) (.11735E 2) (.10000E 2)
 (-.92113E- 1, .46221E 0 , -.42576E- 1, .46025E 0)
 (-.15437E 0, .20424E 2 , -.31527E 1, .20179E 2)
 <-.10758E- 2>

TABLE XXXXIII

CLOSED-LOOP TRANSFER FUNCTIONS FOR LATERAL NONLINEAR SYSTEM B

PROJECT: LD F-4 VT0333F/SF UP

DENOMINATOR:

-.29759E- 1
 (.11240E- 1) (.21071E 0) (.60993E 0) (.11522E 1) (.10000E 2)
 (.36326E 0, .20633E 0 , .74952E- 1, .19224E 0)
 (.99554E 0, .10119E 2 , .10074E 2, .95514E 0)
 (.11566E 0, .17489E 1 , .20229E 0, .17372E 1)
 <-.66047E- 2>

NUMERATOR: B /YC FILE NAME? /1/ OLD FILE

-.78467E- 7
 (.00000E 0) (.10000E- 1) (.00000E 0) (.74542E 0) (.48557E 0)
 (.10000E 2) (-.10000E 2) (-.71764E 2)
 <-.20382E- 5>

NUMERATOR: PSD/YC FILE NAME? /2/ OLD FILE

.65353E- 5
 (.00000E 0) (.10000E- 1) (.00000E 0) (.68273E 0) (.10000E 2)
 (-.10000E 2)
 (.20363E- 1, .21093E 1 , .42952E- 1, .21089E 1)
 <-.19852E- 4>

NUMERATOR: PHI/YC FILE NAME? /3/ OLD FILE

.86664E- 4
 (.00000E 0) (.10000E- 1) (.00000E 0) (.10000E 2) (-.10000E 2)
 (.12027E 0, .15562E 1 , .18718E 0, .15449E 1)
 <-.20989E- 3>

TABLE XXXXIII(cont'd)

CLOSED-LOOP TRANSFER FUNCTIONS FOR LATERAL NONLINEAR SYSTEM B

NUMERATOR: DS /YC FILE NAME? /4/ OLD FILE

.71333E- 2
 (.42665E- 1) (.00000E 0) (.10000E- 1) (.00000E 0) (.13917E1)
 (.10000E 2) (-.10000E 2)
 (.11356E 0, .17249E 1 , .19588E 0, .17138E 1)
 <-.12602E- 2>

NUMERATOR: YE /YC FILE NAME? /5/ OLD FILE

-.29759E- 1
 (.00000E 0) (.00000E 0) (.11321E 1) (.70600E 0) (.10000E 2)
 (.48700E 0, .30500E 0, .14854E 0, .26639E 0)
 (.99600E 0, .10120E 2, .10080E 2, .90425E0)
 (.11600E 0, .17490E 1, .20288E0, .17372E 0)
 <-.69139E 1>

NUMERATOR: YP /YC FILE NAME? /6/ OLD FILE

.13000E- 3
 (.10000E- 1) (.10000E 2) (-.10000E 2)
 (.12200E 0, .15250E 1, .18631E 0, .15138E 1)
 (.18026E- 1, .46720E 1, .84213E-1, .46711E 1)
 <-.66047E- 2>

NUMERATOR: B /VG FILE NAME? /7/ OLD FILE

-.10731E- 4
 (.11239E- 1) (.21832E 0) (.11521E 1) (.61261E 0) (.10000E2)
 (.25626E 2)
 (.37113E 0, .20231E 0 , .75084E- 1, .18786E 0)
 (.99739E 0, .10083E 2 , .10057E 2, .72870E 0)
 <-.19818E- 4>

TABLE XXXXIII(concluded)

CLOSED-LOOP TRANSFER FUNCTIONS FOR LATERAL NONLINEAR SYSTEM B

NUMERATOR: PSD/VG FILE NAME? /8/ OLD FILE

.14637E- 3
 (.00000E 0) (.10000E- 1) (.11548E 1) (.10000E 2)
 (.95662E 0, .72771E 0 , .69614E 0, .21201E 0)
 (-.28776E 0, .14608E 0 , -.42035E- 1, .13990E 0)
 (.99320E 0, .10188E 2 , .10119E 2, .11857E 1)
 < .19825E- 4>

NUMERATOR: PHI/VG FILE NAME? /9/ OLD FILE

-.88994E- 3
 (-.91548E- 2) (.10222E 2) (.11508E 1) (.10000E 2) (.97647E 1)
 (.70315E 0, .55463E- 2 , .38999E- 2, .39437E- 2)
 (-.99251E- 1, .45586E 0 , -.45244E- 1, .45361E 0)
 < .59824E- 7>

NUMERATOR: DS /VG FILE NAME? /10/ OLD FILE

-.30116E 0
 (.52327E- 1) (.16977E- 1) (.13402E- 1) (.11516E 1) (-.16597E 0)
 (-.41126E 0) (.10000E 2) (-.10000E 2)
 < .28183E- 4>

NUMERATOR: YE /VG FILE NAME? /11/ OLD FILE

.71741E- 4
 (.15835E- 3) (.11508E 1) (.82818E 1) (.11683E 2) (.10000E 2)
 (-.82305E- 1, .45066E 0 , -.37092E- 1, .44914E 0)
 (-.15439E 0, .20419E 2 , -.31526E 1, .20175E 2)
 < .10712E- 2>

NUMERATOR: YP /VG FILE NAME? /12/ OLD FILE

-.71741E- 4
 (.15835E- 3) (.82818E 1) (.11508E 1) (.11683E 2) (.10000E2)
 (-.82305E- 1, .45066E 0 , -.37092E- 1, .44914E 0)
 (-.15439E 0, .20419E 2 , -.31526E 1, .20175E 2)
 <-.10712E- 2>

TABLE XXXIV

CLOSED-LOOP TRANSFER FUNCTIONS FOR LATERAL LINEAR SYSTEM C

PROJECT: LD F-4 VT0333F/S F UP

DENOMINATOR:

```

-.29759E- 1
( .10690E- 1) ( .28088E 1) ( .10000E 2) ( .31460E 1) ( .14440E 2)
( .51644E 0, .28970E 0 , .14962E 0, .24808E 0)
( .54222E 0, .59313E 0 , .32160E 0, .49837E 0)
( .34427E 0, .19436E 1 , .66912E 0, .18248E 1)
<-.45275E- 1>

```

NUMERATOR: B /VG FILE NAME? /1/ OLD FILE

```

-.10731E- 4
( .10689E- 1) ( .10000E 2) ( .63333E 1) ( .19678E 1) ( .26383E 2)
( .11991E 2)
( .42424E 0, .28481E 0 , .12083E 0, .25791E 0)
( .78648E 0, .60836E 0 , .47846E 0, .37574E 0)
<-.13577E- 3>

```

NUMERATOR: PSD/VG FILE NAME? /2/ OLD FILE

```

.14637E- 3
( .10000E- 1) ( .00000E 0) ( .10000E 2) ( .14678E 2)
(-.29337E 0, .22111E 0 , -.64868E- 1, .21138E 0)
( .95177E 0, .97359E 0 , .92663E 0, .29872E 0)
( .85272E 0, .36936E 1 , .31496E 1, .19294E 1)
< .13583E- 3>

```

NUMERATOR: PHI/VG FILE NAME? /3/ OLD FILE

```

-.88994E- 3
(-.12918E- 1) ( .15792E 1) ( .10000E 2) ( .10441E 2) ( .95009E 1)
( .74535E 0, .67076E- 2 , .49995E- 2, .44718E- 2)
(-.29865E 0, .79197E 0 , -.23652E 0, .75583E 0)
< .50825E- 6>

```

TABLE XXXIV(cont'd)

CLOSED-LOOP TRANSFER FUNCTIONS FOR LATERAL LINEAR SYSTEM C

NUMERATOR: DA /VG FILE NAME? /4/ OLD FILE

-.16019E 0
 (.61537E- 1) (.21428E- 1) (.11329E- 1) (-.19834E 0) (.10000E 2)
 (-.42753E 0) (-.10000E 2)
 (.95811E 0, .15535E 1, .14885E 1, .44493E 0)
 < .48971E- 4>

NUMERATOR: YE /VG FILE NAME? /5/ OLD FILE

.71741E- 4
 (.45180E- 4) (.15719E 1) (.10000E 2)
 (-.28082E 0, .76867E 0, -.21586E 0, .73774E 0)
 (.96646E 0, .10107E 2, .97676E 1, .25956E 1)
 (-.14665E 0, .20249E 2, -.29696E 1, .20030E 2)
 < .12608E- 2>

PROJECT: LD F-4 VT0333F/S F, LG UP

DENOMINATOR:

-.29759E- 1
 (.10690E- 1) (.28088E 1) (.10000E 2) (.31460E 1) (.14440E 2)
 (.51644E 0, .28970E 0, .14962E 0, .24808E 0)
 (.54222E 0, .59313E 0, .32160E 0, .49837E 0)
 (.34427E 0, .19436E 1, .66912E 0, .18248E 1)
 <-.45275E- 1>

NUMERATOR: B /YC FILE NAME? /1/ OLD FILE

-.40903E- 6
 (.00000E 0) (.10000E- 1) (.14546E 0) (.00000E 0) (.11867E 1)
 (.10000E 2) (-.10000E 2) (-.25025E 3)
 <-.17669E- 4>

NUMERATOR: PSD/YC FILE NAME? /2/ OLD FILE

.10467E- 4
 (.00000E 0) (.10000E- 1) (.00000E 0) (.62070E 0) (.10000E 2)
 (-.10000E 2)
 (-.41233E 0, .45768E 1, -.18871E 1, .41696E 1)
 <-.13609E- 3>

TABLE XXXXIV(concluded)

CLOSED-LOOP TRANSFER FUNCTIONS FOR LATERAL LINEAR SYSTEM C

NUMERATOR: PHI/YC FILE NAME? /3/ OLD FILE

.80230E- 3
 (.00000E 0) (.10000E- 1) (.00000E 0) (.10000E 2) (-.10000E 2)
 (.13227E 0, .13412E 1 , .17741E 0, .13294E 1)
 <-.14432E- 2>

NUMERATOR: DA /YC FILE NAME? /4/ OLD FILE

.12395E- 1
 (.42665E- 1) (.00000E 0) (.10000E- 1) (.00000E 0) (.13917E 1)
 (.10000E 2) (-.10000E 2)
 (.11356E 0, .17249E 1 , .19588E 0, .17138E 1)
 <-.21897E- 2>

NUMERATOR: YE /YC FILE NAME? /5/ OLD FILE

-.29759E- 1
 (.00000E 0) (.00000E 0) (.54255E 0) (.27376E 1) (.31909E 1)
 (.10000E 2) (.14440E 2)
 (.36520E 0, .60996E 0 , .22276E 0, .56783E 0)
 (.34244E 0, .19414E 1 , .66481E 0, .18241E 1)
 <-.28560E 2>

NUMERATOR: YP /YC FILE NAME? /6/ NEW FILE

.11408E- 3
 (.10000E- 1) (.10000E 2) (-.10000E 2)
 (.11935E 0, .13245E 1 , .15808E 0, .13150E 1)
 (-.32200E 0, .15041E 2 , -.48432E 1, .14240E 2)
 <-.45275E- 1>

TABLE XXXV

CLOSED-LOOP TRANSFER FUNCTIONS FOR LATERAL NONLINEAR SYSTEM C

PROJECT: LD F-4 VT0333F/S F UP

DENOMINATOR:

```

-.29759E- 1
( .11067E- 1) ( .11145E 1) ( .10000E 2)
( .50888E 0, .21552E 0 , .10967E 0, .18553E 0)
( .77538E 0, .41497E 0 , .32176E 0, .26205E 0)
( .99201E 0, .10215E 2 , .10133E 2, .12889E 1)
( .11831E 0, .18214E 1 , .21549E 0, .18086E 1)
<-.10164E- 1>
    
```

NUMERATOR: YD /YC FILE NAME? /Y/ NEW FILE

```

-.30546E- 4
( .10000E- 1) ( .00000E 0) ( .13505E 2) ( .10000E 2) (-.10000E2)
(-.11611E 2)
( .56559E- 1, .14567E 1 , .82387E- 1, .14543E 1)
<-.10164E- 1>
    
```

NUMERATOR: B /YC FILE NAME? /1/ OLD FILE

```

-.91823E- 7
( .00000E 0) ( .10000E- 1) ( .14546E 0) ( .00000E 0) (.11867E1)
( .10000E 2) (-.10000E 2) (-.25025E 3)
<-.39666E- 5>
    
```

NUMERATOR: PSD/YC FILE NAME? /2/ OLD FILE

```

.23497E- 5
( .00000E 0) ( .10000E- 1) ( .00000E 0) ( .62070E 0) ( .10000E 2)
(-.10000E 2)
(-.41233E 0, .45768E 1 , -.18871E 1, .41696E 1)
<-.30550E- 4>
    
```

TABLE XXXV(cont'd)

CLOSED-LOOP TRANSFER FUNCTIONS FOR LATERAL NONLINEAR SYSTEM C

NUMERATOR: PHI/YC FILE NAME? /3/ OLD FILE

.18011E- 3
 (.00000E 0) (.10000E- 1) (.00000E 0) (.10000E 2) (-.10000E 2)
 (.13227E 0, .13412E 1, .17741E 0, .13294E 1)
 <-.32398E- 3>

NUMERATOR: YE /YC FILE NAME? /4/ OLD FILE

-.29759E- 1
 (.00000E 0) (.00000E 0) (.10876E 1) (.51042E 0) (.10000E2)
 (.48212E 0, .40578E 0, .19563E 0, .35551E 0)
 (.99201E 0, .10215E 2, .10133E 2, .12889E 1)
 (.11810E 0, .18213E 1, .21509E 0, .18086E 1)
 <-.94154E 1>

NUMERATOR: YP /YC FILE NAME? /5/ OLD FILE

.25611E- 4
 (.10000E- 1) (.10000E 2) (-.10000E 2)
 (.11935E 0, .13245E 1, .15808E 0, .13150E 1)
 (-.32200E 0, .15041E 2, -.48432E 1, .14240E 2)
 <-.10164E- 1>

NUMERATOR: DA /YC FILE NAME? /11/ NEW FILE

.27825E- 2
 (.42665E- 1) (.00000E 0) (.10000E- 1) (.00000E 0) (.13917E 1)
 (.10000E 2) (-.10000E 2)
 (.11356E 0, .17249E 1, .19588E 0, .17138E 1)
 <-.49156E- 3>

NUMERATOR: B /VG FILE NAME? /6/ OLD FILE

-.10731E- 4
 (.11065E- 1) (.11104E 1) (.10000E 2) (.25612E 2)
 (.88879E 0, .45184E 0, .40159E 0, .20709E 0)
 (.46480E 0, .20820E 0, .96769E- 1, .18434E 0)
 (.99782E 0, .10099E 2, .10077E 2, .66578E 0)
 <-.30480E- 4>

TABLE XXXV(concluded)

CLOSED-LOOP TRANSFER FUNCTIONS FOR LATERAL NONLINEAR SYSTEM C

NUMERATOR: PSD/VG FILE NAME? /7/ OLD FILE

.14637E- 3
 (.00000E 0) (.10000E- 1) (.97525E 0) (.10000E 2)
 (-.26440E 0, .15900E 0 , -.42041E- 1, .15334E 0)
 (.83206E 0, .89667E 0 , .74608E 0, .49737E 0)
 (.99098E 0, .10251E 2 , .10159E 2, .13741E 1)
 < .30493E- 4>

NUMERATOR: PHI/VG FILE NAME? /8/ OLD FILE

-.88994E- 3
 (-.10757E- 1) (.10000E 2) (.12190E 1) (.10257E 2) (.97240E 1)
 (.72112E 0, .60744E- 2 , .43803E- 2, .42084E- 2)
 (-.14850E 0, .51543E 0 , -.76540E- 1, .50971E 0)
 < .11410E- 6>

NUMERATOR: YE /VG FILE NAME? /9/ NEW FILE

.71741E- 4
 (.12218E- 3) (.12214E 1) (.91912E 1) (.10757E 2) (.10000E 2)
 (-.13706E 0, .50544E 0 , -.69277E- 1, .50067E 0)
 (-.15459E 0, .20359E 2 , -.31473E 1, .20114E 2)
 < .11208E- 2>

NUMERATOR: YP /VG FILE NAME? /10/ NEW FILE

-.71741E- 4
 (.12218E- 3) (.91912E 1) (.12214E 1) (.10757E 2) (.10000E 2)
 (-.13706E 0, .50544E 0 , -.69277E- 1, .50067E 0)
 (-.15459E 0, .20359E 2 , -.31473E 1, .20114E 2)
 < -.11208E- 2>

NUMERATOR: DA /VG FILE NAME? /12/ NEW FILE

-.10412E 0
 (.54495E- 1) (.18607E- 1) (.12481E- 1) (.11530E 1) (-.18042E 0)
 (-.40104E 0) (.10000E 2) (-.10000E 2)
 < .10993E- 4>

APPENDIX VI

MEAN SQUARE PERFORMANCE DATA AND PILOT OPINION RATINGS RESULTING FROM HONEYWELL, INC. FIXED-BASE, PILOTED SIMULATOR EXPERIMENTS (REPRODUCED AND SUMMARIZED FROM REF. 1)

Mean square performance data for the glide slope and localizer tracking task for back-up system A, B and C are given in Tables XXXXVI, XXXXVII and XXXXVIII respectively. These data were generated by means of fixed-base piloted simulation. The only disturbance inputs acting were normal and side gusts. (No model of the ILS beam bends is included.) Definitions of the quantities recorded in Tables XXXXVI, XXXXVII and XXXXVIII are given below.

$$\bar{u}_e^2 = \frac{1}{T} \int_0^T (u(t) - u_0)^2 dt \quad (\text{knots})^2 \quad (61)$$

$$\bar{\theta}_e^2 = \frac{1}{T} \int_0^T (\theta(t) - \theta_0)^2 dt \quad (\text{deg})^2 \quad (62)$$

$$\bar{\delta}_{se}^2 = \frac{1}{T} \int_0^T (\delta_s(t) - \delta_{s0})^2 dt \quad (\text{deg})^2 \quad (63)$$

$$\bar{\delta}_s^2 = \frac{1}{T} \int_0^T \dot{\delta}_s(t)^2 dt \quad (\text{deg/sec})^2 \quad (64)$$

$$\bar{GS}^2 = \frac{1}{T} \int_0^T GS(t)^2 dt \quad (\text{deg})^2 \quad (65)$$

$$\bar{n}_z^2 = \frac{1}{T} \int_0^T n_z(t)^2 dt \quad (\text{ft/sec}^2)^2 \quad (66)$$

Etc.

where the nominal trim point is defined:

TABLE XXXXVI

EVALUATIONS - REDUNDANT ACTUATOR/BACK-UP POWER SYSTEMS

Mean Square Errors	Pilot	JN	JN	JN	JN	DS	DS	DS	DS	DS	DJ	TL
	Date	12/16/69	12/16/69	12/16/69	12/16/69	11/21/69	11/21/69	11/21/69	12/3/69	12/3/69	12/2/69	12/2/69
	Run No.	21	26	27	28	19	20	21	18	19	39	12
No. of Engines		2	1	1	1	1	1	1	1	1	1	1
Gusts		No	No	No	No	Yes						Yes
δ_g max (deg/sec)		1	2	2	2	2	2	2	1	1	1	1
δ_g min (deg)		-4										-4
δ_s max (deg)		-1										-1
δ_g power (HP)		.1	.2	.2	.2	.2	.2	.2	.1	.1	.1	.1
$\overline{u_e^2}$		2490.	3260.	1320.	1350.	212.	7590.	3040.	2560.	1190.	883.	4500.
$\overline{q_e^2}$		66.1	38.3	10.3	49.3	227.	333.	691.	45.3	4.75	34.2	22.7
$\overline{\delta_{sc}^2}$		1.08	5.84	4.06	.34	2.22	.26	.56	.884	.864	7.48	.58
$\overline{\delta_s^2}$		8.38	2.32	2.19	7.75	1.03	.983	1.81	.376	.404	.389	.019
$\overline{GS^2}$		1.97	1.08	.776	.778	1.69	2.79	.108	.229	.683	.501	1.95
$\overline{n_z^2}$		128.	189.	107.	207.	774.	853.	1079.	156.	111.	258.	36.1
$\overline{S_L^2}$.539	.845	.314	.506	.0983	.0800	.331	.049	.0569	.155	.0051
$\overline{Q^2}$		25.8	6.7	6.2	23.3	56.9	52.5	206.	7.96	11.0	20.2	.54
$\overline{\phi^2}$		53.2	145.	22.9	99.8	888.	117.	216.	53.9	69.1	353.	68.0
$\overline{\psi^2}$		18.8	73.2	9.6	139.	1410.	1330.	4290.	18.9	28.8	71.0	34.4
$\overline{P^2}$		6.13	54.8	6.18	16.2	84.2	60.8	86.8	26.1	32.8	143.	9.82
$\overline{R^2}$.842	1.55	.268	1.35	11.2	4.19	11.2	1.11	1.70	10.4	1.13
$\overline{B^2}$.083	.455	.089	.734	3.02	3.10	6.50	.766	1.00	8.15	1.14
$\overline{LOC^2}$.423	35.3	.254	41.8	148.	172.	165.	4.70	.190	1.48	3.58
$\overline{F_{PR}^2}$		109.	167.	155.	208.	254.	235.	234.	199.	186.	217.	212.
$\overline{\delta_a^2}$		0	0	0	0	0	0	0	0	0	0	0
$\overline{\delta_a^2}$		0	0	0	0	0	0	0	0	0	0	0
$\overline{\delta_r^2}$.048	1.15	.812	3.23	4.92	4.00	3.97	2.13	2.10	3.93	2.94
$\overline{\delta_r^2}$		3.26	2.33	1.02	2.85	3.08	2.29	1.97	1.81	2.06	9.30	.910
$\overline{S_{LD}^2}$.61	1.28	.321	2.98	.240	.123	.321	.050	.0912	.067	.214
$\overline{P_r^2}$.0008	.0088	.0062	.246	.0375	.0304	.0302	.016	.0160	.0301	.222
$\overline{\delta_{SP}^2}$		82.8	141.	42.8	395.	32.5	16.7	42.7	6.65	12.3	9.16	29.4
$\overline{\delta_{SP}^2}$		72.4	167.	47.3	92.2	25.6	11.2	67.1	12.8	19.8	3.79	2.06

TABLE XXXXVI(cont'd)

EVALUATIONS - REDUNDANT ACTUATOR/BACK-UP POWER SYSTEMS

Pilot Opinion - Landability				
Question	Pilot	Date	Comment	
1. Is the aircraft difficult to trim?	JN	12/16	No problem	
	JN	12/16	No problem	
	DS	11/21	Yes	
	LF	12/3	No	
	DS	12/3	No	
	DJ	12/2	OK	
2. Is attitude control satisfactory?	JN	12/16	OK	
	JN	12/16	No real problem (with practice)	
	DS	11/21	Extremely difficult	
	LF	12/3	Yes	
	DS	12/3	OK	
	DJ	12/2	OK	
Is heading control satisfactory?	JN	12/16	OK	
	JN	12/16	No real problem (with practice)	
	DS	11/21	No comment	
	LF	12/3	Less than desirable	
	DS	12/3	OK	
	DJ	12/2	OK	
3. Is holding altitude a problem?	a. Straight and level	JN	12/16	---
		JN	12/16	No problem
		DS	11/21	---
		LF	12/3	No, did not increase problem
		DS	12/3	---
		DJ	12/2	OK
	b. Turns	JN	12/16	Actually easier (but this is pilot technique); unfamiliarity with basic configuration
		JN	12/16	No problem
		DS	11/21	Unsatisfactory
		LF	12/3	---
		DS	12/3	---
		DJ	12/2	---
4. What is maximum usable bank angle?	JN	12/16	45°	
	JN	12/16	30° maximum	
	DS	11/21	20°	
	LF	12/3	No problem; did not exceed 15° bank angle	
	DS	12/3	10-15°	
	DJ	12/2	25°	
5. Is maintaining airspeed a problem?	JN	12/16	Only due to unfamiliarity	
	JN	12/16	No problem	
	DS	11/21	Very difficult	
	LF	12/3	No	
	DS	12/3	Kept 200-220 knots	
	DJ	12/2	High	
6. Are there any problems associated with the landing task?	JN	12/16	No	
	JN	12/16	No problem	
	DS	11/21	---	
	LF	12/3	Yes, direction control	
	DS	12/3	---	
	DJ	12/2	---	

TABLE XXXXVI(cont'd)

EVALUATIONS - REDUNDANT ACTUATOR/BACK-UP POWER SYSTEMS

Pilot Opinion - Landability			
Question	Pilot	Date	Comment
a. How well can you accomplish the task?	JN	12/16	Satisfactory
	JN	12/16	Satisfactory +
	DS	11/21	Unsuccessful
	LF	12/3	Acceptable
	DS	12/3	Satisfactory
	DJ	12/2	OK
b. How much fatigue is involved?	JN	12/16	No factor
	JN	12/16	Not a factor other than getting behind on the cross check
	DS	11/21	Extreme
	LF	12/3	Normal
	DS	12/3	Moderate
	DJ	12/2	---
7. What are the effects of random gust inputs on handling quality?	JN	12/16	Not noticeable
	JN	12/16	Not noticeable
	DS	11/21	---
	LF	12/3	Aggravates problem
	DS	12/3	Moderate
	DJ	12/2	No problem
8. Are special piloting techniques required for the configuration?	JN	12/16	None
	JN	12/16	None other than use of rudders (not applicable in some jets)
	DS	11/21	Yes; extreme lead
	LF	12/3	No more than qualified pilot
	DS	12/3	---
	DJ	12/2	High airspeed
9. What instruments are used most?	JN	12/16	Not angle of attack
	JN	12/16	Not angle of attack or vertical speed; used attitude indicator to cross check, flight director, airspeed, and altitude
	DS	11/21	All
	LF	12/3	Flight direction
	DS	12/3	---
	DJ	12/2	---
10. Are any of the instruments inadequate for the configuration?	JN	12/16	Flight direction is hidden behind stick
	JN	12/16	Flight direction is hidden behind stick
	DS	11/21	---
	LF	12/3	No
	DS	12/3	---
	DJ	12/2	---
11. Pilot rating?	JN	12/16	2
	JN	12/16	2
	DS	11/21	9
	LF	12/3	5
	DS	12/3	5
	DJ	12/2	5
12. PIO rating?	JN	12/16	1
	JN	12/16	2
	DS	11/21	6
	LF	12/3	3
	DS	12/3	2
	DJ	12/2	5

NOTE: The dash denotes no comment by the pilot.

TABLE XXXXVI (concluded)

EVALUATIONS - REDUNDANT ACTUATOR/BACK-UP POWER SYSTEMS

Pilot Opinion - Landability				
Question	Pilot	Date	Comment	
1. Is the aircraft difficult to trim?	DS	12/3	Ran out of time on this run; trouble with transducer, roll uncertainties	
	DJ	12/2	OK	
2. Is attitude control satisfactory?	DS	12/3	---	
	DJ	12/2	OK	
Is heading control satisfactory?	DS	12/3	---	
	DJ	12/2	OK	
3. Is holding altitude a problem?				
	a. Straight and level	DS	12/3	---
	DJ	12/2	OK	
	b. Turns	DS	12/3	---
	DJ	12/2	OK	
4. What is maximum usable bank angle?	DS	12/3	---	
	DJ	12/2	OK	
5. Is maintaining airspeed a problem?	DS	12/3	---	
	DJ	12/2	OK	
6. Are there any problems associated with the landing task?	DS	12/3	---	
	DJ	12/2	---	
a. How well can you accomplish the task?	DS	12/3	---	
	DJ	12/2	---	
b. How much fatigue is involved?	DS	12/3	---	
	DJ	12/2	---	
7. What are the effects of random gust inputs on handling quality?	DS	12/3	---	
	DJ	12/2	---	
8. Are special piloting techniques required for the configuration?	DS	12/3	---	
	DJ	12/2	Keep airspeed above 160 knots	
9. What instruments are used most?	DS	12/3	---	
	DJ	12/2	---	
10. Are any of the instruments inadequate for the configuration?	DS	12/3	---	
	DJ	12/2	---	
11. Pilot rating?	DS	12/3	---	
	DJ	12/2	4	
12. PIO rating?	DS	12/3	---	
	DJ	12/2	3	

NOTE: The dash denotes no comment by the pilot.

TABLE XXXXVII

EVALUATIONS - MECHANICAL BACK-UP SYSTEM NO. 1

Mean Square Errors	Pilot		LF	LF	LF	LF	LF	LF	LF	LF	LF	LF	LF	
	Date	Run No.	12/8/69	12/8/69	12/8/69	12/8/69	12/8/69	12/8/69	12/8/69	12/8/69	12/8/69	12/8/69	12/8/69	
No. of Engines			2	2	2	2	2	2	2	2	2	2	2	
Gusts			Yes										Yes	
δ_s max (deg/sec)														
δ_s min (deg)			Depends on pilot											
δ_s max (deg)														
δ_s power (HP)														
$\overline{u_e}^2$			5250.	4560.	1060.	254.	1230.	440.	896.	91.	1160.	1370.	362.	3540.
$\overline{\theta_e}^2$			18.9	14.8	13.6	12.8	.375	15.1	34.6	60.3	.109x10 ⁵	34.1	.435	12.9
$\overline{\delta_{se}}^2$			5.84	2.94	2.10	2.10	2.84	2.23	1.48	1.68	.24	.888	1.24	.16
$\overline{\delta_s}^2$.318	2.77	.199	1.03	.238	.406	.703	.267	.229	.648	.108	1.33
\overline{GS}^2			.0565	.822	5.92	.939	5.95	.778	.861	3.95	.785	1.16	.376	.217
$\overline{n_z}^2$			168.	263.	83.7	88.8	43.6	110.	52.4	54.4	88.8	70.3	107.	107.
$\overline{S_L}^2$.0639	.143	.0538	.0529	.0416	.0322	.0745	.0845	.0151	.0559	.0172	.0499
\overline{Q}^2			2.09	14.9	1.49	6.77	1.51	3.26	3.43	1.80	2.37	4.78	1.70	6.10
$\overline{\phi}^2$			309.	172.	224.	153.	50.4	145.	115.	118.	81.2	102.	143.	123.
$\overline{\psi}^2$			234.	80.9	40.3	151.	66.8	76.4	31.4	20.7	19.3	25.3	32.6	34.3
\overline{P}^2			14.2	20.5	16.8	16.5	10.2	18.1	17.9	21.1	46.8	30.9	39.1	57.4
\overline{R}^2			2.25	1.89	1.78	1.85	.730	1.89	1.48	1.20	2.10	2.55	2.18	2.63
$\overline{\beta}^2$			1.15	1.09	.987	1.15	1.14	1.03	.981	.895	2.02	2.14	1.59	2.54
$\overline{I.O.C}^2$			204.	26.3	8.29	11.6	114.	5.85	40.3	21.5	2.45	.572	6.96	4.51
$\overline{F_{PR}}^2$			117.	112.	118.	.128.	118.	117.	114.	114.	238.	231.	228.	221.
$\overline{\delta_a}^2$			0	0	0	0	0	0	0	0	0	0	0	0
$\overline{\delta_a}^2$			0	0	0	0	0	0	0	0	0	0	0	0
$\overline{\delta_r}^2$.0360	.0478	.0447	.135	.0426	.0448	.0114	.0111	5.39	5.78	4.80	5.32
$\overline{\delta_r}^2$.326	.843	.537	.815	.513	.728	.350	.315	7.49	9.47	5.85	10.7
$\overline{S_{LD}}^2$			1.19	.977	1.22	1.98	1.38	1.53	1.13	1.00	.788	.729	.767	.844
$\overline{P_r}^2$.000529	.000427	.000385	.00110	.000363	.000398	.000113	.00107	.0412	.0441	.0366	.0407
$\overline{\delta_{SP}}^2$			290.	134.	167.	273.	189.	210.	155.	137.	107.	100.	105.	116.
$\overline{\delta_{SP}}^2$			9.42	12.3	14.0	15.7	9.93	12.7	27.6	24.7	10.1	7.79	10.1	29.9

TABLE XXXXVII(cont'd)

EVALUATIONS - MECHANICAL BACK-UP SYSTEM NO. 1

Mean Square Errors	Pilot	LF	LF	LF	LF	DS							
	Date	12/8/69	12/8/69	12/8/69	12/5/69	12/5/69	12/5/69	12/5/69	12/5/69	12/5/69	12/5/69	12/5/69	12/5/69
	Run No.	28	29	31	32	9	10	16	27	28	29	31	32
No. of Engines		2	2	2	2	2	2	2	2	2	2	2	2
Gusts	Yes												Yes
δ_s max (deg/sec)	Depends on pilot												
δ_s min (deg)													
δ_s max (deg)													
δ_s power (HP)													
$\overline{u_e}^2$		509.	687.	5970.	3700.	1390.	1710.	302.	303.	173.	1200.	571.	819.
$\overline{\theta_e}^2$		12.1	26.6	64.6	12.7	4.85	9.29	39.6	11.1	5.71	2.32	22.9	13.0
$\overline{\delta_{se}}^2$.80	1.49	.360	-1.08	.508	.020	1.15.	.680	.200	.712	.116	.704
$\overline{\delta_s}^2$.0634	.0811	1.56	.214	.276	.181	.033	.0622	.0511	.0599	.0267	.0489
\overline{GS}^2		5.10	1.46	1.43	3.29	1.09	.722	1.52	.238	1.12	2.05	.844	.460
$\overline{n_z}^2$		35.7	40.2	82.4	25.4	33.6	67.6	40.7	43.5	14.2	79.2	48.7	23.0
$\overline{S_L}^2$.00979	.0106	.0539	.0580	9.88	.00649	.00693	.00851	.00626	.0222	.00776	.0272
\overline{Q}^2		.590	.592	6.55	1.32	.973	.867	.288	.314	.300	1.14	.360	.666
$\overline{\phi}^2$		126.	113.	.174.	118.6	17.5	188.	79.4	47.2	59.4	192.	58.8	52.9
$\overline{\psi}^2$		38.0	38.6	14.3	21.9	7.43	76.6	28.6	29.0	16.0	86.1	17.2	42.5
\overline{P}^2		42.9	35.8	50.0	40.5	13.6	109.	21.0	23.2	26.0	33.1	26.3	12.3
\overline{R}^2		2.37	1.84	2.27	2.28	.664	4.88	1.54	1.18	1.25	2.90	1.44	.927
$\overline{\beta}^2$		1.70	1.20	1.30	1.19	.585	4.18	.833	.877	.908	1.43	1.10	.591
\overline{LOC}^2		3.44	30.6	22.2	8.85	.463	16.4	.987	4.09	.940	4.22	1.37	.914
$\overline{F_{PR}}^2$		216.	191.	179.	153.	126.	145.	244.	234.	203.	271.	239.	265.
$\overline{\delta_a}^2$		0	0	0	0	0	0	0	0	0	0	0	0
$\overline{\delta_r}^2$		4.26	2.97	3.10	2.38	.236	2.94	4.64	1590.	2.76	7.94	4.75	6.29
$\overline{\delta_r}^2$		4.13	3.76	8.98	8.16	1.40	21.0	2.12	2.88	2.45	2.92	2.42	1.91
$\overline{S_{LD}}^2$.659	.371	.325	.284	.0614	.103	.059	.446	.110	.146	.0965	.113
$\overline{F_r}^2$.0323	.0227	.0239	.0184	.00189	.023	.035	.0320	.0210	.0602	.0362	.0477
$\overline{\delta_{SP}}^2$		90.2	51.0	44.2	40.0	8.80	14.0	8.01	60.8	14.8	19.9	13.1	15.4
$\overline{\delta_{SP}}^2$		8.78	10.9	30.6	11.5	8.20	20.9	7.31	13.8	19.1	19.0	4.43	4.10

TABLE XXXXVII(cont'd)

EVALUATIONS - MECHANICAL BACK-UP SYSTEM NO. 1

Mean Square Errors	Pilot	LF												
	Date	12/5/69	12/5/69	12/5/69	12/5/69	12/5/69	12/5/69	12/5/69	12/5/69	12/5/69				
	Run No.	45	46	48	49	51	52	53	54					
No. of Engines		2	2	2	2	2	2	2	2					
Gusts		Yes	←—————→							Yes				
δ_s max (deg/sec)	} Depends on pilot													
δ_s min (deg)														
δ_s max (deg)														
δ_s power (HP)														
$\overline{u_e^2}$		1850.	1400.	3060.	3060.	812.	1420.	3060.	17900.					
$\overline{n_e^2}$		69.9	41.8	24.2	40.4	4.68	42.2	9.43	16.4					
$\overline{\delta_{se}^2}$		2.46	3.46	.872	.208	.032	.676	.172	3.08					
$\overline{\delta_s^2}$.119	.218	.0692	.0473	.0214	.329	.00452	.150					
$\overline{GS^2}$.419	1.55	1.27	.702	.861	1.95	.347	1.22					
$\overline{\tilde{n}_z^2}$		224.	180.	97.3	56.1	108.	170.	28.6	576.					
$\overline{s_l^2}$.0655	.0138	.0125	.0124	.0106	.0206	4.43	.0195					
$\overline{Q^2}$		2.20	2.43	.939	.846	.863	3.43	.125	1.29					
$\overline{\sigma^2}$		143.	328.	303.	73.1	296.	354.	62.9	209.					
$\overline{\psi^2}$		396.	98.6	32.6	20.4	54.5	67.5	15.5	53.4					
$\overline{P^2}$		44.4	64.1	85.0	30.6	65.8	147.	35.4	48.1					
$\overline{R^2}$		2.70	4.31	5.09	1.59	4.41	8.05	1.94	3.31					
$\overline{\beta^2}$		1.60	2.08	3.64	1.62	2.72	7.49	1.60	2.17					
$\overline{LOC^2}$		86.6	7.18	.468	.515	14.9	.571	4.97	4.05					
$\overline{F_{PR}^2}$		185.	214.	235.	212.	224.	256.	196.	320.					
$\overline{\delta_a^2}$		0	0	0	0	0	0	0	0					
$\overline{\delta_a^2}$		0	0	0	0	0	0	0	0					
$\overline{\delta_r^2}$		2.34	4.93	6.72	3.54	5.52	8.94	2.85	6.42					
$\overline{\delta_r^2}$		5.30	9.51	17.4	5.63	8.41	27.3	6.87	13.3					
$\overline{s_{l,d}^2}$.174	.268	.218	.232	15.2	.230	.208	.303					
$\overline{T_r^2}$.0179	.0376	.0515	.0271	.0421	.0687	.0218	.0482					
$\overline{\delta_{SP}^2}$		23.8	36.6	29.7	31.7	20.7	31.4	28.4	41.4					
$\overline{c_{SP}^2}$		3.85	13.5	10.1	.687	2.37	10.0	1.03	2.64					

TABLE XXXXVII(cont'd)

EVALUATIONS - MECHANICAL BACK-UP SYSTEM NO. 1

Pilot Opinion - Landability				
Question	Pilot	Date	Comment	
1. Is the aircraft difficult to trim?	LF	12/8	Yes	
	DS	12/5	No	
	LF	12/5	Trimable, but effort on stick and rudder	
2. Is attitude control satisfactory?	LF	12/8	Fair	
	DS	12/5	Recoverable	
	LF	12/5	Good	
Is heading control satisfactory?	LF	12/8	Poor	
	DS	12/5	Recoverable	
	LF	12/5	More difficult	
3. Is holding altitude a problem? a. Straight and level	LF	12/8	OK	
	DS	12/5	---	
	LF	12/5	OK	
	b. Turns	LF	12/8	OK
		DS	12/5	---
		LF	12/5	OK
4. What is maximum usable bank angle?	LF	12/8	30°	
	DS	12/5	30°	
	LF	12/5	40°	
5. Is maintaining airspeed a problem?	LF	12/8	No	
	DS	12/5	No	
	LF	12/5	No	
6. Are there any problems associated with the landing task? a. How well can you accomplish the task? b. How much fatigue is involved?	LF	12/8	---	
	DS	12/5	---	
	LF	12/5	Maintaining precision direction	
	a. How well can you accomplish the task?	LF	12/8	Marginal acceptable
		DS	12/5	N/A
		LF	12/5	Satisfactory
	b. How much fatigue is involved?	LF	12/8	Moderately heavy
		DS	12/5	---
		LF	12/5	Moderately heavy
7. What are the effects of random gust inputs on handling qualities?	LF	12/8	Disturbs heading	
	DS	12/5	None	
	LF	12/5	More difficult to hold heading	
8. Are special piloting techniques required for the configuration?	LF	12/8	Gain airspeed to 220K	
	DS	12/5	No	
	LF	12/5	Use large amount of rudder	
9. What instruments are used most?	LF	12/8	---	
	DS	12/5	---	
	LF	12/5	Flight director and heading	
10. Are any of the instruments inadequate for the configuration?	LF	12/8	---	
	DS	12/5	---	
	LF	12/5	---	
11. Pilot rating?	LF	12/8	5	
	DS	12/5	5	
	LF	12/5	5	
12. PIO rating?	LF	12/8	2	
	DS	12/5	2	
	LF	12/5	2	

NOTE: The dash denotes no comment by the pilot.

TABLE XXXVII(concluded)

EVALUATIONS - MECHANICAL BACK-UP SYSTEM NO. 1

Pilot Opinion - Landability			
Question	Pilot	Date	Comment
1. Is the aircraft difficult to trim?	DS	12/4	---
2. Is attitude control satisfactory?	DS	12/4	---
Is heading control satisfactory?	DS	12/4	---
3. Is holding altitude a problem?			
a. Straight and level	DS	12/4	OK
b. Turns	DW	12/4	OK
4. What is maximum usable bank angle?	DS	12/4	Full bank up to 60° after recovery completed
5. Is maintaining airspeed a problem?	DS	12/4	OK
6. Are there any problems associated with the landing task?	DS	12/4	---
a. How well can you accomplish the task?	DS	12/4	---
b. How much fatigue is involved?	DS	12/4	Normal
7. What are the effects of random gust inputs on handling qualities?	DS	12/4	No effect
8. Are special piloting techniques required for the configuration?	DS	12/4	Recovery from manual attitudes - noseup dying airspeed
9. What instruments are used most?	DS	12/4	---
10. Are any of the instruments inadequate for the configuration?	DS	12/4	---
11. Pilot rating?	DS	12/4	---
12. PIO rating?	DS	12/4	---
13. Special comments	DS	12/4	Aircraft is recoverable to straight and level flight if backup controls are activated immediately; M = 0.3, M = 0.5, M = 0.8 (roll necessary to drop airspeed)

NOTE: The dash denotes no comment by the pilot.

TABLE XXXVIII

EVALUATIONS - MECHANICAL BACK-UP SYSTEM NO. 2

Mean Square Errors	Pilot	DS	DS																
	Date	12/5/69	12/5/69																
	Run No.	24	25																
No. of Engines		2	2																
Gusts		Yes	Yes																
δ_s max (deg/sec)																			
δ_s min (deg)		Depends on pilot																	
δ_s max (deg)																			
δ_s power (HP)																			
$\overline{u_e}^2$		1390.	2580.																
$\overline{\theta_e}^2$		39.9	33.6																
$\overline{\delta_{se}}^2$.104	.452																
$\overline{\delta_s}^2$.0940	.0547																
\overline{GS}^2		4.54	1.61																
$\overline{n_z}^2$		1.56	40.2																
$\overline{S_L}^2$.0164	.00653																
\overline{Q}^2		.520	.386																
$\overline{\phi}^2$		38.3	72.5																
\overline{V}^2		7.00	21.3																
\overline{P}^2		30.7	35.3																
\overline{R}^2		1.36	1.42																
$\overline{\beta}^2$.944	.869																
\overline{LOC}^2		.343	1.31																
$\overline{F_{PR}}^2$		135.	148.																
$\overline{\delta_a}^2$		6.72	5.70																
$\overline{\delta_a}^2$		16.5	12.3																
$\overline{\delta_r}^2$.284	.558																
$\overline{\delta_r}^2$		1.21	1.46																
$\overline{S_{LD}}^2$.107	.0807																
$\overline{F_r}^2$.00230	.00431																
$\overline{\delta_{SP}}^2$		0	0																
$\overline{\delta_{SP}}^2$		0	0																

TABLE XXXXVIII (concluded)

EVALUATIONS - MECHANICAL BACK-UP SYSTEM NO. 2

Question	Pilot Opinion		
	Pilot	Date	Comment
1. Is the aircraft difficult to trim?	DS	12/5	No
2. Is attitude control satisfactory?	DS	12/5	Recoverable
Is heading control satisfactory?	DS	12/5	Recoverable
3. Is holding altitude a problem?			
a. Straight and level	DS	12/5	---
b. Turns	DS	12/5	---
4. What is maximum usable bank angle?	DS	12/5	30°
5. Is maintaining airspeed a problem?	DS	12/5	No
6. Are there any problems associated with the landing task?	DS	12/5	
a. How well can you accomplish the task?	DS	12/5	No applicable
b. How much fatigue is involved?	DS	12/5	
7. What are the effects of random gust inputs on handling quality?	DS	12/5	None
8. Are special piloting techniques required for the configuration?	DS	12/5	No
9. What instruments are used most?	DS	12/5	---
10. Are any of the instruments inadequate for the configuration?	DS	12/5	---
11. Pilot rating?	DS	12/5	5
12. PIO rating?	DS	12/5	2

NOTE: The dash denotes no comment by the pilot.

$$u_0 = 198 \text{ knots} \quad (67)$$

$$\theta_0 = 8.0 \text{ deg} \quad (68)$$

$$\delta_{s0} = 2.0 \text{ deg} \quad (69)$$

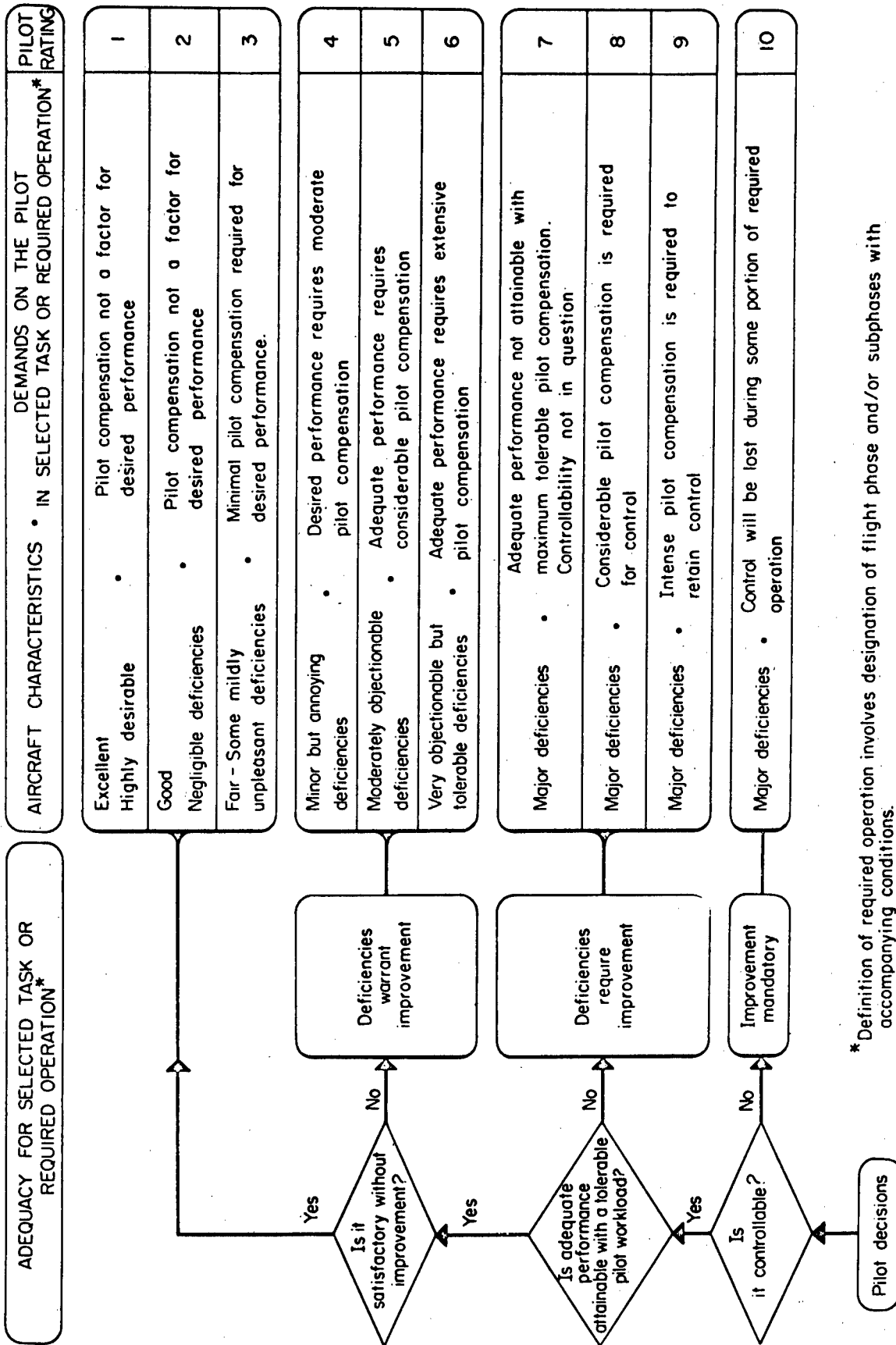
The glide slope and localizer deviations were computed using

$$GS = 57.3 \tan^{-1}(h/x_e) - 2.5 \quad (70)$$

$$LOC = 57.3 \tan^{-1}(y_e/x_e) \quad (71)$$

S_L , S_{LD} and P_r are the actual stick and pedal deflections and F_{SL} , F_{SLD} and F_{PR} are the stick and pedal forces for the F-4 with the existing control system.

Pilot ratings were recorded for both general flying qualities and for PIO tendencies. The general flying qualities rating flow diagram which defines how the numerical ratings were arrived at is given in Fig. 52. The PIO tendency rating scale is defined by Table XXXIX. A summary of the pilot ratings delivered in the experiments has been drawn from the data given in Ref. 1. This summary is presented in Table L. It includes both general flying qualities and PIO tendency ratings.



* Definition of required operation involves designation of flight phase and/or subphases with accompanying conditions.

Figure 52. Handling Qualities Rating Scale

TABLE XXXXIX

PIO TENDENCY RATING SCALE

Description	Numerical Rating
No tendency for pilot to induce undesirable motions.	1
Undesirable motions tend to occur when pilot initiates abrupt maneuvers or attempts tight control. These motions can be prevented or eliminated by pilot technique.	2
Undesirable motions easily induced when pilot initiates abrupt maneuvers or attempts tight control. These motions can be prevented or eliminated but only at sacrifice to task performance or through considerable pilot attention and effort.	3
Oscillations tend to develop when pilot initiates abrupt maneuvers or attempts tight control. Pilot must reduce gain or abandon task to recover.	4
Divergent oscillations tend to develop when pilot initiates abrupt maneuvers or attempts tight control. Pilot must open loop by releasing or freezing the stick.	5
Disturbance or normal pilot control may cause divergent oscillation. Pilot must open control loop by releasing or freezing the stick.	6

TABLE I
SUMMARY OF PILOT OPINION FROM SIMULATION
(Ref. 1)

System Configuration	Flying Qualities Rating	PIO Rating	No. of Subjects	Total No. of Runs	Pilot Comments	
A w/o gusts	2		1	4	airspeed had to be kept higher than recommended for task, rudder used, gusts aggravate problem	
		1 2	1 1	4		
A w/ gusts	2		1	7		
	4					
	5		3			
	9		1			
		1 2 3 5 6	1 2 2 1 1	6		
B w/o gusts						no data taken
B w/ gusts	5		2	32		airspeed had to be kept higher than recommended for task, gusts disturb heading, rudder used
		2	2	32		
C w/o gusts					no data taken	
C w/ gusts	5		1	2		
		2	1	2		

Unclassified

Security Classification

DOCUMENT CONTROL DATA - R & D

(Security classification of title, body of abstract and indexing annotation must be entered when the overall report is classified)

1. ORIGINATING ACTIVITY (Corporate author) SYSTEMS TECHNOLOGY, INC. 13766 South Hawthorne Blvd. Hawthorne, California 90250		2a. REPORT SECURITY CLASSIFICATION Unclassified	
		2b. GROUP NA	
3. REPORT TITLE ANALYSIS OF LIMITED AUTHORITY MANUAL CONTROL SYSTEMS			
4. DESCRIPTIVE NOTES (Type of report and inclusive dates) Final, September 1969 through March 1971			
5. AUTHOR(S) (First name, middle initial, last name) Lee Gregor Hofmann Kishor V. Shah Dunstan Graham			
6. REPORT DATE		7a. TOTAL NO. OF PAGES 228	7b. NO. OF REFS 31
8a. CONTRACT OR GRANT NO. F33615-70-C-1075		9a. ORIGINATOR'S REPORT NUMBER(S) TR-194-1	
b. PROJECT NO. 8219		9b. OTHER REPORT NO(S) (Any other numbers that may be assigned this report)	
c. Task 821904		AFFDL-71-6	
d.			
10. DISTRIBUTION STATEMENT Approved for public release; distribution unlimited.			
11. SUPPLEMENTARY NOTES None		12. SPONSORING MILITARY ACTIVITY Air Force Flight Dynamics Laboratory Wright-Patterson Air Force Base, Ohio	
13. ABSTRACT Systematic procedures for predicting pilot-vehicle-flight control system performance and proneness to pilot induced oscillations and instabilities are here developed and applied to examples. The systems analyzed have very limited maximum control surface rates and deflections. Performance analysis is by means of applying random input describing function theory to predict the root-mean-square level of key system variables as a function of the control surface rate and deflection limit levels. Acceptable limit levels are only two to three times the root mean square value of the variable at the point in the system where each limiter nonlinearity occurs. Pilot induced oscillations and instabilities are predicted by applying sinusoidal input describing function theory. A sinusoidal input describing function is derived for the rate limited integrator having a restricted output range. This is the key element in the model for an actuator having limited maximum rate and deflection. Pilot induced oscillations correspond to a stable limit cycle. Furthermore, pilot induced instabilities may result when conditions derived from the unstable limit cycle solutions are exceeded. A simple design criterion for eliminating pilot induced oscillations and instabilities is Select the linear system gains and equalization so that the locus of closed-loop system roots as a function of the forward-loop actuator gain over the range from zero to its nominal value, does not exhibit conditional stability. Results of analyzing three minimum back-up manual flight control system modifications for the F-4C are compared with data from piloted fixed-base simulator experiments for the same system configurations. The analytically determined minimum limits for the three example back-up systems compare favorably with the minimum limits determined in fixed-base simulation. Predicted and measured pilot opinion ratings also compare favorably. Unfortunately, however, predicted and measured performance do not compare favorably. This may be because of inaccurate or incomplete documentation of the measured performance.			

KEY WORDS	LINK A		LINK B		LINK C	
	ROLE	WT	ROLE	WT	ROLE	WT
Random Input Describing Functions Sinusoidal Input Describing Functions Describing Functions Pilot Induced Oscillations Back-up Flight Control Systems Limited Authority Control Systems Manual Control Actuator Design						